Gravity theories, black holes and compact objects

APRATIM GANGULY

Gravity theories, black holes and compact objects

Author:

Apratim GANGULY

A thesis submitted in fulfilment of the requirements

for the degree of Doctor of Philosophy

in the

Astrophysics and Cosmology Research Unit

School of Mathematics, Statistics and Computer Science

University of KwaZulu-Natal, Westville Campus

March 24, 2016

As the candidate's supervisor I have/have not approved this thesis for submission.

Signed:	Name: Prof. Subharthi RAY	Date:
Signed:	Name: Prof. Sunil MAHARAJ	Date:
Signed:	Name: Dr. Rituparno GOSWAMI	Date:

Declaration 1 - PLAGIARISM

I, Apratim GANGULY, declare that this thesis titled, 'Gravity theories, black holes and compact objects' and the work presented in it are my own. I confirm that:

- This work was done wholly or mainly while in candidature for a research degree at this University.
- Where any part of this thesis has previously been submitted for a degree or any other qualification at this University or any other institution, this has been clearly stated.
- Where I have consulted the published work of others, this is always clearly attributed.
- Where I have quoted from the work of others, the source is always given. With the exception of such quotations, this thesis is entirely my own work.
- I have acknowledged all main sources of help.
- Where the thesis is based on work done by myself jointly with others, I have made clear exactly what was done by others and what I have contributed myself.

Signed:

Date:

Declaration 2 - PUBLICATIONS

The content of this thesis is based on the following research papers published (or submitted or in preparation) in peer-reviewed journals:

- **Global structure of black holes via dynamical system**
  A. Ganguly, *R. Gannouji, R. Goswami, S. Ray*
  Class. Quant. Grav. 32 (2015) 10, 105006

- **Accretion onto a black hole in a string cloud background**
  A. Ganguly, *S. G. Ghosh and S. D. Maharaj*
  Phys. Rev. D 90, 064037 (2014)

- **Neutron stars in Starobinsky model**
  A. Ganguly, *R. Gannouji, R. Goswami, S. Ray*
  Phys. Rev. D 89, 064019 (2014)

- **Global Structure of black holes source by quintessence field**
  M. Cruz, **A. Ganguly**, *R. Gannouji, G. Leon, E. N. Saridakis*
  in preparation

- **Black hole structure via dynamical system in $f(R)$ theories**
  A. Ganguly, *R. Gannouji, R. Goswami, S. Ray*
  in preparation

The work developed in this thesis has been published as news:

- **Can't solve an equation...bypass it !!!**
  R. Gannouji, **A. Ganguly**
  Class. Quant. Grav. +
  (`http://cqgplus.com/2015/07/08/cant-solve-an-equation-bypass-it/`)

Publications not part of this thesis but the work was done during my tenure as a PhD student of UKZN:

- **Dense magnetized plasma associated with a fast radio burst**
  K. Masui, H.-H. Lin, J. Sievers, C. J. Anderson, T.-C. Chang, X. Chen, **A. Ganguly**,*M. Jarvis, C.-Y. Kuo, Y.-C. Li, Y.-W. Liao, M. McLaughlin, U.-L. Pen, J. B. Peterson, A. Roman, P. T. Timbie, T. Voytek, J. K. Yadav*
  Nature 528, 523 (2015)

Signed: ______________________________

Date: ______________________________

"Poets say science takes away from the beauty of the stars – mere globs of gas atoms. I, too, can see the stars on a desert night, and feel them. But do I see less or more?"

Richard Feynman

Abstract

Limitations in solving the nonlinear Einstein field equations can be overcome if we effectively reformulate the equations into an autonomous system of dimensionless, covariantly defined geometrical variables. So, by definition, the system is gauge independent. To avoid solving the equations, we apply the usual tools of dynamical system analysis to the compactified phase space leading to the determination of all important global features of the maximal extension of vacuum (with and without cosmological constant) and electrovacuum spacetimes. The phase plots give a better visualization of how the solutions evolve depending on various initial conditions. The analysis is extended to investigate vacuum spherically symmetric solutions for modified theories of gravity like $f(R)$ and the quintessence model. A variety of new behaviour has been obtained which will extend the framework to study these theories. We have also modelled, for the first time, non-perturbatively with the proper matching of junction conditions and exterior Schwarzschild solution, the full structure of a neutron star in the Starobinsky model. We have shown that the modified field equations are singular in the sense that they develop a boundary layer. Hence all the boundary conditions cannot be satisfied for a generic equation of state, only a particular class are compatible with the model. This particular $f(R)$ model brings two additional fine-tuning problems. First, only a small class of models can be mathematically matched with the exterior Schwarzschild. Second, the central initial conditions of the neutron star should be fine-tuned in order to exactly match Schwarzschild at the surface. Since we are interested in modelling realistic astrophysical compact objects, we will require that the exterior spacetime is static and asymptotically flat, and the exterior static solution should describe a well defined black hole solution. Given these constraints, the fine-tuning problems will be true for a wide range of $f(R)$ models due to the modified Jebsen-Birkhoff theorem. Shifting our focus from interior solutions, we have also investigated stationary, spherically symmetric accretion of a polytropic fluid onto black hole with a string cloud background, where we find that the mass accretion rate increases considerably when compared to the Schwarzschild case. In the process, we also find the gas compression ratios and temperature profiles below the accretion radius and at the event horizon.

Dedication

I dedicate this thesis to my parents, Iva and Asish Ganguly. I hope that this achievement will complete the dream that you had for me for so many years when you chose to give me the best education you could.

Acknowledgements

Research is not a single man's job and it was no exception during my PhD years. To begin with, I want to extend my gratitude to my PhD supervisor, Subharthi Ray, and co-supervisors Sunil Maharaj and Rituparno Goswami. Its been a pleasure working with you guys. The long discussion sessions that we had, both academic and non-academic, has helped me to learn a lot of things which I'm sure will help me in my future endeavors. I would also like to acknowledge the National Research Foundation and University of KwaZulu-Natal (UKZN) for providing the funding that made my research possible. Sunil, thanks for repeatedly scrounging money for me for all the conferences and schools.

I am also grateful to my collaborators Radouane Gannouji, Sushant Ghosh, Migel Cruz, Genly Leon and Emmanuel Saridakis. In particular, Radouane, it has been a pleasure to know and work with you. I think I have found my friend, philosopher and guide in you. Thanks for your endless support and encouragement throughout my PhD years and I sincerely hope this collaboration continues in the future. Also, I want to mention Jonathan Sievers for introducing me to radio astronomy and spending so much time to answer all my queries.

I'm thankful to many people in ACRU and the Mathematics department of UKZN for helping me with my academic and personal problems. Special mention goes to Saumya da, Sergey Shindin, Giovanni, Aymen, Anne, Veeresh and Aurelie for listening to my various problems and boring discussions and trying to find out solutions for them and for the trips, hikes and innumerable lifts that I got from you guys. And, obviously Moumita di and Matt. Saying thanks will be too demeaning for what you guys have done for me. You are practically family to me.

The administrative staffs, particularly Selvie, Sheeren and Soren, thanks for making my life easy. Without your help my life would have been a complete mess. Asok, you are a very kind man. Its been a pleasure knowing you.

I also want to thank the "Bong" group in Durban for making me feel at home away from home. I don't want to take any names because I fear I'll miss someone but all the parties and the food helped me survive. You are the best.

And lastly, I could never adequately thank my family enough. My parents have always expressed how proud they are of me and that meant more to me than they'll ever know. Their

lives have always been their two sons, and they are the two most selfless people I have ever known. They are my heroes. My elder brother and his lovely wife have been the most supportive people in my life. They are always there when I need them and I'm really grateful for that.

Contents

List of Figures

List of Tables

Abbreviations

GR	**G**eneral **R**elativity	**LRS**	**L**ocally **R**otationally **S**ymmetric
EH	**E**instein-**H**ilbert	**CMB**	**C**osmic **M**icrowave **B**ackground
SN	**S**uper**n**ova	**MEMT**	**M**atter **E**nergy **M**omentum **T**ensor
LSS	**L**arge-**S**cale **S**tructure	**CEMT**	**C**urvature **E**nergy **M**omentum **T**ensor
BD	**B**rans-**D**icke	**BAO**	**B**aryon **A**coustic **O**scillation
BH	**B**lack **H**ole	**COBE**	**Co**smic **B**ackground **E**xplorer
NS	**N**eutron **S**tar	**SFEMT**	**S**calar **F**ield **E**nergy **M**omentum **T**ensor
WD	**W**hite **D**warf	**WMAP**	**W**ilkinson **M**icrowave **A**nisotropy **P**robe
EoM	**E**quation **o**f **M**otion	**PNGB**	**P**seudo-**N**ambu-**G**oldstone **B**oson
DE	**D**ark **E**nergy	**LLR**	**L**unar **L**aser **R**anging
EoS	**E**quation **o**f **S**tate	**PSTF**	**P**rojected **S**ymmetric **T**race-**F**ree
AdS	**A**nti-**d**e **S**itter	**FLRW**	**F**riedman-**L**emaître-**R**obertson-**W**alker
AGN	**A**ctiv **G**alactic **N**ucleus	**TOV**	**T**olman-**O**ppenheimer-**V**olkof
PK	**P**ost-**K**eplerian	**SEP**	**S**trong **E**quivalence **P**rinciple
GW	**G**ravity **W**ave	**FAST**	**F**ive hundred meter **A**perture **S**pherical **T**elescope
MS	**M**isner-**S**harp	**LIGO**	**L**aser **I**nterferometer **G**ravitational-Wave **O**bservatory
SKA	**S**quare **K**ilometre **A**rray	**MeerKAT**	**Meer** **K**aroo **A**rray **T**elescope
DGP	**D**vali-**G**abadadze-**P**orrati	**dRGT**	**de** **R**ham-**G**abadadze-**T**olley
		WKB	**W**entzel-**K**ramers-**B**rillouin

Physical Constants

Speed of light	c	$=$	2.99792458×10^{8} m/s
Gravitational constant	G	$=$	6.67408×10^{-11} m^3/Kg s^2
Boltzmann constant	k_B	$=$	$1.38064852 \times 10^{-23}$ m^2 Kg/s^2 K
Solar mass	$M_\odot$	$=$	1.98855×10^{30} Kg
Proton mass	m_p	$=$	$1.6726219 \times 10^{-27}$ Kg

Notations and Conventions

Signature:	$[-,+,+,+]$
Geometrised units:	$8\pi G \;=\; c \;=\; 1$
Greek indices:	$0,\ 1,\ 2,\ 3$
Latin indices:	$1,\ 2,\ 3$
Symmetrization:	$A_{(\mu\nu)} = \frac{1}{2}\left(A_{\mu\nu} + A_{\nu\mu}\right)$
Antisymmetrization:	$A_{[\mu\nu]} = \frac{1}{2}\left(A_{\mu\nu} - A_{\nu\mu}\right)$
Riemann tensor:	$R^{\mu}{}_{\nu\rho\sigma} \;=\; \Gamma^{\mu}{}_{\nu\sigma,\rho} - \Gamma^{\mu}{}_{\nu\rho,\sigma} + \Gamma^{\alpha}{}_{\nu\sigma}\Gamma^{\mu}{}_{\rho\alpha} - \Gamma^{\alpha}{}_{\nu\rho}\Gamma^{\mu}{}_{\sigma\alpha}$
Christoffel symbol:	$\Gamma^{\mu}{}_{(\nu\rho)} \;=\; \frac{1}{2}g^{\mu\sigma}\left(g_{\nu\sigma,\rho} + g_{\sigma\rho,\nu} - g_{\nu\rho,\sigma}\right)$
Ricci tensor:	$R_{\mu\nu} \;=\; R^{\alpha}{}_{\mu\alpha\nu}$

Chapter 1

Introduction

The last century of progress in understanding the fundamental laws of physics has been based on developing our knowledge of the symmetries that these laws respect. Prior to the twentieth century, the accepted laws were based on Galileo's principle of relativity. That is, they do not change over time, and are also invariant under translations and rigid rotations of the three spatial directions. However, in the early 20th century, Einstein [Einstein 1905] and others understood that this Galilean symmetry was only an approximation to a larger symmetry group, the Lorentz group, acting not on space and time separately, but on a four-dimensional spacetime. Crucially, the Lorentz group encodes a notion of causality, and as a result this new theory of *special relativity* predicts that no information is able to travel faster than the speed of light $c \approx 3 \times 10^8 \mathrm{ms}^{-1}$. Galilean symmetry is recovered from special relativity for speeds $v \ll c$, and hence gives a very good approximation for most conventional physics.

Unfortunately, Newton's law of gravitation is inherently inconsistent with special relativity; when a massive body moves, information about the movement is instantaneously transferred across all of space via the change in its gravitational field. This violates causality. This observation motivated the development of general relativity (GR) by Einstein in 1916 [Einstein 1916]. It follows the famous quote by John Wheeler, "*spacetime tells matter how to move; matter tells spacetime how to curve*", according to a particular set of partial differential equations: the Einstein field equations (EFEs)

$$G_{\mu\nu} = \frac{8\pi G}{c^4} T_{\mu\nu}, \tag{1.1}$$

where the Einstein tensor $G_{\mu\nu} = R_{\mu\nu} - \frac{1}{2} R g_{\mu\nu}$ encodes some aspects of the curvature of spacetime, and $T_{\mu\nu}$ encodes information about the matter content and is called the *energy momentum tensor*, with G the Newtonian gravitational constant. The quantities $8\pi G$ and c are set to 1 in the rest of the thesis, unless otherwise stated.

To fix notation and conventions, we first recall some basic concepts of general relativity in four dimensions. Spacetime is a differentiable manifold $(\mathcal{M}, g)$, with local distances measured by a line element

$$ds^2 = g_{\mu\nu} dx^\mu \otimes dx^\nu. \tag{1.2}$$

Summation over repeated indices is implied. Greek indices $\mu, \nu, \dots$ run over spacetime coordinates and can take values $0, 1, 2, 3$ whereas Latin indices $i, j, \dots$ correspond to spatial ones and assume values $1, 2, 3$. The 1-forms dx^μ provide a local coordinate basis for the cotangent space of $\mathcal{M}$. The metric $g_{\mu\nu}$ has signature $[-, +, \dots, +]$, and hence provides an indefinite norm on the tangent space $T(\mathcal{M})$. We will raise and lower indices with the metric $g_{\mu\nu}$ and its inverse $g^{\mu\nu}$.

Unless stated otherwise, we will use ∇ to denote the Levi-Civita connection on $(\mathcal{M}, g)$, with the property that $\nabla g = 0$. The commutator of ∇, acting on an arbitrary vector field V, defines the *Riemann curvature tensor* $R_{\mu\nu\rho\sigma}$ through

$$[\nabla_\mu, \nabla_\nu] V_\rho = R_{\mu\nu\rho\sigma} V^\sigma. \tag{1.3}$$

The Riemann tensor has 20 independent components in 4-D spacetime, and obeys the symmetries $R_{\mu\nu\rho\sigma} = R_{[\mu\nu][\rho\sigma]} = R_{\rho\sigma\mu\nu}$ and $R_{\mu[\nu\rho\sigma]} = 0$, as well as the differential Bianchi identity

$$\nabla_{[\mu} R_{\nu\rho]\sigma\tau} = 0. \tag{1.4}$$

It is often useful to decompose the Riemann tensor into several parts. We write

$$R_{\mu\nu\rho\sigma} = W_{\mu\nu\rho\sigma} + g_{\mu[\rho} R_{\sigma]\nu} - g_{\nu[\rho} R_{\sigma]\mu} - \frac{1}{3} R g_{\mu[\rho} g_{\sigma]\nu}\,, \tag{1.5}$$

where the *Ricci tensor* and *Ricci scalar* are given by

$$R_{\mu\nu} \equiv g^{\rho\sigma} R_{\mu\rho\nu\sigma} \text{ and } R \equiv g^{\mu\nu} R_{\mu\nu}, \tag{1.6}$$

and the *Weyl tensor* $W_{\mu\nu\rho\sigma}$ is totally traceless. The Weyl tensor encodes the information about curvature in the absence of matter. One important property of this tensor is that it is *conformally invariant*. A conformal transformation maps a spacetime $(\mathcal{M}, g)$, to a new spacetime $(\mathcal{M}, \tilde{g})$, where the new metric is given by $\tilde{g} = \Omega^2 g$ for some smooth positive function $\Omega : \mathcal{M} \to \mathbb{R}$. If $\tilde{W}$ is the Weyl tensor for the new spacetime, then the statement of conformal invariance is that $\tilde{W}^\mu{}_{\nu\rho\sigma} = W^\mu{}_{\nu\rho\sigma}$ (see, [Wald 1984]).

1.1 Modifications in the theory of gravity

General relativity is still widely considered as a fundamental theory of gravitation. Being one of the pillars of modern science, it has brought a renaissance in our understanding of the Universe. Though the theory has passed all experimental tests (see [Will 2014] for a review), most of them, except the binary pulsar observations [Kramer and Wex 2009], are in the weak-field regime. This has led to questions related to its short comings which are becoming more and more pertinent from both theoretical and observational points of view. Indeed, looking for modification of the theory of gravity is not a new thing; GR itself is a modification of Newton's gravitational theory which is an extremely good representation of gravity for a host of situations of practical and astronomical interests. Observations of the orbit of Mercury revealed a discrepancy with the prediction of Newtonian gravity in the rate of advance of Mercury's perihelion which was resolved by taking into account the relativistic corrections of Einstein's theory of gravity. Similarly, there is growing evidence that modifications of GR at small and large energies are somehow inevitable.

Ideas to modify GR by considering higher order invariants to the action were invoked as early as the formulation of GR itself [Weyl 1919; Eddington 1923] which were triggered by scientific curiosity. Later, in 1960s, these ideas gained substantial ground when it was realized that GR is not perturbatively renormalizable in the standard quantum field theory sense and hence, cannot be conventionally quantized. Non-renormalizability is seen as a signal that a physical theory is only valid up to a particular energy scale, and there exists new physics that becomes relevant at higher energies. It was soon realized that the theory becomes renormalizable if we add higher order curvature terms to the Einstein-Hilbert action [Utiyama and DeWitt 1962; Stelle 1977]. These lead to high-curvature or high-energy corrections which can avoid the inconsistency of classical GR and quantum mechanics particularly near singularities, as shown by the Hawking-Penrose singularity theorems [Hawking and Penrose 1970]. Also, if theories of quantum gravity (such as string theory and loop quantum gravity) are considered, it can be shown that the effective low energy gravitational action has higher order curvature invariants [Birrell and Davies. 1982; Buchbinder et al. 1992; Vilkovisky 1992].

In recent times, rapid development in observational cosmology confirms that the universe has undergone two phases of cosmic acceleration – the inflationary phase and the late time acceleration. In order to solve the problems of flatness, horizon, monopoles etc., concerning the early Universe in cosmology, a phase of a very rapid accelerated expansion was necessary [Guth 1981; Linde 1982; Albrecht and Steinhardt 1982], i.e., inflation, which is believed to have occurred prior to the radiation dominated era at $\sim 10^{-35} - 10^{-32}$ s after the Big Bang (for reviews, see [Lyth and Riotto 19991; Liddle and Lyth 2000; Bassett et al. 2006]). Furthermore, it naturally provides an initial seed for cosmic microwave background (CMB) anisotropy and large scale structure [Mukhanov and Chibisov 1981; Hawking 1982; Starobinsky 1982; Guth and Pi 1982]. Hence it has become a cornerstone of the Big Bang model. The second accelerating phase has started after the matter domination. Data from type Ia supernovae (SN Ia) [Riess et al. 1998; Riess et al. 1999; Perlmutter et al. 1999], large scale structure (LSS) [Tegmark et al. 4; Tegmark et al. 2006], baryon acoustic oscillations (BAO) [Eisenstein et al. 2005; Percival et al. 2007], and CMB anisotropies [Komatsu et al. 2009; Ade et al. 2015] have concluded that our Universe at present is expanding at an accelerated rate. The unknown component giving rise to this late time cosmic acceleration is called dark energy [Huterer and Turner 1999] (for reviews, see [Copeland, Sami, et al. 2006; Amendola and Tsujikawa 2010]).

These two phases of cosmic acceleration cannot be explained by just standard matter whose equation of state $w = P/\rho$ satisfies the condition $w \geq 0$, where P and ρ are the pressure and the energy density of matter, respectively. In fact, what is required is a fluid of negative pressure, with $w \leq -1/3$, to realize the late time acceleration of the universe. The cosmological constant Λ is the simplest candidate of dark energy, which corresponds to $w = -1$. The cosmological constant is still in remarkably good agreement with almost all cosmological data. However, more than a decade after the observational discovery of cosmic acceleration, our knowledge of the cosmic evolution is so incomplete that it would be totally premature to claim that we are close to understanding the ingredients of the cosmological standard model. There are at least three reasons to prove this point. The first is the so-called *cosmological constant problem* [Weinberg 1989; Martin 2012] which deals with the small but non-zero value of Λ which is 120 orders of magnitude smaller than the energy scale of the vacuum energy of particle physics, from which it is believed to originate from. In fact, its value is too small with respect to any physically meaningful scale, except the current horizon scale. The second is the *coincidence problem* which states that this value is not only small, but also surprisingly close to another unrelated quantity, the present matter energy density. This coincidence is hard to accept as the matter density is diluted rapidly with the expansion of space. Finally, though inflation is an integral part of the standard cosmological model, yet the fact that we exist and are able to observe and describe the universe around us demonstrates that this early accelerated expansion was not due to a constant Λ, thus shedding doubt on the nature of the current accelerated expansion. The very fact that we know so little about the past dynamics of the universe forces us to enlarge the theoretical parameter space and to consider phenomenology that a simple cosmological constant cannot accommodate.

These motivations led many scientists to challenge one of the most basic tenets of physics: Einstein's law of gravity. Two major approaches for modifications (for an extensive review, see [Clifton, Ferreira, et al. 2012]) are as follows:

- **modification of the energy momentum tensor in Einstein's equations**

- **modification of the theory of gravity**

In chapter 2, we formally introduce the modified theories that will be considered in this thesis. The generating Lagrangians will be explicitly given and the field equations derived from them. The form of these field equations will immediately be seen to be more complicated than the general relativistic case.

1.2 Strong gravity regimes in astrophysics

The main focus of this thesis is to study how these modifications to GR are applicable to the strong gravity regime and the constraints they bring thereof. As a common practice, the feasibility of all the modified gravity models are verified by undergoing solar system tests. However, these fields are substantially weaker than the vicinity of astrophysical compact stars and solar mass black holes corresponding to a surface redshift of ~ 1 and a spacetime curvature of $\simeq 2 \times 10^{-13}$ cm^{-2} [Psaltis 2008]. So these compact stars and solar mass black holes give a very good platform to study the behaviour of strong gravity. Ideally, black holes would have been the best candidates to study the strong gravity behaviour of these modified theories. On the other hand, compact stars – like the neutron and quark stars – have additional benefits of studying the behaviour of matter at high density under the modification of gravity.

Black hole (BH), neutron star (NS) and white dwarf (WD) are the three end stages of a star. They are generally termed as "dead" stars and to understand how they are formed, we should start from their "birth". Stars are natural nuclear fusion reactors that take raw materials – hydrogen and helium, and produce a steady supply of heavier elements. In fact, without stars no elements heavier than beryllium could have formed in normal nucleosynthesis [B. W. Carroll and Ostlie 1996].

After a billion years from the birth of the Universe, the slight inhomogeneities in the mass distribution of the early Universe (that were observed by Cosmic Background Explorer (COBE) and Wilkinson Microwave Anisotropy Probe (WMAP), and more recently *Planck*) led to pockets of high density regions. Eventually, clouds of gravitationally bound matter began to form. For such cases, the gravitational attraction is counteracted primarily by the thermal gas pressure, although rotation of the cloud and internal electromagnetic repulsion also play significant roles. If rotation and electromagnetism are neglected, the cloud will collapse under the force of gravity if their mass exceeds the Jeans mass limit, building up ever greater pressure at the core of the cloud triggering hydrogen fusion to helium.

The evolution of the star depends on a number of factors, however mass is the dominant factor which determines the star's ultimate fate. Hydrogen fusion may continue in the star's envelope and some of the energy generated leads to slow expansion of the envelope, thereby decreasing its temperature and shifting it to the red part of the visible spectrum. This type of star is referred to as a red giant. Another situation is that the star may be sufficiently massive to fuse all the elements up to iron, which requires an endothermic reaction to fuse and so will not occur spontaneously. The latter possibility will lead to a particular class of supernova, or catastrophic stellar explosion, which will in turn provide the energy to fuse all the stable elements with atomic numbers higher than iron. Hence, all the naturally occurring elements heavier than beryllium were born from either the evolution or the death of stars.

Eventually, the nuclear fusion reaction in the interior of the star will stop and the thermal pressure of the hot interior can no longer support the gravitational collapse and the star collapses to a smaller and denser state. The star will populate an electron-degenerate core via fusion in its envelope and the gravitational collapse of the core will be supported by electron degeneracy pressure. If the final core is less than 1.44 $M_\odot$, the Chandrasekhar limit, the star will remain electron degenerate and be called a white dwarf. However, if the star's total mass is sufficient for the envelope to populate a more massive core, electron degeneracy will be overcome, and the star will become a neutron star if neutron degeneracy is able to stop the infall and support the mass of the core, or else the star will collapse to a singularity, where all the mass is concentrated at a single point in space. For the latter case, any information contained in the star other than its mass, spin, and charge is erased. This state of complete collapse is known as a black hole, because of its amazing property that, within a certain distance from the singularity, namely the event horizon of the black hole, even a photon lacks sufficient velocity to escape the gravitational pull of the singularity. Because light cannot escape, no information can be sent from inside the event horizon, at least from a classical point of view. The region inside the event horizon is therefore causally disconnected, or in layman's terms, completely cut off from the rest of the Universe.

1.3 Neutron star interior

Neutron stars are truly fascinating objects. They are the densest stars known – while about 10 km in radius, a NS has a mass approximately the same as the Sun (thus its mean density is comparable to the density of an atomic nucleus). They provide an unique site for studying fundamental questions in physics and astrophysics, including the influence of super-strong magnetic fields, superfluidity and superconductivity, the properties of nuclear forces at high densities, possible phase transitions to exotic matter, and gravitational physics in the strong-field regime.

But the main problem is the uncertainty in modeling the dense matter inside NS. The signature of the behaviour of matter at the highest densities lies in observations that depend on the core structure of the neutron star: properties like the star's mass, spin, and size. By observing dynamical neutron star behaviour we can also infer neutron star properties like tidal deformability and the resistance to changes in spin (moment of inertia), which depend on the internal structure of a particular neutron star. All these properties can be traced back to one function: the equation of state (EoS) of the neutron star matter, which describes the relationship between pressure and energy density in the neutron star. The mass, radius and interior structure of a particular neutron star are determined by the precise way the pressure of cold dense matter varies with increasing density. Thus, by observing such properties, the EoS gets constrained.

Alternate theories of gravity can also lead to a change in the interior structure of NS due to modification of the Tolman-Oppenheimer-Volkof (TOV) equation. In chapter 3, we study the structure of neutron stars in the Starobinsky model in an exact and nonperturbative approach. In this model, apart from the standard general relativistic junction conditions, two extra conditions – namely, the continuity of the curvature scalar and its first derivative – need to be satisfied. For the exterior Schwarzschild solution, the curvature scalar and its derivative must be zero at the stellar surface. We show that for some EoS of matter, matching all conditions at the surface of the star is impossible. Hence the model brings two major fine-tuning problems: (*i*) only some particular classes of EoS are consistent with Schwarzschild at the surface, and (*ii*) given the EoS, only a very particular set of boundary conditions at the centre of the star will satisfy the given boundary conditions at the surface. Hence we show that this model [and subsequently many other $f(R)$ models (discussed in chapter 2) where the uniqueness theorem is valid] is highly unnatural for the existence of compact astrophysical objects. This is because the EoS of a compact star should be completely determined by the physics of nuclear matter at high density and not the theory of gravity.

1.4 Black hole accretion

Accretion is the term used by astrophysicists to describe the inflow of matter towards a central gravitating object or towards the centre of mass of an extended system. It is a necessary and ubiquitous phenomenon in the universe which occurs naturally when matter becomes gravitationally bound to a source. Accretion occurs in binary systems, at the centres of galaxies harboring massive black holes, in the hearts of dying stars, and when large clouds pass over compact sources and are bound via collisional angular momentum and energy loss. For example, the accretion of gas onto compact stars of mass $\sim$ $M_\odot$, is the likely source of energy in the observed binary X-ray sources. Similarly, it must be noted that the gravitational binding energy of matter accreting onto super massive black holes, with mass $\sim 10^9\,\mathrm{M}_\odot$, is one of the most promising ideas explaining the highly luminous ($\sim 10^{47}$ ergs/s) active galactic nuclei (AGNs) and quasars.

Black holes are amongst the most striking predictions of Einstein's theory of general relativity but, unlike other astrophysical objects, they cannot be observed directly because of their very nature as described earlier. So the only way to discover its presence is through its gravitational interaction with the surrounding matter. One of the most important effects of the black hole is its tendency to accrete, and hence several aspects of the accretion onto the black hole have been actively investigated (see [Chakrabarti 1996] for a review). What is interesting is while the matter falls through the steep gravitational potential of a black hole, roughly 10% of the accreted rest mass energy gets converted into radiation in different energies depending on the mass of the central black hole. For example, the radiation from an accreting stellar mass black hole is normally in X-rays, and is in optical for a supermassive black hole. This is also how we can observe activity from black holes and indirectly demonstrate their existence. In chapter 4, we examine the accretion process onto the black hole with a string cloud background (discussed in chapter 2), where the horizon of the black hole has an enlarged radius due to the string cloud parameter α. The problem of stationary, spherically symmetric accretion of a polytropic fluid is analyzed to obtain an analytic solution for such a perturbation. It is shown that the mass accretion rate, for both the relativistic and the nonrelativistic fluid by a black hole in the string cloud model, increases with increase in α.

1.5 Global properties of spacetime

In general relativity, to understand how spacetime behaves in presence of a given form of matter, we have to solve the Einstein field equations, which in general, are a set of 10 very complicated coupled nonlinear second order partial differential equations that describes the fundamental interaction of gravitation as a result of spacetime being curved by matter and energy. Once we solve this set of field equations we get the metric of the spacetime that describes all the general important physical features of the spacetime, for example the presence of horizons, spacetime singularities, asymptotic behaviour etc.

However finding exact solutions of this complicated system is a field of research in its own right and can only be obtained for spaces of high symmetry and idealized matter content. Nevertheless, they are very important as they embody the full nonlinearity, allowing study of strong field regimes which is very useful to constrain gravitational theories. They also provide backgrounds on which perturbative analysis can be built, and therefore understand the stability of a solution like the final fate of gravitational collapse. They provide solutions for astrophysical structures like neutron stars, and they enable checks for numerical accuracy.

To find exact solutions the basic problems are

- what is the coordinate choice that can make the calculations simpler.
- the complicated systems are difficult to integrate, this is principally true for realistic matter content as for example neutron stars or for vacuum solutions in the context of modified gravity theories where the equations are often fourth order.

Given the above problems, the key question that arises here is as follows:

Is it possible to identify the general physical properties and global nature of a spacetime without actually solving the Einstein field equations?

In this thesis we tried to answer this question in a transparent manner. To bypass the problem of coordinate choice or coordinate singularities etc. we used the local semi-tetrad splitting of spacetime (which is commonly known as the 1+1+2 covariant formalism) to recast the field equations into an autonomous system of covariantly defined variables. In chapter 5, we present the $1+3$ and $1+1+2$ covariant approach and present the full system of decomposed field equations in general relativity for locally rotationally symmetric (LRS) type II spacetime. This approach enables us to get rid of all the coordinate singularities that may appear due to a bad choice of coordinates while solving the field equations. This autonomous system simplifies considerably when we incorporate the Killing symmetries of the spacetimes. Instead of trying to find particular exact solutions of differential equations, we studied the autonomous system which gives qualitative information on important global features of the spacetime. For that, we used all tools available in dynamical systems as critical points and their stability, Poincare sphere, centre manifold and so on.

It is then very easy, via this formalism, to not only obtain the nature of the central singularity of the black hole, to find whether the solution possesses a horizon or not and the asymptotic behaviour of the solution, but also to obtain the singularity-free nature of e.g. the Nariai solution. It provides an efficient way to understand the global properties of any spacetime, by bypassing the very difficult task of solving the field equations. In chapter 6, we discuss this formalism in the realm of GR whereas in chapters 7 and 8, we study $f(R)$ and quintessence models, respectively, where the field equations become more complicated and exact solutions are hard to find even for idealized cases.

In chapter 9 we summarise our results and provide concluding remarks. This is followed by some useful derivation of relations utilised in our work in the appendices A and B.

Chapter 2

Modified theories of gravity

In this thesis, we define 'General Relativity'as a theory that simultaneously exhibits general covariance, and universal couplings to all matter fields, and satisfies Einstein's field equations. A modification of any of these properties will be referred to as 'modified gravity'theories. To be more precise, any deviation from the standard model of cosmology (with matter, radiation and the cosmological constant) falls in the realm of modified theories of gravity. In this chapter, we will introduce three of these "extended theories" – $f(R)$, quintessence and the cosmic string model, which will be used in the following chapters.

2.1 $f(R)$ gravity theories

We start with a class of models in which gravity is modified with respect to general relativity and invoke new degrees of freedom belonging to the gravitational sector. One of the simplest and most popular schemes of these modifications based upon phenomenological considerations is provided by $f(R)$ theories of gravity (for reviews, see [Sotiriou and Faraoni 2010; De Felice and Tsujikawa 2010]). These theories essentially contain an additional scalar degree of freedom apart from the graviton. Indeed, $f(R)$ theories are conformally equivalent to Einstein's theory plus a canonical scalar degree of freedom dubbed the scalaron [Starobinsky 1980] whose potential is uniquely constructed from the Ricci scalar. One of the most interesting aspects of these models of gravity (contrary to models including the Ricci or Riemann tensor in the action) is the absence of the Ostrogradski ghost despite the fact that the equations of motion are of fourth order.

2.1.1 Action and modified field equations

Generalization of the Einstein-Hilbert (EH) action

$$\mathcal{S}_{GR} = \frac{1}{2}\int d^4x\sqrt{-g}R + \mathcal{S}_M(g_{\mu\nu}, \Psi_M)\,, \tag{2.1}$$

results in the 4-dimensional action in $f(R)$ gravity:

$$\mathcal{S}_{f(R)} = \frac{1}{2}\int d^4x\sqrt{-g}f(R) + \mathcal{S}_M(g_{\mu\nu}, \Psi_M)\,, \tag{2.2}$$

where g denotes the determinant of the metric $g_{\mu\nu}$ and R is the Ricci scalar. S_M and Ψ_M are the matter action and matter fields respectively.

Following the metric formalism from the above action, the field equations are derived by the variation of the action with respect to the metric tensor $g_{\mu\nu}$, and we get (for a detailed derivation, see *appendix* A)

$$f_{,R}R_{\mu\nu} - \frac{1}{2}f(R)g_{\mu\nu} - (\nabla_\mu\nabla_\nu - g_{\mu\nu}\Box)f_{,R} = T^{(M)}_{\mu\nu}\,, \tag{2.3}$$

where $f_{,R} = \frac{df(R)}{dR}$ and $T^{(M)}_{\mu\nu} = -\frac{2}{\sqrt{-g}}\frac{\delta S_M}{\delta g^{\mu\nu}}$ is the matter energy momentum tensor (MEMT) of the matter fields. The trace of Eq. (2.3) is

$$3\Box f_{,R} + f_{,R}R - 2f(R) = T^{(M)}\,, \tag{2.4}$$

where $T^{(M)} = g^{\mu\nu}T^{(M)}_{\mu\nu}$ is the trace of the MEMT. It determines the dynamics of the scalar degree of freedom, $\varphi = f_{,R}$.

The field Eq. (2.3) can also be rewritten in the following form

$$G_{\mu\nu} = \frac{T^{(M)}_{\mu\nu}}{f_{,R}} + T^{(R)}_{\mu\nu}\,, \tag{2.5}$$

where $G_{\mu\nu} = R_{\mu\nu} - \frac{1}{2}g_{\mu\nu}R$ is the Einstein tensor and

$$T^{(R)}_{\mu\nu} = \frac{1}{f_{,R}}\left(\frac{1}{2}g_{\mu\nu}\left(f(R) - Rf_{,R}\right) + (\nabla_\mu\nabla_\nu - g_{\mu\nu}\Box)f_{,R}\right)\,, \tag{2.6}$$

is the curvature energy momentum tensor (CEMT). It corresponds to a modification of the energy momentum tensor (matter and curvature) in Einstein equations.

From the conservation law, we have $\nabla^\mu G_{\mu\nu} = 0$ and $\nabla^\mu T^{(M)}_{\mu\nu} = 0$, which leads to

$$\begin{aligned} &\nabla^\mu \left((1 - f_{,R})G_{\mu\nu} + f_{,R}T^{(R)}_{\mu\nu}\right) = 0\,, \\ \text{or} \quad &\nabla^\mu \left(R_{\mu\nu}(1 - f_{,R}) + \frac{1}{2}g_{\mu\nu}(f(R) - R) + (\nabla_\mu\nabla_\nu - g_{\mu\nu}\Box)f_{,R}\right) = 0\,. \end{aligned} \tag{2.7}$$

2.1.2 Conformal frame

The action, Eq. (2.2), is defined in the Jordan frame where the scalaron is non-minimally coupled to the metric. To derive an action linear in R in the Einstein frame where the scalar field is minimally coupled, we make a conformal transformation of the form [Dicke 1962; Wald 1984; K.-I. Maeda 1989; Wands 1994; Magnano and Sokolowski 1994; Faraoni et al. 1999; Fujii and K.-I. Maeda 2003]

$$\tilde{g}_{\mu\nu} = \Omega^2\, g_{\mu\nu}\,, \tag{2.8}$$

where Ω^2 is a smooth, nonvanishing function of the spacetime called the conformal factor and "$\tilde{\ }$" represent quantities in the Einstein frame. Now, the action (2.2) can be rewritten as

$$\mathcal{S} = \int d^4x\sqrt{-g}\left(\frac{1}{2}f_{,R}R - U\right) + \mathcal{S}_M(g_{\mu\nu}, \Psi_M)\,, \tag{2.9}$$

which can be compared to the action in Brans-Dicke (BD) theory [Brans and Dicke 1961]

$$\mathcal{S}_{BD} = \int d^4x\sqrt{-g}\left(\frac{1}{2}\varphi R - \frac{\omega_{BD}}{2\varphi}(\nabla\varphi)^2 - U(\varphi)\right) + \mathcal{S}_M(g_{\mu\nu}, \Psi_M)\,, \tag{2.10}$$

where φ is the scalaron and ω_{BD} is the BD parameter. Hence the metric formalism of the $f(R)$ theory is equivalent to BD theory when $\omega_{BD} = 0$.

Action (2.9), under conformal transformation, becomes (transformation of these quantities under conformal transformation is shown in *appendix* B),

$$\mathcal{S} = \int d^4x\sqrt{-\tilde{g}}\left(\frac{1}{2}f_{,R}\,\Omega^{-2}\left(\tilde{R} + 6\tilde{\Box}\ln\Omega - 6(\tilde{\nabla}\ln\Omega)^2\right) - \Omega^{-4}U\right) + \mathcal{S}_M(\Omega^{-2}\,\tilde{g}_{\mu\nu}, \Psi_M)\,, \tag{2.11}$$

where

$$U = \frac{f_{,R}R - f(R)}{2}\,. \tag{2.12}$$

The non-minimal coupling to the Ricci scalar can now be removed by making the choice $\Omega^2 = f_{,R}$. Defining a new scalar field $\psi \equiv \sqrt{3/2}\,\ln f_{,R}$, we have $\ln\Omega = \psi/\sqrt{6}$. Hence, the action in the Einstein frame turns out to be

$$\mathcal{S}_E = \int d^4x\sqrt{-\tilde{g}}\left(\frac{1}{2}\tilde{R} - \frac{1}{2}(\tilde{\nabla}\psi)^2 - V(\psi)\right) + \mathcal{S}_M(e^{-\sqrt{\frac{2}{3}}\,\psi}\,\tilde{g}_{\mu\nu}, \Psi_M)\,, \tag{2.13}$$

where

$$V(\psi) = \frac{U}{(f_{,R})^2} = \frac{f_{,R}R - f(R)}{2(f_{,R})^2}\,. \tag{2.14}$$

The equations of motion (EoM) in the Einstein's frame are given by (for a detailed derivation, see *appendix* A)

$$\tilde{G}_{\mu\nu} = \tilde{T}^{(M)}_{\mu\nu} + \tilde{T}^{(\psi)}_{\mu\nu} \qquad \text{(Modified Einstein Equation)}\,, \tag{2.15a}$$

$$\tilde{\Box}\psi = V_{,\psi} - \frac{1}{\sqrt{6}}\tilde{T}^{(M)} \qquad \text{(Klein} - \text{Gordon Equation)}\,, \tag{2.15b}$$

where $V_{,\psi} \equiv \mathrm{d}V/\mathrm{d}\psi$ and

$$\tilde{T}^{(\psi)}_{\mu\nu} = \psi_{,\mu}\psi_{,\nu} - \tilde{g}_{\mu\nu}\left(\frac{1}{2}(\tilde{\nabla}\psi)^2 + V(\psi)\right)\,, \tag{2.16}$$

is the scalar field energy momentum tensor (SFEMT).

2.2 Quintessence

In order to modify the theory of gravity, various paths might be used. For clarity, Lovelock's theorem is particularly useful to define an extension of the theory of GR. The theorem says that

In 4D the only action constructed solely from the metric $g_{\mu\nu}$ preserving the diffeomorphism and which have field equations involving derivatives of the metric tensor only up to second order is Einstein-Hilbert action.

Therefore following these assumptions, GR emerges as an unique theory. But any violation of these axioms gives rise to a different class of modified theories of gravity. Even if the number of models is infinite, we might find clarity. In fact, in this very rich zoo of models, we can find a fundamental common idea:

- In higher dimensional theories, the models have more than 2 degrees of freedom. For example, the Dvali-Gabadadze-Porrati (DGP) model has 5 degrees of freedom which can be split into a massless graviton, a massless vector field and a scalar field. But the main interesting parts of the model are contained in the additional scalar field (along with the massless graviton). In fact, integrating out the additional dimension [Luty et al. 2003] gives rise to an effective theory describing the brane bending mode, known as galileon theory [Nicolis et al. 2009]. Higher dimensional models often contain scalar fields which can be very relevant in cosmology. In fact, more generically many theories of high energy physics, such as string theory and supergravity, predict light gravitationally coupled scalar fields [Binetruy 2006; Linde 2008].

- In higher derivative theories such as $f(R)$ in the metric formalism, we have also an additional degree of freedom, the scalaron which appears explicitly in the Einstein frame of the theory as we have seen.
- Obviously additional extra fields might be scalar fields such as the Horndeski model [Horndeski 1974] or beyond Horndeski [Gleyzes et al. 2015].
- In the case we break the diffeomorphism invariance such as de Rham-Gabadadze-Tolley (dRGT) model [deRham et al. 2011] we have additional degrees of freedom. And as in extra dimensions, the very interesting aspects of the model are encoded in the scalar degree of freedom which become transparent in the so-called decoupling limit [deRham 2014].

Therefore we see that even if the models appear very different, they can be unified in a single structure. They all have in common an additional degree of freedom, a scalar field, which encodes various interesting aspects of the model. Even if the scalar tensor theories are not the most general models, they possess various properties of the underlying theory and they have many interesting features to study such as screening mechanisms (see e.g. [Tolley 2009]), spontaneous scalarization [Damour and Esposito-Farese 1993], superradiance [Press and Teukolsky 1972], etc.

We see therefore how important, models with a scalar field are, because they encode most of the phenomenology of modified gravity theories but also because they are viable models such as in inflation and interesting alternative models such as for dark energy. In this section, we introduce the simplest of this class of models, quintessence, but which remains the best model to describe the early Universe, the inflation and often used as a toy model to describe and study the interaction of matter with compact objects.

We refer to scalar field models with canonical kinetic energy and minimally coupled to gravity as “quintessence models” (for a review, see [Martin 2008; Tsujikawa 2013]). Scalar fields with a slowly varying potential are obvious candidates for inflation as well as for dark energy (DE) for the following reasons:

- simplest fields as they lack internal degrees of freedom,
- do not introduce preferred directions,
- typically weakly clustered,
- can easily drive an accelerated expansion.

Due to its many advantages, quintessence models are the protoypical DE models [Caldwell, Dave, et al. 1998] and the most studied ones [Amendola and Tsujikawa 2010]. If the kinetic energy has a canonical form, the only degree of freedom is then provided by the field potential (and of course by the initial conditions).

The quintessence model is described by the action

$$S = \int \mathrm{d}^4x\sqrt{-g}\,\left[\frac{1}{2}R + \frac{1}{2}g^{\mu\nu}\partial_\mu\psi\partial_\nu\psi - V(\psi)\right] + S_M\,, \tag{2.17}$$

which is similar to the action (2.13). *Hence $f(R)$ theories in Einstein frame is equivalent to quintessence model.*

In a Friedmann-Lemaître-Robertson-Walker (FLRW) metric background, given by the metric

$$ds^2 = -dt^2 + a(t)^2\left(\frac{dr^2}{1-kr^2} + r^2d\theta^2 + r^2\sin^2\theta d\varphi^2\right)\,, \tag{2.18}$$

where $a(t)$ is the scale factor and k the spatial curvature, the energy density ρ_ψ and the pressure p_ψ of the scalar field can be obtained from (2.16)

$$\rho_\psi = -{T^0}_0^{(\psi)} = \frac{1}{2}\dot{\psi}^2 + V(\psi)\,,\quad p_\psi = \frac{1}{3}T_i^{i(\psi)} = \frac{1}{2}\dot{\psi}^2 - V(\psi)\,, \tag{2.19}$$

which give the equation of state

$$w_\psi \equiv \frac{p_\psi}{\rho_\psi} = \frac{\dot{\psi}^2 - 2V(\psi)}{\dot{\psi}^2 + 2V(\psi)}\,. \tag{2.20}$$

In the flat universe, using Eqs. (2.15), we get the following equations of motion

$$H^2 = \frac{1}{3}\left[\frac{1}{2}\dot{\psi}^2 + V(\psi) + \rho_M\right]\,, \tag{2.21}$$

$$\dot{H} = -\frac{1}{2}\left[\dot{\psi}^2 + \rho_M + p_M\right]\,, \tag{2.22}$$

$$\ddot{\psi} + 3H\dot{\psi} + V_{,\psi} = 0\,, \tag{2.23}$$

where $H = \dot{a}/a$ is the Hubble function.

During radiation or matter dominated epochs, the energy density ρ_M of the fluid dominates over that of quintessence, i.e. $\rho_M \gg \rho_\psi$. If the potential is steep so that the condition $\dot{\psi}^2/2 \gg V(\psi)$ is always satisfied, the field equation of state is given by $w_\psi \simeq 1$ from Eq. (2.20). In this case the energy density of the field evolves as $\rho_\psi \propto a^{-6}$, which decreases much faster than the background fluid density.

The condition $w_\psi < -1/3$ is required to realize the late time cosmic acceleration, which translates into the condition $\dot{\psi}^2 < V(\psi)$. Hence the scalar potential needs to be shallow enough for the field to evolve slowly along the potential. This situation is similar to that in inflationary cosmology and it is convenient to introduce the following slow-roll parameters [Bassett et al. 2006]

$$\epsilon_s \equiv \frac{1}{2\kappa^2}\left(\frac{V_{,\psi}}{V}\right)^2 , \qquad \eta_s \equiv \frac{V_{,\psi\psi}}{\kappa^2 V} . \tag{2.24}$$

If the conditions $\epsilon_s \ll 1$ and $|\eta_s| \ll 1$ are satisfied, the evolution of the field is sufficiently slow so that $\dot{\psi}^2 \ll V(\psi)$ and $|\ddot{\psi}| \ll |3H\dot{\psi}|$ in Eqs. (2.21) and (2.23).

It is of interest to derive a scalar field potential that gives rise to a power-law expansion

$$a(t) \propto t^p \tag{2.25}$$

An accelerated expansion occurs for $p > 1$. It is also easy to see that the potential giving the power-law expansion corresponds to

$$V(\psi) = V_0 \exp\Big(-\sqrt{\frac{2}{p}}\psi\Big) , \tag{2.26}$$

where V_0 is a constant. The field evolves as $\psi \propto \ln(t)$. The above result shows that the exponential potential may be used for dark energy provided that $p > 1$. Exponential potentials were used in one of the earliest models which could accommodate a period of acceleration today within it, the loitering universe [Sahni, Feldman, et al. 1992]. Therefore such models should be also studied in the context of black holes.

Various other models have been studied in the literature. In fact, depending on the evolution of w_ψ, we can broadly classify quintessence models into two classes [Caldwell and Linder 2005], (i) thawing models and (ii) freezing models.

2.2.1 Thawing models

In this case, the field (with mass m_ψ) is nearly frozen by a Hubble friction (i.e. the term $H\dot{\psi}$ in eq.(2.23)) during the early cosmological epoch and it begins to evolve once H drops below

m_ψ. The equation of state of DE is $w_\psi \simeq -1$ at early times, which is followed by the growth of w_ψ. The representative potentials that belong to this class are

- $V(\psi) = V_0 + M^{4-n}\psi^n \quad (n > 0)\,,$
- $V(\psi) = M^4 \cos^2(\psi/f)\,.$

The former potential is similar to the one of chaotic inflation ($n = 2, 4$) used in the early universe (with $V_0 = 0$) [Linde 1983], while the mass scale M is very different. The model with $n = 1$ was proposed by [Kallosh et al. 2003] in connection with the possibility to allow for negative values of $V(\psi)$. The universe will collapse in the future if the system enters the region with $V(\psi) < 0$. The latter potential appears as a potential for the Pseudo-Nambu-Goldstone Boson (PNGB). This was introduced by [Frieman et al. 1995] in response to the first tentative suggestions that the universe may be dominated by the cosmological constant. In this model the field is nearly frozen at the potential maximum during the period in which the field mass m_ψ is smaller than H, but it begins to roll down around the present ($m_\psi \simeq H_0$).

2.2.2 Freezing models

In these models, the field was rolling along the potential in the past, but the evolution of the field gradually slows down after the system enters the phase of cosmic acceleration because the potential tends to be shallow at late times. The representative potentials that belong to this class are

- $V(\psi) = M^{4+n}\psi^{-n} \quad (n > 0)\,,$
- $V(\psi) = M^{4+n}\psi^{-n}\exp(\alpha\psi^2/m_{\rm pl}^2)\,.$

The former potential does not possess a minimum and hence the field rolls down the potential toward infinity. This appears, for example, in the fermion condensate model as a dynamical supersymmetry breaking [Binetruy 1999]. There is also a so-called tracker solution [Steinhardt et al. 1999] for this solution along which w_ψ is nearly constant during the matter era and then starts to decrease after that. The latter potential has a minimum at which the field is eventually trapped (corresponding to $w_\psi = -1$). This potential can be constructed in the framework of supergravity [Brax and Martin 1999].

2.3 Cosmic strings

Cosmic strings are a generic outcome of symmetry breaking phase transitions in the early universe [Kibble 1976], and further motivation comes from a potential role in large scale structure formation [Vilenkin 1981]. Strings may have been present in the early universe, and they play a role in the seeding of density inhomogeneities [Mitchell and Turok 1987]. The magnitude of such strings are determined by the dimensionless parameter

$$\frac{G\mu}{c^2} = \left(\frac{\eta}{m_{Pl}}\right)^2 , \tag{2.27}$$

where η is the energy scale of string and $m_{Pl} = \sqrt{hc/G}$ is the Planck mass. For the Nambu-Goto string model, using the *Planck* data, it has been shown that a constraint on the string tension of $\frac{G\mu}{c^2} < 1.5 \times 10^{-7}$ at 95 percent confidence can be improved to $\frac{G\mu}{c^2} < 1.3 \times 10^{-7}$ on inclusion of high-l CMB data [Ade et al. 2014b].

It may be also pointed out that strings have become a very important ingredient in many physical theories, and the idea of strings is fundamental in superstring theories [Sen 1998]. The apparent relationship between counting string states and the entropy of the black hole horizon [Larsen 1997; Strominger and Vafa 1996] suggests an association of strings with black holes. Furthermore the intense level of activity in string theory has led to the idea that many of the classic vacuum scenarios, such as the static Schwarzschild point black hole, may have atmospheres composed of a fluid or field of strings [Parthasarathy and Viswanathan 1997]. Many authors have found exact black hole solutions with string cloud backgrounds, for instance, in general relativity [Letelier 1979; Mazharimousavi et al. 2010], in Einstein-Gauss-Bonnet models [Herscovich and Richarte 2010], and in Lovelock gravity [Ghosh and Maharaj 2014], thereby generalizing the pioneering work of Letelier [Letelier 1979] who modified the Schwarzschild black hole for the string cloud model. Glass and Krisch [Glass and Krisch 1998; Glass and Krisch 1999a; Glass and Krisch 1999b] pointed out that allowing the Schwarzschild mass parameter to be a function of radial position creates an atmosphere with a string fluid stress-energy tensor around a static, spherically symmetric object. Here, we briefly review the theory of a cloud of strings (see [Letelier 1979] for further details) and the corresponding modified Schwarzschild black hole.

The Nambu-Goto action of a string evolving in spacetime is given by

$$I_{\mathcal{S}} = \int_{\Sigma} \mathcal{L}\, d\lambda^0 d\lambda^1, \quad \mathcal{L} = m(\Gamma)^{-1/2} , \tag{2.28}$$

where m is a positive constant that characterizes each string, (λ^0, λ^1) is a parametrization of the world sheet Σ with λ^0 and λ^1 being timelike and spacelike parameters [Synge 1960], and

Γ is the determinant of the induced metric on the string world sheet Σ given by

$$\Gamma_{\rho\sigma} = g_{\mu\nu} \frac{\partial x^\mu}{\partial \lambda^\rho} \frac{\partial x^\nu}{\partial \lambda^\sigma}\,, \tag{2.29}$$

and $\Gamma = \det \Gamma_{\rho\sigma}$. Associated with the string worldsheet we have the bivector of the form

$$\Sigma^{\mu\nu} = \epsilon^{\rho\sigma} \frac{\partial x^\mu}{\partial \lambda^\rho} \frac{\partial x^\nu}{\partial \lambda^\sigma}\,, \tag{2.30}$$

where $\epsilon^{\rho\sigma}$ denotes the two-dimensional Levi-Civita tensor given by $\epsilon^{01} = -\epsilon^{10} = 1$. Within this setup, the Lagrangian density becomes

$$\mathcal{L} = m \left[-\frac{1}{2} \Sigma^{\mu\nu} \Sigma_{\mu\nu} \right]^{1/2}\,. \tag{2.31}$$

Further, since $T^{\mu\nu} = 2\partial\mathcal{L}/\partial g^{\mu\nu}$, we obtain the energy momentum tensor for one string as

$$T^{\mu\nu} = m \Sigma^{\mu\rho} \Sigma_\rho{}^\nu / (-\Gamma)^{1/2}\,. \tag{2.32}$$

Hence, the energy momentum tensor for a cloud of string is

$$T^{\mu\nu} = \rho \Sigma^{\mu\sigma} \Sigma_\sigma{}^\nu / (-\Gamma)^{1/2}\,, \tag{2.33}$$

where ρ is the proper density of a string cloud. The quantity $\rho\,(\Gamma)^{-1/2}$ is the gauge invariant quantity called the gauge-invariant density.

The general solution of Einstein's equations for a string cloud in 4-dimensions takes the form [Letelier 1979]

$$\begin{aligned} ds^2 = &-\left(1 - \frac{2M}{r} - \alpha\right) dt^2 + \left(1 - \frac{2M}{r} - \alpha\right)^{-1} dr^2 \\ &+ r^2 (d\theta^2 + \sin^2\theta d\psi^2)\,. \end{aligned} \tag{2.34}$$

Here M arises as an integration constant which is identified as the black hole mass and is not a function of α. The event horizon for the metric (2.34) has radius

$$r_H = \frac{2M}{1-\alpha}, \qquad \alpha \neq 1\,. \tag{2.35}$$

In the limit $\alpha \to 0$, we recover the Schwarzschild radius, and close to unity the event horizon radius tends to infinity. In general the string cloud parameter $\alpha \neq 1$. We note that the case of static spherical symmetry restricts the value of the gauge-invariant density to $\rho(-\Gamma)^{1/2} = \alpha/r^2$ [Letelier 1979], and thereby α is a positive constant. However, for the realistic model under consideration here the string cloud parameter is restricted to $0 < \alpha < 1$. On the other hand, the cloud of strings alone ($M = 0$) does not have a horizon; it generates only a conical singularity at $r = 0$. This solution was first obtained by Letelier [Letelier 1979] and the metric represents the black hole spacetime associated with a spherical mass M centred at the origin of the system of coordinates, surrounded by a spherical cloud of strings. Furthermore it can be interpreted as the metric associated with a global monopole. In the string cloud background, the Schwarzschild radius of the black hole is displaced by the factor $(1 - \alpha)^{-1}$.

Chapter 3

Neutron stars in Starobinsky model

We mentioned in chapter 1 that uncertainty in modeling the equation of state makes the study of the interior of neutron star complicated. In this chapter we show that verifying and constraining the EoS of matter at high density with the aid of modified gravity theories, come at a much later stage, if at all. The challenge we face here is to find a proper matching of the exterior solution with the interior. A few attempts to apply modified gravity models to neutron stars were carried out in the recent past (see e.g. [Kainulainen et al. 2007; Babichev and Langlois 2009; Cooney et al. 2010; Babichev and Langlois 2010; Arapoglu et al. 2011; Orellana et al. 2013; Alavirad and Weller 2013; Astashenok et al. 2013]). But as far as we know, there is no work where the interior solution has been consistently matched with a viable exterior spacetime. As we will see, this will drastically change the conclusions on the viability of the model.

The chapter is organized as follows. We start by giving a brief introduction to the Starobinsky model in Sec. 3.1. After that we very briefly review the basic equations (Tolman-Oppenheimer-Volkoff equation) of the model in Sec. 3.2, followed by the junction conditions at the surface of the star in Sec. 3.3. In Sec. 3.4 we explain why the Schwarzschild solution should be the exterior solution. In Sec. 3.5 we give the laboratory, solar system and cosmological constraints on the parameter α of the model. Sec. 3.6 is devoted to the singular problem of the system with the existence of boundary layers at the surface. In Secs. 3.7 and 3.8, we perform a numerical analysis to confirm the fine-tuned nature of the problem and hence the difficulty of matching all of the boundary conditions. Then, in Sec. 3.9 we propose a semi-analytical approach to solve the problem. The penultimate section 3.10 is devoted to other possible solutions to avoid the fine-tuning problems and we finally end with conclusions in Sec. 3.11. This chapter is based on published work [Ganguly et al. 2014].

3.1 Introduction

As discussed in chapter 1, there are various models where the authors [Ginzburg et al. 1971; Bunch and Davies 1977; Davies 1977] considered Einstein equations with quantum corrections. Following these ideas, Starobinsky studied the cosmology of one of these models [Starobinsky 1980], which was later simplified and is popularly known today as the Starobinsky model, where the action of GR is replaced by $f(R) = R + \alpha R^2$. It was the first internally consistent inflationary model. In this model, the R^2 term produces an accelerated stage in the early Universe preceding the usual radiation and matter stages. Inflation ends when the term αR^2 becomes smaller than the linear term R. Since the term αR^2 is negligibly small relative to R at the present epoch, this model is not suitable to realise the present cosmic acceleration. One should notice that – contrary to the Starobinsky model – generic $f(R)$ models are plagued by various problems; they generally reduce to GR plus cosmological constant [Thongkool et al. 2009], have a ϕMDE (field-matter dominated epoch) instead of a standard matter epoch [Amendola, Gannouji, et al. 2007], hit a curvature singularity [Frolov 2008] (see Ref. [Kobayashi and K.-I. Maeda 2008] for the existence of a singularity in an asymptotic de Sitter universe and Ref. [Upadhye and Hu 2009] for the opposite statement), produce high frequency oscillations and a singularity at finite time in cosmology [Appleby and Battye 2008] or give rise to a fine-tuning [Faraoni 2011].

The recent results from the *Planck* satellite [Ade et al. 2014a] are remarkably compatible with the Starobinsky model. Hence the model remains one of the candidates for gravity at high energies in the early epoch of the Universe and avoids the difficulties listed previously.

3.2 Action and modified TOV equations

The straightforward generalization of the Lagrangian in the Einstein-Hilbert action results in a four-dimensional action in $f(R)$ gravity as given in Eq. (2.2). Following the metric formalism from the above action, the field equations are derived by the variation of the action with respect to the metric tensor $g_{\mu\nu}$, as given in Eq. (2.3) and the trace given in Eq. (2.4).

Substituting $f(R) = R + \alpha R^2$, we get

$$G_{\mu\nu}(1 + 2\alpha R) + \frac{\alpha}{2} g_{\mu\nu} R^2 - 2\alpha(\nabla_\mu \nabla_\nu - g_{\mu\nu}\Box)R = T_{\mu\nu}\,, \tag{3.1}$$

$$6\alpha\Box R - R = T\,, \tag{3.2}$$

where $G_{\mu\nu} = R_{\mu\nu} - \frac{1}{2} g_{\mu\nu} R$ is the Einstein tensor.

As we are interested in spherically symmetric solutions of these field equations inside a neutron star, we choose a spherically symmetric metric of the form

$$ds^2 = -e^{2\Phi(r)}dt^2 + \left(1 - \frac{2m(r)}{r}\right)^{-1} dr^2 + r^2 d\Omega^2 \,. \tag{3.3}$$

Using this metric, the (0,0) and (1,1) components, and the trace of Einstein's equations are

$$\frac{2(1+2\alpha R)}{r^2}m' - 2\alpha\left(1 - \frac{2m}{r}\right)R'' + 2\alpha\left(\frac{m'}{r} + \frac{3m}{r^2} - \frac{2}{r}\right)R' - \frac{1}{2}\alpha R^2 = 8\pi\rho\,, \tag{3.4a}$$

$$\frac{2(1+2\alpha R)}{r^2}\left[\left(1 - \frac{2m}{r}\right)r\Phi' - \frac{m}{r}\right] + 2\alpha\left(1 - \frac{2m}{r}\right)\left(\Phi' + \frac{2}{r}\right)R' + \frac{1}{2}\alpha R^2 = 8\pi P\,, \tag{3.4b}$$

$$-R + 6\alpha\left[\left(1 - \frac{2m}{r}\right)R'' + \left(\left(1 - \frac{2m}{r}\right)\Phi' + \frac{2}{r} - \frac{3m}{r^2} - \frac{m'}{r}\right)R'\right] = 8\pi(-\rho + 3P)\,. \tag{3.4c}$$

The conservation equation $\nabla_\mu T^\mu_1 = 0$ gives

$$P' = -(\rho + P)\Phi'\,. \tag{3.5}$$

From the system of equations (3.4) and Eq. (3.5), we obtain

$$\begin{aligned} m' = \frac{1}{12(1+2\alpha R)(1+2\alpha R+\alpha r R')} \big[& r^2(1+2\alpha R)(48\pi P + R(2+3\alpha R) + 32\pi\rho) \\ &+ 2\alpha(-6m(1+2\alpha R) + r^3(R + 3\alpha R^2 + 16\pi\rho))R' + 24\alpha^2 r(r-2m)R'^2\big]\,, \end{aligned} \tag{3.6}$$

$$P' = -\frac{(P+\rho)(4m + 16\pi r^3 P + 8\alpha m R - \alpha r^3 R^2 - 8\alpha r(r-2m)R')}{4r(r-2m)(1+2\alpha R+\alpha r R')}\,, \tag{3.7}$$

$$\begin{aligned} R'' = \frac{1}{6\alpha r(r-2m)(1+2\alpha R)} \big[& r^2(1+2\alpha R)(24\pi P + R - 8\pi\rho) + \alpha(12m(1+2\alpha R) \\ &+ r(-12 + R(r^2 - 24\alpha + 3\alpha r^2 R) + 16\pi r^2\rho))R' + 12\alpha^2 r(r-2m)R'^2\big]\,, \end{aligned} \tag{3.8}$$

where a prime denotes a derivative with respect to the radial distance r. Finally, an EoS $P = P(\rho)$ closes the set of equations (3.6)–(3.8).

3.3 Junction conditions

In what follows we will be matching the interior of the star to a well defined exterior geometry in order to construct a realistic neutron star model. This requires a set of junction conditions, analogous to the Israel junction conditions from general relativity [Israel 1966]; this problem has been considered in $f(R)$ theories of gravity by Deruelle, Sasaki, and Sendouda [Deruelle et al. 2008], and later by other authors [Clifton, Dunsby, et al. 2013; Senovilla 2013]. We will briefly recap the relevant results from their work here, as it is of central importance to our study.

The prime requirement from Ref. [Deruelle et al. 2008] is that if we allow delta functions on the matter part of the field equations (i.e., if we allow matter fields to be localized on the boundary hypersurface), then delta functions should occur at most linearly in the parts of the field equations that involve geometry only. Here we are interested in the case in which there is no brane located at the boundary. We therefore require that there should be *no* delta function in the part of the field equations containing just the geometry. Therefore, in $f(R)$ gravity theories, apart from the usual GR junction conditions, i.e., the agreement of the first and second fundamental forms on both sides of the matching timelike hypersurface,

$$[h_{\mu\nu}] = 0, \qquad [K_{\mu\nu}] = 0\,, \tag{3.9}$$

(where $h_{\mu\nu}$ and $K_{\mu\nu}$ are the first and second fundamental forms, respectively, and [ ] denotes the jump across the surface), two more conditions need to be satisfied. These are the continuity of the scalar curvature and its first derivative across the boundary,

$$[R] = 0, \qquad [\nabla_\mu R] = 0. \tag{3.10}$$

These extra conditions make the problem of matching the stellar interior with a suitable exterior spacetime extremely restrictive. In fact, most of the compact star models discussed so far in higher order theories of gravity do not rigorously take these restrictions into account [Kainulainen et al. 2007; Babichev and Langlois 2009; Cooney et al. 2010; Babichev and Langlois 2010; Arapoglu et al. 2011; Orellana et al. 2013; Alavirad and Weller 2013; Astashenok et al. 2013].

3.4 Exterior spacetime: Why Schwarzschild?

We know that in general relativity the Jebsen-Birkhoff theorem states that the Schwarzschild solution is the unique spherically symmetric solution of the vacuum Einstein field equations.

In that case a spherically symmetric gravitational field in empty space outside a spherical star must be static, with the metric given by the Schwarzschild metric (for $r > 2M$)

$$ds^2 = -\left(1 - \frac{2M}{r}\right) dt^2 + \frac{dr^2}{\left(1 - \frac{2M}{r}\right)} + r^2 d\Omega^2 \ . \tag{3.11}$$

It represents the spacetime of the solar system (and all other spherically symmetric stellar systems) to a very good approximation, and hence forms the key geometry in much of astrophysics and astronomy.

For higher order gravity theories, the Jebsen-Birkhoff theorem in its original form is violated. As we can easily see, in $f(R)$ theories the trace equation in vacuum is a massive Klein-Gordon equation, which has different classes of nontrivial exact vacuum solutions that can be both static and non-static (see, for example, [Clifton 2006]). Hence, in principle, there exists a larger freedom for the exterior spacetime outside a static star. However, since we are interested in modelling realistic astrophysical compact objects, we will require the exterior spacetime to be static and asymptotically flat, as dictated by observational tests within the solar system. Furthermore, whatever exterior static solution we use for a compact star, it should also describe a well defined black hole solution, as astrophysical black holes are formed via gravitational collapse from these compact objects. Given the above constraints, there are two possible ways to construct a suitable exact exterior for astrophysical compact stars:

1. **Matching the interior with an exact asymptotically flat static solution**. Though very few exact static vacuum solutions are known for the Starobinsky model of $R + \alpha R^2$ gravity, there exists the following uniqueness theorem [Whitt 1984; Mignemi and Wiltshire 1992]: for all functions $f(R)$ which are of class C^3 at $R = 0$ and $f(0) = 0$ while $f'(0) \neq 0$, the only static spherically symmetric asymptotically flat solution with a regular horizon in these models is the Schwarzschild solution, provided that the coefficient of the R^2 term in the Lagrangian polynomial is positive. Since we require $\alpha > 0$ to avoid ghosts in the theory and also require the solution to describe a well defined black hole with a regular horizon, the Schwarzschild solution is the only possible exact asymptotically flat exterior. This is a very well known result that follows the famous BH no-scalar-hair theorems. It states that stationary BH solutions are the same as those in general relativity, namely, the Schwarzschild solution for the non-rotating case. It was proved by Bekenstein [Bekenstein 1995] and Sudarsky [Sudarsky 1995] for a quintessence field with a convex potential, which corresponds to the Starobinsky model in the Einstein frame. Also, an extension was established without assuming any symmetries apart from stationarity in Ref. [Sotiriou and Faraoni 2012]. Obviously if we relax the condition of asymptotic flatness and allow for an asymptotically de Sitter spacetime, we might have other solutions, e.g., by adding a cosmological constant to the model. But the BH

no-scalar-hair theorem was extended to this case in Ref. [Torii et al. 1999]. Therefore, a static BH that is either asymptotically flat or de Sitter is no different than one in general relativity. Finally, we might consider a non-static solution; so far, all the approximate solutions derived in the literature have developed high time oscillating modes because of the presence of the scalaron and should be discarded (see, e.g., Ref. [Starobinsky 2007] in the cosmological case).

2. **Matching the interior to an intermediate static vacuum solution that can be matched to Schwarzschild at a larger distance**. Let us consider an intermediate non-Schwarzschild static exterior matched with the stellar boundary $r = r_s$, which is then matched to Schwarzschild at $r = r_2$, where $r_2 > r_s$. On a superficial level this construction seems to have more freedom as the intermediate static solution need not be asymptotically flat. However, keeping in mind the physicality conditions, we would like this intermediate region to be completely smooth (C^∞). Now from the matching conditions we can immediately see that the Ricci scalar R and its normal derivative R' should vanish at the outer boundary $r = r_2$ of this intermediate solution, where we are matching with the Schwarzschild spacetime. Using the trace equation (3.8), we get $R''(r_2) = 0$ and then the smoothness implies that all the subsequent derivatives of the Ricci scalar must vanish at this boundary. Therefore there exists an open neighbourhood $\mathcal{U} \ni r_2$ where $R = 0$. By continuity, we can then extend this open neighbourhood to the entire exterior asymptotically flat submanifold. Therefore the Ricci scalar vanishes at every point on the exterior submanifold. Using the extension of the Jebsen-Birkhoff theorem to $f(R)$ gravity [Nzioki, Carloni, et al. 2010] which states that for all functions $f(R)$ which are of class C^3 at $R = 0$ and $f(0) = 0$ while $f'(0) \neq 0$, the Schwarzschild solution is the only vacuum spherically symmetric solution with a vanishing Ricci scalar – we can immediately show that this intermediate region has to be Schwarzschild. We also note that this proof remains true even if we consider more than one intermediate region between the stellar boundary and Schwarzschild.

It therefore seems natural to match the spherically symmetric static star with a Schwarzschild exterior. However, the crucial difference with general relativity comes from the fact that for this case the matching surface, the Ricci scalar, and its normal derivative must vanish. This makes the interior solution much more restrictive than GR.

3.5 Constraints on the model

In this section, we derive the various constraints on the parameter α. Let us first consider the experimental bound that comes from the solar system tests of the equivalence principle, lunar laser ranging (LLR). For any chameleon theory with a scalar field ϕ we can define a thin shell parameter ϵ [Khoury and Weltman 2004], which for the Earth is

$$\epsilon \equiv \sqrt{6}\frac{\phi_\infty - \phi_\oplus}{M_{pl}\Phi_\oplus} < 2.2 \times 10^{-6}\,, \tag{3.12}$$

where $(\phi_\infty, \phi_\oplus)$ are, respectively, the minimum of the effective potential at infinity and inside the planet, and $\Phi_\oplus$ is the Newton potential for the Earth. Notice that the constraint on the post-Newtonian parameter γ gives $\epsilon < 2.3 \times 10^{-5}$. Using the value $\Phi_\oplus \simeq 7 \times 10^{-10}$, the previous bound translates into $\phi_\infty/M_{pl} < 10^{-15}$.

We know that any $f(R)$ theory can be written in a chameleon form after a conformal transformation: the two frames are physically equivalent. Hence the model can be cast in the form of a scalar field in an effective potential. The existence of the chameleon mechanism depends on the form of the effective potential, which in turn depends on the local density and pressure. When the pressure is negligible and density is large, the scalar field may acquire a large mass for a suitably chosen potential, leading to a local suppression of the fifth force. The scalar field is assumed to be settled in the minimum of the effective potential. Hence it is easy to find that the minimum of the effective potential can be written in the Jordan frame in the following form

$$2f(R) - Rf'(R) = \frac{\rho - 3P}{M_{pl}^2}\,, \tag{3.13}$$

which corresponds to the trace equation in the constant curvature case. It turns out that the αR^2 term does not change the minimum of the effective potential. Hence the LLR bound leads to [Gannouji et al. 2012]

$$\left| f'\left(\frac{\rho_\infty}{M_{pl}^2}\right) - 1\right| < 10^{-15}. \tag{3.14}$$

For the Starobinsky model and with the density $\rho_\infty \simeq 10^{-24}$ g cm^{-3}, Eq. (3.14) tells us that $\alpha < 10^{-15} M_{pl}^2/\rho_m$ which gives $\alpha < 10^{45}\mathrm{eV}^{-2}$.

But the tightest local constraint comes from the Eöt-Wash experiments, which use torsion balances. We know that a point mass has a Yukawa gravitational potential (see, e.g., Ref. [Stelle 1978]),

$$V(r) = \frac{GM}{r}\left(1 + \frac{1}{3}e^{-r/\sqrt{6\alpha}}\right), \tag{3.15}$$

which gives [Kapner et al. 2007] $\alpha < 4 \times 10^4$ eV^{-2}. Notice that according to the bound from big bang nucleosynthesis and CMB physics, we have $\alpha \ll 10^{35}$ eV^{-2} [Zhang 2007].

We turn now to inflation. According to the latest data set from *Planck*, the Starobinsky model is a viable candidate for the early acceleration phase of the Universe. We have [Starobinsky 2007; Starobinsky 1983] $\alpha \simeq 10^{-45}\big(N/50\big)^2$ eV^{-2} where N is the number of e-folds. Notice that it may not be compatible with the classicality condition of the field [Gannouji et al. 2012; Upadhye, Hu, and Khoury 2012].

Hence we conclude this section by considering $\alpha \simeq 10^{-45}$ eV^{-2} from the cosmological constraints or $\alpha < 4 \times 10^4$ eV^{-2} from the laboratory tests.

3.6 Singular problem

As was noticed in various papers, Eqs. (3.6)-(3.8) are very difficult to solve for realistic cases where α is very small. Also, often in the literature a simple series expansion has been used to carry out these calculations. But, as is known, the solution in powers of the natural small parameter ($\alpha \ll 1$) is invalid if we are considering a boundary layer problem, which is also known as a singular perturbation (see, e.g., Ref. [Nayfeh 1973]). In fact, our equations are among these latter problems because a small parameter α multiplies the highest-order derivative, and we have $\alpha R'' + \cdots$ in Eq. (3.8). We should also mention that it is not *a priori* clear that a nonlinear boundary value problem has a solution.

A singular problem is associated with the approximation of Eq. (3.8) for small values of α. The difficulty near the boundaries arises from the fact that the limit equation with $\alpha = 0$ is algebraic, so that the boundary conditions cannot in general be satisfied. The loss of boundary conditions in a problem usually leads to the occurrence of a boundary layer.

In the case where the equation is linear, a Wentzel-Kramers-Brillouin (WKB) approximation can be performed that introduces transcendentally small terms in the form $\exp(-g(r)/\alpha^n)$, which shows why a simple series expansion $R = \sum_n \alpha^n R_n$ cannot be a correct global approach to the real solution. In fact, we see that in a small region near $g(r) \simeq 0$, the terms of the form $\exp(-g(r)/\alpha^n)$ cannot be neglected, i.e., that small region is called a boundary layer, where the regular expansion fails.

In this section, we consider (m, P, ρ) to be external fields. So, in the limit $\alpha \to 0$, we can write Eq. (3.8) in the form

$$\alpha R'' - 2\alpha^2 R'^2 - \alpha f(r) R R' - \alpha g(r) R' - h(r) R = k(r)\,, \tag{3.16}$$

where (f, g, h, k) are functions of r. There are in fact functions of (m, P, ρ).

We assume that in some subset of $[0, r_s]$, where r_s is the radius of the star, the solution has a regular expansion of the form

$$R(r) = \sum_n \alpha^n R_n(r)\,. \tag{3.17}$$

The substitution in the previous equation gives an algebraic equation at each order,

$$R_0 = -\frac{k(r)}{h(r)}\,, \qquad R_1 = \frac{R_0'' - f(r)R_0R_0' - g(r)R_0'}{h(r)}\,, \cdots \tag{3.18}$$

All the coefficients R_n are determined by the previous coefficients, so we cannot impose the boundary conditions on the regular expansion. Hence the subset where the solution has a regular expansion should not contain the boundary points $r = 0$ and $r = r_s$. This part of the solution is known as the outer expansion.

We note that R_0 corresponds to the solution in GR and by construction (of the EoS) we know that we necessarily have in GR that $R'(0) = 0$, which implies that this condition will also be satisfied for the regular expansion. Therefore the boundary layer exists only near the surface, where the solution will have a fast variation in order to satisfy the conditions $R(r_s) = R'(r_s) = 0$. Notice that it might be seen as a generalization of the well known chameleon mechanism to curved spacetime.

In summary, we have inside the star a solution very close to GR where we can perform a regular expansion of the form (3.17). Near the surface we use the subtraction trick to determine its nature. We define $C = R - \sum_n \alpha^n R_n$, and near $r = r_s$ we introduce the stretching variable $\xi = (r_s - r)\alpha^{-\mu}$, $\mu > 0$, which magnifies the layer. We now assume that there exists a regular expansion for $C(\xi)$, which gives at the lowest order of the expansion near the surface

$$\alpha^{1-2\mu}\frac{d^2C_0}{d\xi^2} - h(r_s)C_0 = 0\,, \tag{3.19}$$

and hence we deduce that $\mu = 1/2$ and $C_0 = Ae^{-\sqrt{h(r_s)}\xi} + Be^{\sqrt{h(r_s)}\xi}$. We can proceed for higher orders by the regular expansion $C = \sum_n \alpha^{n/2}C_n$. This solution is the inner expansion, which should be matched with the outer solution, and hence we fix $B = 0$. Imposing the boundary condition $R(r_s) = 0$, we have

$$R(r) = -\frac{k(r)}{h(r)} + \frac{k(r_s)}{h(r_s)}\; e^{-\sqrt{h(r_s)}(r_s-r)/\sqrt{\alpha}} + O(\sqrt{\alpha})\,. \tag{3.20}$$

We see that it is very difficult to satisfy the second condition $R'(r_s) = 0$; in fact,

$$R'(r_s) = -\frac{k'(r_s)}{h(r_s)} + \frac{k(r_s)h'(r_s)}{h(r_s)^2} + \frac{k(r_s)}{\sqrt{\alpha h(r_s)}}\,. \tag{3.21}$$

The presence of the term $\alpha^{-1/2}$ makes the condition very difficult to satisfy. Notice that if we go to the next order of perturbation, we will have an additional term at the surface for R' in the form $-k(r_s)h'(r_s)/(4h(r_s)^2)$, which does not cancel the term $\propto \alpha^{-1/2}$. Therefore we understand that in order to satisfy both conditions, $R(r_s) = R'(r_s) = 0$, we see from Eq. (3.21) that we need to carefully choose the functions k, h, i.e., the EoS.

We also note from Eq. (3.20) that we have oscillations when $h(r_s) < 0$, which is equivalent to $\alpha < 0$. In fact, from Eq. (3.16) at the linear order, we have

$$\alpha R'' - \alpha g(r) R' - h(r) R = k(r) \,. \tag{3.22}$$

Hence $\{h, k\} \to \{-h, -k\}$ is equivalent to $\alpha \to -\alpha$. Therefore we have an oscillating mode in the ghost case ($\alpha < 0$). We have also noticed numerically that we can kill these oscillations if we reduce the EoS to particular cases where $T(r_s) = T'(r_s) = 0$, where T is the trace of the energy momentum tensor.

3.7 Numerical procedure and results

In this section we will discuss our numerical approach. As a first step, it is convenient to rescale the various quantities involved so as to work directly with dimensionless quantities. We introduce the following rescaled variables:

$$\begin{gathered} r = x\xi_\star, \quad m = \bar{m} M_\odot, \quad P = \bar{P} P_\star, \quad \rho = \bar{\rho}\rho_\star \,, \\ R = \bar{R} R_\star, \quad R' = \bar{R}' \frac{R_\star}{\xi_\star}, \quad R'' = \bar{R}'' \frac{R_\star}{\xi_\star^2}, \quad \alpha = \bar{\alpha}\frac{1}{R_\star} \,, \end{gathered} \tag{3.23}$$

where the barred quantities are dimensionless. Using the above rescaling (3.23), we write the set of equations (3.6)-(3.8) in proper dimensions

$$\bar{m}' = \frac{1}{12c^2GM_\odot(1+2\bar{\alpha}\bar{R})}\Big[\xi_\star^3x^2(48\pi GP_\star\bar{P}+c^4R_\star\bar{R}(2+3\bar{\alpha}\bar{R})+32\pi c^2G\rho_\star\bar{\rho}) \\ +\frac{3\bar{\alpha}\bar{R}'(-4c^2GM_\odot\bar{m}(1+2\bar{\alpha}\bar{R}+4\bar{\alpha}x\bar{R}')+\xi_\star x^2(-16\pi GP_\star\xi_\star^2x\bar{P}+\bar{\alpha}c^4(R_\star\xi_\star^2x\bar{R}^2+8\bar{R}')))}{1+2\bar{\alpha}\bar{R}+\bar{\alpha}x\bar{R}'}\Big], \tag{3.24}$$

$$\bar{P}' = \frac{1}{4c^2P_\star x(c^2\xi_\star x-2GM_\odot\bar{m})(1+2\bar{\alpha}\bar{R}+\bar{\alpha}x\bar{R}')}\big[(P_\star\bar{P}+c^2\rho_\star\bar{\rho})(-4c^2GM_\odot\bar{m}(1+2\bar{\alpha}\bar{R} \\ +4\bar{\alpha}x\bar{R}')+\xi_\star x^2(-16\pi GP_\star\xi_\star^2x\bar{P}+\bar{\alpha}c^4(R_\star\xi_\star^2x\bar{R}^2+8\bar{R}')))\big], \tag{3.25}$$

$$\bar{R}'' = \frac{1}{6\bar{\alpha}c^2x(c^2\xi_\star x-2GM_\odot\bar{m})(1+2\bar{\alpha}\bar{R})}\big[\xi_\star^3x^2(1+2\bar{\alpha}\bar{R})(24\pi GP_\star\bar{P}+c^4R_\star\bar{R}-8\pi c^2G\rho_\star\bar{\rho}) \\ +\bar{\alpha}c^2(12GM_\odot\bar{m}(1+2\bar{\alpha}\bar{R})+c^2\xi_\star x(-12+\bar{R}(-24\bar{\alpha}+R_\star\xi_\star^2x^2\bar{R}))+16\pi G\rho_\star\xi_\star^3x^3\bar{\rho})\bar{R}' \\ +12\bar{\alpha}^2c^2x(c^2\xi_\star x-2GM_\odot\bar{m})\bar{R}'^2\big]. \tag{3.26}$$

Finally, we need to fix the boundary conditions for this system of differential equations. The set of equations (3.24)-(3.26) includes two first order differential equations and one second order differential equation. Thus at least four boundary conditions are required to solve the system completely. In order to obtain physically realistic solutions, these boundary conditions must be chosen from the set of regularity conditions and matching conditions, which are as follows:

1. The regularity conditions at the centre of the star demand that the metric functions and the thermodynamic quantities are at least C^2 functions of the rescaled radial coordinate x. Also, from the form of the interior metric it is clear that the rescaled "mass function" $\bar{m}(x)$ should be zero at the center. Hence at the centre of the star we must have

$$\bar{m}(0)=0\,,\quad \bar{P}'(0)=0\,,\quad \bar{\rho}'(0)=0\,,\quad \bar{R}'(0)=0\,. \tag{3.27}$$

2. As we discussed in Sec. 3.4, the Schwarzschild solution is the natural exterior solution for this gravity model. To match with the Schwarzschild metric, the Ricci scalar and its normal derivative must vanish at the surface. These conditions, along with the matching of the second fundamental form, make the fluid pressure vanish at the surface of the star. Hence we have the following boundary conditions on the matching surface $x=x_s$:

$$\bar{R}(x_s)=0,\qquad \bar{R}'(x_s)=0,\qquad \bar{P}(x_s)=0. \tag{3.28}$$

Any four conditions from the above set of conditions will in principle solve the system of differential equations. However we have to choose the boundary conditions carefully to avoid any "unphysical" solution where the energy condition and/or the regularity conditions are violated at any point in the interior of the star.

3.8 Direct approach

In this section, we directly solve the set of coupled equations (3.24)-(3.26) along with the boundary conditions (3.27) and (3.28). First, we assume the simplest case of constant density star, $\bar{\rho} = 1$. We solve the coupled equations for various values of $\bar{\alpha}$ (see Fig.3.1). We solve the equations by considering random values of $\bar{P}(0)$ and $\bar{R}(0)$. Hence the solution gives a star from which we can read the curvature at the surface Σ $\{\bar{R}_{|\Sigma}, \bar{R}'_{|\Sigma}\}$. We consider $10^{-3} < P(0) < 1/3$. The lower bound corresponds to a realistic choice of the central pressure (in fact, we cannot consider realistic neutron stars with very small central pressure), and the upper bound corresponds to the condition $\rho - 3P > 0$, which is always true for both relativistic and non-relativistic matter. We also notice enlarging the bounds will not affect the results. As we can see from Fig. 3.1, we do not match Schwarzschild at the surface. Hence this equation of state is excluded. It is important to notice that this behaviour is completely different from GR, for which any equation of state is mathematically satisfactory and can only be excluded for physical reasons. It is also important to notice the evolution of the system when $\bar{\alpha}$ decreases; in fact, for smaller $\bar{\alpha}$ the model goes increasingly far from the right boundary conditions at the surface (Schwarzschild). This can be understood from Sec. 3.6. In fact, for smaller values of $\bar{\alpha}$, the system will develop a layer bound and hence the difficulty of having a Schwarzschild solution at the surface increases. Satisfying the two conditions at the surface, namely, $\bar{R} = 0$ and $\bar{R}' = 0$, is impossible for some EoSs. We also perform the same analysis for a more realistic equation of state (polytropic), $\bar{\rho} = k\bar{P}^{5/9}$. We find the same results: we cannot match Schwarzschild at the surface and the star is increasingly far from Schwarzschild at the surface when $\bar{\alpha}$ decreases. Hence we can conclude that the additional junction conditions at the surface of the star provide a constraint on the equation of state inside the compact object. Therefore the equation of state should be fine-tuned.

Also, we find that for the polytropic case we can match with Schwarzschild if $\bar{\alpha} < 0$ (Fig. 3.2), which is obviously excluded because of the ghost condition. But we see that even if an equation of state for $\bar{\alpha} > 0$ is found, we will have to extremely fine-tune the initial conditions $[\bar{P}(0), \bar{R}(0)]$ in order to satisfy the junction conditions. In fact, only a very particular set of initial conditions will match our exterior solution. All other initial conditions will not be correct. Therefore we understand that the model gives rise to two fine-tuning problems: only a class of EoSs can be considered (which might not be consistent with particle physics) and the initial conditions should be extremely fine-tuned in order to match *exactly* the exterior solution.

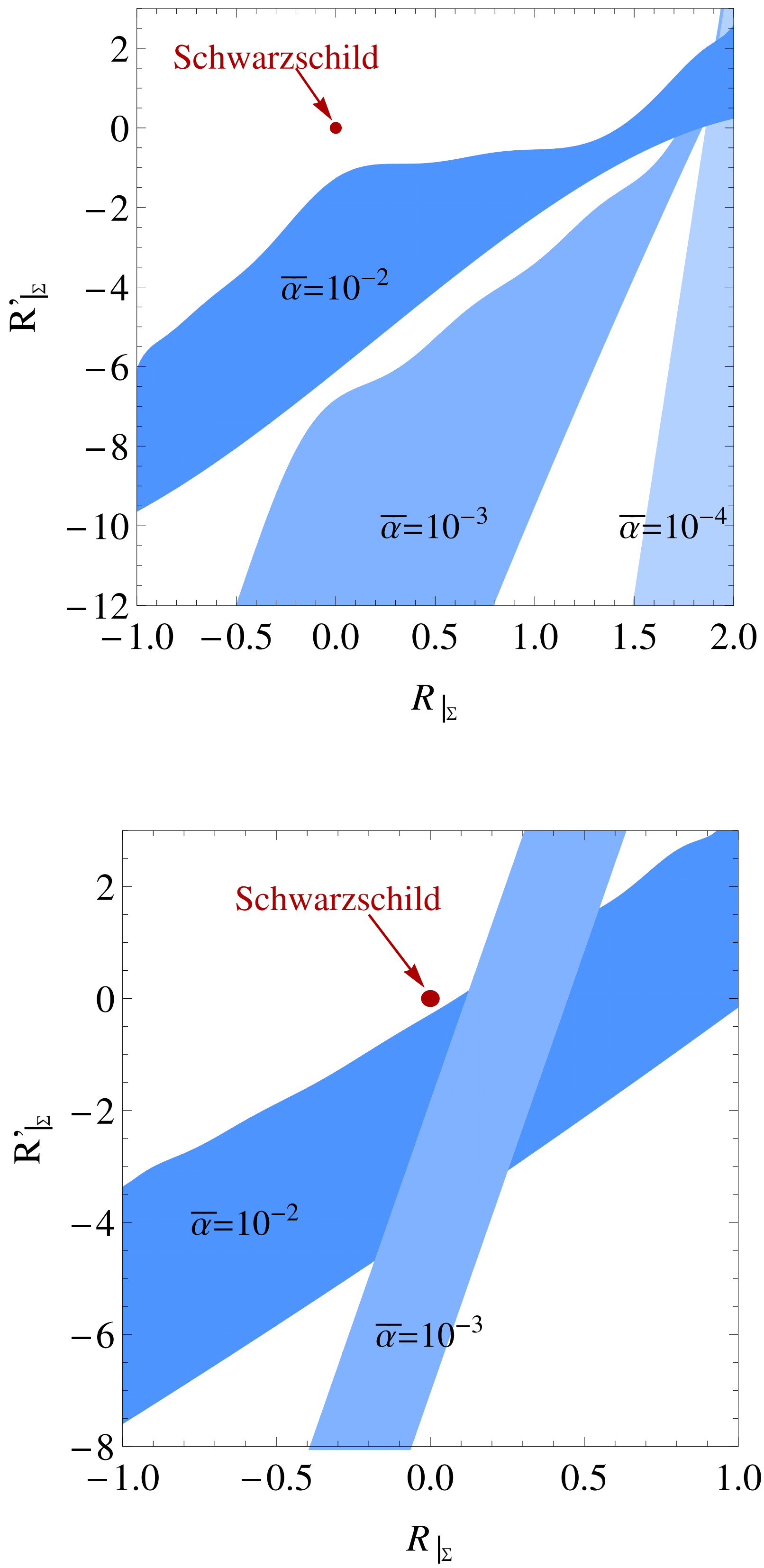

FIGURE 3.1: Top: The contour plot of (R, R') at the surface of the star Σ for $\bar{\rho} = 1$ and we have considered a large range for the initial conditions: $10^{-3} < P(0) < 1/3$ and $R(0) > 0$. Bottom: The contour plot of (R, R') at the surface for the polytropic equation $\bar{\rho} = \bar{P}^{5/9}/0.2$. In both cases, there are no initial condition which match Schwarzschild at the surface. For smaller values of $\bar{\alpha}$ the model goes increasingly far from Schwarzschild in accordance with Eq.(3.21).

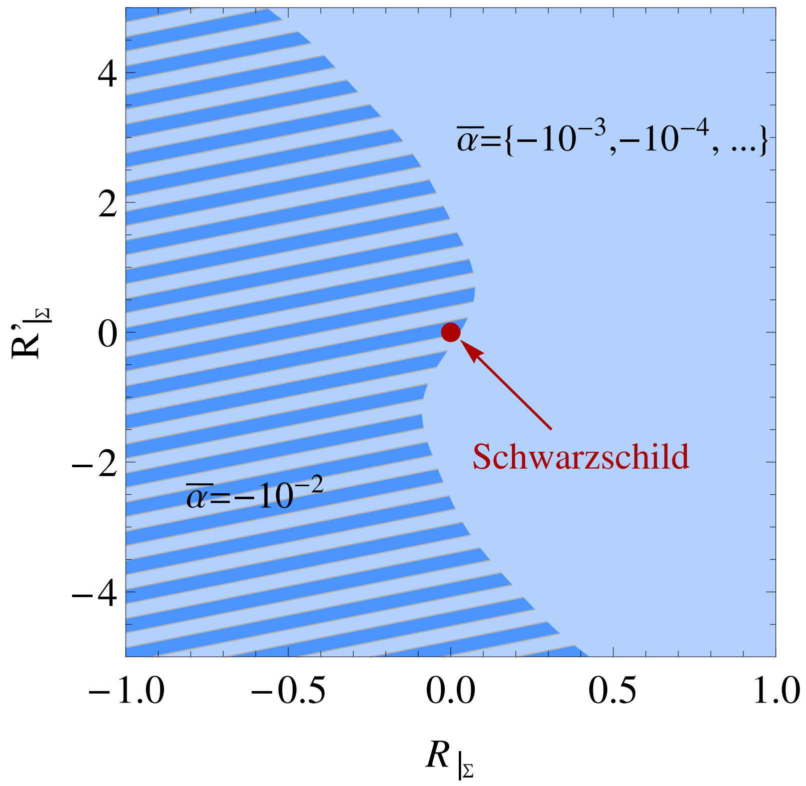

FIGURE 3.2: Contour plot for (R, R') at the surface Σ of the star for the polytropic equation of state $\bar{\rho} = \bar{P}^{5/9}/0.2$ and $\bar{\alpha} < 0$. For a given parameter $\bar{\alpha}$, there will be a unique solution which matches Schwarzschild *exactly* at the surface. The model is extremely fine-tuned.

3.9 Semianalytic approach

As we have seen above, an exact match between the interior and the exterior solutions is sometimes impossible. We have shown the existence of two problems. First, only a class of equations of state can be mathematically matched with Schwarzschild, which can be seen as a fine-tuning of the EoS. Second, we also have a fine-tuning of the initial conditions, because even for a mathematically viable EoS only a particular central condition on the pressure and the curvature will match Schwarzschild at the surface. In this section, we propose a solution to circumvent these difficulties. To avoid these problems, we choose a generic form of the curvature function $\bar{R}(x)$ that satisfies all the regularity and boundary conditions. Hence the problem regarding the boundary conditions will be reduced. Also we do not choose a particular equation of state in order to solve the first problem. The equation of state will be determined by the dynamics of the fields. The only boundary condition to satisfy is the pressure at the surface.

The most general form of the first derivative of the curvature scalar satisfying these conditions should be

$$\bar{R}'(x) = g(x)x(x - x_s)\,, \tag{3.29}$$

where $g(x)$ is an arbitrary and well defined function of x, and x_s is the surface of the star. Integrating $\bar{R}'$, we can fix the integration constant in order to have the last condition $\bar{R}(r_s) = 0$. Notice that, as in GR, we will always consider $R(r) > 0$.

We now choose a suitable ansatz for the function $g(x)$. By doing so, Eq. (3.26) becomes an algebraic constraint between the pressure and the density of the stellar fluid. We also note that by choosing an ansatz for $g(x)$, we can no longer specify the equation of state of the stellar matter without over-specifying the system. Hence the equation of state will be determined by the solution of the system. If a certain class of $g(x)$ gives unphysical EoSs, we will discard the class. As the simplest choice of the ansatz, let us assume the generic function $g(x)$ to be a constant. But the system will not satisfy an additional condition, namely, $R''(r_s) \leq 0$. Indeed, from Eq.(3.8) and the conditions at the surface, $R = R' = P = 0$, we have

$$R'' = -\frac{4\pi r_s}{3\alpha[r_s - 2m(r_s)]}\rho \leq 0. \tag{3.30}$$

Therefore we will assume $g(x) = A(x - x_s)$, which satisfies all conditions and solves the dynamical equations to get the mass and pressure profiles of a neutron star and its corresponding EoS. Hence the curvature scalar has the form

$$\bar{R}(x) = \frac{A}{12}(x - x_s)^3(3x + x_s)\,, \tag{3.31}$$

which satisfies the boundary conditions. The mass and pressure profiles of the star and the corresponding EoS for the given form of $\bar{R}$ are shown in Fig. 3.3. We have taken $x_s = 1$, i.e., we have fixed the radius of the star at 10 km and the central pressure is chosen in order to have $\bar{P}(x_s) = 0$ at the fixed position of the surface $x_s = 1$.

So the mass of the star comes out to be 0.79 $M_\odot$ and its central pressure is 3.73×10^{35} dynes/cm^2. Fitting the EoS, we get a profile of the form

$$\bar{P} \simeq 0.049\;\bar{\rho}^{1.49}\,. \tag{3.32}$$

Therefore we have shown in this section that it is possible to match Schwarzschild exactly at the surface of the star for realistic parameters (e.g., $\alpha = 10^{-45}$ eV^{-2}) and the star obtained is perfectly realistic.

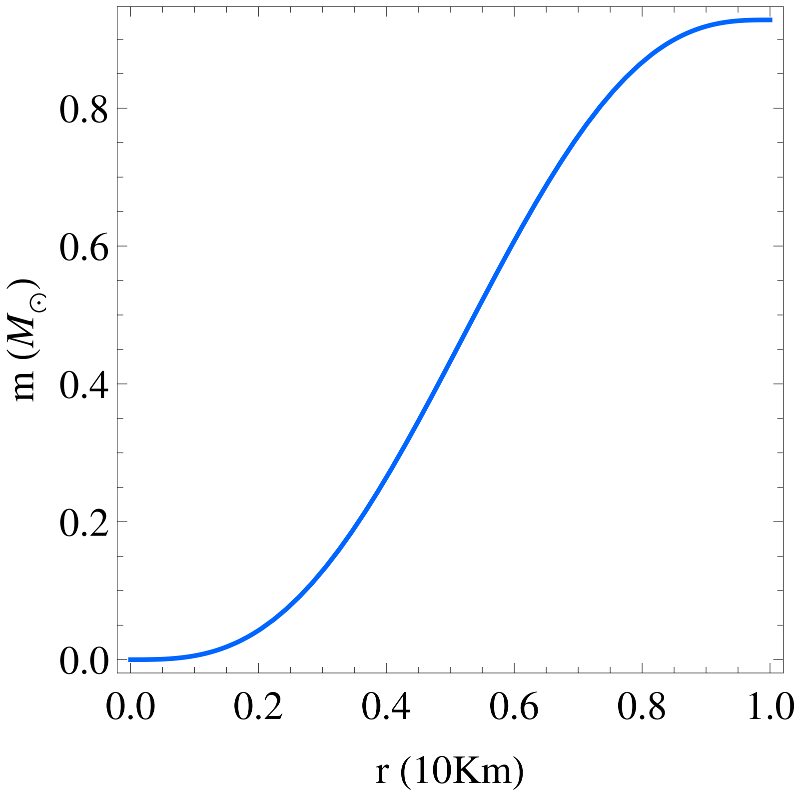
m ($M_\odot$)
0.0
0.2
0.4
0.6
0.8
0.0
0.2
0.4
0.6
0.8
1.0
r (10Km)

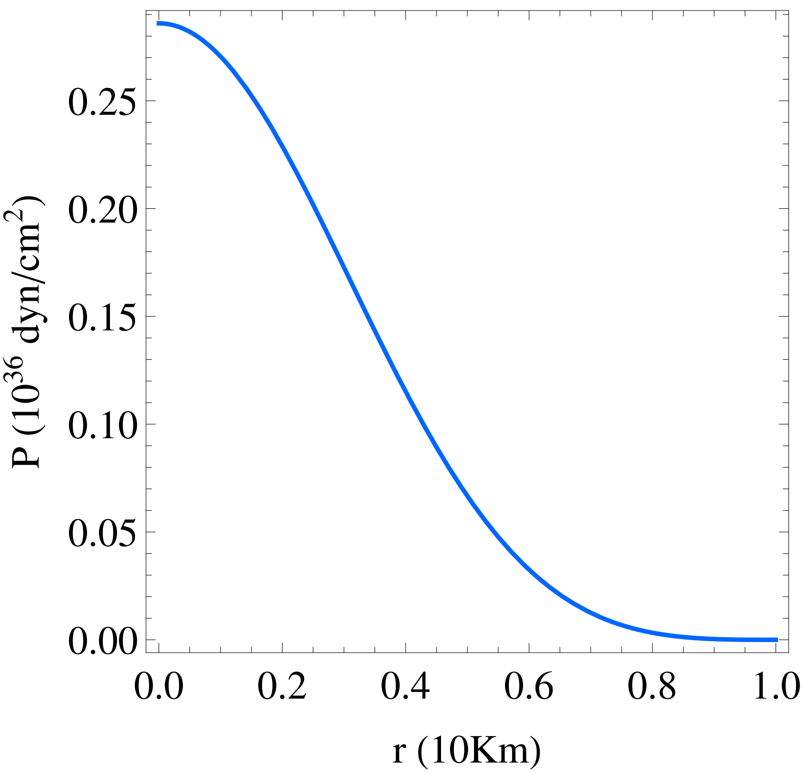
P (10^{36} dyn/cm^2)
0.00
0.05
0.10
0.15
0.20
0.25
0.0
0.2
0.4
0.6
0.8
1.0
r (10Km)

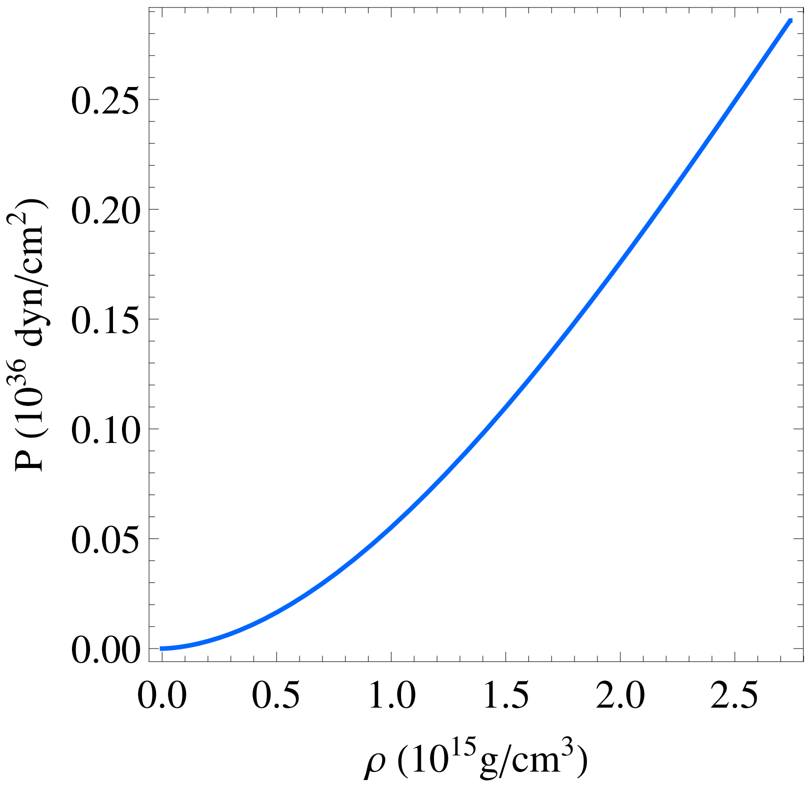

FIGURE 3.3: Mass, pressure and EoS profiles for $\bar{R} = \frac{A}{12}(x-1)^3(3x+1)$, $A = -60$ and $\alpha = 10^{-45}$ eV^{-2}.

3.10 Final Remark

We should emphasize that the matching with any exterior Ricci flat solution will bring the same difficulties because of the boundary conditions $R = R' = 0$ at the surface of the star, and this result can be simply generalized for any viable $f(R)$. Therefore modeling a radiating star with an intermediate Vaidya region is equally fine-tuned and unnatural.

At this point we may argue that in realistic astrophysical scenarios the domain of applicability of the spherically symmetric and vacuum conditions are typically set at astrophysical scales. For example, in the case of our solar system the domain is within the heliopause, which is approximately one light year from the sun. Hence the solar system is not in the *ideal* sense asymptotically flat. However, within this domain the Solar System is definitely "almost" spherically symmetric and "almost" vacuum (with respect to the scales of the problem), and hence the Schwarzschild solution is a very good approximation. Even in the case of $f(R)$ gravity, the conditions regarding the validity and stability of the Jebsen-Birkhoff theorem ensure that the solution will remain "almost" Schwarzschild in the exterior domain for the Starobinsky model provided the value of α is small [Nzioki, Goswami, et al. 2014]. Unfortunately the instability of our solution described in Sec. 3.6 that arises due to the matching of R' at the boundary for very small α still remains.

We would like to emphasize here that our study should not be seen as an exact realization of a real situation, but rather as a limit of various physical and realistic problems. In all cases, we have either rotation or matter in the exterior, and we should keep in mind that in the limit where the spinning goes to zero or the limit where the density of matter goes to zero our result should be recovered. Assuming that the physics is not discontinuous, we can think of our problem as a good approximation of a real situation.

A possible solution will be a matching with an exterior solution of the following form:

$$m(r) = M - ae^{-br} \tag{3.33}$$

This solution is asymptotically Schwarzschild, and hence it can match with the standard constraints in the Solar System provided b is large enough. For this solution, we have

$$R = 2ab(br - 2)\frac{e^{-br}}{r^2} \tag{3.34}$$

Hence we will be able to alleviate the fine-tuning problem. In fact, any numerical solution can be matched at the surface with Eq. (3.34) by choosing different values of a and b.

Even if this class of solutions exists for other $f(R)$ models, it is well known that for the Starobinsky model, the Schwarzschild is the unique asymptotically flat solution. Hence the fine-tuning problem cannot be circumvented in this case.

Another way to address this fine-tuning problem would be to neglect the extra matching conditions at the surface (namely the matching of the Ricci scalar and its normal derivative) and to allow a delta function in the field equations, which will give rise to a surface stress-energy term. This procedure was used to model static gravastars in GR [Mazur and Mottola 2004]. However this will radically change the structure of the crust of the neutron stars and should have, in principle, observational signatures [Lattimer and Prakash 2001].

3.11 Conclusions

Moving to the interior of neutron stars, in this chapter, we have derived for the first time the full exact solution for a neutron star in the Starobinsky model with the exterior matching solution, namely Schwarzschild. However, in this model (as well as in other $f(R)$ modified gravity models in general) the field equations are highly nonlinear. Difficulties appear due to the fourth order of the field equations, and hence the necessity of satisfying the extra two junction conditions, namely the continuity of the Ricci scalar and its normal derivative. This makes the problem more stringent and has not been considered before for studying compact stars in these models. Also, for the $R + \alpha R^2$ model that we have considered in this work, Schwarzschild is the only static spherically symmetric asymptotically flat solution with a regular horizon, which forces us to match the star with a Schwarzschild exterior. We have shown that the equations are singular in the sense that they develop a boundary layer, and hence all boundary conditions cannot be satisfied for a generic EoS. Only a particular class of EoSs will be compatible with the model. While trying to solve the system in a direct numerical approach, we faced the typical singularity problem when dealing with small values of the coupling constant α. But for even higher values of α and when choosing a constant density and polytropic EoS, we found that matching with the Schwarzschild exterior is not possible. In fact, we have also shown that as we go to smaller values of α, the system moves further away from Schwarzschild. This clearly indicates that in this model some EoSs can be ruled out even without considering observational constraints, unlike in GR. Also, for negative α which has an inherent ghost problem – we found the Schwarzschild exterior solution only for certain fine-tuned initial conditions. Therefore, the model brings two additional fine-tuning problems. First, only a class of EoS can be mathematically matched with Schwarzschild. Second, the central initial conditions should be fine-tuned in order to exactly match Schwarzschild at the surface. From our point of view, if we assume that the EoS is fixed and cannot fluctuate and hence only a very particular set of boundary conditions will produce the star, an extremely small deviation from that set of conditions will not be a solution, which implies an instability of the solution.

So the obvious question that arises is whether any solution exists in this model that smoothly matches with Schwarzschild. To check this, we took a semi-analytical approach to choose a form of the Ricci scalar and its first derivative that satisfies all the boundary conditions. We solved the resultant system to get a mass and a pressure profile that are physically viable, and we also found an acceptable EoS. This proves that there exists a class of solutions which – apart from satisfying all the boundary and junction conditions – matches smoothly with the Schwarzschild exterior solution. Therefore we have shown that the matching with Schwarzschild at the surface is possible but highly unnatural. And this phenomenon is true for a wide class of $f(R)$ theories that permit the Schwarzschild spacetime and also satisfy the uniqueness theorem. This is unnatural because the EoS of compact star matter should be completely determined by nuclear physics and the macroscopic description of quantum field theory for a highly dense star, and not by the theory of gravity.

Chapter 4

Accretion onto a black hole in a string cloud background

In this chapter, we consider the steady state spherical accretion onto a black hole that has a cloud of strings in the background and study the changes it brings out in comparison to a Schwarzschild black hole. As discussed in chapter 2, it has been recognized that certain gauge theories allow the possibility of topological defects, such as strings, and that these defects represent objects which might have been created in the very early Universe. Cosmic strings are strands of matter which could be created in a cosmological phase transition. It may be noted that the study of Einstein's equations coupled with a *string cloud* may be very important as the relativistic strings at a classical level can be used to construct applicable models [Letelier 1979]. Hence the study of the gravitational effects of matter, in the form of clouds of both cosmic and fundamental strings, has generated considerable attention [Synge 1960].

The chapter is organized as follows: After giving a brief account of the work that has been done in regards to spherical accretion to date in Sec. 4.1, in Sec. 4.2 the analytic general relativistic accretion onto a Schwarzschild black hole is appropriately generalized to model spherical steady state accretion onto a black hole surrounded by a cloud of strings. We calculate how the presence of a string cloud would affect the mass accretion rate $\dot{M}$ of a gas onto a black hole. We also determine analytic corrections to the critical radius, the critical fluid velocity and the sound speed, and subsequently to the mass accretion rate. Finally, we obtain expressions for the asymptotic behaviour of the fluid density and the temperature near the event horizon in Sec. 4.3 and conclude in Sec. 4.4. This chapter is based on the work [Ganguly, Ghosh, et al. 2014].

4.1 Introduction

The first study of spherical accretion onto compact objects dates back more than forty years in the seminal paper due to Bondi [Bondi 1952]. In this classic work, the hydrodynamics of polytropic flow is studied within the Newtonian framework, and it is found that either a settling or transonic solution is mathematically possible for the gas accreting onto compact objects. Note that the accretion rate is highest for the transonic solution. The relativistic version of the same problem was solved by Michel [Michel 1972] twenty years later. Michel [Michel 1972] investigated the steady state spherically symmetric flow of a test gas onto a Schwarzschild black hole in the framework of general relativity. He showed that accretion onto the black hole should be transonic. Michel's relativistic results attracted several researchers [Carr and Hawking 1974; Begelman 1978; Ray 1980; Thorne et al. 1981; Bettwieser and Glatzel 1981; Chang 1985; Pandey 1987; Shapiro and Teukolsky 1983]. Spherical accretion and winds in the context of general relativity have also been analyzed using equations of state other than the polytrope. Other extensive studies include the calculation of the frequency and luminosity spectra [Shapiro 1973a], the influence of an interstellar magnetic field in ionized gases [Shapiro 1973b], and the changes in accreting processes when the black hole rotates [Shapiro 1974]. Several radiative processes have been included by Blumenthal and Mathews [Blumenthal and Mathews 1976], and Brinkmann [Brinkmann 1980]. In addition Malec [Malec 1999] considered general relativistic spherical accretion with and without back-reaction, and showed that relativistic effects increase mass accretion when back-reaction is absent. Accretion of a perfect fluid with a general equation of state onto a Schwarzschild black hole has been investigated in [Babichev et al. 2004; Babichev et al. 2006; Babichev et al. 2005], and a similar analysis for a charged black hole has been done in [Pacheco 2012]. Accretion processes related to a charged black hole were analyzed in [Michel 1972] and investigated further in [Babichev, Chernov, et al. 2011; Jamil et al. 2008; Sharif and Abbas 2011; Sharif and Abbas 2012]. Also note that the mass accretion rate is affected by the presence of higher dimensions [John et al. 2013]. The main aim of these studies is to obtain the net energy output emitted by infalling gas with application of black hole accretion to several classes of astrophysical sources. It is understood that accretion onto a black hole might be an important source of radiant energy. This may be related to the accretion rate $\dot{M}$, and we may expect that an increase in $\dot{M}$ should lead to an increase in the luminosity [Shapiro 1973a].

We thereby generalize the previous work of Michel [Michel 1972]. Interestingly, it turns out that the mass accretion rate $\dot{M}$ increases with the string cloud as a background in comparison to the standard black hole.

4.2 General equations for spherical accretion

We now present the basic relations in spherical symmetry with accreting matter, and describe the flow of gas into the modified Schwarzschild black hole (2.34). Also we probe how the string cloud background affects the accretion rate $\dot{M}$, the asymptotic compression ratio, and the temperature profiles. We consider the steady state radial inflow of gas onto a central mass M by following the approach of Michel [Michel 1972] and Shapiro [Shapiro and Teukolsky 1983]. The gas is approximated as a perfect fluid described by the energy momentum tensor

$$T^{\mu\nu} = (\rho + p)\, u^{\mu} u^{\nu} + p g^{\mu\nu}\,, \tag{4.1}$$

where ρ and p are the fluid proper energy density and pressure respectively, and

$$u^{\mu} = \frac{dx^{\mu}}{ds}\,, \tag{4.2}$$

is the fluid 4-velocity which obeys the normalization condition $u^{\mu}u_{\mu} = -1$. We also define the proper baryon number density n, and the baryon number flux $J^{\mu} = nu^{\mu}$. All these quantities are measured in the local inertial rest frame of the fluid. The spacetime curvature is dominated by the compact object and we ignore the self-gravity of the fluid. The accretion process is based on two important conservation laws. Firstly, if no particles are created or destroyed then particle number is conserved and

$$\nabla_{\mu} J^{\mu} = \nabla_{\mu}(nu^{\mu}) = 0\,. \tag{4.3}$$

Secondly, the conservation law is that of energy momentum which is governed by

$$\nabla_{\mu} T^{\mu}_{\nu} = 0\,. \tag{4.4}$$

The non-null components of the 4-velocity are $u^0 = dt/ds$ and $v(r) = u^1 = dr/ds$. Since $u_{\mu}u^{\mu} = -1$, and the velocity components vanish for $\mu > 1$, we have

$$u^0 = \left[\frac{v^2 + 1 - \frac{2M}{r} - \alpha}{\left(1 - \frac{2M}{r} - \alpha\right)^2}\right]^{1/2}\,, \tag{4.5}$$

where α is the string cloud parameter introduced in chapter 2. Equation (4.3) can be written as

$$\frac{1}{r^2}\frac{d}{dr}\left(r^2 nv\right) = 0\,. \tag{4.6}$$

Our assumptions of spherical symmetry and steady state flow make (4.4) comparatively easier to tackle. The $\nu = 0$ component is

$$\frac{1}{r^2}\frac{d}{dr}\left[r^2(\rho+p)v\left(1-\frac{2M}{r}-\alpha+v^2\right)^{1/2}\right]=0\,. \tag{4.7}$$

The $\nu = 1$ component can be simplified to

$$v\frac{dv}{dr}=-\frac{dp}{dr}\left(\frac{1-\frac{2M}{r}-\alpha+v^2}{\rho+p}\right)-\frac{M}{r^2}\,. \tag{4.8}$$

The above equations are generalizations of the results obtained for the standard Schwarzschild black hole [Michel 1972; Shapiro and Teukolsky 1983].

4.2.1 Accretion onto a black hole

The accretion of matter onto black holes remains a classic problem of contemporary astrophysics, as it does on the related problems of active galactic nuclei and quasars, the mechanism of jets, and the nature of certain galactic X-ray sources. Let us consider spherical steady state accretion onto a Schwarzschild black hole of mass M in a string cloud background to obtain the mass accretion rate from a qualitative analysis of (4.6) and (4.8). For an adiabatic fluid there is no entropy production and the conservation of mass energy is governed by

$$Tds=0=d\left(\frac{\rho}{n}\right)+p\;d\left(\frac{1}{n}\right)\,, \tag{4.9}$$

which may be put in the form

$$\frac{d\rho}{dn}=\frac{\rho+p}{n}\,. \tag{4.10}$$

We define the adiabatic sound speed a via [Shapiro and Teukolsky 1983]

$$a^2\equiv\frac{dp}{d\rho}=\frac{dp}{dn}\frac{n}{\rho+p}\,, \tag{4.11}$$

and we have used equation (4.10). Using (4.11), the baryon and momentum conservation equations can be written as

$$\frac{v'}{v}+\frac{n'}{n}+\frac{2}{r}=0\,, \tag{4.12}$$

$$vv'+a^2\left(1-\frac{2M}{r}-\alpha+v^2\right)\frac{n'}{n}+\frac{M}{r^2}=0\,, \tag{4.13}$$

with $p' = (dp/dn)n'$ where a dash ($'$) denotes a derivative with respect to r. With the help of the above equations, we obtain the system

$$v' = \frac{N_1}{N}\,,$$
$$n' = -\frac{N_2}{N}\,, \tag{4.14}$$

where

$$N_1 = \frac{1}{n}\left[\left(1 - \frac{2M}{r} - \alpha + v^2\right)\frac{2a^2}{r} - \frac{M}{r^2}\right]\,, \tag{4.15a}$$
$$N_2 = \frac{1}{v}\left(\frac{2v^2}{r} - \frac{M}{r^2}\right)\,, \tag{4.15b}$$
$$N = \frac{v^2 - \left(1 - \frac{2M}{r} - \alpha + v^2\right)a^2}{vn}\,. \tag{4.15c}$$

In the stationary accretion of gas onto the black hole, the amount of infalling matter per unit time $\dot{M}$, and other parameters are determined by the gas properties and the gravitational field at large distances. For large r, the flow is subsonic i.e. $v < a$ and since the sound speed must be subluminal, i.e., $a < 1$, we have $v^2 \ll 1$. The denominator (4.15c) is therefore

$$N \approx \frac{v^2 - a^2(1-\alpha)}{vn}\,, \tag{4.16}$$

and so $N < 0$ as $r \to \infty$ if we demand $v^2 < a^2(1-\alpha)$. At the event horizon $r_H = 2M/(1-\alpha)$, and we have

$$N = \frac{v(1-a^2)}{n}\,. \tag{4.17}$$

Under the causality constraint $a^2 < 1$, we have $N > 0$. Therefore N should pass through a critical point r_s where it goes to zero. As the flow is assumed to be smooth everywhere, so N_1 and N_2 should also vanish at r_s, i.e., to avoid discontinuities in the flow, we must have $N = N_1 = N_2 = 0$ at the radius r_s. This is nothing but the so-called *sonic condition*. Hence, the flow must pass through a critical point outside the event horizon, i.e., $r_H < r_s < \infty$. At the critical point the system (4.15) satisfies the condition

$$v_s^2 = \frac{a_s^2(1-\alpha)}{1+3a_s^2} = \frac{M}{2r_s}\,, \tag{4.18}$$

where $v_s \equiv v(r_s)$ and $a_s \equiv a(r_s)$. The quantities with a subscript s are defined at the critical point or the sonic points of the flow. It can be clearly seen that the critical velocity in this model is modified by the factor $(1-\alpha)$, and the physically acceptable solution $v_s^2 > 0$ is ensured since $0 \le \alpha < 1$.

To calculate the mass accretion rate, we integrate (4.6) over a 4-dimensional volume and multiply by m_b, the mass of each baryon, to obtain

$$\dot{M} = 4\pi r^2 m_b n v \,, \tag{4.19}$$

where $\dot{M}$ is an integration constant, independent of r, having dimensions of mass per unit time. It is similar to the Schwarzschild case. Equations (4.6) and (4.7) can be combined to yield

$$\left(\frac{\rho + p}{n}\right)^2 \left(1 - \frac{2M}{r} - \alpha + v^2\right) = \left(\frac{\rho_\infty + p_\infty}{n_\infty}\right)^2 , \tag{4.20}$$

which is the modified relativistic Bernoulli equation for the steady state accretion onto black holes surrounded by a cloud of strings. Equations (4.19) and (4.20) are the basic equations that characterize accretion onto a black hole with parameter α where we have ignored the back-reaction of matter. In the limit $\alpha = 0$, our results reduce to those obtained in [Michel 1972; Shapiro and Teukolsky 1983] for the standard Schwarzschild black hole.

4.2.2 The polytropic solution

In order to calculate $\dot{M}$ explicitly and all the fundamental characteristics of the flow, (4.19) and (4.20) must be supplemented with an equation of state which is a relation that characterizes the state of matter of the gas. Following Bondi [Bondi 1952] and Michel [Michel 1972], we introduce a polytropic equation of state

$$p = K n^\gamma \,, \tag{4.21}$$

where K and the adiabatic index γ are constants. On inserting (4.21) into the energy equation (4.9) and integrating, we obtain

$$\rho = \frac{K}{\gamma - 1} n^\gamma + m_b n \,, \tag{4.22}$$

where m_b is an integration constant obtained by matching with the total energy density equation $\rho = m_b n + U$, where $m_b n$ is the rest mass energy density of the baryons and U is the internal energy density. Equations (4.21) and (4.22) give

$$\gamma K n^{\gamma - 1} = \frac{a^2 m_b}{(1 - \frac{a^2}{\gamma - 1})} \,. \tag{4.23}$$

Using (4.22) and (4.23) we can easily rewrite the Bernoulli equation (4.20) as

$$\left(1+\frac{a^2}{\gamma-1-a^2}\right)^2\left(1-\frac{2M}{r}-\alpha+v^2\right)=\left(1+\frac{a_\infty^2}{\gamma-1-a_\infty^2}\right)^2. \tag{4.24}$$

At the critical radius r_s, using the relation (4.18) and inverting the above equation, we get

$$\left(1+3a_s^2\right)\left(1-\frac{a_s^2}{\gamma-1}\right)^2=\left(1-\frac{a_\infty^2}{\gamma-1}\right)^2. \tag{4.25}$$

It must be noted that, in general, the Bernoulli equation is modified due to a string cloud background. However at the critical radius, the form remains unchanged from the Schwarzschild case [Shapiro and Teukolsky 1983].

For large but finite values of r, i.e. $r \geq r_s$ the baryons will be non-relativistic, i.e., $T \ll mc^2/k = 10^{13}K$ for neutral hydrogen. In this regime we should have $a \leq a_s \ll 1$. Expanding (4.25) up to second order in a_s and a_∞, we obtain

$$\begin{aligned} a_s^2 &\approx \frac{2}{5-3\gamma}a_\infty^2\,, \quad && \gamma\neq\frac{5}{3} \\ &\approx \frac{2}{3}a_\infty\,, && \gamma=\frac{5}{3}. \end{aligned} \tag{4.26}$$

We thus obtain the critical radius r_s in terms of the black hole mass M and the boundary condition a_∞ from (4.18) and (4.26):

$$\begin{aligned} r_s &\approx \frac{5-3\gamma}{4}\frac{M}{a_\infty^2(1-\alpha)}\,, \quad && \gamma\neq\frac{5}{3} \\ &\approx \frac{3}{4}\frac{M}{a_\infty(1-\alpha)}\,, && \gamma=\frac{5}{3}. \end{aligned} \tag{4.27}$$

Also, for $a^2/(\gamma-1)\ll 1$, we get from (4.23)

$$\frac{n}{n_\infty}\approx\left(\frac{a}{a_\infty}\right)^{2/(\gamma-1)}. \tag{4.28}$$

We are now in a position to evaluate the accretion rate $\dot{M}$. Since $\dot{M}$ is independent of r, (4.19) must also hold for $r = r_s$. We use the critical point to determine the Bondi accretion rate $\dot{M} = 4\pi r_s^2 m_b n_s v_s$. By virtue of eqs. (4.18), (4.26), (4.27) and (4.28) the accretion rate becomes

$$\dot{M}=\frac{4\pi}{(1-\alpha)^{3/2}}\lambda_s M^2 m_b n_\infty a_\infty^{-3}\,, \tag{4.29}$$

where we have defined the dimensionless accretion eigenvalue

$$\lambda_s = \left(\frac{1}{2}\right)^{(\gamma+1)/2(\gamma-1)} \left(\frac{5-3\gamma}{4}\right)^{-(5-3\gamma)/2(\gamma-1)} . \tag{4.30}$$

From (4.29), it is evident that the mass accretion in a string cloud background is increased by the factor $(1-\alpha)^{-3/2}$, which may result in a more luminous source. However, the accretion rate still scales as $\dot{M} \sim M^2$ which is similar to that of the Newtonian model [Bondi 1952] as well as the relativistic case [Michel 1972; Shapiro and Teukolsky 1983]. In the limiting case $\alpha = 0$, we obtain the well known relations derived in [Michel 1972; Shapiro and Teukolsky 1983] for the Schwarzschild black hole. In Fig. 4.1, we have plotted the logarithm of the accretion rate $\dot{M}$ against the string cloud parameter α for various polytropic indices γ. Here $\dot{M}$ is calculated in ergs/sec. We see that $\dot{M}$ increases rapidly with increasing α $(0 \leq \alpha < 1)$, and interestingly $\dot{M} \to \infty$ as $\alpha \to 1$.

4.2.3 Some numerical results

The radial motion of the relativistic fluid accreting onto the black hole in a string cloud background is governed by (4.6) and (4.24). These equations are difficult to solve analytically and we solve them numerically as in ref. [Pacheco 2012]. We consider only the case of the relativistic fluid with $\gamma = \frac{4}{3}$ to study the radial velocity of the flow. Following [Pacheco 2012], we introduce dimensionless variables, the radial distance in terms of the gravitational radius $(x = (r/2M))$ and the particle number density with respect to its value at infinity $(y = n/n_\infty)$. Now considering $a \ll 1$, Eq. (4.24) can be rewritten, in terms of a new variable, as

$$\left(1 + \frac{a_\infty^2}{\gamma-1} y^{\gamma-1}\right)^2 \left(1 - \frac{1-\alpha}{x} - \alpha + v^2\right) = \left(1 + \frac{a_\infty^2}{\gamma-1}\right)^2 . \tag{4.31}$$

On the other hand, using the same notation, the baryon conservation equation (4.6) can be recast as

$$yv = \left(\frac{x_s}{x}\right)^2 a_\infty \left(\frac{2}{5-3\gamma}\right)^{\gamma+1/2(\gamma-1)} (1-\alpha)^{1/2} , \tag{4.32}$$

where the constant of integration is calculated by applying baryon conservation at the critical point. Observe that (4.31) and (4.32) are corrected equations for the string cloud model and when $\alpha \to 0$ we recover the familiar model of Michel [Michel 1972]. Clearly, the equations (4.31) and (4.32) form a nonlinear system of algebraic equations which is solved numerically for the fluid velocity v given in terms of the velocity of light and y. The parameters defining the flow are the sound velocity at infinity a_∞, the adiabatic coefficient γ and the string cloud parameter α. The velocity profile of the flow as a function of the dimensionless variable x for

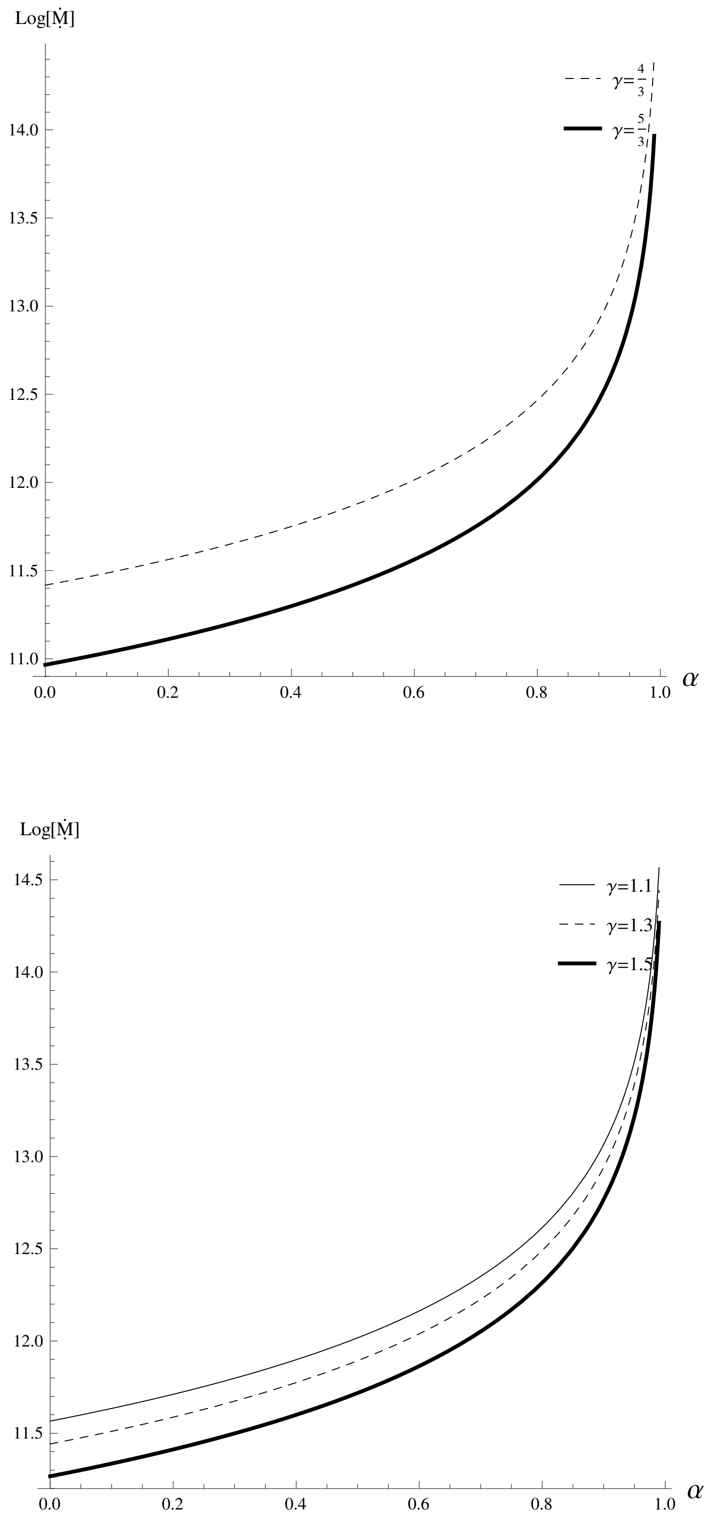

FIGURE 4.1: Plots showing the logarithm of the accretion rate $\dot{M}$ as a function of α for different values of γ.

different values of the parameter α is plotted in Fig. 4.2. The solution is obtained by assuming an asymptotic temperature at infinity of $10^{-9}\ m_pc^2/k_B$ for the relativistic case, i.e., $\gamma = \frac{4}{3}$. The event horizons for the model are located at $x = 1/(1-\alpha)$, and hence the event horizon varies with α. Interestingly a string cloud in the background has a profound influence on the radial velocity, and the result is strikingly different from the Schwarzschild case ($\alpha = 0$). In the familiar Schwarzschild case ($\alpha = 0$, Fig. 4.2), we note that the flow speed of the accreting gas crosses the event horizon at the speed of light. This feature is consistent with the treatment of de Freitas [Pacheco 2012] who considered relativistic accretion onto a charged black hole. The critical radius is far away from the event horizon ($x_c = 1.25\times10^8$) where the flow velocity is much less the value at the event horizon. To conserve space we have plotted velocity profile for $\gamma = 4/3$, as the radial velocity v for other values of γ have similar profiles. The velocity profile are plotted for some specific values of string cloud parameter $\alpha = 0,\ 0.2,\ 0.4,\ 0.6,\ 0.75$ and 0.8, respectively for which the event horizons are located at $r = 1, 1.25, 1.67, 2.5, 4$ and 5. It is clear from Fig. 4.2, the fluid always crosses event horizon with the velocity of light for all values of α.

We have also plotted the compression ratio y as a function of radial coordinate for a relativistic accreting gas with $\gamma = \frac{4}{3}$ in Fig. 4.3 for different values of string cloud parameter. More specifically for $\alpha = 0,\ 0.2,\ 0.4,\ 0.6,\ 0.75$ and 0.8. This graph shows that the compression factor profiles are also affected by a change in the string cloud parameter α; this is in contrast to analogous compression factor of an accreting charged black hole [Pacheco 2012]. The compression ratio for a black hole in string cloud background increases with increase in α. In general, it may attain the value of the order of $10^{14} - 10^{16}$.

4.3 Asymptotic behaviour

In the last section, we found that the accretion rate at some sonic point $r = r_s$ far away from event horizon, i.e., $r_s \gg 2M$ is not influenced by nonlinear gravity. Next we estimate the flow characteristics for $r_H < r \ll r_s$ and at the event horizon $r = r_H$.

4.3.1 Sub-Bondi radius $r_H < r \ll r_s$

At distances below the Bondi radius the gas is supersonic so that $v > a$ when $r_H < r \ll r_s$. From (4.24) we find the upper bound on the radial dependence of the gas velocity

$$v^2 \approx \frac{2M}{r}, \qquad \gamma \neq \frac{5}{3}\,. \tag{4.33}$$

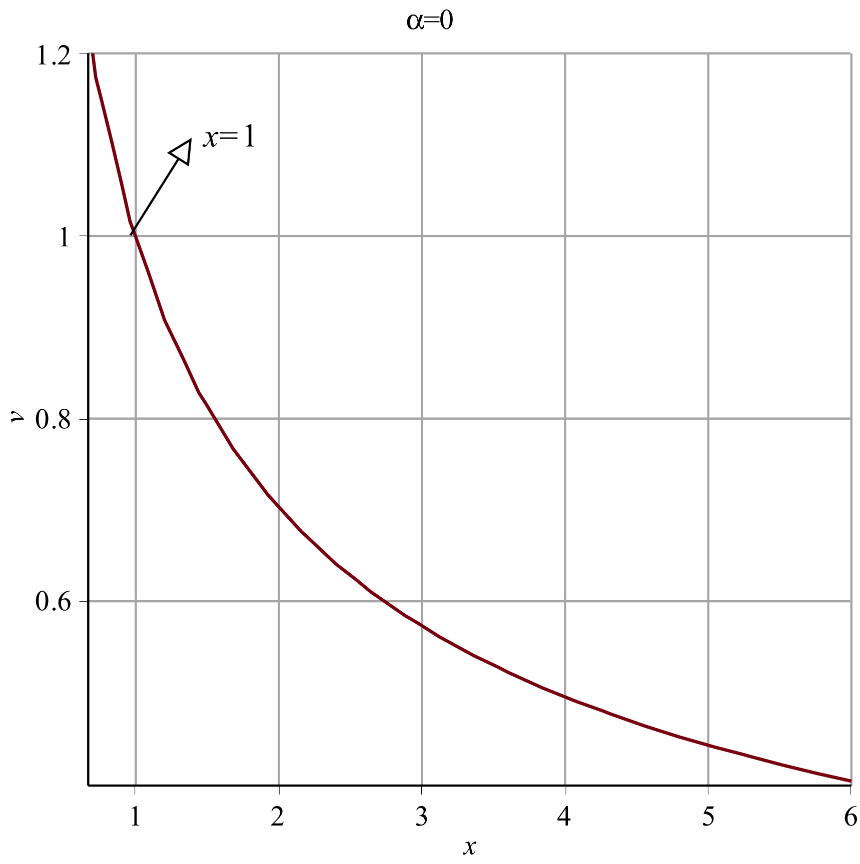
α=0
x=1
1.2
1
0.8
0.6
v
1
2
3
4
5
6
x

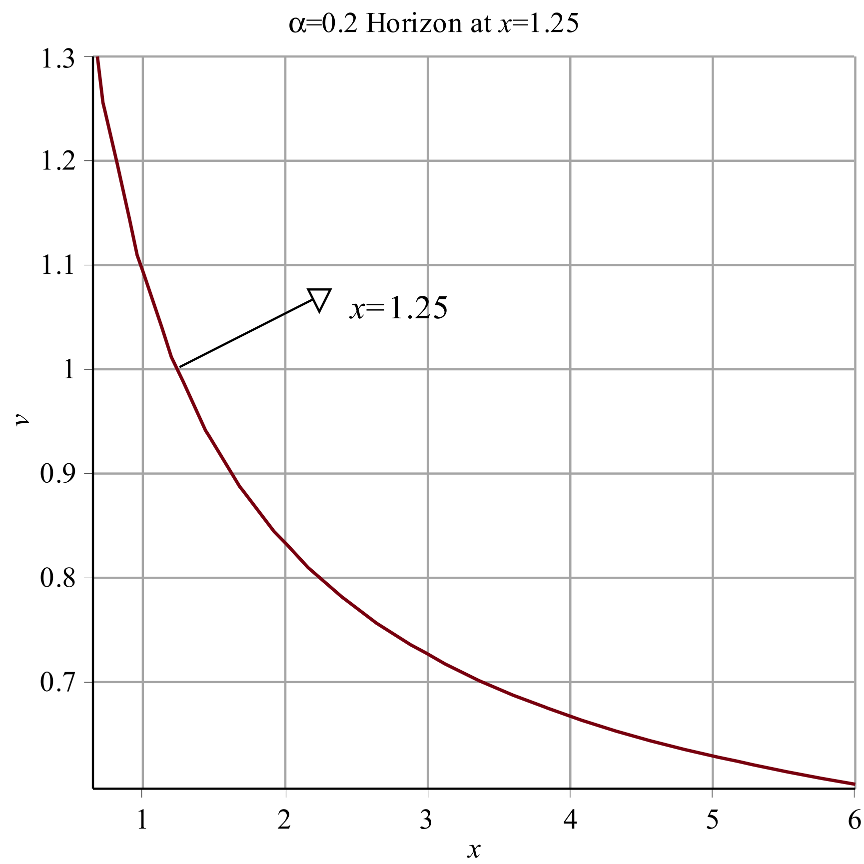
α=0.2 Horizon at x=1.25
x=1.25
1.3
1.2
1.1
1
0.9
0.8
0.7
v
1
2
3
4
5
6
x

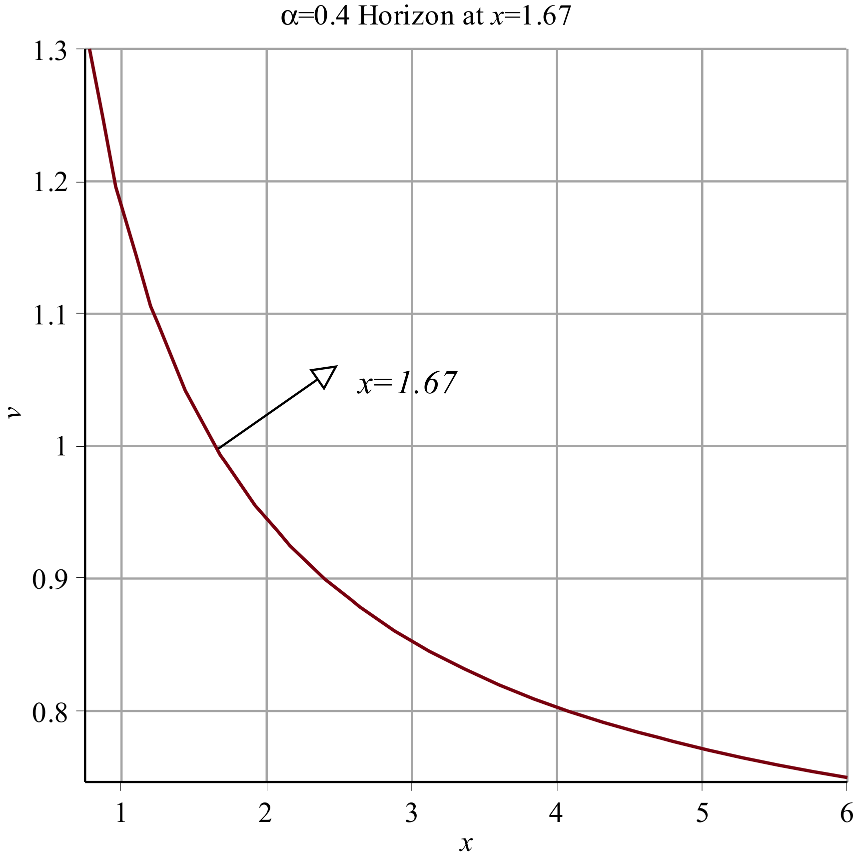
α=0.4 Horizon at x=1.67
1.3
1.2
1.1
1
0.9
0.8
v
x=1.67
1
2
3
4
5
6
x

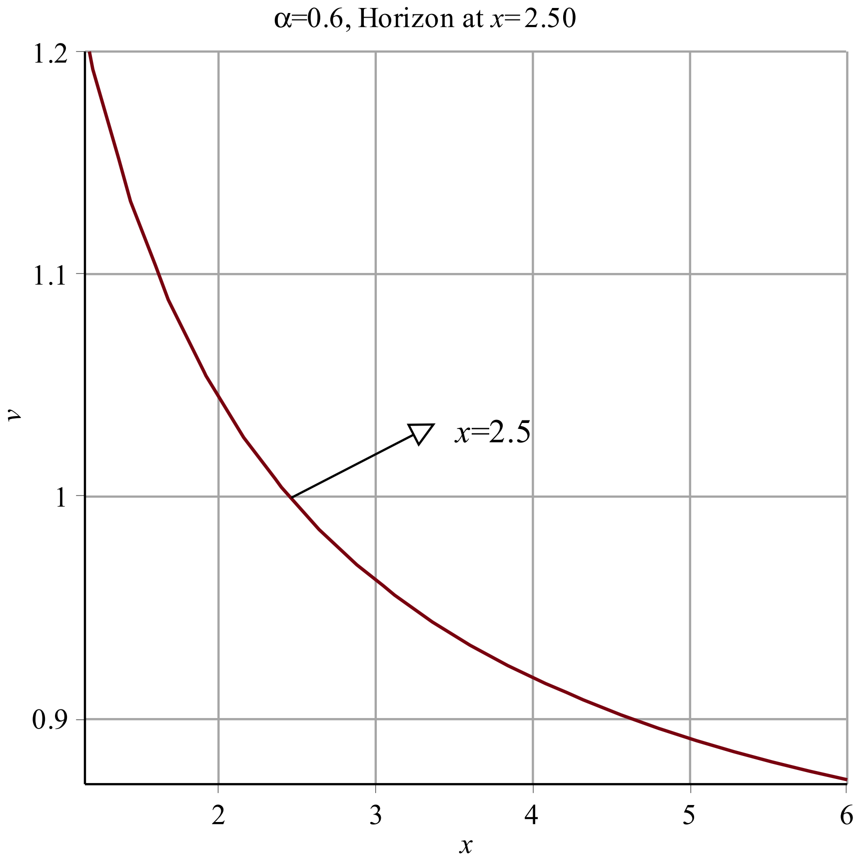
α=0.6, Horizon at x=2.50
1.2
1.1
1
0.9
v
x=2.5
2
3
4
5
6
x

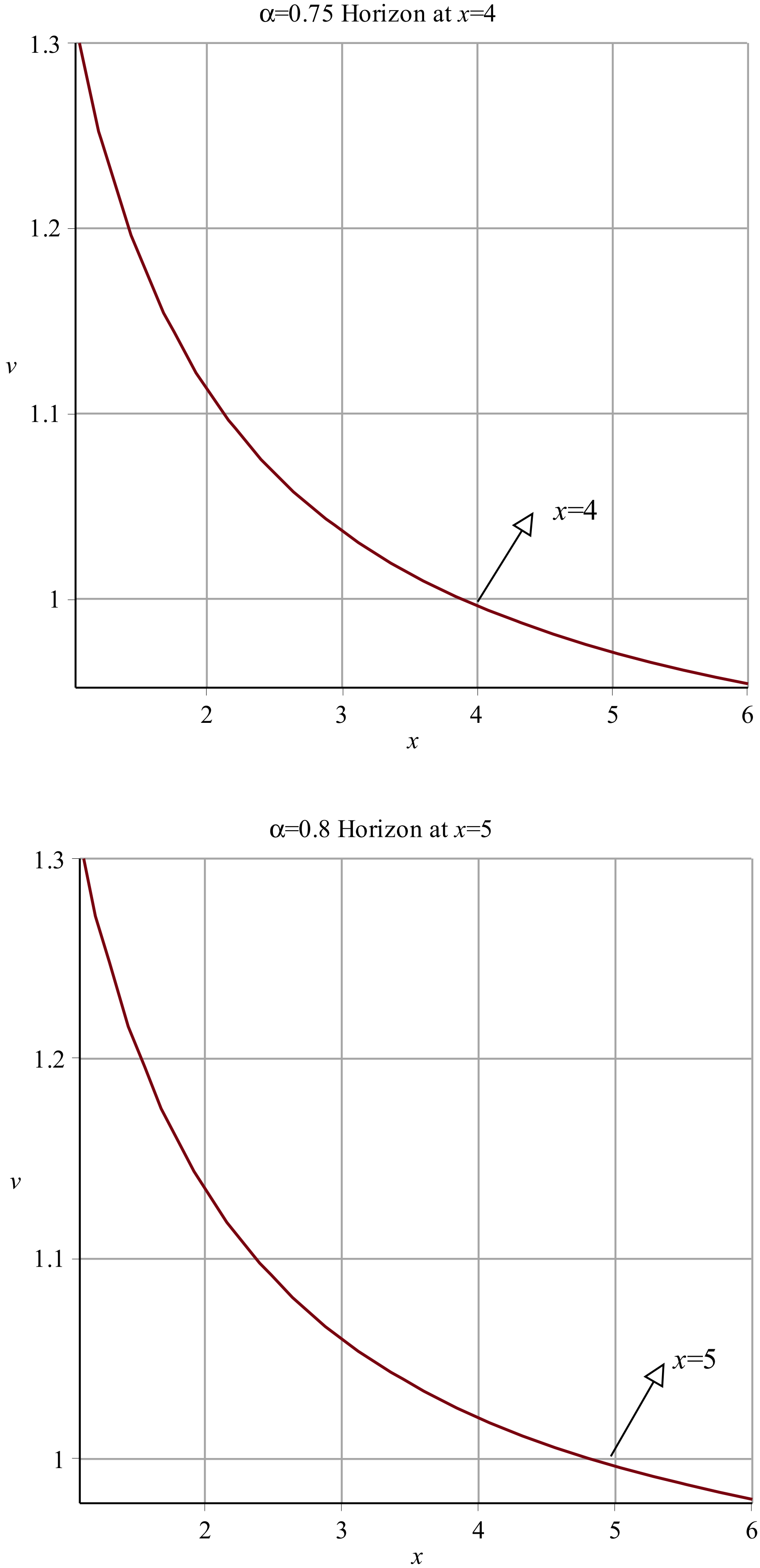

FIGURE 4.2: The radial velocity profile v for a relativistic fluid $\gamma = 4/3$ accreting onto the black hole as a function of the dimensionless radius $x = (r/2M)$ for different values of the string cloud parameter α. The arrows point to the location of the horizon for each case.

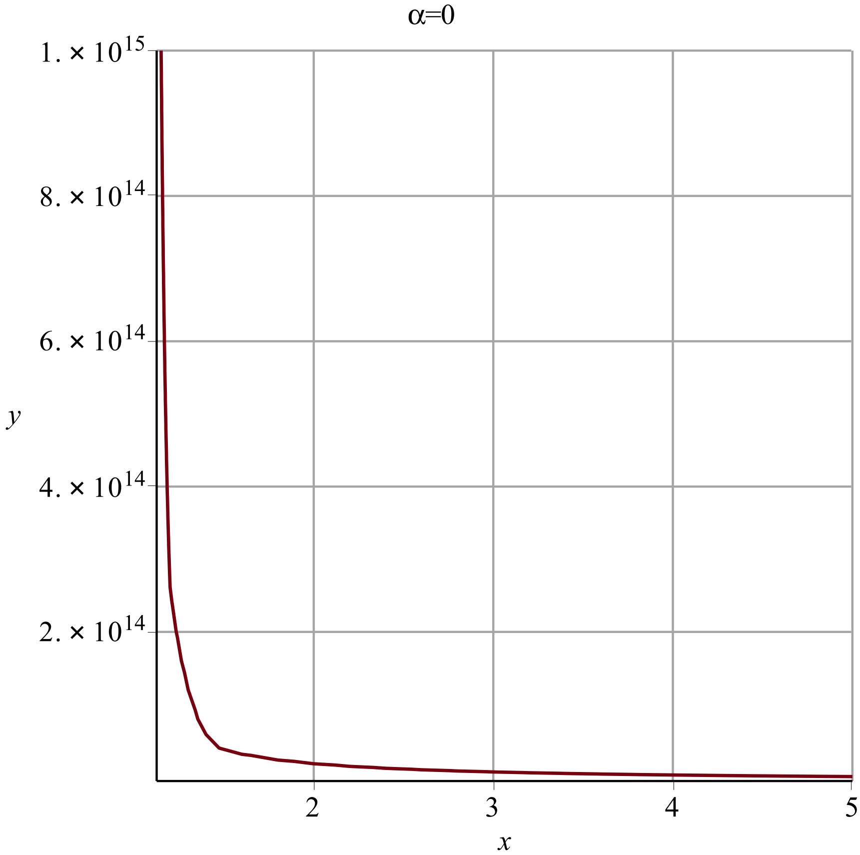
α=0
1. × 10^15
8. × 10^14
6. × 10^14
4. × 10^14
2. × 10^14
y
2
3
4
5
x

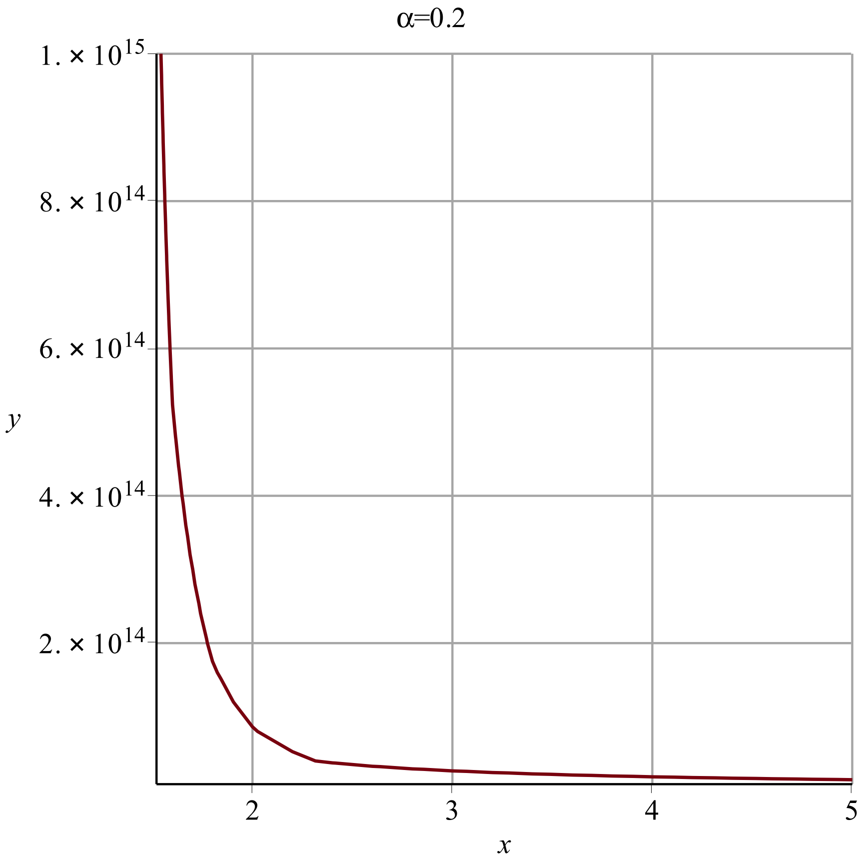
α=0.2
1. × 10^15
8. × 10^14
6. × 10^14
4. × 10^14
2. × 10^14
y
2
3
4
5
x

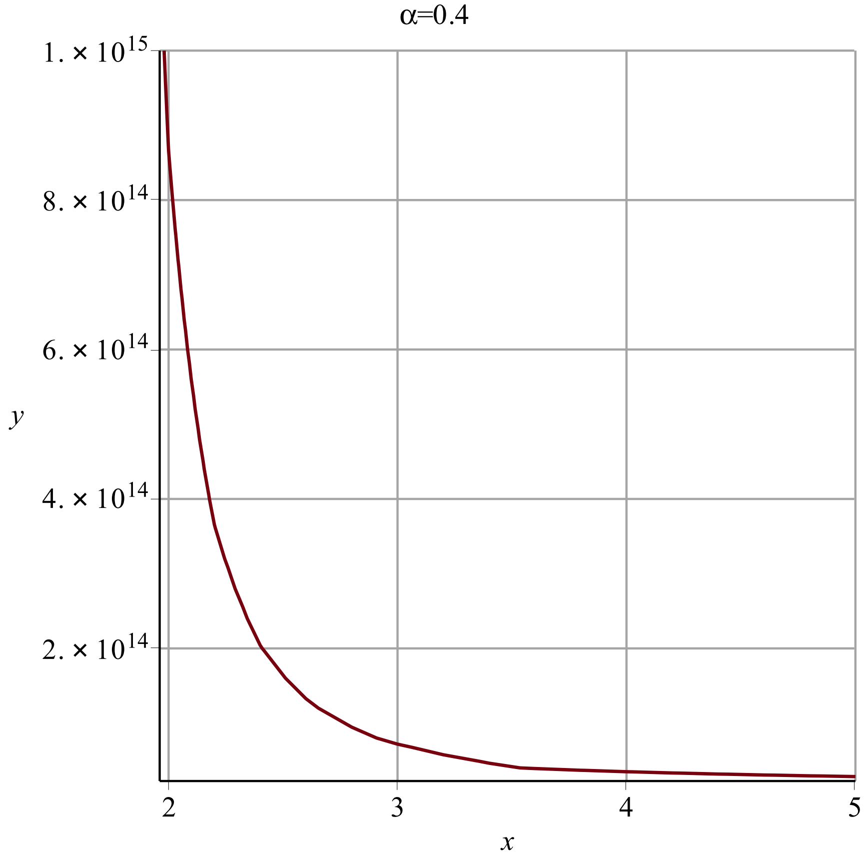
α=0.4
1. × 10^15
8. × 10^14
6. × 10^14
4. × 10^14
2. × 10^14
y
2
3
4
5
x

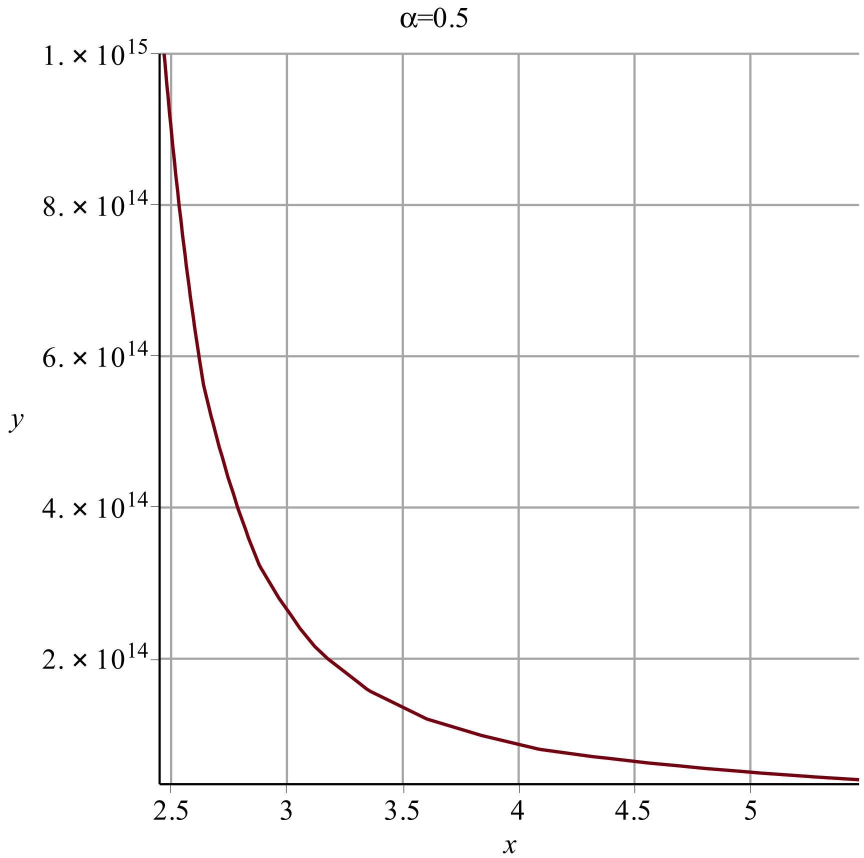
α=0.5
1. × 10^15
8. × 10^14
6. × 10^14
4. × 10^14
2. × 10^14
y
2.5
3
3.5
4
4.5
5
x

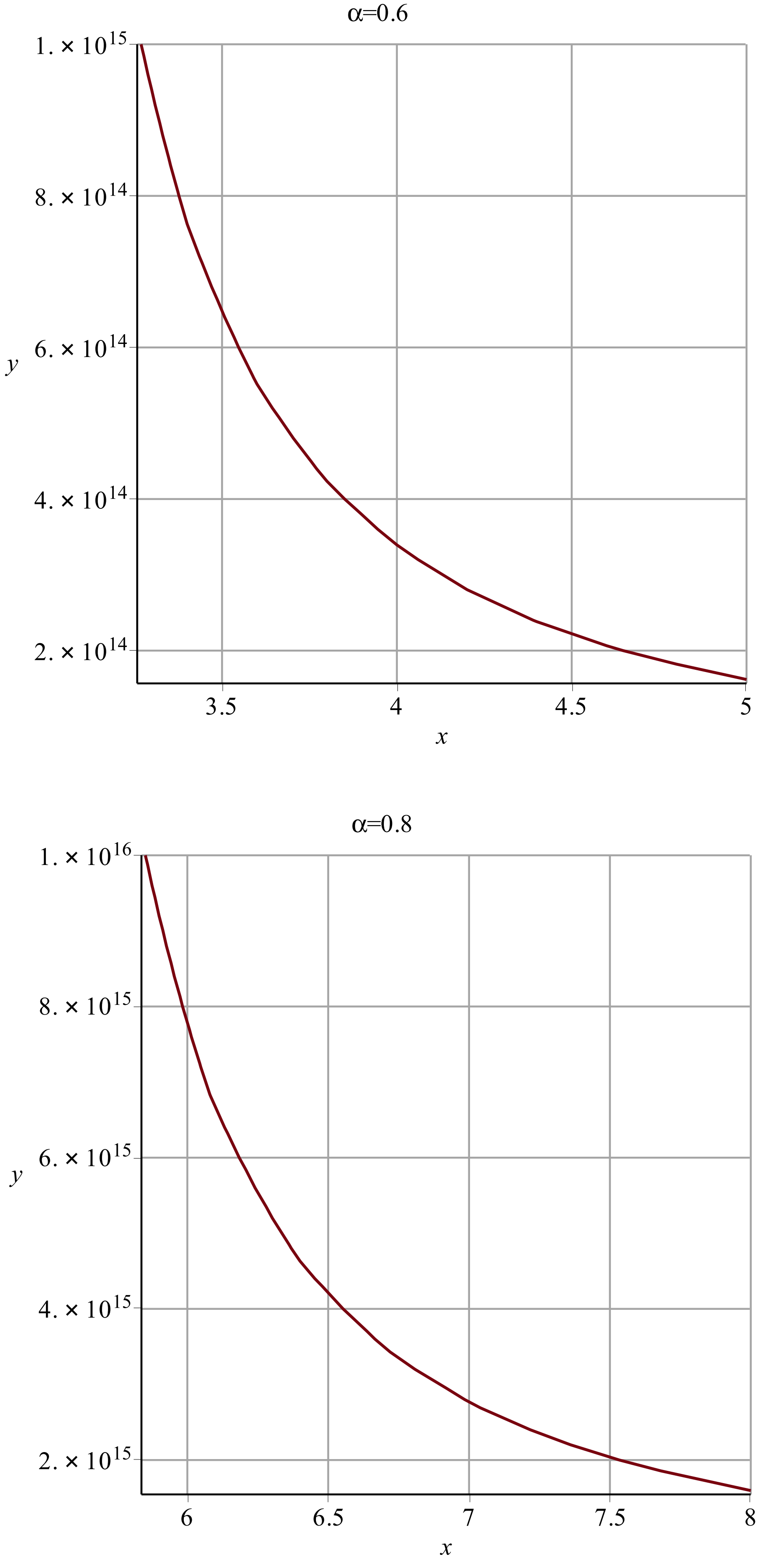

FIGURE 4.3: The compression factor y for a relativistic fluid $\gamma = 4/3$ accreting onto the black hole as a function of the dimensionless radius $x = (r/2M)$ for different values of the string cloud parameter α.

We can now estimate the gas compression on these scales. With the help of (4.19), (4.29) and (4.33) we obtain

$$\frac{n(r)}{n_\infty} \approx \frac{\lambda_s}{\sqrt{2}(1-\alpha)^2}\left(\frac{M}{a_\infty^2 r}\right)^{3/2}. \tag{4.34}$$

For a Maxwell-Boltzmann gas, $p = nk_BT$, we generate the adiabatic temperature profile

$$\frac{T(r)}{T_\infty} = \left(\frac{n(r)}{n_\infty}\right)^{\gamma-1} \approx \left[\frac{\lambda_s}{\sqrt{2}(1-\alpha)^2}\left(\frac{M}{a_\infty^2 r}\right)^{3/2}\right]^{\gamma-1}, \tag{4.35}$$

using (4.21) and (4.34).

4.3.2 Event horizon

At the event horizon we have $r = r_H = 2M/(1-\alpha)$. As the flow is supersonic since we are well below the Bondi radius, it is reasonable to assume that the fluid velocity is approximated by $v^2 \approx \frac{2M}{r}$. At r_H, $v_H^2 \equiv v^2(r_H) \approx 1-\alpha$, i.e., the flow speed at the horizon is always less than the speed of light. Therefore, using the fact $M/r_H = (1-\alpha)/2$, we obtain the gas compression at the event horizon from (4.34):

$$\frac{n_H}{n_\infty} \approx \frac{\lambda_s}{4(1-\alpha)^{1/2}}\left(\frac{c}{a_\infty}\right)^3. \tag{4.36}$$

Again assuming the presence of a Maxwell-Boltzmann gas, $p = nk_BT$, we find the adiabatic temperature profile at the event horizon using (4.35) and the horizon assumption

$$\frac{T_H}{T_\infty} \approx \left[\frac{\lambda_s}{4(1-\alpha)^{1/2}}\left(\frac{c}{a_\infty}\right)^3\right]^{\gamma-1}, \tag{4.37}$$

where, following [Shapiro and Teukolsky 1983], we have re-introduced the speed of light c in the above expressions. The limit $\alpha \to 0$ in the above equation gives us the corresponding result of accretion of the fluid onto the Schwarzschild black hole [Shapiro and Teukolsky 1983].

4.4 Conclusions

In this chapter, we deal with static, spherically symmetric accretion onto black holes. Historically the accretion problem with a polytropic equation of state was addressed by Bondi [Bondi 1952]. He showed that subsonic flow far from a black hole will inevitably become supersonic, and that the requirement of a smooth traversal of the sonic surface uniquely specifies the accretion rate as a function of two thermodynamic variables, namely the density and temperature of the gas at infinity. The relativistic version of the same problem was solved by Michel [Michel 1972] twenty years later, after the discovery of celestial X-ray sources. He showed that accretion onto the black hole should be transonic. Accretion onto compact objects such as black holes and neutron stars is the most efficient method of releasing energy; up to 10 percent of the rest mass energy of the matter accreting on the black hole is liberated. Recent developments in the theory of accretion are significant steps toward understanding various astronomical sources that are believed to be powered by the accretion onto black holes. Spherical accretion onto a black hole is generally specified by the mass accretion rate $\dot{M}$ which is a key parameter, and there is evidence that a higher accretion rate can provide higher luminosity values. In view of this, we analyzed the steady state and spherical accretion of a fluid onto the Schwarzschild black hole in a string cloud background. We determined exact expressions for the mass accretion rate at the critical radius. It turns out that this quantity is modified so that $\dot{M} \approx M^2/(1-\alpha)^{3/2}$ with $r_s \approx M/(1-\alpha)$. Thus the accretion rate by the black hole in a string cloud background is higher than that for a Schwarzschild black hole. Thus the parameter α can be introduced in the problem of accretion onto black hole to extend the work of Michel [Michel 1972], and this quantity determines the accretion rate and other flow parameters. In principle, the accretion rate and other parameters still have the same characteristics as in the Schwarzschild black hole; in this sense we may conclude that the familiar steady state spherical accretion solution onto the Schwarzschild black hole is stable. In the limit $\alpha \to 0$, our results reduce exactly to those obtained in [Michel 1972; Shapiro and Teukolsky 1983] for the standard Schwarzschild black hole. We can attempt to work out the effect of string cloud background on the luminosity, the frequency spectrum and the energy conversion efficiency of the accretion flow. It is possible to deviate from spherical symmetry, e.g., include rotation, which may lead to a higher accretion rate. These and other related issues are currently under investigation.

Chapter 5

Covariant formalism

In general relativity, to understand how the spacetime behaves in presence of a given form of matter, we have to solve the Einstein field equations that describe the fundamental interaction of gravitation as a result of spacetime being curved by matter and energy. But the spacetime can be described in several ways:

- **metric formalism:** metric $g_{\mu\nu}$ defined in a particular coordinate basis, with connection given by Christoffel symbols.
- **tetrad formalism:** metric defined by a locally defined set of four linearly independent vector fields called a tetrad, with its connection given by the Ricci rotation coefficients.
- **semi-tetrad formalism:** via covariantly defined variables with respect to a partial frame formalism such as the 1+3 or 1+1+2 decompositions.

Though the metric and the tetrad formalism is widely used, the covariant formalism has the advantage of being gauge independent and physics can be described completely by tensor quantities which are invariant under choice of coordinates.

The chapter is organized as follows. We begin in Sec. 5.1 with the $1+3$ formalism followed by the $1+1+2$ approach in Sec. 5.2. After introducing LRS spacetime in Sec. 5.3, we mention LRS-II spacetime in Sec. 5.4 in which we will be working on in the next three chapters and also give the complete set of covariant equations in this spacetime. We conclude in Sec. 5.5.

5.1 1+3 Covariant approach

The $1+3$ decomposition or threading of spacetime [Ellis and H. v. Elst 1999; Ellis 2009; Ehlers 1993; Kundt and Trümper 1962; Maartens 1997] (see [Roy 2014] for a comparison with the so-called 3+1 formalism), where we split the spacetime into a timelike and an orthogonal three-dimensional spacelike hypersurface provides a covariant description of spacetime in terms of scalars, 3-vectors and projected symmetric trace-free (PSTF) 3-tensors governed by the Ricci and twice-contracted Bianchi identities. All informations are captured in a set of kinematic and dynamic variables.

5.1.1 Formalism

For the $1+3$ splitting of spacetime, we define a unit timelike vector (4-velocity) u^μ

$$u^\mu = \frac{dx^\mu}{d\tau} \qquad\qquad u_\mu\, u^\mu = -\,1\,, \tag{5.1}$$

where τ is the proper time along the observer's worldline. This defines the projection tensors along the timelike direction and on the 3-space as

$$\begin{aligned} U^\mu{}_\nu &= -\,u^\mu\, u_\nu\,, && \text{(parallel to } u^\mu\text{)} \\ h^\mu{}_\nu &= g^\mu{}_\nu + u^\mu u_\nu\,. && \text{(orthogonal to } u^\mu\text{)} \end{aligned}$$

The tensors satisfy the relations

$$U^\mu{}_\alpha\, U^\alpha{}_\nu = -\,U^\mu{}_\nu\;, \qquad U^\mu{}_\nu\, u^\nu = u^\mu\;, \qquad U^\mu{}_\mu = 1\,, \tag{5.2}$$

$$\text{and} \qquad h_{\mu\nu}\, u^\nu = 0\;, \qquad h^\mu{}_\alpha\, h^\alpha{}_\nu = h^\mu{}_\nu\;, \qquad h^\mu{}_\mu = 3\,. \tag{5.3}$$

The standard $1+3$ decomposition is performed in the following manner: any 4-vector b_μ is split into a scalar, B (parallel to u^μ), and a 3-vector, B_μ (orthogonal to u^μ):

$$b_\mu = -\,u_\mu B + B_\mu, \qquad \text{where} \qquad B \equiv b_\mu u^\mu \qquad \text{and} \qquad B^\mu \equiv h^\mu{}_\nu b^\nu\,; \tag{5.4}$$

and any projected rank-2 tensor $A_{\mu\nu}$ is split into

$$A_{\mu\nu} = A_{\langle\mu\nu\rangle} + \frac{1}{3} A\, h_{\mu\nu} + \epsilon_{\mu\nu\rho} A^\rho\,, \tag{5.5}$$

where $A \equiv h_{\mu\nu} A^{\mu\nu}$ is the spatial trace, $A_{\langle\mu\nu\rangle}$ is the PSTF 3-tensor defined as

$$A_{\langle\mu\nu\rangle} = \left(h^\rho{}_{(\mu} h^\sigma{}_{\nu)} - \frac{1}{3} h_{\mu\nu} h^{\rho\sigma} \right) A_{\rho\sigma}\,, \tag{5.6}$$

A_μ is the spatial vector which is spatially dual to the anti-symmetric part $\left(A_{[\mu\nu]}\right)$ of the rank-2 tensor defined as

$$A_\mu = \frac{1}{2}\epsilon_{\mu\nu\rho}A^{[\nu\rho]} \qquad \Leftrightarrow \qquad A_{[\mu\nu]} = \epsilon_{\mu\nu\rho}A^\rho\,, \tag{5.7}$$

and $\epsilon_{\mu\nu\delta}$ is the 3-volume element, defined as:

$$\epsilon_{\mu\nu\rho} = \eta_{\mu\nu\rho\sigma}u^\sigma = \sqrt{|g|}\delta^0{}_{[\mu}\delta^1{}_\nu\delta^2{}_\rho\delta^3{}_{\sigma]}u^\sigma\,. \qquad (\eta_{\mu\nu\rho\sigma}\text{ is the 4-volume element})$$

We can also define two derivatives: the covariant time derivative along the vector u^μ defined as

$$\dot{A}^{\mu..\nu}{}_{\rho..\sigma} = u^\alpha\nabla_\alpha A^{\mu..\nu}{}_{\rho..\sigma}\ , \tag{5.8}$$

and the orthogonally projected derivative defined as

$$D_\alpha A^{\mu..\nu}{}_{\rho..\sigma} = h^\mu{}_\gamma h^\delta{}_\rho ... h^\nu{}_\epsilon h^\xi{}_\sigma h^\beta{}_\alpha\nabla_\beta A^{\gamma..\epsilon}{}_{\delta..\xi}\ , \tag{5.9}$$

with projection on all the free indices. It is worth noting that these derivatives do not generally commute and give rise to various commutator relations, which play an integral part in partial frame formalisms.

5.1.2 Variables

Using Eqs. (5.8) and (5.9), we can define the splitting of the covariant derivative of the scalar field Ψ as

$$\nabla_\mu\Psi = -u_\mu\dot{\Psi} + D_\mu\Psi\,, \tag{5.10}$$

and that of the 4-velocity u^μ into its irreducible parts as

$$\begin{aligned}\nabla_\mu u_\nu &= -u_\mu\dot{u}_\nu + D_\mu u_\nu \\ &= -u_\mu\dot{u}_\nu + \frac{1}{3}\theta\, h_{\mu\nu} + \sigma_{\mu\nu} + \omega_{\mu\nu}\,.\end{aligned} \tag{5.11}$$

The geometrical quantities in Eq. (5.11), arising from the relative motion of the comoving observers are listed below

- Relativistic acceleration vector: $\dot{u}^\mu \ = \ u^\nu\nabla_\nu u^\mu$
  (represents effect of forces other than gravity on the observer)

- Rate of (volume) expansion of the fluid: $\theta \equiv D_\mu u^\mu$
- Trace-free symmetric rate of shear tensor: $\sigma_{\mu\nu} = \sigma_{\langle\mu\nu\rangle} \equiv D_{\langle\mu}u_{\nu\rangle}$
  (represents rate of distortion of the congruence)
- Antisymmetric vorticity tensor: $\omega_{\mu\nu} = \omega_{[\mu\nu]} \equiv D_{[\mu}u_{\nu]}$
  (represents rotation of the congruence relative to the non-rotating frame)

The Riemann curvature tensor represents the spacetime completely which is fully determined by the Weyl tensor $W_{\mu\nu\rho\sigma}$ (free gravitational field) and the Ricci tensor, which is determined locally at each point by the energy momentum tensor ($R = -T$), as given in Eq. (1.5).

So, in a fully $1+3$ covariant approach, we can split the Weyl curvature tensor relative to u^μ into

- Electric part: $E_{\mu\nu} = E_{\langle\mu\nu\rangle} = W_{\mu\rho\nu\sigma}u^\rho u^\sigma$
- Magnetic part: $H_{\mu\nu} = H_{\langle\mu\nu\rangle} = \frac{1}{2}\epsilon_{\mu\rho\sigma}W^{\rho\sigma}{}_{\nu\xi}u^\xi$

Also the energy momentum tensor $T_{\mu\nu}$ can be decomposed relative to u^μ as

$$T_{\mu\nu} = \rho u_\mu u_\nu + p h_{\mu\nu} + q_\nu u_\mu + q_\mu u_\nu + \pi_{\mu\nu}\,. \tag{5.12}$$

The matter variables defined in Eq. (5.12) are as follows:

- Relativistic energy density relative to u^μ: $\rho \equiv T_{\mu\nu}u^\mu u^\nu$
- Total isotropic pressure: $p \equiv \frac{1}{3}T_{\mu\nu}h^{\mu\nu}$
- Relativistic momentum density (energy flux relative to u^μ): $q^\mu \equiv -T_{\nu\rho}u^\nu h^{\rho\mu}$
- PSTF anisotropic pressure (stress): $\pi_{\mu\nu} = \pi_{\langle\mu\nu\rangle} \equiv T_{\rho\sigma}h^\rho{}_{\langle\mu}h^\sigma{}_{\nu\rangle}$

Hence, any arbitrary spacetime can be completely characterized by the irreducible set of geometrical and matter variables

$$\{\dot{u}^\mu,\ \theta,\ \sigma_{\mu\nu},\ \omega_{\mu\nu},\ E_{\mu\nu},\ H_{\mu\nu}\} \qquad \{\rho,\ p,\ q^\mu,\ \pi_{\mu\nu}, \Lambda\}\,, \tag{5.13}$$

where Λ is the cosmological constant which acts as an energy density term in the field equations. A set of tensor equations for the above mentioned variables from the Ricci identity

$$2\nabla_{[\mu}\nabla_{\nu]}u^\rho = R_{\mu\nu}{}^\rho{}_\sigma u^\sigma\,, \tag{5.14}$$

and the twice-contracted Bianchi identity

$$\nabla_\mu R^\mu{}_\rho + \nabla_\nu R^\nu{}_\rho - \nabla_\rho R = 0 \qquad \Leftrightarrow \qquad \nabla^\mu G_{\mu\nu} = 0\,, \tag{5.15}$$

covariantly describe the spacetime as an alternative formulation of EFEs.

5.2 1+1+2 Covariant approach

The covariant 1+3 approach works extremely well in cosmological applications when the background model is homogeneous and isotropic, that is of Friedman-Lemaître-Robertson-Walker (FLRW) type. By virtue of the symmetry, the $1+3$ decomposition gives rise to equations involving only scalars. However, if the spacetime under consideration has less symmetry, the 1+3 approach is no longer ideally suited because its splitting in 'time' and 'space' relative to the fundamental observer is not sensitive to another preferred direction apart from 'time'. The description of spacetime through covariant quantities, defined in the observer's rest space, is simply blind to a second distinguished direction. The formalism follows the same strategy as the 1+3 decomposition where we further decompose the 3-hypersurface into a spacelike vector and a 2-space. This strategy was developed in [C. A. Clarkson and Barrett 2003; C. Clarkson 2007] (see also [K. Maeda et al. 1980] for the so-called $2+1+1$ formalism). Analogously, the quantities of the rest space are further covariantly split in such a way that obtained quantities still have a clear geometrical or physical meaning. The 1+1+2 approach thus naturally extends the 1+3 approach and keeps its many benefits.

5.2.1 Formalism

To deal with the preferred radial direction in spherical symmetric case, we split the 3-space by introducing a unit spacelike vector n^μ orthogonal to u^μ:

$$n_\mu u^\mu = 0\;, \quad n_\mu n^\mu = 1. \tag{5.16}$$

with a projection tensor on the 2-space (sheet) orthogonal to n^μ and u^μ

$$N_\mu{}^\nu \equiv h_\mu{}^\nu - n_\mu n^\nu = g_\mu{}^\nu + u_\mu u^\nu - n_\mu n^\nu\,, \tag{5.17}$$

with

$$N^\mu{}_\mu = 2\,, \qquad \text{and} \qquad n^\mu N_{\mu\nu} = 0 = u^\mu N_{\mu\nu}\,. \tag{5.18}$$

Any 3-vector ψ^μ can now be irreducibly split into a scalar, Ψ (parallel to n^μ), and a vector, Ψ^μ (orthogonal to n^μ) on the sheet:

$$\psi^\mu = \Psi n^\mu + \Psi^\mu \,, \qquad \text{where} \qquad \Psi \equiv \psi_\mu n^\mu \qquad \text{and} \qquad \Psi^\mu \equiv N^{\mu\nu}\psi_\nu \,. \tag{5.19}$$

Similarly, any PSTF 3-tensor, $\psi_{\mu\nu}$, can be split into:

$$\psi_{\mu\nu} = \psi_{\langle\mu\nu\rangle} = \Psi\left(n_\mu n_\nu - \frac{1}{2}N_{\mu\nu}\right) + 2\Psi_{(\mu}n_{\nu)} + \Psi_{\mu\nu} \,, \tag{5.20}$$

where $\Psi \equiv n^\mu n^\nu \psi_{\mu\nu} = -N^{\mu\nu}\psi_{\mu\nu}$ is the scalar, $\Psi_\mu \equiv N_\mu{}^\nu n^\rho \psi_{\nu\rho}$ is the 2-vector and $\Psi_{\mu\nu}$ is the 2-tensor defined as:

$$\Psi_{\mu\nu} = \Psi_{\mu\nu} \equiv \left(N_{(\mu}{}^\rho N_{\nu)}{}^\sigma - \frac{1}{2}N_{\mu\nu}N^{\rho\sigma}\right)\psi_{\rho\sigma} \,. \tag{5.21}$$

The curly brackets denote the PSTF tensors on the 2-sheet.

Hence we can define two additional derivatives: along n^μ in the surface orthogonal to u^μ

$$\hat{A}_{\mu..\nu}{}^{\rho..\sigma} \equiv n^\alpha D_\alpha A_{\mu..\nu}{}^{\rho..\sigma} \;, \tag{5.22}$$

and a projected derivative onto the sheet defined

$$\delta_\alpha A_{\mu..\nu}{}^{\rho..\sigma} \equiv N_\mu{}^\beta ... N_\nu{}^\gamma N_\delta{}^\rho .. N_\xi{}^\sigma N_\alpha{}^k D_k A_{\beta..\gamma}{}^{\delta..\xi} \,, \tag{5.23}$$

with projection on all free indices. As in $1+3$ formalism, these derivatives do not commute in general.

5.2.2 Variables

According to Eqs. (5.19) and (5.19), the $1+3$ geometric quantities can be split as follows

$$\dot{u}^\mu = \mathcal{A}n^\mu + \mathcal{A}^\mu \,, \tag{5.24}$$

$$\omega^\mu = \Omega n^\mu + \Omega^\mu \,, \tag{5.25}$$

$$\sigma_{\mu\nu} = \Sigma\left(n_\mu n_\nu - \frac{1}{2}N_{\mu\nu}\right) + 2\Sigma_{(\mu}n_{\nu)} + \Sigma_{\mu\nu} \,, \tag{5.26}$$

$$E_{\mu\nu} = \mathcal{E}\left(n_\mu n_\nu - \frac{1}{2}N_{\mu\nu}\right) + 2\mathcal{E}_{(\mu}n_{\nu)} + \mathcal{E}_{\mu\nu} \,, \tag{5.27}$$

$$H_{\mu\nu} = \mathcal{H}\left(n_\mu n_\nu - \frac{1}{2}N_{\mu\nu}\right) + 2\mathcal{H}_{(\mu}n_{\nu)} + \mathcal{H}_{\mu\nu} \,. \tag{5.28}$$

The covariant derivative of the radial unit vector n^μ in its irreducible form can be obtained in the similar way as Eq. (5.11)

$$\nabla_\mu n_\nu = -\mathcal{A} u_\mu u_\nu - u_\mu \alpha_\nu + \left(\frac{1}{3}\theta + \Sigma\right) n_\mu u_\nu + \left(\Sigma_\mu - \epsilon_{\mu\rho}\Omega^\rho\right) u_\nu$$
$$+ n_\mu a_\nu + \frac{1}{2}\phi N_{\mu\nu} + \xi \epsilon_{\mu\nu} + \zeta_{\mu\nu}\,, \tag{5.29}$$

from which the covariant spatial derivative of n^μ can be obtained as:

$$D_\mu n_\nu = n_\mu a_\nu + \frac{1}{2}\phi N_{\mu\nu} + \xi \epsilon_{\mu\nu} + \zeta_{\mu\nu}\,, \tag{5.30}$$

where $\epsilon_{\mu\nu}$ is the 2-volume element on the sheet defined as:

$$\epsilon_{\mu\nu} = \epsilon_{\mu\nu\rho} n^\rho\,. \tag{5.31}$$

The new kinematic variables are as follows:

- Acceleration of the sheet: $a_\mu \;\equiv\; n^\nu D_\nu n_\mu \;=\; \hat{n}_\mu$
- Expansion of the sheet: $\phi \;\equiv\; \delta_\mu n^\mu$
- Twisting of the sheet (rotation of n^μ): $\xi \;\equiv\; \frac{1}{2}\epsilon^{\mu\nu}\delta_\mu n_\nu$
- Shear of the sheet (distortion): $\zeta_{\mu\nu} \;\equiv\; \delta_{\mu_\nu} n$

The derivative of n^μ along u^μ is given by

$$\dot{n}_\mu = \mathcal{A} u_\mu + \alpha_\mu\,, \tag{5.32}$$

where $\mathcal{A} \equiv n^\mu \dot{u}_\mu$ and $\alpha_\mu \equiv N_{\mu\nu}\dot{n}^\nu$.

Also, the full decomposition of the covariant derivative of u^μ in terms of $1+1+2$ variables is given by

$$\nabla_\mu u_\nu = -u_\mu \left(\mathcal{A} n_\nu + \mathcal{A}_\nu\right) + n_\mu n_\nu \left(\frac{1}{3}\theta + \Sigma\right) + n_\mu \left(\Sigma_\nu + \epsilon_{\nu\rho}\Omega^\rho\right)$$
$$+ \left(\Sigma_\mu - \epsilon_{\mu\rho}\Omega^\rho\right) n_\nu + N_{\mu\nu}\left(\frac{1}{3}\theta - \frac{1}{2}\Sigma\right) + \Omega\epsilon_{\mu\nu} + \Sigma_{\mu\nu}\,, \tag{5.33}$$

which implies the relation

$$\hat{u}_\mu = \left(\frac{1}{3}\theta + \Sigma\right) n_\mu + \Sigma_\mu + \epsilon_{\mu\nu}\Omega^\nu\,. \tag{5.34}$$

Finally, the matter variables are split as follows

$$q^\mu = Qn^\mu + Q^\mu \,, \tag{5.35}$$

$$\pi_{\mu\nu} = \Pi\left(n_\mu n_\nu - \frac{1}{2}N_{\mu\nu}\right) + 2\Pi_{(\mu}n_{\nu)} + \Pi_{\mu\nu} \,, \tag{5.36}$$

which leads to the EMT in terms of $1+1+2$ variables as

$$T_{\mu\nu} = \rho u_\mu u_\nu + p h_{\mu\nu} + 2u_{(\mu}\left[Qn_{\nu)} + Q_{\nu)}\right] + \Pi\left(n_\mu n_\nu - \frac{1}{2}N_{\mu\nu}\right) + 2\Pi_{(\mu}n_{\nu)} + \Pi_{\mu\nu} \,. \tag{5.37}$$

So, in the $1+1+2$ formalism, any arbitrary spacetime can be completely characterized irreducibly by the following geometrical and matter variables:

$$\begin{gathered}\{\theta,\ \mathcal{A},\ \Omega,\ \Sigma,\ \phi,\ \xi,\ \mathcal{E},\ \mathcal{H},\ \mathcal{A}^\mu,\ \Omega^\mu,\ \Sigma^\mu,\ \alpha^\mu,\ a^\mu,\ \mathcal{E}^\mu,\ \mathcal{H}^\mu,\ \Sigma_{\mu\nu},\ \zeta_{\mu\nu},\ \mathcal{E}_{\mu\nu},\ \mathcal{H}_{\mu\nu}\} \\ \{\rho,\ p,\ Q,\ \Lambda,\ \Pi,\ Q^\mu,\ \Pi^{\mu\nu}\} \,.\end{gathered} \tag{5.38}$$

5.3 LRS spacetime

Locally rotationally symmetric spacetimes possess a continuous isotropy group at each point and hence a multi-transitive isometry group [H. v. Elst and Ellis 1996]. Since LRS spacetimes exhibit locally a preferred spatial direction, the 1+1+2 formalism is therefore ideally suited for covariant description of these spacetimes, yielding a complete characterization in terms of invariant scalar quantities that have physical or direct geometrical meaning [C. A. Clarkson and Barrett 2003; Betschart and C. A. Clarkson 2004]. The preferred spatial direction in the LRS spacetimes constitutes a local axis of symmetry and in this case n^μ is a vector pointing along the axis of symmetry and is thus called a 'radial' vector. Since LRS spacetimes are defined to be isotropic, this allows for the vanishing of all 1+1+2 vectors and tensors, such that there are no preferred directions in the sheet. Thus, all the non-zero 1+1+2 covariantly defined scalars that fully describe LRS spacetimes are

$$\{\mathcal{A},\ \theta,\ \phi,\ \xi,\ \Sigma,\ \Omega,\ \mathcal{E},\ \mathcal{H},\ \rho,\ p,\ Q,\ \Pi,\ \Lambda\} \,. \tag{5.39}$$

5.4 LRS-II spacetime

A subclass of the LRS spacetimes, called LRS class II spacetimes [Ellis 1967; Stewart and Ellis 1968; H. v. Elst and Ellis 1996], contains all the LRS spacetimes that are rotation free. Also, the spacetime is vorticity free which further constrains the magnetic Weyl curvature $\mathcal{H} = 0$

[Betschart and C. A. Clarkson 2004]. As a consequence, in LRS-II spacetimes the variables Ω, ξ and $\mathcal{H}$ are identically zero and the variables

$$\{\mathcal{A},\ \theta,\ \phi,\ \Sigma,\ \mathcal{E},\ \rho,\ p,\ Q,\ \Pi,\ \Lambda\}\,, \tag{5.40}$$

fully characterise the kinematics. To describe these spacetimes in terms of metric components, it is well known that the most general interval for LRS-II is written as [Stewart and Ellis 1968]

$$ds^2 = -A^2(t,\chi)\,dt^2 + B^2(t,\chi)\,d\chi^2 + C^2(t,\chi)\,[\,dy^2 + D^2(y,k)\,dz^2\,]\,, \tag{5.41}$$

where t and χ are parameters along the integral curves of the timelike vector field $u^\mu = A^{-1}\delta^\mu_0$ and the preferred spacelike vector field $n^\mu = B^{-1}\delta^\mu_1$. The function $D(y,k) = \sin y, y, \sinh y$ for $k = (1, 0, -1)$ respectively. The 2-metric $dy^2 + D^2(y,k)\,dz^2$ describes spherical, flat, or open homogeneous and isotropic 2-surfaces for $k = (1, 0, -1)$. Spherically symmetric spacetimes are the $k = 1$ subclass of these spacetimes. One can easily see that all the physically interesting spherically symmetric spacetimes fall in the class LRS-II.

5.4.1 Equations

The complete set of propagation and/or evolution equations which define these spacetimes, namely LRS class II spacetimes, are

Propagation equations:

$$\hat{\phi} = -\frac{1}{2}\phi^2 + \left(\frac{1}{3}\theta + \Sigma\right)\left(\frac{2}{3}\theta - \Sigma\right) - \frac{2}{3}\left(\rho + \Lambda\right) - \frac{1}{2}\Pi - \mathcal{E}\ , \tag{5.42a}$$

$$\hat{\Sigma} - \frac{2}{3}\hat{\theta} = -\frac{3}{2}\phi\Sigma - Q\ , \tag{5.42b}$$

$$\hat{\mathcal{E}} - \frac{1}{3}\hat{\rho} + \frac{1}{2}\hat{\Pi} = -\frac{3}{2}\phi\left(\mathcal{E} + \frac{1}{2}\Pi\right) + \left(\frac{1}{2}\Sigma - \frac{1}{3}\theta\right)Q\ , \tag{5.42c}$$

Evolution equations:

$$\dot{\phi} = -\left(\Sigma - \frac{2}{3}\theta\right)\left(\mathcal{A} - \frac{1}{2}\phi\right) + Q\ , \tag{5.43a}$$

$$\dot{\Sigma} - \frac{2}{3}\dot{\theta} = -\mathcal{A}\phi + 2\left(\frac{1}{3}\theta - \frac{1}{2}\Sigma\right)^2 + \frac{1}{3}\left(\rho + 3p - 2\Lambda\right) - \mathcal{E} + \frac{1}{2}\Pi\ , \tag{5.43b}$$

$$\dot{\mathcal{E}} - \frac{\dot{\rho}}{3} + \frac{\dot{\Pi}}{2} = \left(\frac{3}{2}\Sigma - \theta\right)\mathcal{E} + \frac{\Pi}{4}\left(\Sigma - \frac{2}{3}\theta\right) + \frac{\phi Q}{2} - \frac{\rho + p}{2}\left(\Sigma - \frac{2}{3}\theta\right)\ . \tag{5.43c}$$

Mixed (Propagation/Evolution) equations:

$$\hat{\mathcal{A}} - \dot{\theta} = -(\mathcal{A} + \phi)\,\mathcal{A} + \frac{1}{3}\theta^2 + \frac{3}{2}\Sigma^2 + \frac{1}{2}(\rho + 3p - 2\Lambda)\ , \tag{5.44a}$$

$$\dot{\rho} + \hat{Q} = -\theta(\rho + p) - (\phi + 2\mathcal{A})\,Q - \frac{3}{2}\Sigma\Pi\ , \tag{5.44b}$$

$$\dot{Q} + \hat{p} + \hat{\Pi} = -\left(\frac{3}{2}\phi + \mathcal{A}\right)\Pi - \left(\frac{4}{3}\theta + \Sigma\right)Q - (\rho + p)\,\mathcal{A}\ , \tag{5.44c}$$

where Λ is the cosmological constant. We also define the Gaussian curvature on the 2-sheet via the Ricci tensor on the sheet ${}^2R_{\mu\nu} = KN_{\mu\nu}$ which can be written in the form [Betschart and C. A. Clarkson 2004]

$$K = \frac{1}{3}(\rho + \Lambda) - \mathcal{E} - \frac{\Pi}{2} + \frac{\phi^2}{4} - \left(\frac{1}{3}\theta - \frac{1}{2}\Sigma\right)^2\ , \tag{5.45}$$

which from Eqs. (5.42a)-(5.43c) give

$$\hat{K} = -\phi K\ , \tag{5.46}$$

$$\dot{K} = -\left(\frac{2}{3}\theta - \Sigma\right)K\ . \tag{5.47}$$

From Eq. (5.47), it follows that whenever the Gaussian curvature of the sheet is non-zero and constant in time, the shear is always proportional to the expansion:

$$\dot{K} = 0 \implies \Sigma = \frac{2}{3}\theta \quad \text{for} \quad K \neq 0\,. \tag{5.48}$$

5.4.2 Misner-Sharp mass

For the metric (5.41), we can define the mass function as [Stephani et al. 2004]:

$$\mathcal{M}(\chi, t) = \frac{C}{2}\left(k - \nabla_\mu C \nabla^\mu C\right)\ . \tag{5.49}$$

For spherically symmetric spacetimes, $k = 1$, and we can write $C = \frac{1}{\sqrt{K}}$. Then Eq. (5.49) becomes

$$\mathcal{M} = \frac{1}{2\sqrt{K}}\left(1 - \frac{1}{4K^3}\nabla_\mu K \nabla^\mu K\right)\ . \tag{5.50}$$

Geometrically, the above expression gives the amount of mass enclosed within the spherical shell at a given value of affine parameter of the integral curves of n^μ at a given instant of time. This is the Misner-Sharp (MS) mass. The square of the covariant derivative of the Gaussian curvature can be written as

$$\nabla_\mu K \nabla^\mu K = \left(-u^\mu u^\nu + n^\mu n^\nu\right) \nabla_\mu K \nabla_\nu K = -\dot{K}^2 + \hat{K}^2 \,. \tag{5.51}$$

Using the 1+1+2 decomposition of the covariant derivative for LRS-II spacetime with Eqs. (5.45)-(5.47), the MS mass takes the form

$$\mathcal{M}_{MS} = \frac{1}{2K^{3/2}} \left(\frac{1}{3}(\rho + \Lambda) - \mathcal{E} - \frac{1}{2}\Pi \right) \,. \tag{5.52}$$

It can be easily seen that even in the case of vacuum spacetimes, the mass does not vanish due to the electric part of the Weyl Curvature $\mathcal{E}$, which acts as a mass source.

5.5 Conclusions

This chapter provided an extensive review of both the $1+3$ and $1+1+2$ covariant approaches to general relativity. In the $1+3$ formalism, a time like flow u^a is introduced which splits spacetime into 'time' and 'space'. The $1+1+2$ further decomposes the '3-space' relative to a preferred spatial vector n^a . Locally rotationally symmetric spacetime is then introduced and the full system of field equations (evolution, propagation and mixed) for LRS-II spacetime is given in the $1+1+2$ formalism which are derived from the Bianchi and Ricci identities and are gauge invariant (coordinate independent). From the structure of these equations we can already obtain some important information about the spacetime in general since the covariant decomposition of the spacetime introduces quantities that have a clear physical or geometrical meaning, which gives a better understanding of the underlying physics which sometimes remains obscure in the metric approach.

Chapter 6

Global structure of black holes via dynamical system

As mentioned in chapter 1, in general relativity, any spacetime can be regarded as a solution to the Einstein field equations $G_{\mu\nu} = T_{\mu\nu}$, if we define the energy momentum tensor of the matter according to the left hand side of the equation, which can be calculated from the metric tensor of the spacetime. However, the matter tensor so defined will in general have nonphysical properties and, in most of the cases, will have no resemblance to the standard matter around us. Hence by the term *exact solution* of Einstein field equations, we shall mean the following: A spacetime $(\mathcal{M}, \mathbf{g})$ in which the field equations are satisfied with the energy momentum tensor $T_{\mu\nu}$ of some specific form of matter which obeys the postulate of local causality and at least one of the physically reasonable energy conditions [Hawking and Ellis 1973]. Most of the well known exact solutions are thus for the empty space ($T_{\mu\nu} = 0$), for an electromagnetic field, for a perfect fluid or for combination of these. Because of the extreme complexity of the field equations, which are in general 10 coupled nonlinear second order partial differential equations, it is impossible to find exact solutions except in spaces of high symmetry (e.g. spherical symmetry) and for relatively simple matter content. In this regard these exact solutions are rather idealised.

Nevertheless, the exact solutions give the idea of important qualitative features that can arise in GR and hence also the possible properties of the realistic solutions of field equations. One of the most intriguing and challenging tasks is to find the global properties of the field equations by the maximal analytic extension of the local solutions. Study of global structures of the solutions are important as we get the maximal manifold $(\mathcal{M}, \mathbf{g})$ on which the solution is valid and hence the maximal complete atlas. This enables us to get rid of all coordinate singularities that may appear due to bad choice of coordinates while solving the field equations. Obtaining such a maximal extension may be tedious and tricky as we need to cleverly redefine the spacetime coordinates so that the region around the coordinate singularity becomes regular. By this step, we get rid of the coordinate singularity and the metric tensor becomes nondegenerate even in the locus of the previous coordinate singularity. We may continue it as far as we can till this process ultimately stops because the spacetime is surrounded either by asymptotic infinity - infinite volume where trajectories may be extended to an infinite proper length - or by genuine (curvature) singularities that cannot be extended by any coordinate. Geodesics physically terminate at such real singularities.

We know the dynamical systems approach has proven to be a very important mathematical tool in studying the global properties of various cosmologies in GR [Wainwright and Ellis 1997] and also other higher order theories of gravity [Carloni et al. 2005; Amendola, Gannouji, et al. 2007; Goheer et al. 2009; Zhou et al. 2009; Xiao and Zhu 2011; Leon and Saridakis 2013; Heisenberg et al. 2014; Chiba et al. 2014; Kofinas et al. 2014]. Similar analysis were performed to study the properties of spherically symmetric solutions in dimensionally reduced spacetimes and diatonic black holes in GR and other higher order theories of gravity [Mignemi and Wiltshire 1989; Wiltshire 1991; Mignemi and Wiltshire 1992; Poletti and Wiltshire 1994; Mignemi 2000; Melis and Mignemi 2005; Clifton and Barrow 2005]. The most important advantage of the dynamical systems technique is that without solving the system completely we can have qualitative informations on important global features of the phase space, in terms of the fixed points of the system, their stabilities and different invariant submanifolds of the complete phase space.

The aim of this work is as follows:

- Using a semi-tetrad covariant formalism, we show that we can recast the field equations (which are the combination of Ricci and doubly contracted Bianchi identities) for vacuum (with or without a cosmological constant) or electrovacua Locally rotationally symmetric type II (LRS-II) spacetimes into an autonomous system of covariantly defined variables. Hence by definition, this autonomous system is gauge independent.
- Using the usual Poincaré compactification, we compactify the phase space of this autonomous system.
- Using the general symmetries of LRS-II spacetimes and the properties of the phase space of the above defined autonomous system, we show that we can have the qualitative idea of all the important global features of these spacetimes, without actually solving the system.

Thus the analysis developed in this work can be effectively used to find the important global properties of other more realistic solutions of Einstein field equations, without solving these equations.

In this work, we confine our attention to spherically symmetric vacuum (with or without a cosmological constant) or electrovacuum, see chapters 7 and 8 for applications to modified gravity theories. For technical reasons, it is convenient to consider a class of spacetimes which is a small generalization of spherically symmetric metrics: namely *Locally rotationally symmetric* class II spacetimes [Ellis 1967; Stewart and Ellis 1968; H. v. Elst and Ellis 1996] described in chapter 5.

It has been recently shown in [Goswami and Ellis 2011], that a vacuum or electrovac LRS-II spacetime (with or without a cosmological constant) has an extra symmetry in terms of existence of a Killing vector in the local $[u, n]$-plane, where u^μ and n^μ are timelike and spacelike vector fields respectively, defined above. This extra Killing vector, if timelike, makes the spacetime locally static and, if spacelike, makes the spacetime locally spatially homogeneous. In the maximally extended manifold these two sections are joined via a 3-dimensional submanifold, commonly known as the event horizon. Using this extra symmetry of LRS-II spacetimes, we recast the field equations into a covariantly defined autonomous system separately for both these sections, compactify the phase spaces and show that we can recover all the important features of the global properties of these solutions.

The chapter is organized as follows. We write down the general autonomous equations for both static and nonstatic cases in LRS-II spacetime in Sec. 6.1. In Sec. 6.2, we study the vacuum solutions followed by adding the cosmological constant in Sec. 6.3. Finally in Sec. 6.4, we study the charged spacetime and conclude in Sec. 6.5. This chapter is based on published work [Ganguly et al. 2015]

6.1 Autonomous system

In the most general case we will consider only electromagnetic field. Assuming that we do not have magnetic monopoles or using the duality rotation [Plebanski and Krasinski 2006], we can always suppress the magnetic field in the vacuum. Also the electric field can be decomposed in the form $E^\mu = En^\mu$ which is a solution of $\hat{E} = -\phi E$ and $\dot{E} = (\Sigma - \frac{2}{3}\theta)E$. We have $F_{\mu\nu} = \frac{1}{2}u_{[\mu}E_{\nu]}$ from which we have

$$T_{\mu\nu} = \frac{E^2}{\mu_0}\left[\frac{1}{2}g_{\mu\nu} + u_\mu u_\nu - n_\mu n_\nu\right], \tag{6.1}$$

where μ_0 is the permeability in free space. This gives $Q = 0$, $\Pi = -4\rho/3$, $P = \rho/3$ and $\rho = E^2/2\mu_0$. We can always absorb the constants and work with the variable ρ which is solution of the equations

$$\hat{\rho} = -2\phi\rho \ , \tag{6.2}$$

$$\dot{\rho} = 2(\Sigma - \frac{2}{3}\theta)\rho \ . \tag{6.3}$$

Also, notice that Eq. (5.45) is a constraint because for any surface K is fixed, e.g. in Schwarzschild coordinates we have $K = 1/r^2$. This equation will be used to define the dimensionless variables as the Friedmann equation is used in cosmology.

6.1.1 Static case

In this part, we will consider spacetime with an additional timelike killing vector. Therefore all the time derivatives are zero, hence it can easily be seen from the previous equations that $\theta = \Sigma = Q = 0$. As a consequence the variables $\{\mathcal{A}, \phi, \mathcal{E}, \rho, \Lambda\}$ fully characterize the kinematics. We define the dimensionless geometrical variables in the following way

$$x_1 = -\frac{\mathcal{E}}{K}, \ x_2 = \frac{\phi}{2\sqrt{K}}, \ x_3 = \frac{\mathcal{A}}{\sqrt{K}}, \ x_4 = \frac{\Lambda}{3K}, \ x_5 = \frac{\rho}{K} \ . \tag{6.4}$$

Using Eqs. (6.2) and (6.3), we have from Eqs. (5.42a)-(5.47):

$$x_1' = x_2(2x_5 - x_1) \ , \tag{6.5a}$$

$$x_2' = \frac{x_1}{2} - x_4 \ , \tag{6.5b}$$

$$x_3' = x_5 - 3x_4 - x_3(x_2 + x_3) \ , \tag{6.5c}$$

$$x_4' = 2x_2x_4 \ , \tag{6.5d}$$

$$x_5' = -2x_2x_5 \ , \tag{6.5e}$$

$$0 = x_1 - 2x_4 - 2x_2x_3 \ , \tag{6.5f}$$

$$1 = x_1 + x_2^2 + x_4 + x_5 \ , \tag{6.5g}$$

where we have defined the dimensionless spatial derivative $x' = \hat{x}/\sqrt{K}$.

6.1.2 Nonstatic case

In the previous subsection, we discussed the static case. Here we will assume the presence of spacelike killing vector. Hence all space-derivatives will be zero. Therefore, for the nonstatic

Universe, $\phi = \mathcal{A} = Q = 0$ and the variables $\{\theta, \Sigma, \mathcal{E}, \rho, \Lambda\}$ completely characterize the system. Along with the definitions in (6.4), we further define two new variables

$$x_6 = \frac{\theta}{3\sqrt{K}}, \; x_7 = -\frac{\Sigma}{2\sqrt{K}} \; . \tag{6.6}$$

Here the propagation of the variables will be zero and only the evolution terms remain. Similar to the static case, using Eqs. (6.2) and (6.3), the system of equations from (5.42a)-(5.47), turns out to be

$$\mathring{x}_1 = (2x_5 - x_1)(x_6 + x_7) \; , \tag{6.7a}$$
$$\mathring{x}_4 = 2x_4(x_6 + x_7) \; , \tag{6.7b}$$
$$\mathring{x}_5 = -2x_5(x_6 + x_7) \; , \tag{6.7c}$$
$$\mathring{x}_6 = x_7(x_6 - 2x_7) + x_4 - \frac{x_5}{3} \; , \tag{6.7d}$$
$$\mathring{x}_7 = x_7(2x_7 - x_6) + \frac{x_5}{3} - \frac{x_1}{2} \; , \tag{6.7e}$$
$$1 = x_1 + x_4 + x_5 - (x_6 + x_7)^2 \; , \tag{6.7f}$$
$$0 = x_1 - 2x_4 + 2(x_6 - 2x_7)(x_6 + x_7) \; . \tag{6.7g}$$

where we define the dimensionless temporal derivative $\mathring{x} = \dot{x}/\sqrt{K}$.

6.2 Vacuum spacetime

In this section we will assume vacuum, i.e. $\rho = p = \Pi = \Lambda = 0$.

6.2.1 Static

Only the variables x_1, x_2 and x_3 are nonzero. We use the last constraint (6.5g) to reduce the system to

$$x_2' = x_2 x_3 \, , \tag{6.8}$$
$$x_3' = -x_3(x_2 + x_3) \, , \tag{6.9}$$
$$1 = 2x_2 x_3 + x_2^2 \, . \tag{6.10}$$

The analysis of the system is carried out in the standard way. Notice that the full knowledge of the dynamical system should comprise its behaviour at infinity. Hence we transform the phase space into the so-called Poincaré sphere, a sphere with unit radius, tangent to the plane (x_2, x_3) at the origin. Every point of the plane (x_2, x_3) is mapped into 2 points on the surface

Dynamical system	Critical points	Stability	Nature
$x_2' = x_2 x_3$	$P_M : (x_2, x_3) = (1, 0)$	Attractor	Minkowski
$x_3' = -x_3(x_2 + x_3)$	$\bar{P}_M : (x_2, x_3) = (-1, 0)$	Repeller	Minkowski
$2x_2 x_3 + x_2^2 = 1$			
$X_2' = X_2 X_3(X_2 X_3 + 2X_3^2 + Z^2)$	$P_H : (X_2, X_3) = (0, 1)$	Repeller	Horizon
$X_3' = -X_2^2 X_3(X_2 + 2X_3) - X_3(X_2 + X_3)Z^2$	$\bar{P}_H : (X_2, X_3) = (0, -1)$	Attractor	Horizon
$X_2^2 + X_3^2 + Z^2 = 1$	$P_S : (X_2, X_3) = (\frac{2}{\sqrt{5}}, -\frac{1}{\sqrt{5}})$	Repeller	Singularity
$X_2^2 + 2X_2 X_3 = Z^2$	$\bar{P}_S : (X_2, X_3) = (-\frac{2}{\sqrt{5}}, \frac{1}{\sqrt{5}})$	Attractor	Singularity

TABLE 6.1: Critical points and their stability in both finite and infinite (Poincaré sphere) domains corresponding to static black hole and white hole.

of the sphere which are situated on the line passing through the point (x_2, x_3) and the centre of the sphere. Therefore, infinitely distant points of the plane are mapped into the equator of the sphere. Finally, we will represent the orthogonal projection of any one of the hemispheres (to do away with duplicate points) of the sphere onto the tangent plane. This is the projective plane. In the compactified phase portrait, we will use capital letters (X_2, X_3). Under Poincaré transformation, the equations become

$$X_2' = X_2 X_3(X_2 X_3 + 2X_3^2 + Z^2)\,, \tag{6.11}$$

$$X_3' = -X_2^2 X_3(X_2 + 2X_3) - X_3(X_2 + X_3)Z^2\,, \tag{6.12}$$

$$Z' = Z X_3(-1 + X_2 X_3 + 2X_3^2 + Z^2)\,, \tag{6.13}$$

$$Z^2 = 2X_2 X_3 + X_2^2\,, \tag{6.14}$$

$$1 = X_2^2 + X_3^2 + Z^2\,, \tag{6.15}$$

where we have defined $x_i = X_i/Z$ with the constraint $X_2^2 + X_3^2 + Z^2 = 1$ and rescaled the derivative $ZX' \to X'$. The analysis of the dynamical system for vacuum is summarized in Table 6.1 and the phase portrait is shown in Fig.6.1. Notice that for each point we have given the stability. A hyperbolic equilibrium can be an attractor, repeller or saddle point. But there are many more types for non-hyperbolic equilibria. Most of these equilibria do not have names. A complete classification doesn't exist. Therefore for non-hyperbolic critical points we will specify only if it is stable or unstable. Finally, we need to find the nature of each critical point. There are various ways to do it. It can be derived by solving the linearized equations around the critical points. First, we need to define a coordinate system. We will use the spherical coordinates with a metric in the following form

$$ds^2 = -Adt^2 + \frac{dr^2}{B} + r^2 d\Omega^2\,, \tag{6.16}$$

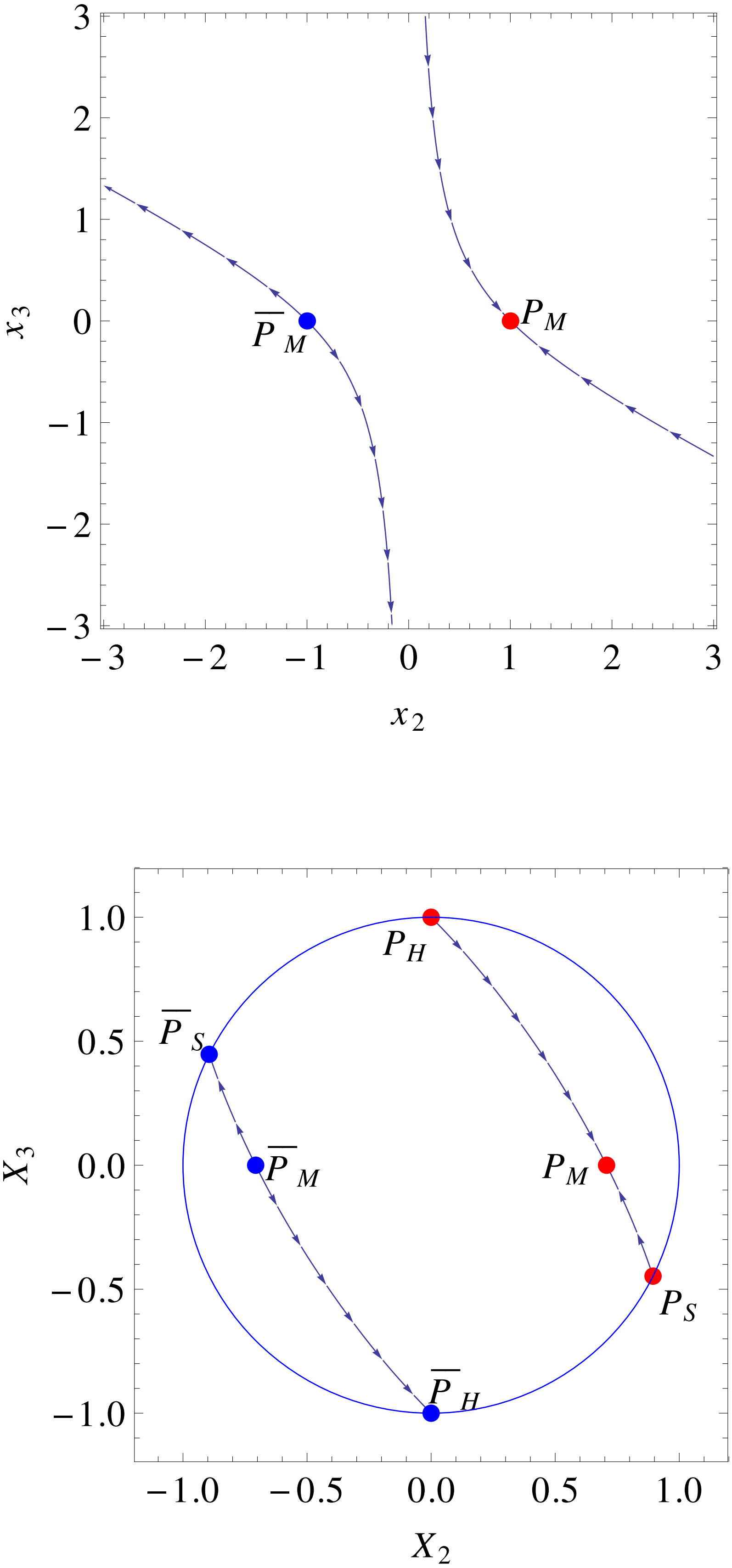

FIGURE 6.1: The phase portrait for static vacuum in both finite and infinite (Poincaré sphere) domains is displayed. The points (P_M, P_H, P_S) corresponds to the black hole solution while $(\bar{P}_M, \bar{P}_H, \bar{P}_S)$ corresponds to the white hole.

where $d\Omega^2 = d\theta^2 + \sin^2\theta d\varphi^2$. In order to understand the nature of the critical point, we need to determine the different variables in terms of the metric. From the definition (6.16), we define the four-velocity $u^t = 1/\sqrt{A}$ and the radial vector $n^r = \sqrt{B}$. Hence we get

$$\mathcal{A} \equiv -u^\mu u^\nu \nabla_\mu n_\nu = \frac{\sqrt{B}}{2A}\frac{\mathrm{d}A}{\mathrm{d}r}\,, \tag{6.17}$$

$$\phi = N_\nu{}^\mu \nabla_\mu n^\nu = \frac{2}{r}\sqrt{B}\,. \tag{6.18}$$

Also we can rewrite the derivatives in the following form

$$x' = \frac{\hat{x}}{\sqrt{K}} = r\hat{x} = r\frac{r\phi}{2}\frac{\mathrm{d}x}{\mathrm{d}r} = x_2\frac{\mathrm{d}x}{\mathrm{d}\ln r}\,, \tag{6.19}$$

where $K = 1/r^2$ and we have used $\hat{x} = n^\mu D_\mu x = \sqrt{B}\frac{\mathrm{d}x}{\mathrm{d}r} = r\frac{\phi}{2}\frac{\mathrm{d}x}{\mathrm{d}r}$. The last equality comes from (6.18). Hence we have

$$B = x_2^2\,, \qquad \frac{d\ln A}{d\ln r} = 2\frac{x_3}{x_2}\,, \tag{6.20}$$

from which we can easily recover the metric at each critical point. Notice that each critical point is at a fixed value of radial distance r, hence it is necessary to perform a linearisation around the point in order to do an integration and recover the gravitational potential A. For example, the solution of the dynamical system reduces around the critical point $(1, 0)$ to

$$x_2 \simeq 1 + \frac{\epsilon}{r}\,, \tag{6.21}$$

$$x_3 \simeq -\frac{\epsilon}{r}, \quad \text{with} \quad \epsilon \ll 1\,. \tag{6.22}$$

From (6.20) we get

$$A = B = 1 \pm \frac{2\epsilon}{r}\,. \tag{6.23}$$

The point P_M corresponds to the limit where $\epsilon \to 0$, therefore P_M is the Minkowski spacetime. Notice from (6.18) that $x_2 = \sqrt{B}$, hence we have $x_2 > 0$. But if we take the inner normal to the surface $n^r = -\sqrt{B}$ we will have $x_2 = -\sqrt{B} < 0$. Hence the phase space $x_2 < 0$ will be opposite to the subspace $x_2 > 0$, the nature of the points will be reversed, e.g. an attractor will be repeller (because of sign change in derivative (6.19)). Also we see from (6.17) and (6.18) that reversing the direction of u^μ has no effect, because of the static nature of the spacetime. We also notice that in the Kruskal-Szekeres coordinates, we have $U^2 - V^2 = C^{\mathrm{st}}$ when $r = C^{\mathrm{st}}$. Therefore the normal vector to this hypersurface is $n^\mu = (U, -V, 0, 0)$ or $n^\mu = (-U, V, 0, 0)$. In these coordinates, inner/outer direction of the spacelike normal vector n corresponds to the transformation $(U \to -U, V \to -V)$ which is equivalent to the transformation from the exterior region to parallel exterior region. Therefore the phase space corresponding to $x_2 < 0$ is the parallel exterior region. The analysis covers the static part of the black hole and the white hole.

We can do the same for the points at infinity, e.g. the point P_S. In this case, we have $(X_2, X_3, Z) = (\frac{2}{\sqrt{5}}, -\frac{1}{\sqrt{5}}, 0)$. The solution of the dynamical system around this point (the dynamical system is given in the Table 6.1) is

$$X_2 = \frac{2}{\sqrt{5}}\,, \tag{6.24}$$

$$X_3 = -\frac{1}{\sqrt{5}}\,, \tag{6.25}$$

$$Z = \epsilon\sqrt{r}, \quad \text{with} \quad \epsilon \ll 1\,. \tag{6.26}$$

which gives

$$x_2 \equiv \frac{X_2}{Z} \simeq \frac{2}{\epsilon\sqrt{5r}}\,, \tag{6.27}$$

$$x_3 \equiv \frac{X_3}{Z} \simeq -\frac{1}{\epsilon\sqrt{5r}}\,, \tag{6.28}$$

after redefinition of time (constant is absorbed for A), we have

$$A = B = \frac{4}{5\epsilon^2 r}\,. \tag{6.29}$$

Therefore in the limit $\epsilon \to 0$, we conclude that P_S corresponds to the singularity at $r = 0$.

Finally P_H is a little more subtle. In fact we can't linearize the equations around this point. We notice that in a stationary spacetime, the apparent horizon coincides with the event horizon and the apparent horizon is a marginally trapped surface on which the outgoing null geodesics have zero expansion [Hawking and Ellis 1973]. We define 2 spacelike vectors (a^μ, b^μ) on the 2-surface, which define an orthonormal basis with n^μ the normal spacelike vector to the 2-surface and u^μ the timelike vector. Hence we can write the metric as

$$g_{\mu\nu} = -u_\mu u_\nu + n_\mu n_\nu + a_\mu a_\nu + b_\mu b_\nu\,. \tag{6.30}$$

Also the expansion of the outgoing null geodesics is [Hawking and Ellis 1973; Sasaki et al. 1980]

$$\Theta = \frac{1}{2}\nabla_\mu k_\nu (a^\mu a^\nu + b^\mu b^\nu) = \frac{1}{2}\nabla_\mu k_\nu N^{\mu\nu}\,, \tag{6.31}$$

where $k^\mu = u^\mu + n^\mu$ is the outgoing null vector. Hence (6.31) can be written as

$$\Theta = \frac{1}{2}\Big(N^{\mu\nu}K_{\mu\nu} + \delta_\mu n^\mu\Big)\,, \tag{6.32}$$

where $K_{\mu\nu} = h_\mu^{\ \alpha} h_\nu^{\ \beta}\nabla_\alpha u_\beta$ is the extrinsic curvature. Using the decomposition of the extrinsic curvature and the definition of sheet expansion, we have

$$\Theta = \frac{1}{2}\Big(\frac{2}{3}\theta - \Sigma + \phi\Big) = \sqrt{K}\Big(x_2 + x_6 + x_7\Big)\,. \tag{6.33}$$

Therefore we conclude that $x_2 + x_6 + x_7 = 0$ [Hamid et al. 2014] for the apparent horizon ($\Theta = 0$) and hence $x_2 = 0$ for static case, which implies P_H is a horizon.

Hence we see from Fig. 6.1 that if the system starts from the horizon (P_H) it goes asymptotically to the Minkowski spacetime (P_M) which corresponds to the standard Schwarzschild black hole solution with a positive mass and, if the system starts from the singularity (P_S), it also propagates till Minkowski spacetime but without crossing the horizon. That solution corresponds to a naked singularity where the mass is negative. The transformation to the extended spacetime ($U \to -U, V \to -V$) is equivalent to ($x_2 \to -x_2, x_3 \to -x_3$) which gives the other part of the phase space where $\phi < 0$ which means anti-gravity or defocusing of geodesics.

6.2.2 Nonstatic

For this case, only the variables x_1, x_6 and x_7 are nonzero. We also use the constraint (6.7g) to reduce the system to

$$\mathring{x}_6 = x_7(x_6 - 2x_7)\,, \tag{6.34}$$

$$\mathring{x}_7 = x_6(x_6 - 2x_7)\,, \tag{6.35}$$

$$1 = 3\Big(x_7^2 - x_6^2\Big)\,. \tag{6.36}$$

There are no finite fixed points. Under the Poincaré transformation, the equations become

$$\mathring{X}_6 = -X_7(X_6 - 2X_7)(X_6^2 - X_7^2 - Z^2)\,, \tag{6.37}$$

$$\mathring{X}_7 = X_6(X_6 - 2X_7)(X_6^2 - X_7^2 + Z^2)\,, \tag{6.38}$$

$$\mathring{Z} = -2X_6X_7Z(X_6 - 2X_7)\,, \tag{6.39}$$

$$Z^2 = 3\Big(X_7^2 - X_6^2\Big)\,, \tag{6.40}$$

$$1 = X_6^2 + X_7^2 + Z^2\,, \tag{6.41}$$

Dynamical system	Critical points	Stability	Nature
$\mathring{x}_6 = x_7(x_6 - 2x_7)$ $\mathring{x}_7 = x_6(x_6 - 2x_7)$ $1 = 3\left(x_7^2 - x_6^2\right)$	No fixed points		
$\mathring{X}_6 = -X_7(X_6 - 2X_7)(X_6^2 - X_7^2 - Z^2)$ $\mathring{X}_7 = X_6(X_6 - 2X_7)(X_6^2 - X_7^2 + Z^2)$ $Z^2 = 3\left(X_7^2 - X_6^2\right)$ $1 = X_6^2 + X_7^2 + Z^2$	$P_H : (X_6, X_7) = (\frac{1}{\sqrt{2}}, -\frac{1}{\sqrt{2}})$ $\bar{P}_H : (X_6, X_7) = (-\frac{1}{\sqrt{2}}, \frac{1}{\sqrt{2}})$ $P_S : (X_6, X_7) = (-\frac{1}{\sqrt{2}}, -\frac{1}{\sqrt{2}})$ $\bar{P}_S : (X_6, X_7) = (\frac{1}{\sqrt{2}}, \frac{1}{\sqrt{2}})$	Repeller Attractor Attractor Repeller	Horizon Horizon Singularity Singularity

Table 6.2: Critical points, stability and their nature in both finite and infinite (Poincaré sphere) domains for nonstatic vacuum.

where we have rescaled the derivative $Z\mathring{X} \to \mathring{X}$.

We perform the same analysis as before except that the metric takes the following form

$$ds^2 = -\frac{dt^2}{B(t)} + A(t)dr^2 + t^2 d\Omega^2 \,. \tag{6.42}$$

We define the normal vectors as $u^\mu = (\pm\sqrt{B}, 0, 0, 0)$ and $n^\mu = (0, \pm 1/\sqrt{A}, 0, 0)$. It is easy to see that for any field X, we have $\dot{X} = u^\mu \nabla_\mu X = \pm\sqrt{B} dX/dt$. We can also get $\theta = \nabla_\mu u^\mu = (\frac{d\ln A}{dt}/2 + 2/t)u^0$ and $\theta/3 - \Sigma/2 = N^{\mu\nu}\nabla_\mu u_\nu/2 = u^0/t$ which gives $u^0 = x_6 + x_7$. Hence $u^\mu = (x_6 + x_7, 0, 0, 0)$. The position of the horizon corresponds to $x_6 + x_7 = 0$. Also the line of constant time are in the Kruskal coordinates defined by $V^2 - U^2 = C^{st}$ so in these coordinates we have $u^\mu = (V, -U, 0, 0)$ or $u^\mu = (-V, U, 0, 0)$. The transformation from nonstatic black hole to nonstatic white hole is $(U \to -U,\ V \to -V)$ or equivalently by reversing the sign of $x_6 + x_7$. As previously the metric can be written in terms of the normalized variables

$$B = (x_6 + x_7)^2 \,, \qquad \frac{d\ln A}{d\ln t} = 2\frac{x_6 - 2x_7}{x_6 + x_7} \,, \tag{6.43}$$

and the derivative $\mathring{x} = (x_6 + x_7)\frac{dx}{d\ln t}$.

Hence it is easy to analyze the system and find the nature of each critical points. The final result is summarized in the Table 6.2 and the phase portrait is shown on Fig. 6.2. We see that on the black hole side (ie., $x_6 + x_7 < 0$), there is a flow of the trajectory from the horizon to the singularity and vice-versa for the white hole (ie., $x_6 + x_7 > 0$). This exactly corresponds to what we already know.

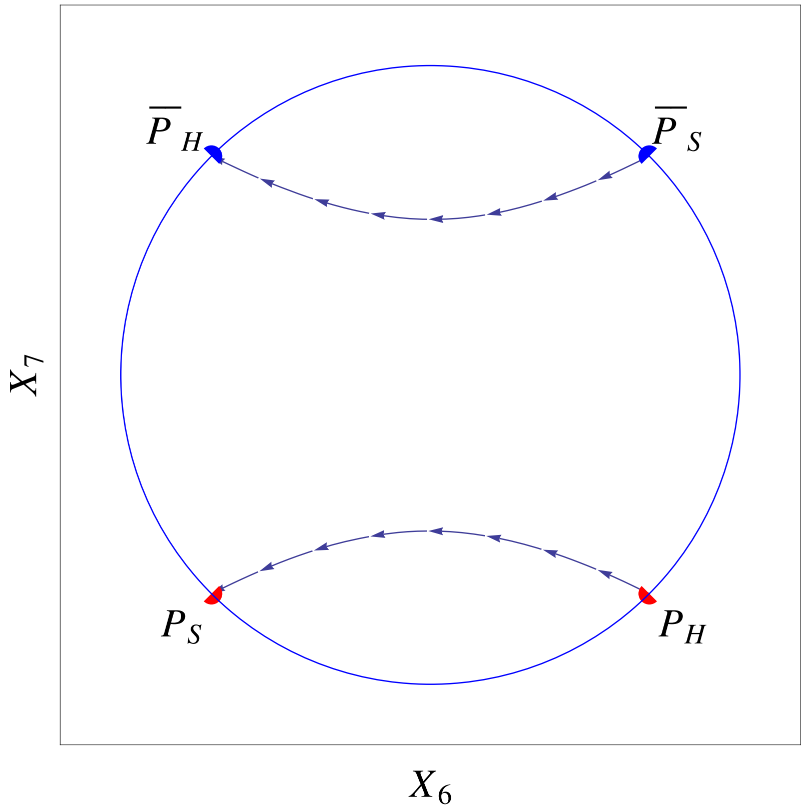

FIGURE 6.2: The phase portrait for nonstatic vacuum within Poincaré sphere for black hole and white hole.

6.3 Vacuum spacetime with cosmological constant

We follow the same analysis done previously in the presence of a cosmological constant. In this case, $\rho = p = \Pi = 0$, so we include x_4 other than the variables defined in the previous section.

6.3.1 Static

Using the constraints (7.8g) and (7.8h)) the system reduces to

$$x_2' = x_2 x_3 \,, \tag{6.44}$$

$$x_3' = -x_3(x_3 - x_2) + x_2^2 - 1 \,. \tag{6.45}$$

We see that $x_2 = 0$ is an invariant submanifold of the dynamical system contrary to $x_3 = 0$, meaning the system cannot go through the subspace $x_2 = 0$ and can only approach it asymptotically, which corresponds to the horizon as seen previously. Like before, we have the Minkowski critical point $(x_2, x_3) = (\pm 1, 0)$. Using the transformation $x_i = X_i/Z$ with

$X_2^2 + X_3^2 + Z^2 = 1$, the Poincaré sphere, we have

$$X_2' = -X_2 X_3 (X_2^2 + X_2 X_3 - 2X_3^2 - 2Z^2)\,, \tag{6.46}$$

$$X_3' = X_2^2 (X_2 - X_3)(X_2 + 2X_3) + (X_2 - X_3) X_3 Z^2 - Z^4\,, \tag{6.47}$$

$$1 = X_2^2 + X_3^2 + Z^2\,, \tag{6.48}$$

where we performed a rescaling of the derivative $ZX' \to X'$.

As usual the nature can be derived by making a linearisation around the critical point. Let us consider the point $(\frac{1}{\sqrt{2}}, \frac{1}{\sqrt{2}})$. The linearisation gives

$$X_2 \simeq \frac{1}{\sqrt{2}} + \frac{\epsilon_1}{r^3}\,, \tag{6.49}$$

$$X_3 \simeq \frac{1}{\sqrt{2}} - \frac{\epsilon_1}{r^3}\,, \tag{6.50}$$

$$Z \simeq \frac{\epsilon_2}{r}\,, \tag{6.51}$$

which gives

$$x_2 \simeq \frac{r}{\sqrt{2}\epsilon_2} + \frac{\epsilon_1}{r^2}\,, \tag{6.52}$$

$$x_3 \simeq \frac{r}{\sqrt{2}\epsilon_2} - \frac{\epsilon_1}{r^2}\,, \tag{6.53}$$

which at the leading order gives

$$B \simeq \frac{r^2}{2\epsilon_2^2} \simeq -\frac{\Lambda}{3} r^2\,, \quad \Lambda < 0\,, \tag{6.54}$$

$$A \simeq \alpha r^2\,, \tag{6.55}$$

where α is a constant of integration and we used the constraint (7.8g) and (7.8h) to get $x_4 = \Lambda r^2/3 \simeq -r^2/2\epsilon_2^2$. Hence we conclude the point is the anti-de Sitter Universe.

Finally, $(P_{H1}, \bar{P}_{H1}, P_{H2}, \bar{P}_{H2})$ are the horizons. First, we notice that because we want a static universe, the sign of the metric can't flip, hence $A > 0$ and $B > 0$. Also from (6.20) we have $\mathrm{sign}(dA/dr) = \mathrm{sign}(x_2 x_3)$. Finally, following standard convention, we have $dA/dr > 0$ for event horizon and the cosmological horizon is the null surface for which $dA/dr < 0$ (or also a Cauchy horizon). We conclude that P_{H1} and $\bar{P}_{H2}$ are event horizons while de Sitter horizons for $\bar{P}_{H1}$ and P_{H2}. The results are summarized in Table 6.3. To avoid the singularity, we see from Fig. 6.3 that the sign of the cosmological constant is not important but we avoid it by imposing $\mathcal{E} < 0$. Fig. 6.3 represents the complete static manifold. We can, for example, start an evolution from the event horizon of the BH (P_{H1}). Depending on the initial conditions, we

Dynamical system	Critical points	Stability	Nature
$x_2' = x_2x_3$	$P_M : (x_2, x_3) = (1, 0)$	Saddle point	Minkowski
$x_3' = -x_3(x_3 - x_2) + x_2^2 - 1$	$\bar{P}_M : (x_2, x_3) = (-1, 0)$	Saddle point	Minkowski
	$(P_{H1}, \bar{P}_{H1}) : (X_2, X_3) = (0, 1)$	Repeller	Horizon
$X_2' = -X_2X_3(X_2^2 + X_2X_3 - 2X_3^2 - 2Z^2)$	$(P_{H2}, \bar{P}_{H2}) : (X_2, X_3) = (0, -1)$	Attractor	Horizon
$X_3' = X_2^2(X_2 - X_3)(X_2 + 2X_3)$	$P_S : (X_2, X_3) = (\frac{2}{\sqrt{5}}, -\frac{1}{\sqrt{5}})$	Repeller	Singularity
$+(X_2 - X_3)X_3Z^2 - Z^4$			
$Z' = ZX_3(-2X_2^2 - X_2X_3 + X_3^2 + Z^2)$	$\bar{P}_S : (X_2, X_3) = (-\frac{2}{\sqrt{5}}, \frac{1}{\sqrt{5}})$	Attractor	Singularity
$X_2^2 + X_3^2 + Z^2 = 1$	$P_{AdS} : (X_2, X_3) = (\frac{1}{\sqrt{2}}, \frac{1}{\sqrt{2}})$	Attractor	Anti-de Sitter
	$\bar{P}_{AdS} : (X_2, X_3) = (-\frac{1}{\sqrt{2}}, -\frac{1}{\sqrt{2}})$	Repeller	Anti-de Sitter

TABLE 6.3: Critical points and their stability in both finite and infinite (Poincaré sphere) domains for general relativity with cosmological constant (static case).

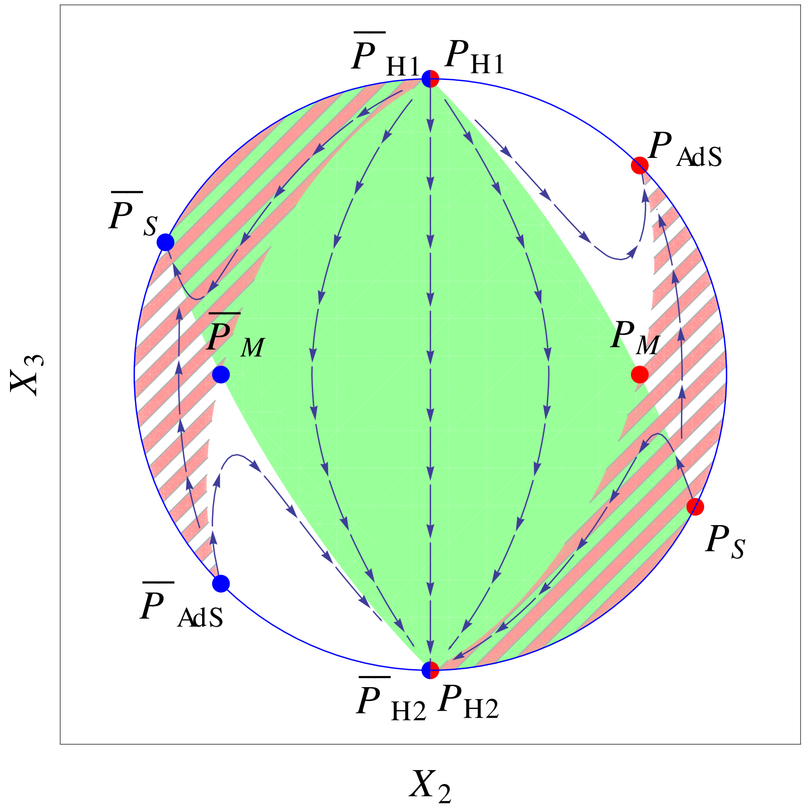

FIGURE 6.3: The phase portrait for general relativity with cosmological constant within Poincaré sphere. The green region corresponds to positive cosmological constant while the dashed red part corresponds to positive electric part of the Weyl tensor $\mathcal{E} > 0$.

can choose a path towards the anti-de Sitter space or propagate to the de Sitter horizon in P_{H2}. Localized at the cosmological horizon we can imagine a coordinate transformation which is going to smoothen that coordinate singularity, but we don't get rid of the central singularity. That transformation is going to reverse x_2 and x_3 hence we will be at the point $\bar{P}_{H1}$ which corresponds to the cosmological horizon where now $\phi < 0$, hence we are on the other side of the extension of the spacetime. The system will propagate till the point $\bar{P}_{H2}$, which corresponds to the event horizon. Now, close to that horizon, we can use another transformation which is going to transform the system into P_{H1} which is again the event horizon, we can proceed to the same thing again and again which shows the infinite structure of the complete manifold. Notice also that we have a straight trajectory from P_{H1} to P_{H2}, this corresponds to both horizons indistinguishably, it's the degenerate solution. In fact we have in that case $\phi = 0$ and from the equations we have $K = \Lambda$ and

$$\frac{B}{2A}\frac{d^2A}{dr^2} + \frac{1}{4A}\frac{dB}{dr}\frac{dA}{dr} - \frac{B}{4A^2}\Big(\frac{dA}{dr}\Big)^2 + \Lambda = 0\,. \tag{6.56}$$

Notice that this equation is equivalent to $R_{\mu\nu} = \Lambda g_{\mu\nu}$ with a metric given by $ds^2 = -Adt^2 + dr^2/B + d\Omega^2/\Lambda$. In case where $A = B$, we have $A = \alpha + \beta r - \Lambda r^2$ corresponding to Nariai spacetime. It is interesting to notice from Fig.6.3 how easily we deduce the absence of singularity for Nariai spacetime and anti-de Sitter asymptotic region.

6.3.2 Nonstatic

In this part, we investigate the nonstatic case with a cosmological constant. Using the constraints (6.7f) and (6.7g) the system reduces to

$$\mathring{x}_6 = x_6x_7 - 3{x_7}^2 + {x_6}^2 + \frac{1}{3}\,, \tag{6.57}$$

$$\mathring{x}_7 = {x_7}^2 - 2x_6x_7 - \frac{1}{3}\,. \tag{6.58}$$

We see that $x_6 + x_7$ is an invariant submanifold and hence can't be crossed. Horizons are always invariant submanifolds in our formalism. We have 2 fixed points at finite distance corresponding to horizons. Under Poincaré transformation, the equations become

$$\begin{aligned}
\mathring{X}_6 &= 3X_7^2(X_6^2 - X_7^2) + (3X_6^2 + 4X_6X_7 - 8X_7^2)\frac{Z^2}{3} + \frac{Z^4}{3}\,,\\
\mathring{X}_7 &= -3X_6X_7(X_6^2 - X_7^2) - (X_6^2 + 7X_6X_7 - 3X_7^2)\frac{Z^2}{3} - \frac{Z^4}{3}\,,\\
1 &= X_6^2 + X_7^2 + Z^2\,,
\end{aligned} \tag{6.59}$$

where we rescaled the derivative ($Z\mathring{X} \to \mathring{X}$). The analysis follows the same previous strategy

Dynamical system	Critical points	Stability	Nature
$\mathring{x}_6 = x_6x_7 - 3{x_7}^2 + {x_6}^2 + \frac{1}{3}$	$(P_{H3}, \bar{P}_{H3}) : (x_6, x_7) = (\frac{1}{3}, -\frac{1}{3})$	Saddle point	Horizon
$\mathring{x}_7 = {x_7}^2 - 2x_6x_7 - \frac{1}{3}$	$(P_{H2}, \bar{P}_{H2}) : (x_6, x_7) = (-\frac{1}{3}, \frac{1}{3})$	Saddle point	Horizon
	$P_{dS} : (X_6, X_7) = (-1, 0)$	Repeller	de Sitter
$\mathring{X}_6=3X_7^2(X_6^2-X_7^2)+(3X_6^2+4X_6X_7-8X_7^2)\frac{Z^2}{3}+\frac{Z^4}{3}$	$\bar{P}_{dS} : (X_6, X_7) = (1, 0)$	Attractor	de Sitter
$\mathring{X}_7=-3X_6X_7(X_6^2-X_7^2)-(X_6^2+7X_6X_7-3X_7^2)\frac{Z^2}{3}-\frac{Z^4}{3}$	$P_S : (X_6, X_7) = (-\frac{1}{\sqrt{2}}, -\frac{1}{\sqrt{2}})$	Attractor	Singularity
$\mathring{Z}=-(X_6^3+X_6^2X_7-5X_6X_7^2+X_7^3)Z+(-X_6+X_7)\frac{Z^3}{3}$	$\bar{P}_S : (X_6, X_7) = (\frac{1}{\sqrt{2}}, \frac{1}{\sqrt{2}})$	Repeller	Singularity
$1=X_6^2+X_7^2+Z^2$	$(P_{H1}, \bar{P}_{H1}) : (X_6, X_7) = (-\frac{1}{\sqrt{2}}, \frac{1}{\sqrt{2}})$	Attractor	Horizon
	$(P_{H4}, \bar{P}_{H4}) : (X_6, X_7) = (\frac{1}{\sqrt{2}}, -\frac{1}{\sqrt{2}})$	Repeller	Horizon

TABLE 6.4: Critical points and their stability in both finite and infinite (Poincaré sphere) domains for general relativity with cosmological constant (nonstatic case).

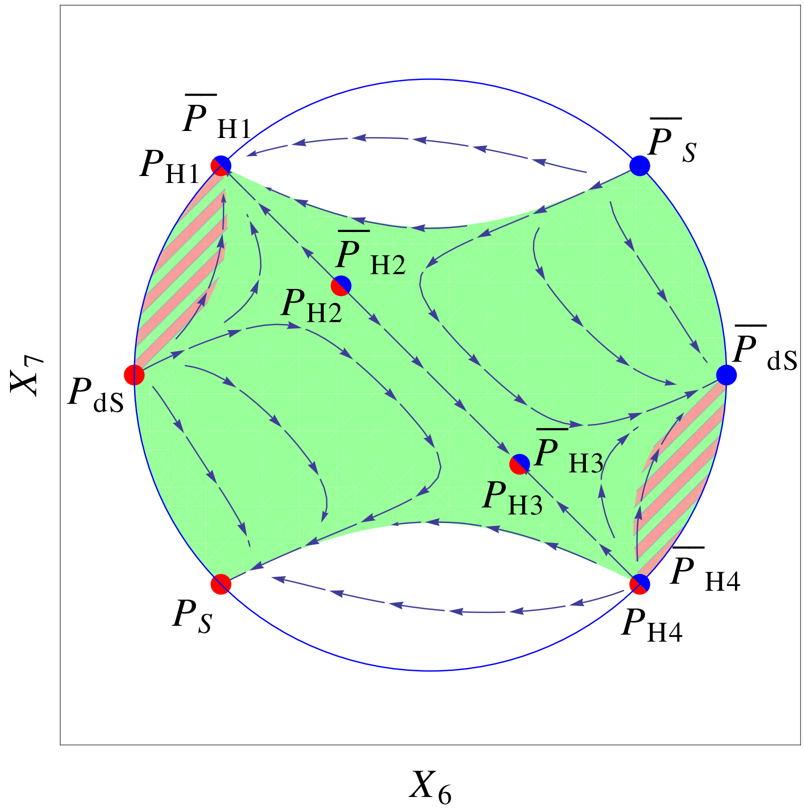

FIGURE 6.4: The phase portrait for nonstatic with Λ in infinite (Poincaré sphere) domain. The green part corresponds to $\Lambda > 0$ and the red dashed region corresponds to $\mathcal{E} > 0$.

and is summarized in Table 6.4 and phase space is displayed in Fig. 6.4. We notice from Fig. 6.4 that condition $\mathcal{E} > 0$ is sufficient to avoid singularity. We can start the evolution from either the horizon or the de Sitter space in the black hole and depending on the initial conditions, the path evolve either towards the singularity (from both horizon and de Sitter) or towards the horizon (from the de Sitter space). Finally the degenerate case where $x_6 + x_7 = 0$ reduces to

$$K = \Lambda \,, \tag{6.60}$$

$$\dot{\theta} + \theta^2 - \Lambda = 0 \,, \tag{6.61}$$

which gives in terms of metric

$$\frac{B}{2A}\frac{d^2A}{dt^2} - \frac{B}{4A^2}\left(\frac{dA}{dt}\right)^2 + \frac{1}{4A}\frac{dA}{dt}\frac{dB}{dt} - \Lambda = 0 \tag{6.62}$$

In the case where $B = \Lambda$ we have $A = \alpha \cosh(t + \beta)^2$ corresponding to Nariai solution in global coordinates. We see from the Fig. 6.4 the solution is singularity-free and does not have asymptotic de Sitter region as expected [Bousso 2002].

6.4 Charged spacetime

In this section, we will consider the presence of a charge hence the additional variable x_5.

6.4.1 Static

Using the constraints (7.8g) and (7.8h) the equations reduce to 3-dimensional autonomous system

$$x_2' = x_2 x_3 \,, \tag{6.63}$$

$$x_3' = 1 - 3x_2x_3 - x_2^2 - x_3^2 - 6x_4 \,, \tag{6.64}$$

$$x_4' = 2x_2x_4 \,, \tag{6.65}$$

with the constraint (positivity of density $\rho = E^2/2\mu_0$)

$$x_5 = 1 - x_2^2 - 3x_4 - 2x_2x_3 \geq 0 \,. \tag{6.66}$$

We see that $x_4 = 0$ and $x_2 = 0$ are invariant submanifolds. The latter defines the horizon while $x_4 \propto \Lambda$ does not change sign. The critical points and their nature are summarized in Table 6.5. We have 2 types of singularities which are calculated by a linearisation around the

Dynamical system	Critical points	Stability	Nature
	$(P_{H1}, \bar{P}_{H1}) : (x_2, x_3, x_4) = (0, x_3, \frac{1-x_3^2}{6})$	Saddle line (if $x_3 \neq 0$)	Horizon
Finite distance	$P_M : (x_2, x_3, x_4) = (1, 0, 0)$	Saddle point	Minkowski
	$\bar{P}_M : (x_2, x_3, x_4) = (-1, 0, 0)$	Saddle point	Minkowski
	$(P_{H2}, \bar{P}_{H2}) : (X_2, X_3, X_4) = (0, 1, 0)$	Repeller	Horizon
	$(P_{H3}, \bar{P}_{H3}) : (X_2, X_3, X_4) = (0, -1, 0)$	Attractor	Horizon
Points at infinity	$(P_{H4}, \bar{P}_{H4}) : (X_2, X_3, X_4) = (0, 0, 1)$	Stable ($X_2 > 0$), Unstable ($X_2 < 0$)	Horizon
	$(P_{AdS}, \bar{P}_{AdS}) : (X_2, X_3, X_4) = (0, 0, -1)$	Stable ($X_2 > 0$), Unstable ($X_2 < 0$)	Anti-de Sitter
	$P_{S1} : (X_2, X_3, X_4) = (\frac{2}{\sqrt{5}}, -\frac{1}{\sqrt{5}}, 0)$	Saddle point	Singularity ($\sim 1/r$)
	$\bar{P}_{S1} : (X_2, X_3, X_4) = (-\frac{2}{\sqrt{5}}, \frac{1}{\sqrt{5}}, 0)$	Saddle point	Singularity ($\sim 1/r$)
	$P_{S2} : (X_2, X_3, X_4) = (\frac{1}{\sqrt{2}}, -\frac{1}{\sqrt{2}}, 0)$	Repeller	Singularity ($\sim 1/r^2$)
	$\bar{P}_{S2} : (X_2, X_3, X_4) = (-\frac{1}{\sqrt{2}}, \frac{1}{\sqrt{2}}, 0)$	Attractor	Singularity ($\sim 1/r^2$)

TABLE 6.5: Critical points and their stability in both finite and infinite (Poincaré sphere) domains for general relativity with charge and cosmological constant (static case).

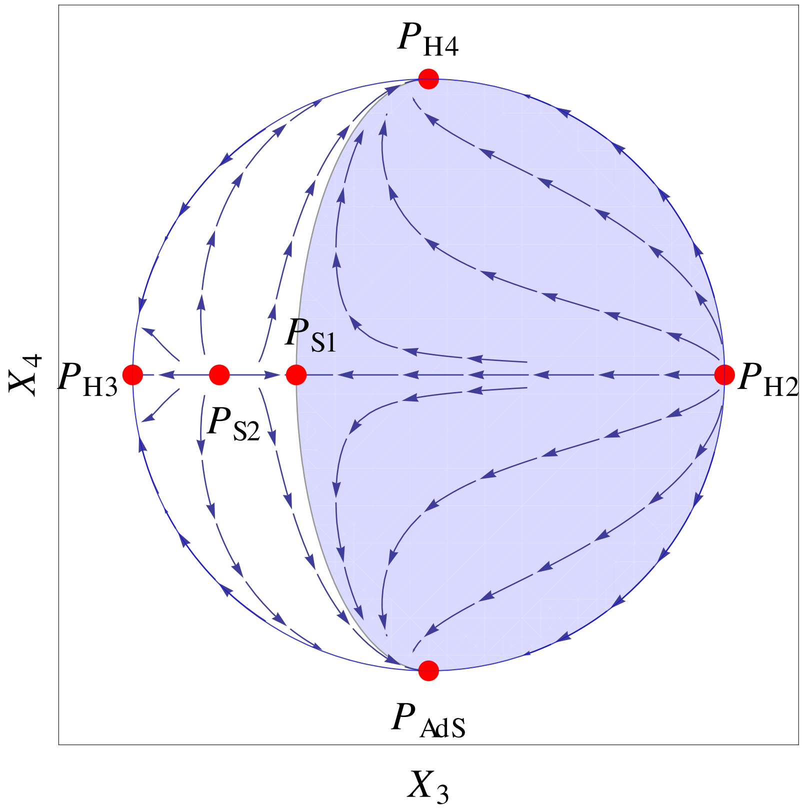

FIGURE 6.5: The phase portrait at infinity for general relativity with charge and cosmological constant. Only the black hole region is shown $X_2 > 0$. The white hole phase space can be easily deduced. The blue region represents violation of energy condition $x_5 < 0$ which is equivalent to $q^2 < 0$ where q is black hole charge.

critical point. The weakest singularity ($B \sim 1/r$) is always a saddle point if $x_5 \neq 0$ while the strongest singularity ($B \sim 1/r^2$) is a repeller for black hole ($x_2 > 0$) and an attractor for the white hole. Notice also that $(X_2, X_3, X_4) = (0, 0, -1)$ is not a horizon and, in fact, $X_2 = 0$ doesn't imply x_2 zero. This critical point corresponds to the end point of the saddle line in Table 6.5. It is stable for the black hole ($X_2 > 0$) while unstable for the white hole. In Fig.6.5, we have the behaviour of the dynamical system at infinity and Fig.6.6 shows the full phase space for a spacetime without cosmological constant, this is the Reissner-Nordström solution.

Finally the critical solution $x_2 = 0$ gives $x_3' + x_3^2 + 1 = 0$ which corresponds to Nariai solution. More generically if we impose $\phi = 0$ to the equations (5.42a)-(5.47) in the static case, and assuming $\Pi = 0$, we have $Q = 0, p = -\rho, K = \Lambda$ and

$$\hat{\mathcal{A}} + \mathcal{A}^2 + \Lambda = 0\,. \tag{6.67}$$

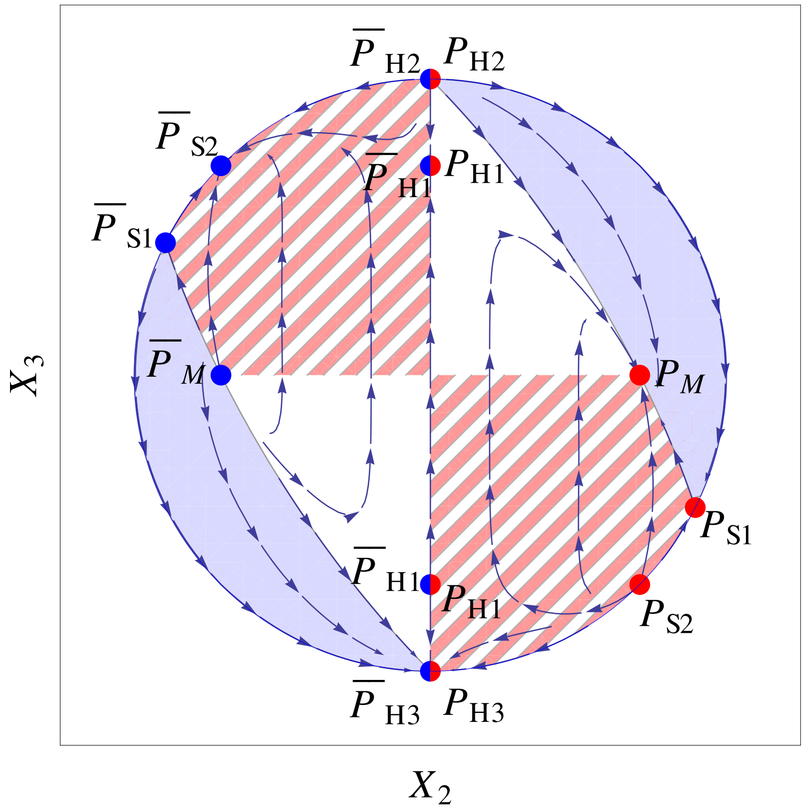

FIGURE 6.6: The phase portrait for general relativity with charge without cosmological constant in infinite (Poincaré sphere) domain. The blue region represents $x_5 < 0$ and should not be included. The dashed red part represents positive electric part of Weyl tensor $\mathcal{E} > 0$.

It can be integrated easily by defining an affine parameter ξ by $\sqrt{B}d\xi = dr$ which gives $\mathcal{A} = -\sqrt{\Lambda}\tan(\sqrt{\Lambda}\xi + \alpha) = 2^{-1}\frac{d\ln A}{d\xi}$ and hence we have the line element

$$\mathrm{d}s^2 = -\cos^2(\xi)dt^2 + \frac{d\xi^2 + d\Omega^2}{\Lambda}, \tag{6.68}$$

Therefore we can define the static Nariai solution as spacetime without sheet expansion $\phi = 0$.

6.4.2 Nonstatic

Using the constraints (6.7f) and (6.7g) the nonstatic system reduces to

$$\mathring{x}_4 = 2x_4(x_6 + x_7), \tag{6.69}$$

$$\mathring{x}_6 = x_6x_7 - x_6^2 - x_7^2 + 2x_4 - \frac{1}{3}, \tag{6.70}$$

$$\mathring{x}_7 = 2x_6(x_6 - x_7) - x_7^2 - 2x_4 + \frac{1}{3}, \tag{6.71}$$

Dynamical system	Critical points	Stability	Nature
Finite distance	$(P_{H1}, \bar{P}_{H1}) : (x_4, x_6, x_7) = (\frac{1+9x_6^2}{6}, x_6, -x_6)$	Saddle line (if $x_6 \neq 0$)	Horizon
Points at infinity	$(P_{dS}, \bar{P}_{dS}) : (X_4, X_6, X_7) = (1, 0, 0)$	Unstable ($X_6 + X_7 < 0$)	de Sitter
	$(P_{H2}, \bar{P}_{H2}) : (X_4, X_6, X_7) = (-1, 0, 0)$	Unstable ($X_6 + X_7 < 0$)	Horizon
	$(P_{H3}, \bar{P}_{H3}) : (X_4, X_6, X_7) = (0, \frac{1}{\sqrt{2}}, -\frac{1}{\sqrt{2}})$	Repeller	Horizon
	$(P_{H4}, \bar{P}_{H4}) : (X_4, X_6, X_7) = (0, -\frac{1}{\sqrt{2}}, \frac{1}{\sqrt{2}})$	Attractor	Horizon
	$\bar{P}_{S1} : (X_4, X_6, X_7) = (0, \frac{1}{\sqrt{2}}, \frac{1}{\sqrt{2}})$	Saddle point	Singularity ($\sim 1/t$)
	$P_{S1} : (X_4, X_6, X_7) = (0, -\frac{1}{\sqrt{2}}, -\frac{1}{\sqrt{2}})$	Saddle point	Singularity ($\sim 1/t$)
	$\bar{P}_{S2} : (X_4, X_6, X_7) = (0, \frac{1}{\sqrt{5}}, \frac{2}{\sqrt{5}})$	Repeller	Singularity ($\sim 1/t^2$)
	$P_{S2} : (X_4, X_6, X_7) = (0, -\frac{1}{\sqrt{5}}, -\frac{2}{\sqrt{5}})$	Attractor	Singularity ($\sim 1/t^2$)

TABLE 6.6: Critical points and their stability in both finite and infinite (Poincaré sphere) domains for general relativity with charge and cosmological constant (nonstatic case).

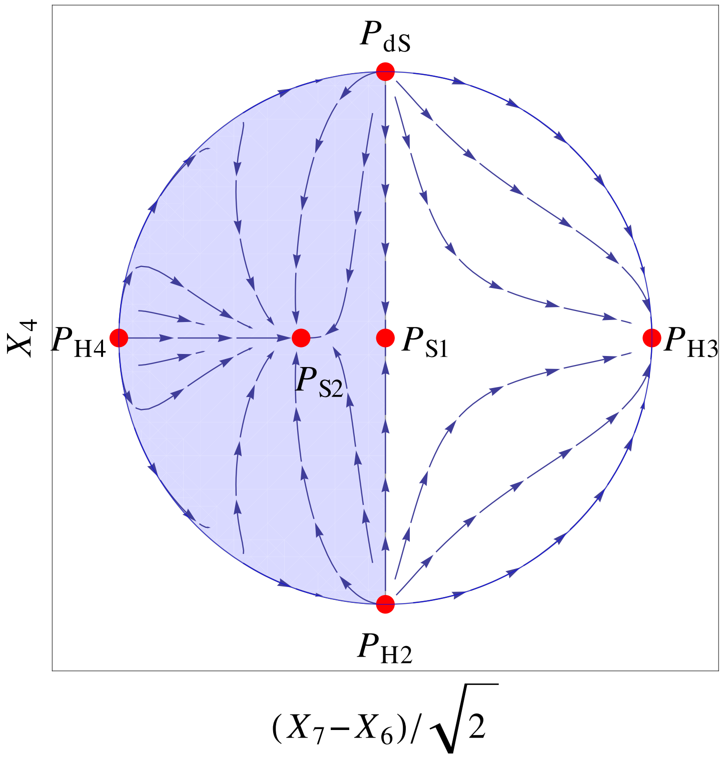

FIGURE 6.7: The phase portrait at infinity for general relativity with charge and cosmological constant in nonstatic case. Only one side of the extended manifold is shown. The white region is $\rho > 0$.

with the constraint on the positivity of density

$$x_5 = 1 - 3x_4 + 3x_6^2 - 3x_7^2 \geq 0\,. \tag{6.72}$$

As expected $x_4 = 0$ is invariant submanifold but also $x_6 + x_7 = 0$ which defines the horizon. The full analysis of the dynamical system is summarized in Table 6.6. We have 2 types of singularities but as in static case $B \sim 1/t$ is a saddle point. The point $(1, 0, 0)$ corresponds to de Sitter ($\Lambda > 0$), it is stable for the white hole while unstable for black hole $X_6 + X_7 < 0$.
The behaviour of the full system at infinity is shown in Fig.6.7 while Fig.6.8 shows the full phase space for $\Lambda = 0$. We see that we can't reach the singularity P_{S2} where the metric goes like $1/t^2$ as soon as we assume $\rho = E^2/2\mu_0 > 0$. In fact to reach the singularity we need to cross another horizon (Cauchy horizon) therefore the spacetime becomes static around this singularity.

Finally, very generically assuming $x_6+x_7 = 0$ gives from equations (5.42a)-(5.47) (and assuming $\Pi = 0$)

$$K = \Lambda\,, \tag{6.73}$$

$$\dot{\theta} + \theta^2 - \Lambda = 0\,. \tag{6.74}$$

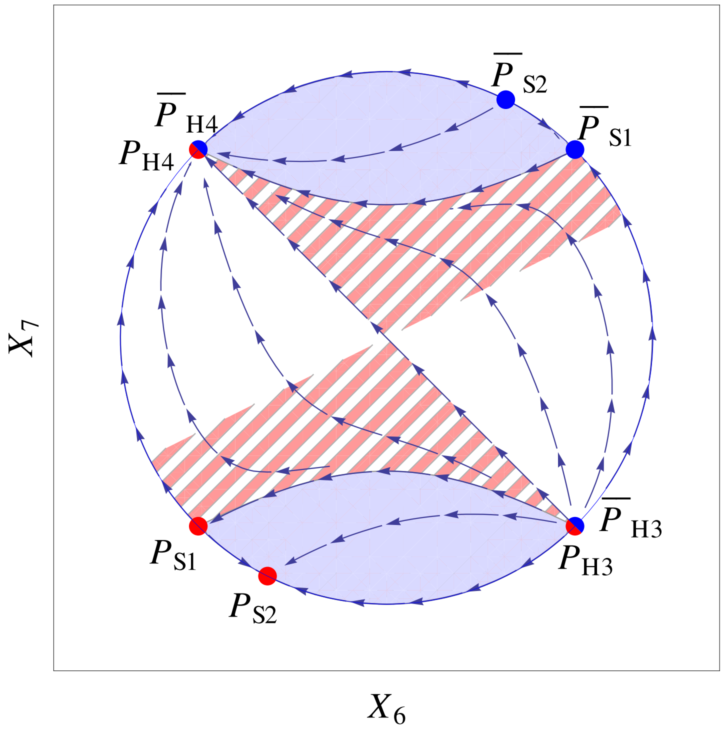

FIGURE 6.8: The phase portrait for general relativity with charge without cosmological constant in infinite (Poincaré sphere) domain. The dashed red region is $\mathcal{E} > 0$ while blue represents forbidden region $x_5 < 0$.

As previously, by introducing an affine parameter, it is easy to integrate the equation, we find

$$\mathrm{d}s^2 = -\frac{dt^2}{\Lambda} + \cosh^2(t)\mathrm{d}r^2 + \frac{\mathrm{d}\Omega^2}{\Lambda}\,. \tag{6.75}$$

Hence imposing the condition $\Sigma = 2\theta/3$ ($x_6 + x_7 = 0$) for a nonstatic spherically symmetric spacetime gives the Nariai solution.

6.5 Conclusions

In this chapter, we effectively reformulated the system of Einstein field equations, for LRS-II spacetimes, into an autonomous system of dimensionless, covariantly defined geometrical variables. By compactifying the phase space of this system and using the usual tools of dynamical system analysis, we qualitatively found all the important global features of the maximal extension of these spacetimes. Through the construction of this autonomous system of covariant variables, we eliminated the problems of coordinate singularities. It is quite interesting that horizons manifest themselves as invariant submanifolds of the phase space of the autonomous system. It is also very easy, via this formalism, to see the singularity-free nature of the Nariai solution. This analysis provides an efficient way to understand the global properties of any spacetime, by bypassing the very difficult task of solving the field equations and maximally extending the solution.

Chapter 7

Black holes structure via dynamical system in *f(R)* theories

The models of $f(R)$ gravity were introduced in the early days of GR to explore the possible alternatives to the Einstein-Hilbert action. It also appeared as a model for inflation and it is still consistent with all observations but, with the 1998 discovery of the acceleration of the Universe, $f(R)$ gravity became extremely popular. In fact, using type Ia supernovae [Riess et al. 1998], dark energy was introduced in the standard cosmological model to account for 68% of the energy content of the universe [Ade et al. n.d.]. It is difficult to conceive of a cosmological constant Λ whose energy density is fine-tuned by $\sim$ 55 orders of magnitude to account for the present acceleration [Martin 2012]. Various attempts to explain the cosmic acceleration in the context of GR and without dark energy, for example, using the backreaction of inhomogeneities on the cosmic dynamics [Buchert 2000] or by postulating that we live near the centre of a giant void in a dust-dominated universe [Alnes et al. 2006], have so far been unconvincing. Therefore an alternative is to abandon GR and modify the Einstein-Hilbert action by replacing the Ricci scalar R with a nonlinear function $f(R)$. On cosmological scales this modification of gravity deviates from GR in that it can cause cosmic acceleration without an unphysical, negative pressure fluid.

The $f(R)$ theory is equivalent to the standard degree of freedom, the massless graviton, plus a scalar field, the scalaron, which is not a ghost if $f_{,R} > 0$ [Nunez and Solganik 2004]. Also it can been shown that the scalaron has a rest mass in the WKB regime $M^2 = f_{,R}/3f_{,RR}$ ($M \gg R$) which implies the condition that $f_{,RR} > 0$. This condition can be derived in various contexts as, for example, an instability in the matter sector [Dolgov and Kawasaki 2003], stability of stars [Seifert 2007], cosmological perturbations [Sawicki and Hu 2007], well defined post-Newtonian limit [Olmo 2005], stability of the de-Sitter [Faraoni 2005] and Anti-de Sitter (AdS) space [Myung 2011] or the stability of the Schwarzschild solution [Myung et al. 2011].

Also, in order to have a viable matter phase during the cosmological expansion we need to impose the condition $Rf_{,RR}/f_{,R} > 0$ which during matter phase $R > 0$ imposes $f_{,RR}/f_{,R} > 0$ [Amendola, Gannouji, et al. 2007; Amendola, Polarski, et al. 2007]. It is also required for the stability of the cosmological perturbations [S. M. Carroll et al. 2006; Song et al. 2007; Bean et al. 2007; Faulkner et al. 2007]

Therefore we see that all the conditions for a physically viable model converge towards the conditions of positivity of the first and the second derivative of the lagrangian and hence we will restrict to models satisfying $f_{,R} > 0$ and $f_{,RR} > 0$ for $R > R_0$. In cosmology, R_0 represents the curvature of the universe in the future which means $R_0 \simeq 4\Lambda \simeq 10^{-47}\text{GeV}^4$. Also notice that if for some $R > R_0$ we have $f_{,R} = 0$, the universe becomes strongly anisotropic and inhomogeneous [Nariai 1973; Gurovich and Starobinsky 1979]. Therefore we will impose a stronger condition:

$$\forall R, \quad f_{,R} > 0 \text{ and } f_{,RR} > 0\,. \tag{7.1}$$

For example, the model $f(R) = R - \alpha/R^n$ ($\alpha > 0$, $n > 0$) does not satisfy the condition $f_{,RR} > 0$ and hence will not be considered in this analysis.

Having these conditions in mind, we will study very generically these models in the context of static spherically spacetimes without assuming a particular Lagrangian. For that, we will extend the formalism developed in chapter 6 for $f(R)$ theories.

The chapter is organized as follows. The autonomous system for the static case in $f(R)$ theories is given Sec. 7.1 and we study the vacuum solutions in both finite and infinite regime. Sec. 7.2 makes an analysis of the critical points or lines from a physical point of view. In Sec. 7.3, we study a special $f(R)$ model, αR^{n+1}, where the dimension of the autonomous system reduces by 1. We intend to study other $f(R)$ models in greater detail. The conclusions are given in Sec. 7.4. This chapter is based on a work in progress [Ganguly et al. n.d.].

7.1 $f(R)$ gravity

As we have seen in chapter 2, field equations in $f(R)$ theories can be effectively written as Eq. (2.5). In case of vacuum, $T^{(M)}_{\mu\nu} = 0$ and the effective energy momentum is given by $T^{(R)}_{\mu\nu}$. Using Eq. (5.37), quantities like ρ, P, Π and Q are defined in $f(R)$ gravity as [Nzioki, Goswami, et al. 2014]:

$$\rho = \frac{1}{f_{,R}}\left[\frac{1}{2}(Rf_{,R}-f)+f_{,RR}\hat{X}+f_{,RR}X\phi+f_{,RRR}X^2\right], \tag{7.2}$$

$$p = \frac{1}{f_{,R}}\left[\frac{1}{2}(f-Rf_{,R})-\mathcal{A}f_{,RR}X-\frac{2}{3}\left(f_{,RR}\hat{X}+f_{,RR}X\phi+f_{,RRR}X^2\right)\right], \tag{7.3}$$

$$\Pi = \frac{1}{3f_{,R}}\left[2f_{,RRR}X^2+2f_{,RR}\hat{X}-f_{,RR}X\phi\right], \tag{7.4}$$

$$Q = 0\,, \tag{7.5}$$

where $X = \hat{R}$ and $f_{,R} = df/dR$. The trace of the modified Einstein's equation leads to an additional equation

$$Rf_{,R}-2f = -3\left[f_{,RR}\left(\hat{X}+(\phi+\mathcal{A})X\right)+f_{,RRR}X^2\right]. \tag{7.6}$$

In chapter 6, we studied both the static and the nonstatic Universe for the different spacetimes but in this chapter and the following one, we will only concentrate on the static Universe. This is because the nonstatic case is not very interesting from an observational point of view since we are mainly concerned about the exterior solutions. We know that for a static Universe, $\theta = \Sigma = Q = 0$, hence we can define the variables as:

$$x_1 = -\frac{\mathcal{E}}{K}\,,\quad x_2 = \frac{\phi}{2\sqrt{K}}\,,\quad x_3 = \frac{\mathcal{A}}{\sqrt{K}}\,,\quad x_4 = \frac{R}{6K}\,,\quad x_5 = -\frac{f}{6Kf_{,R}}\,,\quad x_6 = \frac{Xf_{,RR}}{\sqrt{K}f_{,R}}\,. \tag{7.7}$$

The evolution of the variables will be zero. Using Eqs. (7.2)-(7.6), we get from the system of equations (5.42a)-(5.47) the following set for the autonomous system:

$$x_1' = \frac{1}{2}\left(-x_1\left(2x_2+x_6\right)+x_6^2\left(x_2-x_3\right)\right), \tag{7.8a}$$

$$x_2' = \frac{1}{2}\left(x_1+x_2x_6+x_3x_6\right)+x_5\,, \tag{7.8b}$$

$$x_3' = -x_3\left(x_2+x_3+x_6\right)-2x_4-x_5\,, \tag{7.8c}$$

$$x_4' = x_4\left(2x_2+\frac{x_6}{m}\right), \tag{7.8d}$$

$$x_5' = x_5\left(2x_2-x_6\right)-\frac{x_4x_6}{m}\,, \tag{7.8e}$$

$$x_6' = -2x_4-4x_5-x_6\left(x_2+x_3+x_6\right), \tag{7.8f}$$

$$1 = x_1+x_2^2+x_2x_6+x_4+x_5\,, \tag{7.8g}$$

$$0 = x_1-x_2\left(2x_3+x_6\right)-x_3x_6-2x_4-2x_5\,, \tag{7.8h}$$

where $m = Rf_{,RR}/f_{,R}$. We define also $u = -Rf_{,R}/f \equiv x_4/x_5$, reversing that equation we will have $m \equiv m(x_4/x_5)$.

Using the constraints Eqs. (7.8g) and (7.8h), we can reduce two degrees of freedom of the system (7.8), say

$$x_1 = \frac{1}{3}\left(2 - (x_2 - x_3)(2x_2 + x_6)\right) , \tag{7.9a}$$

$$x_5 = \frac{1}{3}\left(1 - x_2^2 - 3x_4 - x_3 x_6 - 2x_2(x_3 + x_6)\right) . \tag{7.9b}$$

Then the system (7.8) reduces to

$$x_2' = \frac{2 - 2x_2^2 - 3x_4 + x_3x_6 - x_2(x_3 + x_6)}{3} , \tag{7.10a}$$

$$x_3' = \frac{-1 + x_2^2 - x_2x_3 - 3x_3^2 - 3x_4 + 2x_2x_6 - 2x_3x_6}{3} , \tag{7.10b}$$

$$x_4' = x_4\left(2x_2 + \frac{x_6}{m}\right) , \tag{7.10c}$$

$$x_6' = \frac{-4 + 4x_2(x_2 + 2x_3) + 6x_4 + (5x_2 + x_3)x_6 - 3x_6^2}{3} , \tag{7.10d}$$

for $m \neq 0$.

Next, we will find out the critical points of the above system and study its stability and nature. For understanding the nature, we will study the behaviour of the dynamical system around the critical point as described in chapter 6. We define a metric with spherical coordinates:

$$ds^2 = -A(r)dt^2 + \frac{dr^2}{B(r)} + r^2 d\Omega^2 . \tag{7.11}$$

Now, following chapter 6, we calculate the relations which essentially boils down to:

$$x_2 = \sqrt{B} , \tag{7.12}$$

$$2\frac{x_3}{x_2} = \frac{\mathrm{d}(\ln A)}{\mathrm{d}(\ln r)} , \tag{7.13}$$

$$\frac{6}{r^2}x_4 = R , \tag{7.14}$$

$$\frac{x_6}{x_2} = \frac{\mathrm{d}(\ln f_{,R})}{\mathrm{d}(\ln r)} , \tag{7.15}$$

where $K = 1/r^2$.

The derivatives can be written as

$$x' = \frac{\hat{x}}{\sqrt{K}} = r\hat{x} = rn^{\mu}D_{\mu}x = r\frac{r\phi}{2}\frac{\mathrm{d}x}{\mathrm{d}r} = x_2\frac{\mathrm{d}x}{\mathrm{d}\ln r} . \tag{7.16}$$

Using Eq. (5.52), we can define the Misner-Sharp mass with the help of Eqs. (7.2), (7.4) and (7.9) as

$$\begin{aligned}\mathcal{M}_{MS} &= \frac{1}{2\sqrt{K}}\left(x_1 + x_2x_6 + x_4 + x_5\right) \\ &= \frac{1-x_2^2}{2\sqrt{K}}\,,\end{aligned} \tag{7.17}$$

along with the derivative

$$\hat{\mathcal{M}}_{MS} = x_2\Big[\frac{x_2^2-1}{6} + \frac{x_2x_6 + x_2x_3 - x_3x_6}{3} + x_4\Big]\,. \tag{7.18}$$

The critical points of the above system of equations are:

$\mathbf{P_1}:\ (x_2,x_3,x_4,x_6) = (1,0,0,0)$
$\mathbf{\bar{P}_1}:\ (x_2,x_3,x_4,x_6) = (-1,0,0,0)$
$\mathbf{P_2}:\ (x_2,x_3,x_4,x_6) = \left(\frac{2}{\sqrt{7}},\frac{1}{\sqrt{7}},0,\frac{4}{\sqrt{7}}\right)$
$\mathbf{\bar{P}_2}:\ (x_2,x_3,x_4,x_6) = \left(-\frac{2}{\sqrt{7}},-\frac{1}{\sqrt{7}},0,-\frac{4}{\sqrt{7}}\right)$
$\mathbf{P_3}:\ (x_2,x_3,x_4,x_6) = \left(\frac{1-m}{\sqrt{(1-2m-2m^2)(1-2m+4m^2)}},\frac{m(1+2m)}{\sqrt{(1-2m-2m^2)(1-2m+4m^2)}},\right.$
$\left.-\frac{m(1+m)}{1-2m-2m^2},\frac{2m(m-1)}{\sqrt{(1-2m-2m^2)(1-2m+4m^2)}}\right)$
$\mathbf{\bar{P}_3}:\ (x_2,x_3,x_4,x_6) = \left(-\frac{1-m}{\sqrt{(1-2m-2m^2)(1-2m+4m^2)}},-\frac{m(1+2m)}{\sqrt{(1-2m-2m^2)(1-2m+4m^2)}},\right.$
$\left.-\frac{m(1+m)}{1-2m-2m^2},-\frac{2m(m-1)}{\sqrt{(1-2m-2m^2)(1-2m+4m^2)}}\right)$

In what follows we shall consider the properties of each fixed point. It must be stressed that the barred points will not be analyzed in great detail as they have the same nature but their stabilities are complimentary to the corresponding unbarred points.

- P_1: Minkowski point
  The linearized system around this point has the eigenvalues $(2,2,-1,-1)$, hence it is a saddle point and the eigenvectors are

  $$\left(-\frac{1}{8},\frac{1}{4},0,1\right),\ \left(-\frac{1}{4},-\frac{1}{2},1,0\right),\ (-1,0,0,1)\,,\ (-1,1,0,0)\,.$$

  This point is found in chapter 6 where it is shown to be Minkowski spacetime. In fact we can also show that $\mathcal{M}_{MS} = \hat{\mathcal{M}}_{MS} = 0$.

  Notice that if we reduce the system to the 2-D subsystem where the eigenvalues are $(-1,-1)$ then the point will be an attractor. We notice that this subsystem is defined by

$$x_4 = 0\,, \tag{7.19}$$

$$x_2^2 + 2x_2x_3 + x_6(2x_2 + x_3) - 1 = 0\,. \tag{7.20}$$

It is easy to show that it is an invariant submanifold, therefore any trajectory on this surface remains on the surface. Hence the only possibility to have a spacetime for $f(R)$ theories which is asymptotically flat is to consider initial conditions on this surface. Along with these constraints the system reduces to

$$x_2' = x_2x_3 + x_2x_6 + x_3x_6\,, \tag{7.21}$$

$$x_3' = -x_3(x_2 + x_3 + x_6)\,, \tag{7.22}$$

$$x_6' = -x_6(x_2 + x_3 + x_6)\,. \tag{7.23}$$

We have two different cases, from $x_4 = 0$ we have $R = 0$ and $R' = 0$ and hence (i) $x_6 = 0$ if $f'(0)/f''(0) \neq 0$ and (ii) x_6 can be nonzero if $f'(0)/f''(0) = 0$. But as we said previously we will not consider the case $f'(R) = 0$, which is trivial. Therefore we will focus only on the case $x_6 = 0$. Also, notice that we have $x_5 = 0$ which implies $f(0)/f'(0) = 0$. Under all these conditions, the system reduces to

$$x_2' = x_2x_3\,, \tag{7.24}$$

$$x_3' = -x_3(x_2 + x_3)\,, \tag{7.25}$$

with the constraint $x_2^2 + 2x_2x_3 - 1 = 0$. Remember that $x_2' = x_2(dx_2/d\ln r) = 1/2(dx_2^2/d\ln r) = 1/2(dB/d\ln r)$. Substituting this relation in Eq. (7.24) and using the constraint to remove x_3, we get $dB/d\ln r = 1 - B$ which gives $x_2^2 = B = 1 - m/r$ where m is a constant of integration. Using this result in Eq. (7.13), we can easily get $A = \alpha(1 - m/r)$ where α is a constant of integration which can be absorbed by the re-definition of time. *Therefore we can conclude that for any $f(R)$ gravity theory for which $f'(0)/f''(0) \neq 0$, the unique asymptotically flat solution is Schwarzschild. Hence if we consider a general polynomial $f(R) = \sum_n a_nR^n$, the necessary condition gives $a_1 = 0$ which implies that any theory in the form $f(R) = R + h(R)$ where h is a polynomial, does not have an asymptotically flat spacetime except Schwarzschild.*

Notice that we could derive the condition differently, in fact once we understand from the dynamical system that an asymptotically flat spacetime exists only for $R = 0$ we have from the equations of motion

$$f'(0)R_{\mu\nu} - \frac{1}{2}f(0)g_{\mu\nu} - f''(0)\nabla_\mu R\nabla_\nu R - f'(0)\nabla_{\mu\nu}R + f''(0)(\nabla R)^2 g_{\mu\nu} + f'(0)\Box R g_{\mu\nu} = 0\,. \tag{7.26}$$

Because we assume $f'(0) \neq 0$, this equation becomes

$$R_{\mu\nu} - \frac{1}{2}\frac{f(0)}{f'(0)}g_{\mu\nu} - \frac{f''(0)}{f'(0)}\nabla_\mu R\nabla_\nu R - \nabla_{\mu\nu}R + \frac{f''(0)}{f'(0)}(\nabla R)^2 g_{\mu\nu} + \Box R g_{\mu\nu} = 0\,. \tag{7.27}$$

And hence if $f'(0)/f''(0) \neq 0$, we have for $R = 0$

$$R_{\mu\nu} - \frac{1}{2}\frac{f(0)}{f'(0)}g_{\mu\nu} = 0\,, \tag{7.28}$$

which by contraction gives

$$R = 2\frac{f(0)}{f'(0)} = 0\,, \tag{7.29}$$

and therefore $R_{\mu\nu} = 0$. Therefore we recover that under the same conditions $f'(0)/f''(0) \neq 0$ and $f(0)/f'(0) = 0$, the unique asymptotically flat solution is Schwarzschild ($R_{\mu\nu} = R = 0$).

We have learned something very important here, the phase space is 4D but on the surface $x_4 = 0$ it reduces to 2D because of an additional induced constraint which is $x_6 = 0$.

- $\bar{P}_1$: Anti-Minkowski point
  The linearized system around this point has the eigenvalues $(-2, -2, 1, 1)$, hence it is a saddle point.

- P_2: Isothermal point
  The eigenvalues of the linearized system are $\left(-\sqrt{7}, \frac{4(1+m(0))}{\sqrt{7}m(0)}, \frac{-\sqrt{7}+i}{2}, -\frac{\sqrt{7}+i}{2}\right)$. It is an attractor when $-1 < m(0) < 0$ and saddle point elsewhere except $m(0) = -1$. At $m(0) = -1$, it is a non-hyperbolic point and the system is stable.

  For this spacetime, $rA'/A = 1$, $B = 4/7$, $R = 0$ and $rR'f''(0)/f'(0) = 2$, which gives $\mathrm{ds}^2 = -rdt^2 + (7/4)dr^2 + r^2 d\Omega^2$. This spacetime corresponds to a special case of isothermal metric ($\alpha = 1/3$ in the article [Saslaw et al. 1996]) where the solution corresponds to a perfect fluid with $\rho = 3/7r^2$, $P_r = P_t = 1/7r^2$, ie. the EoS is $P = (1/3)\rho$.

  For this spacetime we have a positive and increasing mass $\mathcal{M}_{MS} = 3/14\sqrt{K} > 0$ and $\hat{\mathcal{M}}_{MS} = 3/7\sqrt{7} > 0$.

- $\bar{P}_2$: Anti-Isothermal point
  The eigenvalues of the linearized system are $\left(\sqrt{7}, -\frac{4(1+m(0))}{\sqrt{7}m(0)}, \frac{\sqrt{7}-i}{2}, \frac{\sqrt{7}+i}{2}\right)$. It is a repeller when $-1 < m(0) < 0$ and saddle point otherwise.

- P_3: Clifton-Barrow point
  This point exists only if $-\frac{1+\sqrt{3}}{2} < m < \frac{\sqrt{3}-1}{2}$. We notice that P_3 satisfy $x_4 = -x_5(1+m)$ ie. $m = -u-1$. We must solve this equation to get the explicit coordinates of P_3. For example if we consider the model $f(R) = R + a\sqrt{R}$ we have $m = -a/(2a+4\sqrt{R})$ and $u = -(a+2\sqrt{R})/(2a+2\sqrt{R})$ which gives for this model $m(u) = (1+u)/2u$. Therefore the equation $m(u) = -u-1$ gives $u = -1$ and $u = -1/2$ which implies $m = 0$ and $m = -1/2$. We define the system (7.10) for $m \neq 0$, therefore for this model, we have 1 critical point

$$P_{3a} = \left(\frac{\sqrt{2}}{2}, 0, \frac{1}{6}, \frac{\sqrt{2}}{2}\right) . \tag{7.30}$$

  More generically, we have $u' = u(1+m+u)\frac{x_6}{m}$, hence the critical line $m = -u-1$ is an invariant submanifold if x_6/m doesn't diverge.

  The eigenvalues of the linearized system are
  $$\left(-\sqrt{\frac{1-2m+4m^2}{1-2m-2m^2}}, \frac{-\sqrt{1-2m+4m^2}+\sqrt{-7+14m+20m^2}}{2\sqrt{1-2m-2m^2}}, \frac{-\sqrt{1-2m+4m^2}-\sqrt{-7+14m+20m^2}}{2\sqrt{1-2m-2m^2}}, \frac{2(1-m^2)(1+m')}{\sqrt{(1-2m-2m^2)(1-2m+4m^2)}}\right),$$
  where $m' = dm/du$. It is an attractor for $\{m' < -1; -1 \leq m < (\sqrt{3}-1)/2\}$ and $\{m' > -1; -(\sqrt{3}+1)/2 < m \leq -1\}$ saddle point for $\{m' < -1; -(\sqrt{3}+1)/2 \leq m < -1\}$ and $\{m' > -1; -1 < m \leq (\sqrt{3}-1)/2\}$. The critical point is non-hyperbolic when $m' = -1$ and $m = -1$, but we can show that it is stable.

  The solution of the dynamical system at the critical point comes out to be

$$A = r^{\frac{2m(1+2m)}{1-m}}, \quad B = \frac{(1-m)^2}{(1-2m-2m^2)(1-2m+4m^2)},$$
$$R = -\frac{6m(1+m)}{r^2(1-2m-2m^2)}, \quad f_{,R} = Nr^{-2m},$$

  where N is an arbitrary constant. This point is the asymptotic behaviour of the solution found by Clifton and Barrow [Clifton and Barrow 2005].

  Notice that in the case $m = -1$, $P_3 = P_2$, hence we understand that P_2 is also the asymptotic behaviour of a Clifton-Barrow solution but this critical point exists for any $f(R)$ theory .

For this spacetime, the Misner-Sharp mass and its derivative is

$$\mathcal{M}_{MS} = -\frac{m(2-5m+4m^2+8m^3)}{2(1-2m-2m^2)(1-2m+4m^2)\sqrt{K}}\,, \tag{7.31}$$

$$\hat{\mathcal{M}}_{MS} = \frac{m(m-1)(2-5m+4m^2+8m^3)}{2\Big[(1-2m-2m^2)(1-2m+4m^2)\Big]^{3/2}}\,. \tag{7.32}$$

The mass of the spacetime is positive for

$$-1.2 \simeq -\frac{1}{6}\Big(1+\frac{17}{(314-18\sqrt{183})^{1/3}}+\frac{(157-9\sqrt{183})^{1/3}}{2^{2/3}}\Big) < m < 0\,, \tag{7.33}$$

and negative elsewhere. Notice also that the curvature scalar is positive for $-1 < m < 0$ and negative elsewhere.

- $\bar{P}_3$: Anti-Clifton-Barrow point
  This point exists only if $-\frac{1+\sqrt{3}}{2} < m < \frac{\sqrt{3}-1}{2}$. We notice that P_3 satisfies $x_4 = -x_5(1+m)$ ie. $m = -u-1$. We must solve this equation to get the explicit coordinates of P_3.

  The eigenvalues of the linearized system are

$$\Bigg(\sqrt{\tfrac{1-2m+4m^2}{1-2m-2m^2}},\ \tfrac{\sqrt{1-2m+4m^2}+\sqrt{-7+14m+20m^2}}{2\sqrt{1-2m-2m^2}},\ \tfrac{\sqrt{1-2m+4m^2}-\sqrt{-7+14m+20m^2}}{2\sqrt{1-2m-2m^2}},\ -\tfrac{2(1-m^2)(1+m')}{\sqrt{(1-2m-2m^2)(1-2m+4m^2)}}\Bigg)\,.$$

To complete the analysis we need to study the structure of the phase space at infinity, for this we use the Poincaré transformation $x_i = X_i/Z$, with the constraint $X_2^2+X_3^2+X_4^2+X_6^2+Z^2=1$, therefore the system (7.12)-(7.15) becomes

$$\bar{X}_2 \equiv ZX_2' = -\frac{X_2X_6X_4^2}{m} + \frac{1}{3}\Big[X_3X_6 - X_2^3(X_3+4X_6) + (-3X_4+2Z)Z - X_2^2(X_3^2+8X_4^2 + 11X_3X_6 + 7X_6^2 - 3X_4Z + 4Z^2) + 2X_2X_3^3 + X_2X_3^2X_6 - X_2X_3(X_4^2+2X_6^2-3X_4Z) + X_2X_6(-X_4^2+2X_6^2-6X_4Z+3Z^2)\Big], \tag{7.34}$$

$$\bar{X}_3 \equiv ZX_3' = -\frac{X_3X_6X_4^2}{m} + \frac{1}{3}\Big[X_2^4 + X_2^3X_3 + X_3(-3X_3X_4^2 - 2X_4^2X_6 - 4X_3X_6^2 + X_6^3) + 3X_4(-1+X_3^2-2X_3X_6)Z - (1+2X_3(X_3-X_6))Z^2 + X_2^2(-2X_3^2+X_4^2-5X_3X_6+X_6^2+Z^2) - X_2X_3(7X_4^2+11X_3X_6+6X_6^2-3X_4Z+3Z^2) + 2X_2X_6\Big], \tag{7.35}$$

$$\bar{X}_4 \equiv ZX_4' = \frac{X_4X_6(1-X_4^2)}{m} + \frac{X_4}{3}\Big[8X_2^3 + 7X_2X_3^2 + 3X_3^3 - 3X_2^2X_6 - 11X_2X_3X_6 + 2X_3^2X_6 + X_2X_6^2 - X_3X_6^2 + 3X_6^3 + 3X_4(X_2+X_3-2X_6)Z + (4X_2+X_3+4X_6)Z^2\Big], \tag{7.36}$$

$$\bar{X}_6 \equiv ZX_6' = -\frac{X_4^2X_6^2}{m} + \frac{1}{3}\Big[2(1-X_6^2)\Big(2X_2(X_2+2X_3) + Z(3X_4-2Z)\Big) - X_6^2((3Z^2 + (X_2+X_3)(2X_2+X_3)) + 3X_4^2) + X_6(7X_2^3 + X_2^2X_3 + X_2(3Z^2+6X_3^2+3ZX_4-X_4^2) + X_3(4X_3^2+(Z+X_4)(2Z+X_4)))\Big]. \tag{7.37}$$

Notice that we have redefined the derivative. The critical points or lines at infinity ($Z=0$) are

$\mathbf{P_4}:\ (X_2,X_3,X_4,X_6) = (0,1,0,0)$
$\mathbf{P_5}:\ (X_2,X_3,X_4,X_6) = (0,-1,0,0)$
$\mathbf{P_6}:\ (X_2,X_3,X_4,X_6) = (0,0,1,0)$
$\mathbf{P_7}:\ (X_2,X_3,X_4,X_6) = (0,0,-1,0)$
$\mathbf{P_8}:\ (X_2,X_3,X_4,X_6) = (0,0,0,1)$
$\mathbf{P_9}:\ (X_2,X_3,X_4,X_6) = (0,0,0,-1)$
$\mathbf{P_{10}}:\ (X_2,X_3,X_4,X_6) = \left(\frac{1}{3\sqrt{2}}, \frac{1}{3\sqrt{2}}, 0, \frac{2\sqrt{2}}{3}\right)$
$\bar{\mathbf{P}}_{\mathbf{10}}:\ (X_2,X_3,X_4,X_6) = \left(-\frac{1}{3\sqrt{2}}, -\frac{1}{3\sqrt{2}}, 0, -\frac{2\sqrt{2}}{3}\right)$
$\mathbf{L_1}:\left(X_2, X_3 = \frac{-2X_2+\sqrt{1+X_2^2}+\sqrt{1-7X_2^2+4X_2\sqrt{1+X_2^2}}}{2}, X_4=0, X_6 = \frac{-2X_2+\sqrt{1+X_2^2}-\sqrt{1-7X_2^2+4X_2\sqrt{1+X_2^2}}}{2}\right)$
$\mathbf{L_2}:\left(X_2, X_3 = \frac{-2X_2+\sqrt{1+X_2^2}-\sqrt{1-7X_2^2+4X_2\sqrt{1+X_2^2}}}{2}, X_4=0, X_6 = \frac{-2X_2+\sqrt{1+X_2^2}+\sqrt{1-7X_2^2+4X_2\sqrt{1+X_2^2}}}{2}\right)$
$\mathbf{L_3}:\left(X_2, X_3 = \frac{-2X_2-\sqrt{1+X_2^2}+\sqrt{1-7X_2^2-4X_2\sqrt{1+X_2^2}}}{2}, X_4=0, X_6 = \frac{-2X_2-\sqrt{1+X_2^2}-\sqrt{1-7X_2^2-4X_2\sqrt{1+X_2^2}}}{2}\right)$
$\mathbf{L_4}:\left(X_2, X_3 = \frac{-2X_2-\sqrt{1+X_2^2}-\sqrt{1-7X_2^2-4X_2\sqrt{1+X_2^2}}}{2}, X_4=0, X_6 = \frac{-2X_2-\sqrt{1+X_2^2}+\sqrt{1-7X_2^2-4X_2\sqrt{1+X_2^2}}}{2}\right)$
$\mathbf{L_5}:\left(X_2, X_3 = \frac{2-3m_0+\sqrt{4-8m_0-11m_0^2}}{2m_0}X_2, X_4 = \sqrt{1-a_+X_2^2}, X_6 = -\frac{2+3m_0+\sqrt{4-8m_0-11m_0^2}}{2(1+m_0)}X_2\right)$

$\mathbf{L_6}: \left(X_2, X_3 = \frac{2-3m_0+\sqrt{4-8m_0-11m_0^2}}{2m_0}X_2, X_4 = -\sqrt{1-a_+X_2^2}, X_6 = -\frac{2+3m_0+\sqrt{4-8m_0-11m_0^2}}{2(1+m_0)}X_2\right)$
$\mathbf{L_7}: \left(X_2, X_3 = \frac{2-3m_0-\sqrt{4-8m_0-11m_0^2}}{2m_0}X_2, X_4 = \sqrt{1-a_-X_2^2}, X_6 = -\frac{2+3m_0-\sqrt{4-8m_0-11m_0^2}}{2(1+m_0)}X_2\right)$
$\mathbf{L_8}: \left(X_2, X_3 = \frac{2-3m_0-\sqrt{4-8m_0-11m_0^2}}{2m_0}X_2, X_4 = -\sqrt{1-a_-X_2^2}, X_6 = -\frac{2+3m_0-\sqrt{4-8m_0-11m_0^2}}{2(1+m_0)}X_2\right)$
where

$$a_\pm = \frac{4-2m_0-11m_0^2-6m_0^3 \pm (2+m_0-2m_0^2)\sqrt{4-8m_0-11m_0^2}}{2m_0^2(1+m_0)^2}\,, \quad m_0 \equiv m(0)\,. \tag{7.38}$$

Notice that we have additional points at infinity for special cases when $m = -4/3$ or $m = -1$. We will not study them but for sake of completeness we give them here. For $m = -1$, we have the surface $X_4^2 + X_6^2 = 1$ along with $X_2 = X_3 = 0$ and a second surface $X_3 = -3X_2,\ X_6 = -5X_2$ and $35X_2^2 + X_4^2 = 1$. While for $m = -4/3$ we have $X_3 = X_2,\ X_6 = 4X_2$ with $18X_2^2 + X_4^2 = 1$.

- P_4: Horizon point
  The eigenvalues are $(2,2,1,0)$, with eigenvectors

$$\left(\frac{1}{4},0,0,1\right), (-1,1,0,0), (0,0,1,0), \left(-\frac{1}{2},0,0,1\right).$$

  This point corresponds to a horizon and is unstable. This is a point that we had in general relativity. Remember that $\mathrm{d}\ln\mathrm{A}/\mathrm{d}\ln\mathrm{r} = 2\mathrm{x}_3/\mathrm{x}_2 = 2\mathrm{X}_3/\mathrm{X}_2$ and this point has $X_3 = 1 > 0$, hence $d\ln A/d\ln r > 0$ which corresponds to an event horizon. Also notice that one of the eigenvalues is zero because this point is part of the line L_1.

- P_5: Horizon point
  The eigenvalues are $(-2,-2,-1,0)$, with eigenvectors

$$\left(\frac{1}{4},0,0,1\right), (-1,1,0,0), (0,0,1,0), \left(-\frac{1}{2},0,0,1\right).$$

  The same analysis can be performed for this point, for which we have $d\ln A/d\ln r < 0$ hence the point is a horizon corresponding to a cosmological or Cauchy horizon depending if the point predates a singularity or an event horizon. The point is stable and one of the eigenvalues is zero because this point is part of the line L_4.

- P_6: Horizon point
  This point was also found in GR, it corresponds to horizon and this is an attractor.

- P_7: AdS point
  This point was studied in GR. This is AdS and it's stable.

- P_8:

  This point is typical of $f(R)$ theories where $x_6 \neq 0$ while we have $x_6 = 0$ in general relativity. The eigenvalues are $\left(0, 2, 1, \frac{1+m(0)}{m(0)}\right)$, with eigenvectors

$$\left(-\frac{1}{2}, 1, 0, 0\right), (-1, 0, 0, 1), , (1, 1, 0, 0), (0, 0, 1, 0).$$

  Hence the point is an repeller iff $m(0) < -1$ or $m(0) > 0$. Notice that one of the eigenvalues is zero because this point is part of the line L_2.

- P_9:

  This point is also typical of $f(R)$ theories since $x_6 \neq 0$. The eigenvalues are $\left(0, -2, -1, -\frac{1+m(0)}{m(0)}\right)$, with eigenvectors

$$\left(-\frac{1}{2}, 1, 0, 0\right), (-1, 0, 0, 1), , (1, 1, 0, 0), (0, 0, 1, 0).$$

  Hence the point is an attractor iff $m(0) < -1$ or $m(0) > 0$. Notice that one of the eigenvalues is zero because this point is part of the line L_3.

- P_{10}:

  The eigenvalues are

$$\left(-\frac{5}{3\sqrt{2}}, -\frac{5}{3\sqrt{2}}, \frac{\sqrt{2}}{3}, \frac{4+3m(0)}{3\sqrt{2}m}\right),$$

  with following eigenvectors

$$(-4, 0, 0, 1), (-1, 1, 0, 0), \left(-\frac{3}{4}, \frac{1}{4}, 0, 1\right), (0, 0, 1, 0).$$

  which implies that the point is saddle.

  For this spacetime, $X_2 \neq 0$ which implies $x_2 = \infty$ and hence $\mathcal{M}_{MS} < 0$. In fact the Misner-Sharp mass will be negative for all points and lines at infinity if $X_2 \neq 0$. The linearization around this point shows that the metric behaves like

$$A \propto r^2, \quad B \propto r^{-2}. \tag{7.39}$$

- $\bar{P}_{10}$:

  The eigenvalues are

$$\left(\frac{5}{3\sqrt{2}}, \frac{5}{3\sqrt{2}}, -\frac{\sqrt{2}}{3}, -\frac{4+3m(0)}{3\sqrt{2}m}\right),$$

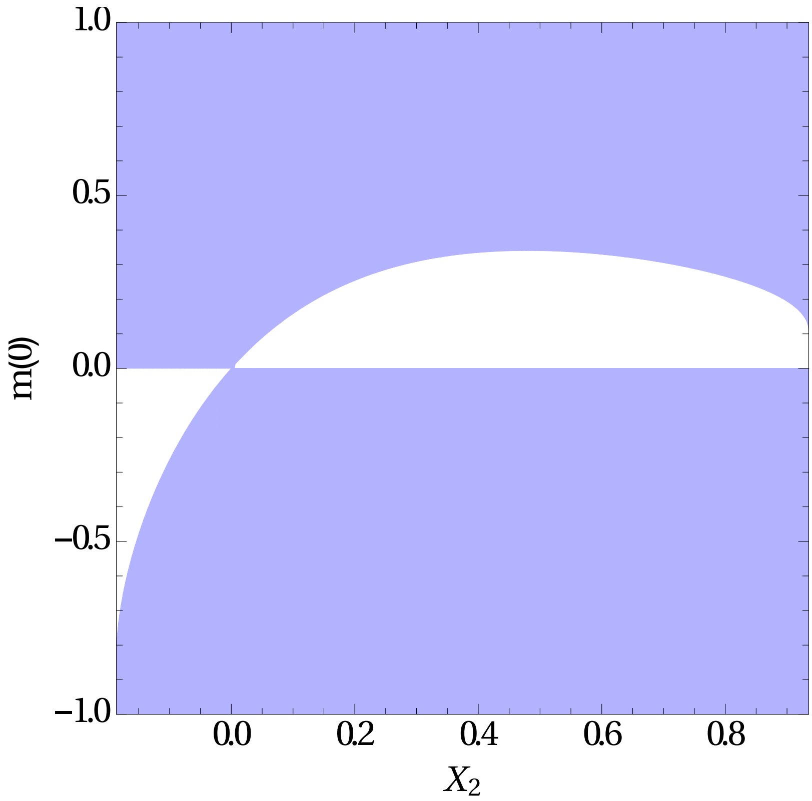

FIGURE 7.1: Stability plot of critical line L_1 (blue is the repelling region).

with following eigenvectors

$$(-4,0,0,1)\,,(-1,1,0,0)\,,\left(-\frac{3}{4},\frac{1}{4},0,1\right)\,,(0,0,1,0)\,,$$

which implies that the point is saddle.

- L_1: Critical line
  This line is defined for $-\sqrt{\frac{15-8\sqrt{3}}{33}} < X_2 < \sqrt{\frac{15+8\sqrt{3}}{33}}$. The line is a repeller when

$$1+\frac{-2X_2+\sqrt{1+X_2^2}-\sqrt{1-7X_2^2+4X_2\sqrt{1+X_2^2}}}{2(X_2+\sqrt{1+X_2^2})m(0)}>0\,,$$

and saddle elsewhere (Fig. 7.1). The stability of a critical point can change along the critical line depending on $m(0)$. Thus this system might be considered as the case of bifurcation. The linearization around this line shows that the metric behaves like

$$A\propto r^{-2+\frac{\sqrt{1+X_2^2}}{X_2}+\frac{\sqrt{1-7X_2^2+4X_2\sqrt{1+X_2^2}}}{X_2}}\,,\quad B\propto r^{2-2\frac{\sqrt{1+X_2^2}}{X_2}}\,. \tag{7.40}$$

We notice that this line is symmetric to L_4 under the transformation $X_2\to -X_2$. Therefore it is sufficient to study $X_2>0$. This is a singularity which is a repeller

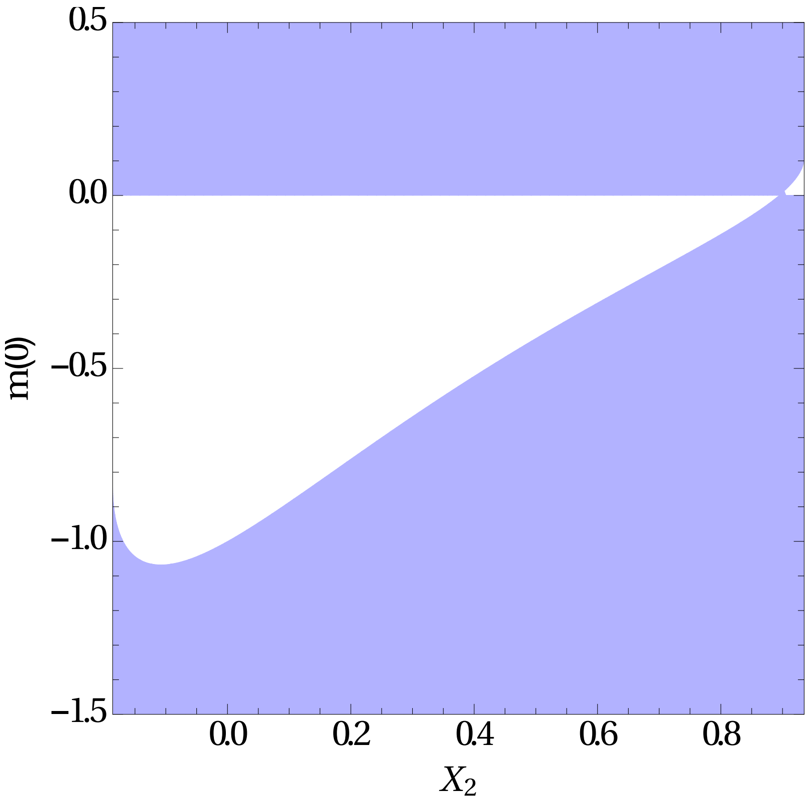

FIGURE 7.2: Stability plot of critical line L_2 (blue is the repelling region).

for some models depending on $m(0)$. Therefore we have a continuum of singularity behaviours $B \propto r^{\alpha}$ where $\alpha < 6 - 4\sqrt{3}$ while $A \propto r^{\beta}$ with $\beta > -2(2-\sqrt{3})$.

- L_2: Critical line
  This line is defined for $-\sqrt{\frac{15-8\sqrt{3}}{33}} < X_2 < \sqrt{\frac{15+8\sqrt{3}}{33}}$. The line is a repeller when

$$1 + \frac{-2X_2 + \sqrt{1+X_2^2} + \sqrt{1 - 7X_2^2 + 4X_2\sqrt{1+X_2^2}}}{2(X_2 + \sqrt{1+X_2^2})m(0)} > 0\,,$$

and saddle elsewhere (Fig. 7.2). The linearization around this line shows that the metric behaves like

$$A \propto r^{-2+\frac{\sqrt{1+X_2^2}}{X_2}-\frac{\sqrt{1-7X_2^2+4X_2\sqrt{1+X_2^2}}}{X_2}}\,, \quad B \propto r^{2-2\frac{\sqrt{1+X_2^2}}{X_2}} \tag{7.41}$$

We notice that this line is symmetric to L_3 under the transformation $X_2 \to -X_2$. Therefore it is sufficient to study $X_2 > 0$. This is a singularity which is a repeller for some models depending on $m(0)$. Therefore we have a continuum of singularity behaviours $B \propto r^{\alpha}$ where $\alpha < 6 - 4\sqrt{3}$ while $A \propto r^{\beta}$ with $\beta < -2(2-\sqrt{3})$.

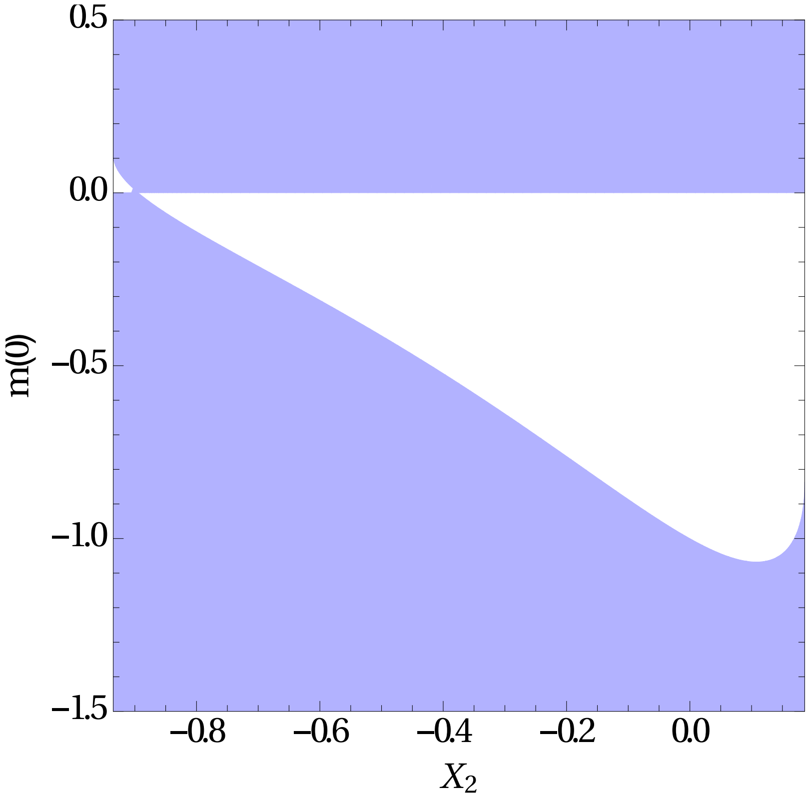

FIGURE 7.3: Stability plot of critical line L_3 (blue is the attracting region).

Notice that there are 2 particular values of X_2 for which $A = B$, this is for $X_2 = 1/\sqrt{3}$ or $X_3 = 2/\sqrt{5}$ for which the metric is respectively $A = B = 1/r^2$ or $A = B = 1/r$.

- L_3: Critical line
  This line is defined for $-\sqrt{\frac{15+8\sqrt{3}}{33}} < X_2 < \sqrt{\frac{15-8\sqrt{3}}{33}}$. The line is an attractor when

$$1 + \frac{-2X_2 - \sqrt{1+X_2^2} - \sqrt{1 - 7X_2^2 - 4X_2\sqrt{1+X_2^2}}}{2(X_2 - \sqrt{1+X_2^2})m(0)} > 0\,,$$

and saddle elsewhere (Fig. 7.3). The linearization around this line shows that the metric behaves like

$$A \propto r^{-2-\frac{\sqrt{1+X_2^2}}{X_2}+\frac{\sqrt{1-7X_2^2-4X_2\sqrt{1+X_2^2}}}{X_2}}\,, \quad B \propto r^{2+2\frac{\sqrt{1+X_2^2}}{X_2}}\,. \tag{7.42}$$

As we said it is sufficient to study $X_2 > 0$. This is an attractor for some models depending on $m(0)$. Therefore we have a continuum of behaviours at infinity $B \propto r^{\alpha}$ where $\alpha > 6 + 4\sqrt{3}$ while $A \propto r^{\beta}$ with $-2(2 + \sqrt{3}) < \beta < -4$.

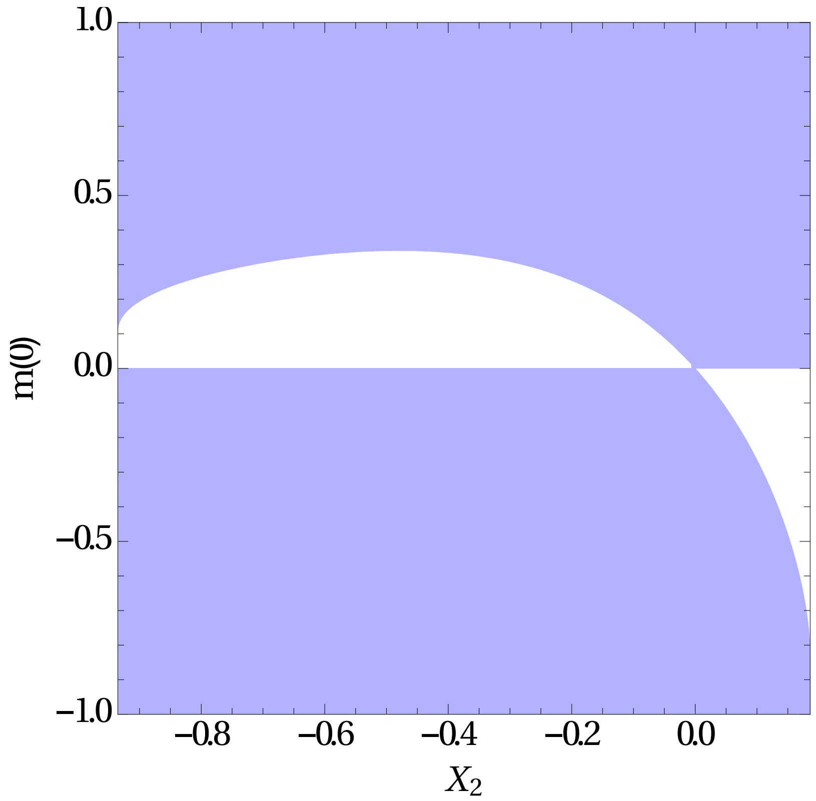

FIGURE 7.4: Stability plot of critical line L_4 (blue is the attracting region).

- L_4: Critical line

  This line is defined for $-\sqrt{\frac{15+8\sqrt{3}}{33}} < X_2 < \sqrt{\frac{15-8\sqrt{3}}{33}}$. The line is an attractor when

$$1+\frac{-2X_2-\sqrt{1+X_2^2}+\sqrt{1-7X_2^2-4X_2\sqrt{1+X_2^2}}}{2(X_2-\sqrt{1+X_2^2})m(0)}>0\,,$$

  and saddle elsewhere (Fig. 7.4). The linearization around this line shows that the metric behaves like

$$A \propto r^{-2-\frac{\sqrt{1+X_2^2}}{X_2}-\frac{\sqrt{1-7X_2^2-4X_2\sqrt{1+X_2^2}}}{X_2}}\,, \qquad B \propto r^{2+2\frac{\sqrt{1+X_2^2}}{X_2}}\,. \tag{7.43}$$

  As we said it is sufficient to study $X_2 > 0$. This is an attractor for some models depending on $m(0)$. Therefore we have a continuum of behaviorus at infinity $B \propto r^{\alpha}$ where $\alpha > 6+4\sqrt{3}$ while $A \propto r^{\beta}$ with $\beta < -2(2+\sqrt{3})$.

- $L_{5,6,7,8}$: Critical lines

  These lines are defined for $-\frac{2}{11}(\sqrt{15}+2) < m(0) < \frac{2}{11}(\sqrt{15}-2)$ and $0 < X_2 < \sqrt{\frac{4}{33}+\frac{14}{33\sqrt{15}}}$ for $L_{5,6}$ and $0 < X_2 < \sqrt{\frac{15+8\sqrt{3}}{33}}$ for $L_{7,8}$. As previously we consider only $X_2 > 0$.

These lines are difficult to study, so they should be considered for specific models. We will see that for most of the models, these lines do not exist.

Notice that contrary to cosmology it is not possible to study the models in the $u - m$ plane because of a large degeneracy of the solutions. In fact, we can have various spacetimes with the same curvature scalar R and hence with the same (u, m). Also some of the critical points like, for example, the Minkowski (P_1) are not localized in the $u - m$ plane.

7.2 Analysis

In this section, we will not consider the lines L_5, L_6, L_7, L_8 because they will not exist for most of the models. Therefore we have 2 repellers: L_1 and L_2, notice that P_4 is part of L_1 while P_8 is part of L_2. Also we have various attractors: P_7 (AdS point), P_6 (horizon), P_3 (Clifton-Barrow point). All the 3 attractors are localized at $x_4 \neq 0$. We also have attractors on the surface $x_4 = 0$ like P_2, L_3, L_4; P_9 is part of L_3 and P_5 is part of L_4.

Hence we see that most of the critical points are localized on the hypersurface $x_4 = 0$ except the Clifton-Barrow point P_3 which is model dependent and the points P_6 which is a horizon and P_7, the AdS point.

We also notice that $x_4 = 0$ can be an invariant submanifold, depending on the functional form of m. For example if $m = u^a$ where $u = x_4/x_5$, the equation for x_4 (Eq. 7.14) reduces to

$$x_4' = x_4^{1-a} \left(2x_2 x_4^a + x_6 x_5^a\right) . \tag{7.44}$$

Therefore in this case $x_4 = 0$ is an invariant submanifold only if $a < 1$. This will be the case for most of the interesting models.

If we assume that the invariant submanifold exists, then we have 2 possibilities. The first case corresponds to initial conditions $x_4 = 0$ (i.e., $R = 0$) and hence we stay on the hypersurface. Going back to the equations of motion, it implies the condition

$$f'(0)R_{\mu\nu} - \frac{1}{2}f(0)g_{\mu\nu} = 0\,, \tag{7.45}$$

which is consistent with $R = 0$ iff $f(0) = f'(0) = 0$. But as we said in the introduction, we will not be considering this case and it is also a trivial case to study without the dynamical approach. Therefore we will only study the flow of the dynamical system which are not on the invariant submanifold but which obviously can converge to it asymptotically.

As we have seen, if the model is not pathological which means $f'(0)/f''(0) \neq 0$, then we have for $R = 0$ necessarily $\hat{R} = 0$ which implies that on the invariant submanifold $x_4 = 0$ we need to also impose $x_6 = 0$ which reduces the lines found into points. The phase space in this invariant submanifold is therefore trivial and defined by (x_2, x_3) but also because in most of the models $f(0)/f'(0) = 0$ we have an additional constraint $x_5 = 0$ which reduces the invariant submanifold to 1D and corresponds to Schwarzschild spacetime with only 3 critical points: Minkowski, the singularity and the horizon.

Moreover, following the same argument, we can say that points $P_8,\ P_9,\ P_{10}$ and $\bar{P}_{10}$ are not physical for the $f(R)$ models that we are interested in.

7.3 Specific Models

In this section, we will study some specific $f(R)$ models.

7.3.1 $f(R) = \alpha R^{n+1}$

This model has been studied extensively in [Clifton and Barrow 2005]. For this model, $m = n$ and $u = x_4/x_5 = -(n+1)$ and this is the only $f(R)$ model where we can further reduce the degrees of freedom of the system by one.

So apart from the two usual constraints, there is a third constraint of the form

$$x_4 = -(n+1)x_5 = \frac{n+1}{3n}(1 - x_2^2 - 2x_2x_6 - 2x_2x_3 - x_3x_6)\,. \tag{7.46}$$

Therefore only the critical points which are localized on this surface should be considered. We see that P_2 should be excluded while P_1 and P_3 remain. Notice that for most of the interesting models like $f(R) = R^2$, P_3 doesn't exist. Hence for these models, only Minkowski exists at finite distance in the phase space. At infinity the constraint becomes $X_4^2 = 1 - (X_2 + X_3)^2 - (X_2 + X_6)^2 - X_3X_6$. P_{10} is then absent. There are two additional critical points that arise due to the reduction of the system. They are

- $\mathbf{P_{11}}$: $(X_2, X_3, X_6) = \left(\frac{1+2n}{\sqrt{6+12n^2}}, \frac{1+2n}{\sqrt{6+12n^2}}, \frac{2(n-1)}{\sqrt{6+12n^2}}\right)$. The point exists for $n \neq -1/2$. Eigenvalues of the linearized system are

$$\left(\frac{2 - 4\delta(1+\delta)}{\delta\sqrt{6 + 12\delta^2}}, \frac{1 - 2\delta(1+4\delta)}{\delta\sqrt{6 + 12\delta^2}}, \frac{1 - 2\delta(1+4\delta)}{\delta\sqrt{6 + 12\delta^2}}\right)\,.$$

It is an attractor when $\left(-\frac{1}{2} < n < 0\right)$ or $\left(n > \frac{\sqrt{3}-1}{2}\right)$, repeller when $\left(n < -\frac{\sqrt{3}+1}{2}\right)$ or $\left(0 < n < \frac{1}{4}\right)$ and saddle otherwise. The linearization around this point shows that the metric behaves like

$$A \propto r^2\,, \quad B \propto r^{\frac{2(2n^2+2n-1)}{n(2n+1)}}\,. \tag{7.47}$$

- $\bar{\mathbf{P}}_{\mathbf{11}}$: $(X_2, X_3, X_6) = \left(-\frac{1+2n}{\sqrt{6+12n^2}}, -\frac{1+2n}{\sqrt{6+12n^2}}, -\frac{2(n-1)}{\sqrt{6+12n^2}}\right)$. The point exists for $n \neq -1/2$. Eigenvalues of the linearized system are

$$\left(-\frac{2-4\delta(1+\delta)}{\delta\sqrt{6+12\delta^2}}, -\frac{1-2\delta(1+4\delta)}{\delta\sqrt{6+12\delta^2}}, -\frac{1-2\delta(1+4\delta)}{\delta\sqrt{6+12\delta^2}}\right)\,,$$

and is an attractor when $\left(n < -\frac{\sqrt{3}+1}{2}\right)$ or $\left(0 < n < \frac{1}{4}\right)$, repeller when $\left(-\frac{1}{2} < n < 0\right)$ or $\left(n > \frac{\sqrt{3}-1}{2}\right)$ and sadlle otherwise.

7.4 Conclusions

In this chapter, we effectively reformulated the system of modified Einstein field equations for $f(R)$ theories in LRS-II spacetimes into an autonomous system of covariantly defined variables. The phase space has been compactified to study the nontrivial behaviours at infinity. We have concentrated on physically viable $f(R)$ models where $f_{,R} > 0$ and $f_{,RR} > 0$ and notice that the system of equations are of higher dimensions and more complex than the GR case, developed in chapter 6. Using the tools of dynamical system analysis, we found the important global features of these spacetimes. We have easily shown that for any theory of the form $f(R) = R + h(R)$, the unique asymptotically flat solution is Schwarzschild. Also, we could recover the Clifton-Barrow solution. The work is still in progress. We are trying to find a way to study the flow of the trajectories in the 4D space and get a complete physical picture.

Chapter 8

Global structure of black holes sourced by quintessence field

As we have seen, scalar degree of freedom encodes most of the interesting aspects of modified gravity. From mass of the graviton to brane-bending mode of the brane models, it is the simplest and the most interesting extension of the standard theory of gravity. Therefore the study of these models is highly legitimate. Also, because these models originate often in high energy theories such as supergravity or as moduli fields in string theory, it is natural to study these models in the context of the most energetic objects in gravity, namely black holes.

In this chapter, the main goal is to show the feasibility of our approach in the study of these models. Therefore we will consider the simplest theory, quintessence. It should be noticed that once the framework has been established, the analysis will become trivial for any scalar-tensor theory and therefore can be trivially generalized. Also this chapter will be a first step to future work, on time dependent spherically symmetric problems, the so called G_2 cosmology which have two commuting Killing vector fields (i.e., models which admit a 2-parameter Abelian isometry group acting transitively on spacelike 2-surfaces). Therefore G_2 models are relevant in the context of early cosmology because of the inhomogeneities included in the analysis.

In this work, we will search for viable potentials in the context of quintessence models which give a proper black hole solution, with a horizon and nice asymptotic behaviour as Minkowski or de Sitter.

The chapter is organized as follows. The autonomous system for the static case in quintessence model is given Sec. 8.1. In Sec. 8.2, we study the system for massless scalar field and for massive field in Sec. 8.3. Finally we conclude in Sec. 8.4. This chapter is also based on a work in progress [Cruz et al. n.d.].

8.1 Quintessence model

As we discussed in chapter 2, quintessence model is equivalent to $f(R)$ theories in Einstein frame with energy momentum tensor

$$T_{\mu\nu}^{(\psi)} := \nabla_\mu\psi\nabla_\nu\psi - \frac{1}{2}g_{\mu\nu}\left[(\nabla\psi)^2 + 2V(\psi)\right], \tag{8.1}$$

where $V(\psi)$ is the scalar field potential.

Since we are interested in the static LRS class II spacetimes, all the time derivatives are zero, thus $\dot{\psi} = 0$ and we already know $\theta = \Sigma = Q = 0$.

The 1+1+2 decomposition of (8.1) leads to

$$\rho = \frac{1}{2}\hat{\psi}^2 + V(\psi), \tag{8.2a}$$

$$p = -\frac{1}{6}\hat{\psi}^2 - V(\psi), \tag{8.2b}$$

$$\Pi = \frac{2}{3}\hat{\psi}^2. \tag{8.2c}$$

For the sake of simplicity we introduce the new variable $\Psi = \hat{\psi}$, and using Eqs. (8.2), we can rewrite the system of equations (5.42a)-(5.47) as

$$\hat{\psi} = \Psi, \tag{8.3a}$$

$$\hat{\phi} = -\frac{1}{2}\phi^2 - \frac{2}{3}\left(\Psi^2 + V(\psi)\right) - \mathcal{E}, \tag{8.3b}$$

$$\hat{\mathcal{E}} = \frac{1}{3}\Psi^2\left(\mathcal{A} - \frac{1}{2}\phi\right) - \frac{3}{2}\phi\mathcal{E}, \tag{8.3c}$$

$$\hat{\mathcal{A}} = -\left(\mathcal{A} + \phi\right)\mathcal{A} - V(\psi), \tag{8.3d}$$

$$\hat{\Psi} = -\left(\mathcal{A} + \phi\right)\Psi + V_{,\psi}, \tag{8.3e}$$

$$\hat{K} = -\phi K, \tag{8.3f}$$

subject to the constraints

$$\mathcal{E} = -\mathcal{A}\phi - \frac{2V(\psi)}{3} + \frac{\Psi^2}{3}, \tag{8.4}$$

$$K = \mathcal{A}\phi + V(\psi) - \frac{\Psi^2}{2} + \frac{\phi^2}{4}. \tag{8.5}$$

Taking the spatial derivative of Eqs. (8.4) and (8.5) and substituting (8.3a)-(8.5), we obtain two identities. This means that the restrictions are preserved by the propagation equations.

8.2 Massless scalar field

We start with the simple problem of massless scalar field. For this case $V(\psi) = \mathrm{dV}/\mathrm{d}\psi = 0$, and the restrictions (8.4) and (8.5) reduces to

$$\mathcal{E} = -\mathcal{A}\phi + \frac{\Psi^2}{3}\,, \tag{8.6a}$$

$$K = \mathcal{A}\phi - \frac{\Psi^2}{2} + \frac{\phi^2}{4} \tag{8.6b}$$

Eq. (8.6b) allows to define a set of normalized variables, defined as

$$x_1 = -\frac{\mathcal{E}}{K},\; x_2 = \frac{\phi}{2\sqrt{K}},\; x_3 = \frac{\mathcal{A}}{\sqrt{K}}, y_1 = \frac{\Psi}{\sqrt{2K}}\,. \tag{8.7}$$

Using the definitions, the constraints can be written as

$$x_2^2 + 2x_2x_3 - y_1^2 = 1\,, \tag{8.8a}$$

$$x_1 - 2x_2x_3 + \frac{2}{3}y_1^2 = 0\,, \tag{8.8b}$$

and the set of autonomous system is as follows:

$$x_1' = \frac{2}{3}y_1^2(x_2 - x_3) - x_1x_2\,, \tag{8.9a}$$

$$x_2' = \frac{1}{6}\left(3x_1 - 4y_1^2\right)\,, \tag{8.9b}$$

$$x_3' = -x_3(x_2 + x_3)\,, \tag{8.9c}$$

$$y_1' = y_1(-x_2 - x_3)\,, \tag{8.9d}$$

where, as in chapters 6 and 7, we define the new radial derivative $f' = \hat{f}/\sqrt{K}$. Taking derivatives of (8.8), and substituting (8.9) and (8.8), we find that the constraints are preserved. Thus, we can eliminate two degrees of freedom from the system, say

$$y_1^2 = x_2^2 + 2x_2x_3 - 1\,, \tag{8.10a}$$

$$x_1 = -\frac{2}{3}\left(x_2^2 - x_2x_3 - 1\right)\,. \tag{8.10b}$$

Using the new constraints (8.10) and substituting in (8.9), we get the reduced dynamical system

$$x_2' = 1 - x_2(x_2 + x_3)\,, \tag{8.11a}$$

$$x_3' = -x_3(x_2 + x_3)\,. \tag{8.11b}$$

Point	X_2	X_3	Stability	Nature
P_H	0	1	Repeller	Horizon
$\bar{P}_H$	0	-1	Attractor	Horizon
P_S	$\frac{2}{\sqrt{5}}$	$-\frac{1}{\sqrt{5}}$	Repeller	Singularity
$\bar{P}_S$	$-\frac{2}{\sqrt{5}}$	$\frac{1}{\sqrt{5}}$	Attractor	Singularity

TABLE 8.1: Critical points at infinity for the Poincaré (global) system (8.13).

defined in the phase space

$$\left\{(x_2, x_3) : x_2^2 + 2x_2 x_3 \geq 1\right\} . \tag{8.12}$$

This condition arises from the fact that y_1^2 needs to be non-negative. The system (8.11) admits two fixed points at the finite region

P$_{\mathbf{M}}$: $(x_2 = 1, x_3 = 0)$: Minkowski point. This critical point is similar to the one that exists in our analysis for GR (chapter 6). The eigenvalues of the linearized system around this point are $(-2, -1)$, hence the point is an attractor.

$\bar{\mathbf{P}}_{\mathbf{M}}$: $(x_2 = -1, x_3 = 0)$: Anti-Minkowski point. The eigenvalues of the linearized system around this point are $(2, 1)$, hence the point is a repeller.

As the system is defined on an unbounded phase space, there might exist nontrivial behaviour at the region where the variables diverge. For this reason, as described in the last two chapters, it is worthy to introduce Poincaré transformation $x_i = X_i/Z$, with the constraint $X_2^2 + X_3^2 + Z^2 = 1$. The infinity boundary $x_2^2 + x_3^2 \to +\infty$ corresponds to the unitary circle $X_2^2 + X_3^2 = 1$ or $Z \to 0$. The propagation equations in the transformed coordinates are:

$$\bar{X}_2 \equiv Z X_2' = (1 - X_2 (2X_2 + X_3)) \left(1 - X_2^2 - X_3^2\right) , \tag{8.13a}$$

$$\bar{X}_3 \equiv Z X_3' = -X_3 (2X_2 + X_3) \left(1 - X_2^2 - X_3^2\right) , \tag{8.13b}$$

defined on the phase space

$$\left\{(X_2, X_3) : 2X_2^2 + 2X_2 X_3 + X_3^2 \geq 1, X_2^2 + X_3^2 \leq 1\right\} . \tag{8.14}$$

The entire infinite space (circumference of the circle in Fig. 8.1) turns out to be critical for the Poincaré (global) system (8.13). In table 8.1, we present the interesting critical points at infinity. The corresponding global phase space for the system (8.13) is given in Fig. 8.1. The shadowed region enclosed by the lines connecting the critical points and the unitary circle, i.e., $2X_2^2 + 2X_2X_3 + X_3^2 > 1, X_2^2 + X_3^2 < 1$ is forbidden since it leads to the violation of the

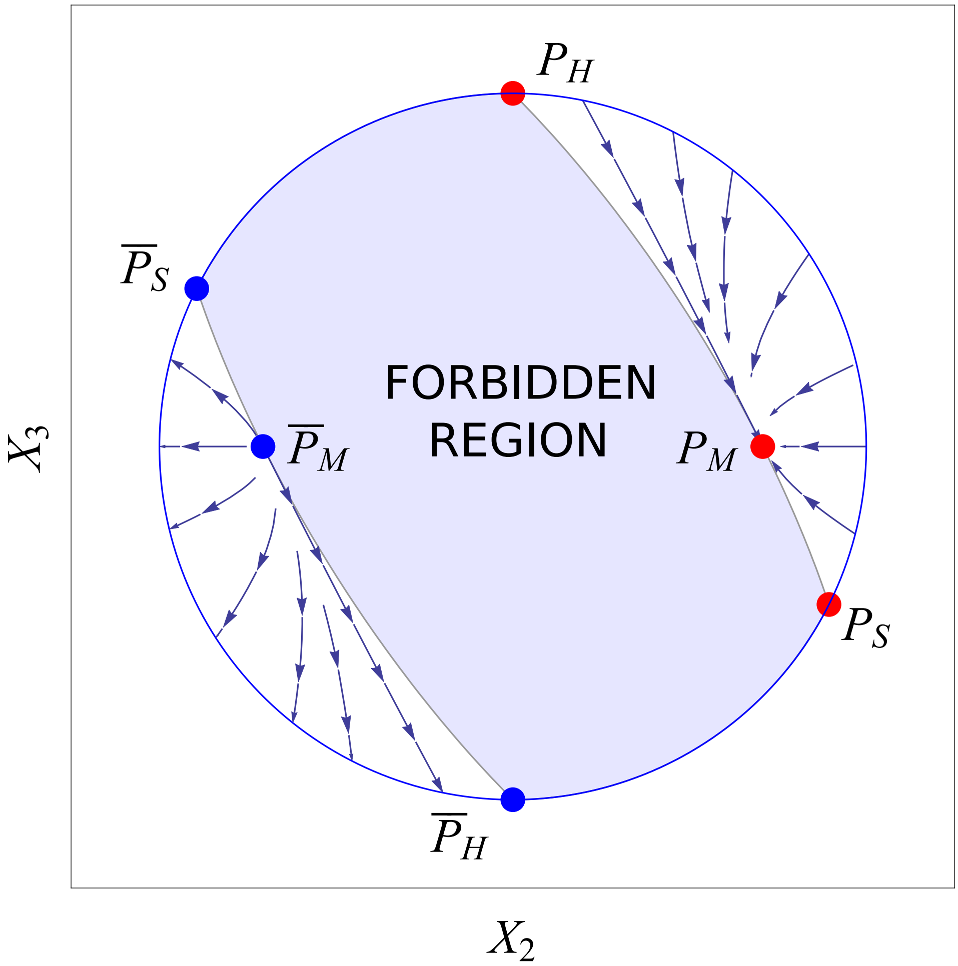

FIGURE 8.1: Global phase space for the system (8.13). The global sink (respectively source) is P_M (respectively $\bar{P}_M$), which belongs to the finite region. P_H and P_S are repellers, whereas $\bar{P}_H$ and $\bar{P}_S$ are attractors. The shadowed region is forbidden since it leads to the violation of the reality condition $y_1^2 \geq 0$.

energy condition $y_1^2 \geq 0$. The trajectories from P_H to P_M or P_S to P_M and the complementary trajectories on the other side of $X_2 = 0$ bears a stark resemblance to the vacuum spacetime in GR (chapter 6) since it corresponds to the trivial solution when the scalar field is constant. Hence, it is the Schwarzschild solution. All other trajectories which start from infinity to P_M (for $X_2 > 0$) or go towards infinity from $\bar{P}_M$ (for $X_2 < 0$) correspond to non-trivial configuration of the scalar field. As none of these trajectories start from $X_2 = 0$, so the non-trivial scalar fields do not have a horizon but a naked singularity. For the sake of completeness, we mention the critical lines

- $\mathbf{L_1}$: $\left(-1 \leq X_2 \leq -\frac{2}{\sqrt{5}} \text{ or } 0 < X_2 \leq 1,\ X_3 = \sqrt{1 - X_2^2}\right)$: The eigenvalues of the linearized system are $\left(0, 2\left(X_2 + \sqrt{1 - X_2^2}\right)\right)$, its an attractor in the region $-1 \leq X_2 \leq -\frac{2}{\sqrt{5}}$, and repeller in the region $0 < X_2 \leq 1$. So, the stability of a critical point changes with X_2 along the critical line. The linearization around the line shows that the metric behaves like

$$A \propto r^{2\frac{\sqrt{1-X_2^2}}{X_2}}\,, \quad B \propto r^{-2\left(1+\frac{\sqrt{1-X_2^2}}{X_2}\right)}\,. \tag{8.15}$$

The critical line is a continuum of singularity.

- $\mathbf{L_2}$: $\left(-1 < X_2 < 0 \text{ or } \frac{2}{\sqrt{5}} \leq X_2 < 1,\ X_3 = -\sqrt{1-X_2^2}\right)$: The eigenvalues of the linearized system are $\left(0, 2\left(X_2 - \sqrt{1-X_2^2}\right)\right)$, its an attractor in the region $-1 < X_2 < 0$, and repeller in the region $\frac{2}{\sqrt{5}} \leq X_2 < 1$. We see that the stability of a critical point changes with X_2 along the critical line. The linearization around the line shows that the metric behaves like

$$A \propto r^{-2\frac{\sqrt{1-X_2^2}}{X_2}}\,, \quad B \propto r^{-2\left(1-\frac{\sqrt{1-X_2^2}}{X_2}\right)}\,. \tag{8.16}$$

The critical line is a continuum of singularity.

The stability can also be verified from the phase space diagram, Fig. 8.1. So, any trajectory which starts from a singularity and not from the horizon describes a naked singularity. The only solution describing a black hole is the Schwarzschild solution. This corresponds to the Fisher solution.

As we have noticed, there is a forbidden region. The Fisher metric can be written as

$$ds^2 = -F^S dt^2 + \frac{dr^2}{F^S} + r^2 F^{1-S} d\Omega^2 \tag{8.17}$$

$$\psi = \sqrt{\frac{1-S^2}{2}}\log F, \qquad F = 1 - \frac{r_S}{r}\,. \tag{8.18}$$

In terms, of this solution, the forbidden region corresponds to $S > 1$. Therefore it corresponds to the reality condition of the scalar field as we have said previously. This is consistent.

Also we see that $x_3 = 0$ is an invariant submanifold. Therefore it is interesting to study this case in particular. The equations reduce to

$$x_2' = 1 - x_2^2\,. \tag{8.19}$$

This equation is easily solved and it gives the metric

$$ds^2 = -dt^2 + \frac{dr^2}{1+\alpha/r^2} + r^2 d\Omega^2\,. \tag{8.20}$$

Since $y_1^2 = \alpha/r^2 > 0$, we have $\alpha > 0$ and therefore this solution describes a naked singularity. This solution can be easily written in the form of the Fisher solution with $S = 0$.

8.3 Massive scalar field

For massive scalar field, potential $V(\psi)$ is nonzero and hence Eq. (8.5) allows us to define the following set of normalized variables

$$x_1 = -\frac{\mathcal{E}}{K},\; x_2 = \frac{\phi}{2\sqrt{K}},\; x_3 = \frac{\mathcal{A}}{\sqrt{K}},$$
$$y_1 = \frac{\Psi}{\sqrt{2K}},\; y_2 = \frac{V(\psi)}{3K}\,. \tag{8.21a}$$

The restrictions now become

$$x_2^2 + 2x_2x_3 - y_1^2 + 3y_2 = 1\,, \tag{8.22a}$$
$$3x_1 - 6x_2x_3 + 2y_1^2 - 6y_2 = 0\,. \tag{8.22b}$$

Now, let's define the auxiliary variables

$$\lambda = -\frac{V_{,\psi}}{V(\psi)},\; \Gamma = \frac{V_{,\psi\psi}V(\psi)}{(V_{,\psi})^2}\,, \tag{8.23}$$

where $V_{,\psi} = dV/d\psi$ and $V_{,\psi\psi} = d^2V/d\psi^2$ and the main hypothesis is that Γ can be written explicitly as a function of λ, i.e., $\Gamma \equiv \Gamma(\lambda)$. The propagation equations for the variables (8.21) and λ are given by

$$x_1' = \frac{2}{3}y_1^2(x_2 - x_3) - x_1x_2\,, \tag{8.24a}$$
$$x_2' = \frac{1}{6}\left(3x_1 - 4y_1^2 - 6y_2\right)\,, \tag{8.24b}$$
$$x_3' = -x_3(x_2 + x_3) - 3y_2\,, \tag{8.24c}$$
$$y_1' = y_1(-x_2 - x_3) - \frac{3\lambda y_2}{\sqrt{2}}\,, \tag{8.24d}$$
$$y_2' = y_2\left(2x_2 - \sqrt{2}\lambda y_1\right)\,, \tag{8.24e}$$
$$\lambda' = -\sqrt{2}(\Gamma - 1)\lambda^2 y_1\,. \tag{8.24f}$$

The restrictions (8.22a) and (8.22b) are conserved, thus we can use them to eliminate two variables, say x_1 and y_2,

$$x_1 = \frac{2}{3}\left(1 - x_2^2 + x_2 x_3\right) , \tag{8.25a}$$

$$y_2 = \frac{1}{2}\left(1 - x_2(x_2 + 2x_3) + y_1^2\right) . \tag{8.25b}$$

Then we get the reduced dynamical system

$$x_2' = x_2 x_3 - y_1^2 , \tag{8.26a}$$

$$x_3' = x_2^2 + x_2 x_3 - x_3^2 - y_1^2 - 1 , \tag{8.26b}$$

$$y_1' = \frac{\lambda\left(x_2^2 + 2x_2 x_3 - y_1^2 - 1\right)}{\sqrt{2}} - y_1(x_2 + x_3) , \tag{8.26c}$$

$$\lambda' = -\sqrt{2}(\Gamma - 1)\lambda^2 y_1 . \tag{8.26d}$$

For nonnegative potentials, ie. $y_2 \geq 0$, the above system define a flow on the unbounded phase space

$$\left\{(x_2, x_3, y_1, \lambda) : x_2(x_2 + 2x_3) - y_1^2 \leq 1, \lambda \in \mathbb{R}\right\} . \tag{8.27}$$

Now let's examine some simpler examples before studying the general case.

8.3.1 Exponential potential: $V = V_0 e^{-\lambda\psi}$

For this case λ is a constant and the tracker parameter $\Gamma = 1$. Thus the last equation is trivially satisfied and we can study the reduced 3D system for (x_2, x_3, y_1).

The fixed points at the finite region of the phase space (8.27) are

$\mathbf{P_M}$: $(x_2 = 1, x_3 = 0, y_1 = 0)$: Minkowski point. The linearized system around this point has eigenvalues $(2, -1, -1)$, hence it is a saddle point. The eigenvectors are

$$\left(\frac{1}{\sqrt{2}\lambda}, \frac{\sqrt{2}}{\lambda}, 1\right) ,\ (0, 0, 1),\ (-1, 1, 0) .$$

Now, we want to reduce the system into an attractor subspace where the eigenvalues are (-1,-1) as we did for the Minkowski point in chapter 7. The subspace will be defined by

$$x_2^2 + 2x_2 x_3 - y_1^2 - 1 = 0 . \tag{8.28}$$

The equation defines an invariant submanifold, so any trajectory on this surface remains on the surface. From Eq. 8.25b, we note that for this configuration, $y_2 = 0$. *Thus it implies that quintessence model with exponential potential does not have an asymptotically flat spacetime.*

$\bar{\mathbf{P}}_{\mathbf{M}}$: $(x_2 = -1, x_3 = 0, y_1 = 0)$: Anti-Minkowski point. The linearized system around this point has eigenvalues $(-2, 1, 1)$, hence it is a saddle point.

For analyzing the stability at the infinite region we introduce the Poincaré transformation $(x_i = X_i/Z,\ y_1 = Y_1/Z)$, with the constraint $X_2^2 + X_3^2 + Y_1^2 + Z^2 = 1$. The infinity boundary $x_2^2 + x_3^2 + y_1^2 \to +\infty$ corresponds to the unitary circle $X_2^2 + X_3^2 + Y_1^2 = 1$. The system (8.26) for the exponential potential ($\lambda =$ const., $\Gamma = 1$) becomes

$$\begin{aligned}\bar{X}_2 \equiv ZX_2' = &-\frac{\lambda}{\sqrt{2}}X_2Y_1\left(2X_2^2 + 2X_2X_3 + X_3^2 - 1\right) + Y_1^2\left(X_2(2X_2 + X_3) - 1\right)\\ &- X_2X_3\left(X_2(3X_2 + X_3) - 2\right)\,,\end{aligned} \tag{8.29a}$$

$$\begin{aligned}\bar{X}_3 \equiv ZX_3' = &-\frac{\lambda}{\sqrt{2}}X_3Y_1\left(2X_2^2 + 2X_2X_3 + X_3^2 - 1\right) - 3X_2^2X_3^2 + 2X_2^2 - X_2X_3^3\\ &+ X_3Y_1^2\left(2X_2 + X_3\right) + X_2X_3 + X_3^2 - 1\,,\end{aligned} \tag{8.29b}$$

$$\begin{aligned}\bar{Y}_1 \equiv ZY_1' = &\frac{\lambda}{\sqrt{2}}\left(1 - Y_1^2\right)\left(2X_2^2 + 2X_2X_3 + X_3^2 - 1\right) - X_2Y_1\left(3X_2X_3 + X_3^2 + 1\right)\\ &+ Y_1^3\left(2X_2 + X_3\right)\,.\end{aligned} \tag{8.29c}$$

defined on the phase space

$$\left\{(X_2, X_3, Y_1) : 2X_2^2 + 2X_2X_3 + X_3^2 \leq 1,\ X_2^2 + X_3^2 + Y_1^2 \leq 1\right\}\,. \tag{8.30}$$

The critical points and lines at infinity are listed below

- $\mathbf{P_1}$: $\left(\lambda \in \mathbb{R},\ X_2 = X_3 = \sqrt{\frac{2}{4+\lambda^2}},\ Y_1 = \frac{\lambda}{\sqrt{4+\lambda^2}}\right)$: The eigenvalues are $\left(\frac{\lambda^2-6}{\sqrt{2(4+\lambda^2)}}, \frac{\lambda^2-6}{\sqrt{2(4+\lambda^2)}}, \frac{\sqrt{2}(\lambda^2-2)}{\sqrt{4+\lambda^2}}\right)$. Its attractor in the region $-\sqrt{2} \leq \lambda \leq \sqrt{2}$, repeller in the region $\lambda > \sqrt{6}$ or $\lambda < -\sqrt{6}$ and saddle point otherwise. The linearization shows that the metric behaves like

$$A \propto r^2\,, \quad B \propto r^{-\lambda^4 - 2\lambda^2 + 8}\,. \tag{8.31}$$

- $\bar{\mathbf{P}}_{\mathbf{1}}$: $\left(\lambda \in \mathbb{R},\ X_2 = X_3 = -\sqrt{\frac{2}{4+\lambda^2}},\ Y_1 = -\frac{\lambda}{\sqrt{4+\lambda^2}}\right)$: The eigenvalues are $\left(-\frac{\lambda^2-6}{\sqrt{2(4+\lambda^2)}}, -\frac{\lambda^2-6}{\sqrt{2(4+\lambda^2)}}, -\frac{\sqrt{2}(\lambda^2-2)}{\sqrt{4+\lambda^2}}\right)$. Its attractor in the region $\lambda \geq \sqrt{6}$ or $\lambda \leq -\sqrt{6}$, repeller in the region $-\sqrt{2} < \lambda < \sqrt{2}$ and saddle point otherwise.

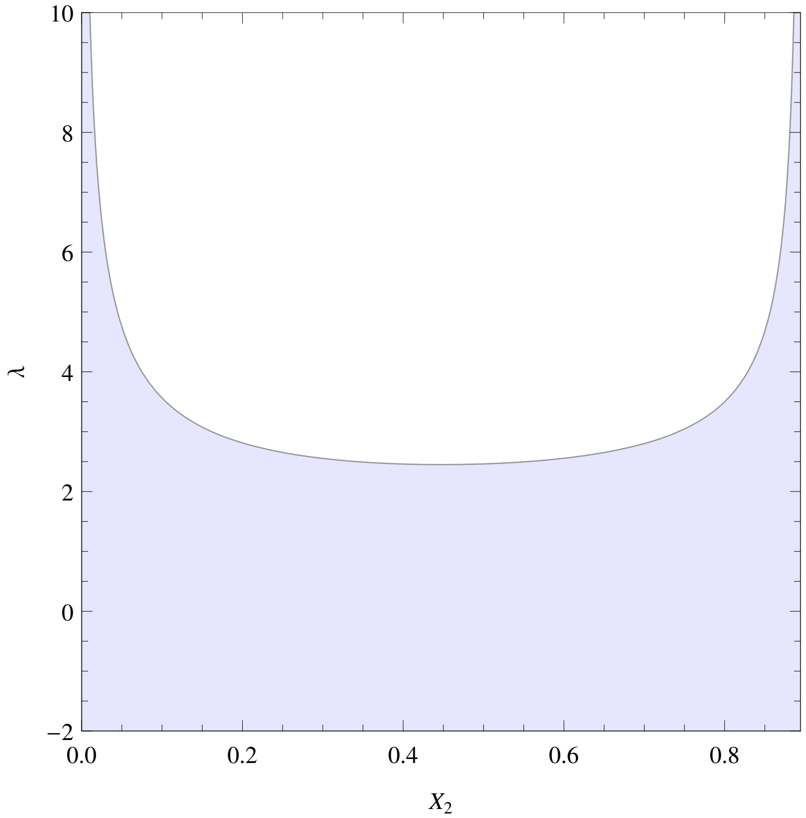

Figure 8.2: Stability plot of critical line L_1 (or L_4 for $X_2 \to -X_2$). Blue is the repelling (attracting) region.

- $\mathbf{L_1}$: $\left(\lambda \in \mathbb{R},\ 0 \le X_2 \le \frac{2}{\sqrt{5}},\ X_3 = -X_2 + \sqrt{1-X_2^2},\ Y_1 = \sqrt{X_2\left(-X_2 + 2\sqrt{1-X_2^2}\right)}\right)$:
  The line is a repeller when

$$\frac{\lambda\sqrt{-X_2\left(X_2 - 2\sqrt{1-X_2^2}\right)} + \sqrt{X_2\left((2-\lambda^2)X_2 + 2\lambda\left(\lambda\sqrt{1-X_2^2} - \sqrt{2X_2(-X_2+2\sqrt{1-X_2^2})}\right)\right)}}{\sqrt{2}\left(X_2 + 2\sqrt{1-X_2^2}\right)} < 1\,,$$

and saddle elsewhere (Fig. 8.2). The linearization shows that the metric behaves like

$$A \propto r^{2\left(-1+\frac{\sqrt{1-X_2^2}}{X_2}\right)}\,, \quad B \propto r^{-2\frac{\sqrt{1-X_2^2}}{X_2}}\,. \tag{8.32}$$

- $\mathbf{L_2}$: $\left(\lambda \in \mathbb{R},\ 0 \le X_2 \le \frac{2}{\sqrt{5}},\ X_3 = -X_2 + \sqrt{1-X_2^2},\ Y_1 = -\sqrt{X_2\left(-X_2 + 2\sqrt{1-X_2^2}\right)}\right)$:
  The line is a repeller when

$$\frac{-\lambda\sqrt{-X_2\left(X_2 - 2\sqrt{1-X_2^2}\right)} + \sqrt{X_2\left((2-\lambda^2)X_2 + 2\lambda\left(\lambda\sqrt{1-X_2^2} + \sqrt{2X_2(-X_2+2\sqrt{1-X_2^2})}\right)\right)}}{\sqrt{2}\left(X_2 + 2\sqrt{1-X_2^2}\right)} < 1\,,$$

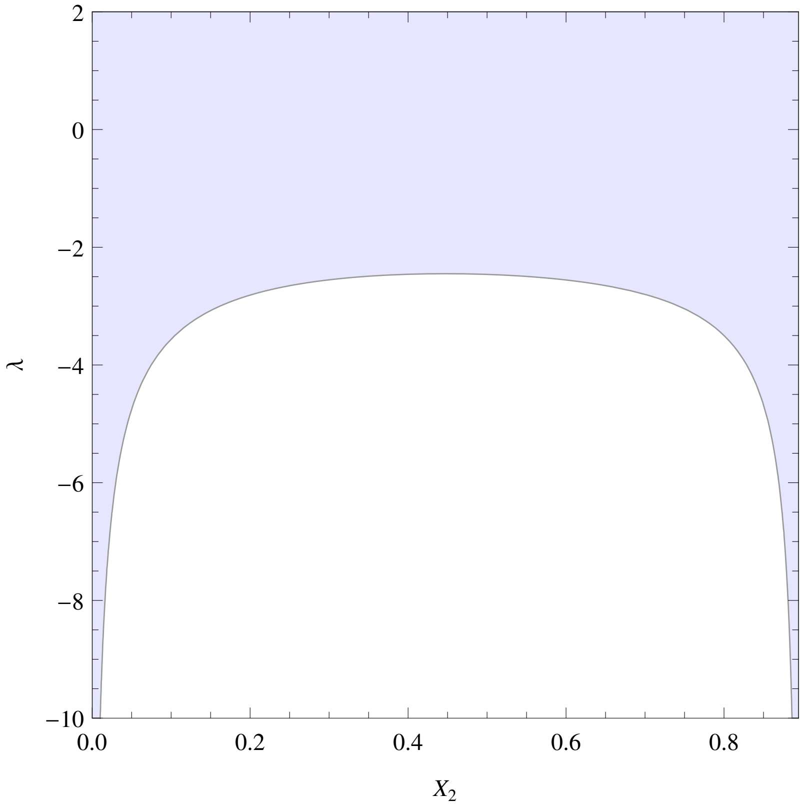

FIGURE 8.3: Stability plot of critical line L_2 (or L_3 for $X_2 \to -X_2$). Blue is the repelling (attracting) region.

and saddle elsewhere (Fig. 8.3).

- $\mathbf{L_3}$: $\left(\lambda \in \mathbb{R},\ -\frac{2}{\sqrt{5}} \leq X_2 \leq 0,\ X_3 = -X_2 - \sqrt{1-X_2^2},\ Y_1 = \sqrt{-X_2\left(X_2 + 2\sqrt{1-X_2^2}\right)}\right)$:
The line is an attractor when

$$\frac{\lambda\sqrt{-X_2\left(X_2+2\sqrt{1-X_2^2}\right)} - \sqrt{X_2\left((2-\lambda^2)X_2 - 2\lambda\left(\lambda\sqrt{1-X_2^2} + \sqrt{-2X_2(X_2+2\sqrt{1-X_2^2})}\right)\right)}}{\sqrt{2}\left(X_2 - 2\sqrt{1-X_2^2}\right)} < 1\,,$$

and saddle elsewhere. We notice that this line is symmetric to L_2 under the transformation $X_2 \to -X_2$, therefore the stability plot for L_3 (Fig. 8.3) will be similar to L_2 with the nature of the stability reversed.

- $\mathbf{L_4}$: $\left(\lambda \in \mathbb{R},\ -\frac{2}{\sqrt{5}} \leq X_2 \leq 0,\ X_3 = -X_2 - \sqrt{1-X_2^2},\ Y_1 = -\sqrt{-X_2\left(X_2 + 2\sqrt{1-X_2^2}\right)}\right)$:
The line is an attractor when

$$-\frac{\lambda\sqrt{-X_2\left(X_2+2\sqrt{1-X_2^2}\right)} + \sqrt{X_2\left((2-\lambda^2)X_2 - 2\lambda\left(\lambda\sqrt{1-X_2^2} - \sqrt{-2X_2(X_2+2\sqrt{1-X_2^2})}\right)\right)}}{\sqrt{2}\left(X_2 - 2\sqrt{1-X_2^2}\right)} < 1\,,$$

and saddle elsewhere. We notice that this line is symmetric to L_1 under the transformation $X_2 \to -X_2$, therefore the stability plot for L_4 (Fig. 8.2) will be similar to L_1 with the nature of the stability reversed.

8.3.2 Powerlaw potential: $V = V_0\psi^N$.

For this case, $\Gamma = 1 - \frac{1}{N}$. The critical points at the finite region of the phase space (8.27) for the powerlaw potential are (for $N \neq 0$):

$\mathbf{P_M}$: $(x_2 = 1, x_3 = 0, y_1 = 0, \lambda \in \mathbb{R})$: Minkowski. The eigenvalues are $(0, -1, -1, 2)$, hence it is a saddle point.

$\bar{\mathbf{P}}_{\mathbf{M}}$: $(x_2 = -1, x_3 = 0, y_1 = 0, \lambda \in \mathbb{R})$. The eigenvalues are $(0, -2, 1, 1)$, hence it is a saddle point.

For analyzing the stability at the infinite region we introduce the Poincaré transformation $(x_i = X_i/Z,\ y_1 = Y_1/Z,\ \lambda = \Lambda/Z)$. The infinity boundary $x_2^2+x_3^2+y_1^2+\lambda^2 \to +\infty$ corresponds to the unitary circle $X_2^2 + X_3^2 + Y_1^2 + \Lambda^2 = 1$. The equations reads:

$$\begin{aligned}\bar{X}_2 \equiv Z^2 X_2' = Z\left(X_2\left(X_3\left(-\Lambda^2 - 3X_2^2 + Y_1^2 + 2\right) - X_2X_3^2 + 2X_2Y_1^2\right) - Y_1^2\right) \\ - \frac{\Lambda X_2 Y_1\left(\Lambda^2(N+2) + N\left(2X_2^2 + 2X_2X_3 + X_3^2 - 1\right)\right)}{\sqrt{2}N},\end{aligned} \tag{8.33a}$$

$$\begin{aligned}\bar{X}_3 \equiv Z^2 X_3' = Z\left(\Lambda^2 + X_2^2\left(2 - 3X_3^2\right) + X_2\left(-X_3^3 + 2X_3Y_1^2 + X_3\right) + X_3^2\left(-\Lambda^2 + Y_1^2 + 1\right) - 1\right) \\ - \frac{\Lambda X_3 Y_1\left(\Lambda^2(N+2) + N\left(2X_2^2 + 2X_2X_3 + X_3^2 - 1\right)\right)}{\sqrt{2}N},\end{aligned} \tag{8.33b}$$

$$\begin{aligned}\bar{Y}_1 \equiv Z^2 Y_1' = Y_1 Z\left(-3X_2^2X_3 - X_2\left(X_3^2 - 2Y_1^2 + 1\right) + X_3(Y_1 - \Lambda)(\Lambda + Y_1)\right) \\ - \frac{\Lambda\left(N\left(Y_1^2 - 1\right)\left(\Lambda^2 + 2X_2^2 + 2X_2X_3 + X_3^2 - 1\right) + 2\Lambda^2Y_1^2\right)}{\sqrt{2}N},\end{aligned} \tag{8.33c}$$

$$\begin{aligned}\bar{\Lambda} \equiv Z^2\Lambda' = -\frac{\Lambda^2 Y_1\left(2\left(\Lambda^2 - 1\right) + N\left(\Lambda^2 + 2X_2^2 + 2X_2X_3 + X_3^2 - 1\right)\right)}{\sqrt{2}N} \\ - \Lambda Z\left(X_3\left(\Lambda^2 + 3X_2^2 - Y_1^2 - 1\right) + X_2X_3^2 - 2X_2Y_1^2\right),\end{aligned} \tag{8.33d}$$

defined on

$$\left\{(X_2, X_3, Y_1, \Lambda) : \Lambda^2 + 2X_2^2 + 2X_2X_3 + X_3^2 \leq 1,\ X_2^2 + X_3^2 + Y_1^2 + \Lambda^2 \leq 1\right\}. \tag{8.34}$$

The points at infinity satisfy $Z \to 0$, thus the leading terms in the system (8.33) which determine the critical points and the dynamics at infinity are

$$\bar{X}_2 \to -\frac{\Lambda X_2 Y_1 \left(\Lambda^2(N+2) + N\left(2X_2^2 + 2X_2X_3 + X_3^2 - 1\right)\right)}{\sqrt{2}N}, \tag{8.35a}$$

$$\bar{X}_3 \to -\frac{\Lambda X_3 Y_1 \left(\Lambda^2(N+2) + N\left(2X_2^2 + 2X_2X_3 + X_3^2 - 1\right)\right)}{\sqrt{2}N}, \tag{8.35b}$$

$$\bar{Y}_1 \to -\frac{\Lambda \left(N\left(Y_1^2 - 1\right)\left(\Lambda^2 + 2X_2^2 + 2X_2X_3 + X_3^2 - 1\right) + 2\Lambda^2 Y_1^2\right)}{\sqrt{2}N}, \tag{8.35c}$$

$$\bar{\Lambda} \to -\frac{\Lambda^2 Y_1 \left(2\left(\Lambda^2 - 1\right) + N\left(\Lambda^2 + 2X_2^2 + 2X_2X_3 + X_3^2 - 1\right)\right)}{\sqrt{2}N}. \tag{8.35d}$$

The critical lines are listed below

- $\mathbf{L_1}$: $\left(X_2 = 0,\ X_3,\ Y_1 = 0,\ \Lambda = \sqrt{1 - X_3^2}\right)$:
- $\mathbf{L_2}$: $\left(X_2 = 0,\ X_3,\ Y_1 = 0,\ \Lambda = -\sqrt{1 - X_3^2}\right)$:
- $\mathbf{L_3}$: $\left(X_2 \neq 0,\ X_3 = -X_2/2,\ Y_1 = 0,\ \Lambda = \sqrt{1 - \frac{5}{4}X_2^2}\right)$:
- $\mathbf{L_4}$: $\left(X_2 \neq 0,\ X_3 = -X_2/2,\ Y_1 = 0,\ \Lambda = -\sqrt{1 - \frac{5}{4}X_2^2}\right)$:
- $\mathbf{L_5}$: $\left(X_2,\ X_3,\ Y_1 = \sqrt{1 - X_2^2 - X_3^2},\ \Lambda = 0\right)$:
- $\mathbf{L_6}$: $\left(X_2,\ X_3,\ Y_1 = -\sqrt{1 - X_2^2 - X_3^2},\ \Lambda = 0\right)$:
- $\mathbf{L_7}$: $\left(N = -2,\ X_2 = 0,\ X_3 = 0,\ Y_1,\ \Lambda = \sqrt{1 - Y_1^2}\right)$: The eigenvalues of the linearized system are $\left(0,\ \frac{Y_1\sqrt{1-Y_1^2}}{\sqrt{2}},\ \frac{Y_1\sqrt{1-Y_1^2}}{\sqrt{2}},\ Y_1\sqrt{2 - 2Y_1^2}\right)$. The line is an attractor when $-1 < Y_1 < 0$, repeller when $0 < Y_1 < 1$ and saddle point when $Y_1 = 0,\ \pm 1$.
- $\mathbf{L_8}$: $\left(N = -2,\ X_2 = 0,\ X_3 = 0,\ Y_1,\ \Lambda = -\sqrt{1 - Y_1^2}\right)$: The eigenvalues of the linearized system are $\left(0,\ -Y_1\sqrt{2 - 2Y_1^2},\ -\frac{Y_1\sqrt{1-Y_1^2}}{\sqrt{2}},\ -\frac{Y_1\sqrt{1-Y_1^2}}{\sqrt{2}}\right)$. The line is an attractor when $0 < Y_1 < 1$, repeller when $-1 < Y_1 < 0$ and saddle point when $Y_1 = 0,\ \pm 1$.

8.3.3 General Case

We consider, $(\Gamma - 1)\lambda^2 = f(\lambda)$, where f is an explicit (arbitrary) function of λ. [Urena-Lopez 2012; Escobar et al. 2012a; Escobar et al. 2012b; Fadragas et al. 2014; Escobar et al. 2014]

Potential	References	$f(\lambda)$	$\mu \equiv \lim_{Z\to 0} Z^2 f(1/Z)$
$V(\psi) = V_0 e^{-k\psi} + V_1$	1	$-\lambda(\lambda - k)$	-1
$V(\psi) = V_0 \left[e^{\alpha\psi} + e^{\beta\psi}\right]$	2	$-(\lambda+\alpha)(\lambda+\beta)$	-1
$V(\psi) = V_0 \left[\cosh(\xi\psi) - 1\right]$	3	$-\frac{1}{2}(\lambda^2 - \xi^2)$	$-\frac{1}{2}$
$V(\psi) = V_0 \sinh^{-\alpha}(\beta\psi)$	4	$\frac{\lambda^2}{\alpha} - \alpha\beta^2$	$\frac{1}{\alpha}$

[1] [Yearsley and Barrow 1996; Pavluchenko 2003; Cardenas et al. 2003]
[2] [Barreiro et al. 2000; Gonzalez, Cardenas, et al. 2007; Gonzalez, Leon, et al. 2006]
[3] [Ratra and Peebles 1988; Wetterich 1988; Matos, Luevano, et al. 2009; Copeland, Mizuno, et al. 2009; Leyva et al. 2009; Pavluchenko 2003; Campo et al. 2013; Sahni and Wang 2000; Sahni and Starobinsky 2000; Lidsey et al. 2002; Matos and Urena-Lopez 2000]
[4] [Ratra and Peebles 1988; Wetterich 1988; Copeland, Mizuno, et al. 2009; Leyva et al. 2009; Pavluchenko 2003; Sahni and Starobinsky 2000; Urena-Lopez and Matos 2000]

TABLE 8.2: The function $f(\lambda)$ for the most common quintessence potentials [Escobar et al. 2014].

The critical points at the finite region of the phase space (8.27) for the arbitrary potential ($(\Gamma - 1)\lambda^2 = f(\lambda)$) are

$\mathbf{P_M}$: $(x_2 = 1, x_3 = 0, y_1 = 0, \lambda \in \mathbb{R})$: Minkowski. The eigenvalues are $(2, -1, -1, 0)$, hence it is a saddle point.

$\bar{\mathbf{P}}_{\mathbf{M}}$: $(x_2 = -1, x_3 = 0, y_1 = 0, \lambda \in \mathbb{R})$: Anti-Minkowski. The eigenvalues are $(-2, 1, 1, 0)$, hence it is a saddle point.

For analyzing the stability at the infinite region we introduce the Poincaré transformation $(x_i = X_i/Z,\ y_1 = Y_1/Z,\ \lambda = \Lambda/Z)$. The infinity boundary $x_2^2+x_3^2+y_1^2+\lambda^2 \to +\infty$ corresponds to the unitary circle $X_2^2 + X_3^2 + Y_1^2 + \Lambda^2 = 1$. The equations reads:

$$\bar{X}_2 \equiv Z^2 X_2' = Z\left(X_2\left(X_3\left(-\Lambda^2-3X_2^2+Y_1^2+2\right)-X_2X_3^2+2X_2Y_1^2\right)-Y_1^2\right)$$
$$-\frac{1}{\sqrt{2}}\Lambda X_2Y_1\left(\Lambda^2+2X_2^2+2X_2X_3+X_3^2-1\right)+\sqrt{2}\Lambda X_2Y_1Z^2f\left(\frac{\Lambda}{Z}\right), \tag{8.36a}$$

$$\bar{X}_3 \equiv Z^2 X_3' = Z\left(\Lambda^2+X_2^2\left(2-3X_3^2\right)+X_2\left(-X_3^3+2X_3Y_1^2+X_3\right)+X_3^2\left(-\Lambda^2+Y_1^2+1\right)-1\right)$$
$$-\frac{1}{\sqrt{2}}\Lambda X_3Y_1\left(\Lambda^2+2X_2^2+2X_2X_3+X_3^2-1\right)+\sqrt{2}\Lambda X_3Y_1Z^2f\left(\frac{\Lambda}{Z}\right), \tag{8.36b}$$

$$\bar{Y}_1 \equiv Z^2 Y_1' = Y_1Z\left(-3X_2^2X_3-X_2\left(X_3^2-2Y_1^2+1\right)+X_3(Y_1-\Lambda)(\Lambda+Y_1)\right)$$
$$-\frac{1}{\sqrt{2}}\Lambda\left(Y_1^2-1\right)\left(\Lambda^2+2X_2^2+2X_2X_3+X_3^2-1\right)+\sqrt{2}\Lambda Y_1^2Z^2f\left(\frac{\Lambda}{Z}\right), \tag{8.36c}$$

$$\bar{\Lambda} \equiv Z^2 \Lambda' = -\Lambda Z\left(X_3\left(\Lambda^2+3X_2^2-Y_1^2-1\right)+X_2X_3^2-2X_2Y_1^2\right)$$
$$-\frac{1}{\sqrt{2}}\Lambda^2Y_1\left(\Lambda^2+2X_2^2+2X_2X_3+X_3^2-1\right)-\sqrt{2}\left(\Lambda^2-1\right)Y_1Z^2f\left(\frac{\Lambda}{Z}\right), \tag{8.36d}$$

defined on

$$\left\{(X_2,X_3,Y_1,\Lambda):\Lambda^2+2X_2^2+2X_2X_3+X_3^2\leq 1,\ X_2^2+X_3^2+Y_1^2+\Lambda^2\leq 1\right\}. \tag{8.37}$$

Let's assume that $\lim_{Z\to 0} Z^2 f\left(\frac{1}{Z}\right)=\mu$ where μ is a (finite) constant. The critical points and the dynamics at infinity is given by the leading terms:

$$\bar{X}_2 \to -\frac{1}{\sqrt{2}}\Lambda X_2Y_1\left(\Lambda^2+2X_2^2+2X_2X_3+X_3^2-1\right)+\sqrt{2}\mu\Lambda^3X_2Y_1, \tag{8.38a}$$
$$\bar{X}_3 \to -\frac{1}{\sqrt{2}}\Lambda X_3Y_1\left(\Lambda^2+2X_2^2+2X_2X_3+X_3^2-1\right)+\sqrt{2}\mu\Lambda^3X_3Y_1, \tag{8.38b}$$
$$\bar{Y}_1 \to -\frac{1}{\sqrt{2}}\Lambda\left(Y_1^2-1\right)\left(\Lambda^2+2X_2^2+2X_2X_3+X_3^2-1\right)+\sqrt{2}\mu\Lambda^3Y_1^2, \tag{8.38c}$$
$$\bar{\Lambda} \to -\frac{1}{\sqrt{2}}\Lambda^2Y_1\left(\Lambda^2+2X_2^2+2X_2X_3+X_3^2-1\right)-\sqrt{2}\mu\left(\Lambda^2-1\right)\Lambda^2Y_1. \tag{8.38d}$$

Observe that the powerlaw-potential discussed in Sec. 8.3.2 corresponds to $\mu=-\frac{1}{N}$. Other examples are given in table 8.2.

The critical points and lines are listed below

- $\mathbf{P_1}$: $(\mu=-1/2,\ X_2=0,\ X_3=0,\ Y_1=1,\ \Lambda=0)$: The point is a repeller.
- $\mathbf{P_2}$: $(\mu=-1/2,\ X_2=0,\ X_3=0,\ Y_1=-1,\ \Lambda=0)$: The point is an attractor.
- $\mathbf{L_1}$: $\left(X_2=0,\ X_3,\ Y_1=0,\ \Lambda=\sqrt{1-X_3^2}\right)$:
- $\mathbf{L_2}$: $\left(X_2=0,\ X_3,\ Y_1=0,\ \Lambda=-\sqrt{1-X_3^2}\right)$:

- **$\mathbf{L_3}$**: $\Big(X_2 \neq 0,\ X_3 = -X_2/2,\ Y_1 = 0,\ \Lambda = \sqrt{1 - \frac{5}{4}X_2^2}\Big)$:
- **$\mathbf{L_4}$**: $\Big(X_2 \neq 0,\ X_3 = -X_2/2,\ Y_1 = 0,\ \Lambda = -\sqrt{1 - \frac{5}{4}X_2^2}\Big)$:
- **$\mathbf{L_5}$**: $\Big(X_2,\ X_3,\ Y_1 = \sqrt{1 - X_2^2 - X_3^2},\ \Lambda = 0\Big)$:
- **$\mathbf{L_6}$**: $\Big(X_2,\ X_3,\ Y_1 = -\sqrt{1 - X_2^2 - X_3^2},\ \Lambda = 0\Big)$:

8.4 Conclusions

In this chapter, we effectively reformulated the system of modified Einstein field equations for quintessence model in LRS-II spacetimes into an autonomous system of covariantly defined variables. The phase space has been compactified to study the nontrivial behaviours at infinity. Using the tools of dynamical system analysis, we have completely studied the massless scalar field case to get the important global features. We are working on the case of massive scalar field.

Chapter 9

Conclusions

Modified gravity necessarily involves additional fields, extra dimensions, or broken symmetries, since we know that GR is the unique interacting theory of a single rank-2 tensor that can be constructed from the metric variation of an action in four dimensions. In this thesis we have discussed how modifications in the theory of gravity brings about changes in the strong field regime, such as neutron stars and black holes. Gravity prevails over all other interactions in these celestial bodies and they are ideal natural laboratories to constrain strong gravity. In this final chapter, we will briefly look at the prospect of future input in this field from observational point of view which will help in constraining the extra degrees of freedom into smaller and smaller parameter space.

Rotating neutron stars or pulsars have proved to be remarkably successful laboratories for testing the predictions of GR [Wex 2014]. By accurately modelling the arrival time of pulses and comparing the model to high precision timing measurements, information can be gleaned about the neutron star, the nature of its companion (if it is in a binary), the interstellar medium and the gravitational potential of the solar system.

Binary pulsar systems have been used to test the predictions of GR to $\sim 0.05\%$ [Kramer 2013]. The analysis proceeds by systematically fitting evolving Keplerian ellipses to the timing data and recording the orbital parameters and their derivatives as the so-called post-Keplerian (PK) timing parameters [Damour and Taylor 1992]. The measured PK parameters are then compared to the values predicted by GR and other theories of gravity. It should be noted that orbital measurement via pulsar timing have the advantage of providing 'clean' direct probes of the spacetime geometry, insensitive to electromagnetic effects of accretion and the magnetosphere. The 1974 discovery of the first binary pulsar PSR B1913+16 by Hulse and Taylor [Hulse and Taylor 1975] provided the first indirect evidence of gravitational waves. The change in the orbital period was shown to be consistent with that predicted by the effects of gravitational radiation reaction.

The most relativistic binary system known to date is the double pulsar system PSR J0737–3039A/B [Burgay et al. 2003; Lyne et al. 2004]. 5 PK parameters have been measured for this binary system, some of them with exquisite precision. In comparison, only 3 PK parameters have been fixed by B1913+16 and J1141–6545 and 4 by B1534+12. For this system the change in the orbital period $\dot{P}_b$ due to gravity wave (GW) damping has been tested to agree with the quadrupole formula of GR to better than 0.1% [Kramer 2013].

In the framework of an alternative gravitation theory that violates the strong equivalence principle (SEP), a binary system may emit dipole gravitational radiation. Such effects arise when the two bodies are very different in terms of their self-gravity, i.e. their compactness. The high asymmetry in the compactness/binding energy of the bodies in the pulsar-WD systems make it particularly sensitive to gravitational dipolar radiation and tests for SEP violation. PSR J1738+0333 and J1713+0747 provides the best constraint for dipolar radiation and hence can test scalar-tensor gravity while violation of SEP is best tested by J0348+0432.

In future, precision measurements made with pulsar timing using radio telescopes such as Meer Karoo Array Telescope (MeerKAT)/Square Kilometre Array (SKA) and Five hundred meter Aperture Spherical Telescope (FAST), will permit us to test the strong field predictions of GR with unprecedented accuracy within the next 20 years. On the one hand, the greatly improved timing precision will allow for better and new tests with existing systems. On the other hand, new instruments and survey techniques promise the discovery of new "gravity labs," like a pulsar-BH system. This will allow us to experimentally explore the possibility of modifications to GR and the validity of alternate theories of gravity.

Another interesting area is the GW observation by the interferometric detectors, such as the current ground-based Laser Interferometer Gravitational-Wave Observatory (LIGO), VIRGO, GEO and TAMA, operating from the tens of Hz through the several kHz range, and the future space-based LISA, which measure the influx of gravitational radiation from the whole sky. Gravitational waves hold the key to testing GR to new exciting levels in the previously unexplored strong field regime. Depending on the type of wave that is detected, e.g., compact binary inspirals, mergers, ringdowns, continuous sources, supernovae, etc, different tests will be possible and we can determine whether a certain modified theory is consistent with the data or not. GR makes very specific and testable predictions on the GW phasing of compact binaries as they inspiral, and on the oscillation frequencies of the compact objects that they produce as a result of the merger. If observed, any deviations from these predictions may identify problems in Einstein's theory, and may even point us to specific ways in which it could be modified.

Einstein developed the general theory of relativity a century ago, and, although it remains a cornerstone of modern physics, we could argue that among all the fundamental forces of nature it is gravity that remains the least well understood. This is almost certainly due to the weakness of the gravitational interaction, which makes it incredibly difficult to test in the laboratory experimentally. Inevitably, experiments on the scale of planets, stars, galaxies, and beyond cannot be performed with the same level of precision and control as those conducted for the other forces on Earth. With the advancement of technology and with bigger and better telescopes coming up, we are starting to catch and we believe that the twenty first century will belong to gravity.

Appendix A

Modified Einstein equations in $f(R)$ theories

Before going into the derivation, we list the following results [S. M. Carroll 2004; Poisson 2004]

$$\delta\sqrt{-g} = -\frac{1}{2}\sqrt{-g}\, g_{\mu\nu}\delta g^{\mu\nu} \tag{A.1}$$

$$\delta g^{\mu\nu} = -g^{\mu\alpha}g^{\nu\beta}\,\delta g_{\alpha\beta} \tag{A.2}$$

$$\delta R = \delta g^{\mu\nu}R_{\mu\nu} + g^{\mu\nu}\delta R_{\mu\nu} \tag{A.3}$$

$$\delta R_{\mu\nu} = \nabla_\lambda\left(\delta\Gamma^\lambda{}_{\nu\mu}\right) - \nabla_\nu\left(\delta\Gamma^\lambda{}_{\lambda\mu}\right) \tag{A.4}$$

A.1 Jordan frame

Variation of the action (2.2) with respect to the metric leads to

$$\begin{aligned}
\delta\mathcal{S}_{f(R)} &= \frac{1}{2}\int d^4x\left[\delta\sqrt{-g}f(R) + \sqrt{-g}\delta f(R)\right] + \delta\mathcal{S}_M \\
&= \frac{1}{2}\int d^4x\left[\left(-\frac{1}{2}\sqrt{-g}\,g_{\mu\nu}\delta g^{\mu\nu}\right)f(R) + \sqrt{-g}f_{,R}\delta R\right] + \delta\mathcal{S}_M && \text{(using A.1)} \\
&= \frac{1}{2}\int d^4x\,\sqrt{-g}\left[-\frac{f(R)}{2}g_{\mu\nu}\delta g^{\mu\nu} + f_{,R}\left(\delta g^{\mu\nu}R_{\mu\nu} + g^{\mu\nu}\delta R_{\mu\nu}\right)\right] + \delta\mathcal{S}_M && \text{(using A.3)} \\
&= \frac{1}{2}\int d^4x\,\sqrt{-g}\left[\left(-\frac{f(R)}{2}g_{\mu\nu} + f_{,R}R_{\mu\nu}\right)\delta g^{\mu\nu}\right. \\
&\left. + f_{,R}\,g^{\mu\nu}\left(\nabla_\lambda\left(\delta\Gamma^\lambda{}_{\nu\mu}\right) - \nabla_\nu\left(\delta\Gamma^\lambda{}_{\lambda\mu}\right)\right)\right] + \delta\mathcal{S}_M && \text{(using A.4)} \\
&= \frac{1}{2}\int d^4x\,\sqrt{-g}\left[\left(-\frac{f(R)}{2}g_{\mu\nu} + f_{,R}R_{\mu\nu}\right)\delta g^{\mu\nu}\right. \\
&\left. + f_{,R}\left(\nabla_\lambda\left(g^{\mu\nu}\,\delta\Gamma^\lambda{}_{\nu\mu}\right) - \nabla_\nu\left(g^{\mu\nu}\,\delta\Gamma^\lambda{}_{\lambda\mu}\right)\right)\right] + \delta\mathcal{S}_M\,,
\end{aligned} \tag{A.5}$$

where we have used metric compatibility $\nabla_\lambda \, g_{\mu\nu} = 0$. Now

$$V^\alpha = g^{\beta\gamma} \, \delta\Gamma^\alpha{}_{\beta\gamma} \, , \tag{A.6}$$

is a tensor since $\delta\Gamma^\alpha_{\beta\gamma}$ is a tensor. Hence

$$\begin{aligned}
\delta\mathcal{S}_{f(R)} = &\frac{1}{2}\int d^4x\,\sqrt{-g}\left[\left(-\frac{f(R)}{2}g_{\mu\nu} + f_{,R}R_{\mu\nu}\right)\delta g^{\mu\nu} + f_{,R}\left(\left(g^{\mu\nu}\,\delta\Gamma^\lambda{}_{\nu\mu}\right)_{,\lambda} + \Gamma^\lambda{}_{\lambda\sigma}V^\sigma\right.\right.\\
&\left.\left.-\left(g^{\mu\nu}\,\delta\Gamma^\lambda{}_{\lambda\mu}\right)_{,\nu} - \Gamma^\nu{}_{\nu\sigma}V^\sigma\right)\right] + \delta\mathcal{S}_M\\
= &\frac{1}{2}\int d^4x\,\sqrt{-g}\left[\left(-\frac{f(R)}{2}g_{\mu\nu} + f_{,R}R_{\mu\nu}\right)\delta g^{\mu\nu} + f_{,R}\left(\left(g^{\mu\nu}\,\delta\Gamma^\lambda{}_{\nu\mu}\right)_{,\lambda}\right.\right.\\
&\left.\left.-\left(g^{\mu\nu}\,\delta\Gamma^\lambda{}_{\lambda\mu}\right)_{,\nu}\right)\right] + \delta\mathcal{S}_M.
\end{aligned} \tag{A.7}$$

So, the variation of the action can be represented as

$$\delta\mathcal{S}_{f(R)} = \frac{1}{2}\left[\delta\mathcal{S}_1 + \delta\mathcal{S}_2\right] + \delta\mathcal{S}_M \, , \tag{A.8}$$

where

$$\begin{aligned}
\delta\mathcal{S}_1 &= \int d^4x\,\sqrt{-g}\left[\left(-\frac{f(R)}{2}g_{\mu\nu} + f_{,R}R_{\mu\nu}\right)\delta g^{\mu\nu}\right]\\
\delta\mathcal{S}_2 &= \int d^4x\,\sqrt{-g}\left[f_{,R}\left(\left(g^{\mu\nu}\,\delta\Gamma^\lambda{}_{\nu\mu}\right)_{,\lambda} - \left(g^{\mu\nu}\,\delta\Gamma^\lambda{}_{\lambda\mu}\right)_{,\nu}\right)\right].
\end{aligned} \tag{A.9}$$

Now, we will calculate $\delta\mathcal{S}_2$ separately and plug it back into Eq. (A.7). The other factors are in the desired form.

$$\begin{aligned}
\delta\mathcal{S}_2 = &-\int d^4x\,\sqrt{-g}\left[\nabla_\lambda(f_{,R})\left(g^{\mu\nu}\,\delta\Gamma^\lambda{}_{\nu\mu}\right) - \nabla_\nu(f_{,R})\left(g^{\mu\nu}\,\delta\Gamma^\lambda{}_{\lambda\mu}\right)\right]\\
&\qquad\text{(Integrating by parts and } \partial_\mu \equiv \nabla_\mu \text{ for scalars)}\\
= &-\int d^4x\,\sqrt{-g}\,\delta\Gamma^\lambda{}_{\nu\mu}\left[\nabla_\lambda(f_{,R})\,g^{\mu\nu} - \nabla_\gamma(f_{,R}\,g^{\mu\gamma}\,\delta^\nu{}_\lambda\right].
\end{aligned} \tag{A.10}$$

The variation of the Christoffel symbol can be obtained, with the help of the relation (A.2), as follows

$$\begin{aligned}
\delta\Gamma^{\lambda}{}_{\nu\mu} &= \delta\left(g^{\lambda\sigma}\,\Gamma_{\sigma\nu\mu}\right)\\
&= \delta g^{\lambda\sigma}\,\Gamma_{\sigma\nu\mu} + \frac{1}{2}g^{\lambda\sigma}\left(\delta g_{\sigma\nu,\mu} + \delta g_{\sigma\mu,\nu} - \delta g_{\nu\mu,\sigma}\right)\\
&= -g^{\lambda\alpha}g^{\sigma\beta}\,\delta g_{\alpha\beta}\,\Gamma^{\gamma}{}_{\nu\mu}\,g_{\sigma\gamma} + \frac{1}{2}g^{\lambda\sigma}\left(\delta g_{\sigma\nu,\mu} + \delta g_{\sigma\mu,\nu} - \delta g_{\nu\mu,\sigma}\right)\\
&= -g^{\lambda\alpha}\,\delta g_{\alpha\beta}\,\Gamma^{\gamma}{}_{\nu\mu}\,\delta^{\beta}{}_{\gamma} + \frac{1}{2}g^{\lambda\sigma}\left(\delta g_{\sigma\nu,\mu} + \delta g_{\sigma\mu,\nu} - \delta g_{\nu\mu,\sigma}\right)\\
&= -g^{\lambda\alpha}\,\delta g_{\alpha\beta}\,\Gamma^{\beta}{}_{\nu\mu} + \frac{1}{2}g^{\lambda\sigma}\left(\delta g_{\sigma\nu,\mu} + \delta g_{\sigma\mu,\nu} - \delta g_{\nu\mu,\sigma}\right)\\
&= \frac{1}{2}g^{\lambda\sigma}\Big(\delta g_{\sigma\nu,\mu} - \Gamma^{\beta}{}_{\mu\nu}\,\delta g_{\sigma\beta} - \Gamma^{\beta}{}_{\mu\sigma}\,\delta g_{\beta\nu} + \delta g_{\sigma\mu,\nu} - \Gamma^{\beta}{}_{\nu\mu}\,\delta g_{\sigma\beta} - \Gamma^{\beta}{}_{\nu\sigma}\,\delta g_{\beta\mu}\\
&\quad -\delta g_{\nu\mu,\sigma} + \Gamma^{\beta}{}_{\sigma\nu}\,\delta g_{\beta\mu} + \Gamma^{\beta}{}_{\sigma\mu}\,\delta g_{\nu\beta}\Big)\\
&\qquad\qquad\qquad\qquad\qquad\qquad \text{(relabelling dummy indices should be noted)}\\
&= \frac{1}{2}g^{\lambda\sigma}\left(\nabla_{\mu}\,\delta g_{\sigma\nu} + \nabla_{\nu}\,\delta g_{\sigma\mu} - \nabla_{\sigma}\,\delta g_{\nu\mu}\right). \qquad \text{(A.11)}
\end{aligned}$$

Substituting the relation (A.11) in Eq. (A.10), we get

$$\delta\mathcal{S}_2 = -\frac{1}{2}\int d^4x\,\sqrt{-g}\,g^{\lambda\sigma}\left(\nabla_{\mu}\,\delta g_{\sigma\nu} + \nabla_{\nu}\,\delta g_{\sigma\mu} - \nabla_{\sigma}\,\delta g_{\nu\mu}\right)\left[\nabla_{\lambda}(f_{,R})\,g^{\mu\nu} - \nabla_{\gamma}(f_{,R})\,g^{\mu\gamma}\,\delta^{\nu}{}_{\lambda}\right]. \qquad \text{(A.12)}$$

The six terms in the above equation can be evaluated in a similar fashion. Here, we will explicitly show two of them:

$$\begin{aligned}
\mathcal{I}_1 &= -\frac{1}{2}\int d^4x\,\sqrt{-g}\,g^{\lambda\sigma}\nabla_{\mu}\,\delta g_{\sigma\nu}\nabla_{\lambda}(f_{,R})\,g^{\mu\nu}\\
&= \frac{1}{2}\int d^4x\,\sqrt{-g}\,g^{\lambda\sigma}g^{\mu\nu}\,\delta g_{\sigma\nu}\nabla_{\mu}\nabla_{\lambda}\left(f_{,R}\right) \qquad \text{(Integrating by parts)}\\
&= -\frac{1}{2}\int d^4x\,\sqrt{-g}\,\delta g^{\lambda\mu}\nabla_{\mu}\nabla_{\lambda}\left(f_{,R}\right) \qquad \text{(A.13)}
\end{aligned}$$

and

$$\begin{aligned}
\mathcal{I}_2 &= \frac{1}{2}\int d^4x\,\sqrt{-g}\,g^{\lambda\sigma}\nabla_{\sigma}\,\delta g_{\nu\mu}\nabla_{\lambda}(f_{,R})\,g^{\mu\nu}\\
&= -\frac{1}{2}\int d^4x\,\sqrt{-g}\,g^{\lambda\sigma}g^{\mu\nu}\,\delta g_{\nu\mu}\nabla_{\sigma}\nabla_{\lambda}\left(f_{,R}\right) \qquad \text{(Integrating by parts)}\\
&= \frac{1}{2}\int d^4x\,\sqrt{-g}\,g_{\mu\nu}\,\delta g^{\mu\nu}\Box\left(f_{,R}\right), \qquad \text{(A.14)}
\end{aligned}$$

where, apart from symmetry of the metric, we have used the relations (A.2) and $g^{\mu\nu}\,\delta g_{\mu\nu} = -g_{\mu\nu}\,\delta g^{\mu\nu}$. So Eq. (A.12) becomes

$$\begin{aligned}\delta\mathcal{S}_2 = -\frac{1}{2}\int d^4x\,\sqrt{-g}\,\Big[&\delta g^{\lambda\mu}\nabla_\mu\nabla_\lambda\,(f_{,R}) + \delta g^{\lambda\nu}\nabla_\nu\nabla_\lambda\,(f_{,R}) - g_{\mu\nu}\,\delta g^{\mu\nu}\Box\,(f_{,R}) \\ &-g_{\nu\sigma}\,\delta g^{\nu\sigma}\Box\,(f_{,R}) - \delta g^{\nu\gamma}\nabla_\nu\nabla_\gamma\,(f_{,R}) + \delta g^{\sigma\gamma}\nabla_\sigma\nabla_\gamma\,(f_{,R})\Big] \\ = -\int d^4x\,\sqrt{-g}\,\delta g^{\mu\nu}&\left[\nabla_\mu\nabla_\nu(f_{,R}) - g_{\mu\nu}\Box(f_{,R})\right]. \end{aligned} \tag{A.15}$$

Substituting Eq. (A.15) in Eq. (A.8), we get

$$\delta\mathcal{S}_{f(R)} = \frac{1}{2}\int d^4x\,\sqrt{-g}\left[-\frac{f(R)}{2}g_{\mu\nu} + f_{,R}R_{\mu\nu} - \left(\nabla_\mu\nabla_\nu - g_{\mu\nu}\Box\right)(f_{,R}) + \frac{2}{\sqrt{-g}}\frac{\delta\mathcal{S}_M}{\delta g^{\mu\nu}}\right]\delta g^{\mu\nu}. \tag{A.16}$$

Setting $\delta\mathcal{S}_{f(R)} = 0$ or setting the co-efficients of $\delta g^{\mu\nu}$ equal to 0, we get the modified Einstein equation (2.3)

$$f_{,R}R_{\mu\nu} - \frac{f(R)}{2}g_{\mu\nu} - \left(\nabla_\mu\nabla_\nu - g_{\mu\nu}\Box\right)(f_{,R}) = T^{(M)}_{\mu\nu} \tag{A.17}$$

where $T^{(M)}_{\mu\nu} = -\frac{2}{\sqrt{-g}}\frac{\delta\mathcal{S}_M}{\delta g^{\mu\nu}}$ is the matter energy-momentum tensor. A different way of deriving the equations can be found in [Guarnizo et al. 2010].

A.2 Einstein frame

To get the Einstein equation, we vary the action (2.13) with respect to the metric

$$\delta\mathcal{S}_E = \int d^4x \left[\delta\sqrt{-\tilde{g}}\left(\frac{1}{2}\tilde{R} - \frac{1}{2}(\tilde{\nabla}\phi)^2 - V(\phi)\right)\right.$$

$$\left. + \frac{1}{2}\sqrt{-\tilde{g}}\left(\delta\tilde{g}^{\mu\nu}\tilde{R}_{\mu\nu} + \tilde{g}^{\mu\nu}\delta\tilde{R}_{\mu\nu} - \delta\tilde{g}^{\mu\nu}\phi_{,\mu}\phi_{,\nu}\right)\right] + \delta\mathcal{S}_M \qquad \text{(using A.3)}$$

$$= \int d^4x \left[\left(-\frac{1}{2}\sqrt{-\tilde{g}}\,\tilde{g}_{\mu\nu}\delta\tilde{g}^{\mu\nu}\right)\left(\frac{1}{2}\tilde{R} - \frac{1}{2}(\tilde{\nabla}\phi)^2 - V(\phi)\right)\right.$$

$$\left. + \frac{1}{2}\sqrt{-\tilde{g}}\left(\delta\tilde{g}^{\mu\nu}\tilde{R}_{\mu\nu} + \tilde{g}^{\mu\nu}\left(\tilde{\nabla}_\lambda\left(\delta\tilde{\Gamma}^\lambda{}_{\nu\mu}\right) - \tilde{\nabla}_\nu\left(\delta\tilde{\Gamma}^\lambda{}_{\lambda\mu}\right)\right) - \delta\tilde{g}^{\mu\nu}\phi_{,\mu}\phi_{,\nu}\right)\right] + \delta\mathcal{S}_M$$

$$\text{(using A.1,A.4)}$$

$$= \frac{1}{2}\int d^4x\,\sqrt{-\tilde{g}}\left[-\tilde{g}_{\mu\nu}\delta\tilde{g}^{\mu\nu}\left(\frac{1}{2}\tilde{R} - \frac{1}{2}(\tilde{\nabla}\phi)^2 - V(\phi)\right)\right.$$

$$\left. + \left(\delta\tilde{g}^{\mu\nu}\tilde{R}_{\mu\nu} + \tilde{\nabla}_\sigma\left(\tilde{g}^{\mu\sigma}\left(\delta\tilde{\Gamma}^\lambda{}_{\lambda\mu}\right) - \tilde{g}^{\mu\nu}\left(\delta\tilde{\Gamma}^\sigma{}_{\mu\nu}\right)\right) - \delta\tilde{g}^{\mu\nu}\phi_{,\mu}\phi_{,\nu}\right)\right] + \delta\mathcal{S}_M$$

$$\text{(using metric compatibility)}$$

$$= \frac{1}{2}\int d^4x\,\sqrt{-\tilde{g}}\left[-\tilde{g}_{\mu\nu}\left(\frac{1}{2}\tilde{R} - \frac{1}{2}(\tilde{\nabla}\phi)^2 - V(\phi)\right) + \left(\tilde{R}_{\mu\nu} - \phi_{,\mu}\phi_{,\nu}\right) + \frac{2}{\sqrt{-\tilde{g}}}\frac{\delta\mathcal{S}_M}{\delta\tilde{g}^{\mu\nu}}\right]\delta\tilde{g}^{\mu\nu}\,, \tag{A.18}$$

where the integral with respect to the natural volume element of the covariant divergence of a vector is equal to a boundary contribution at infinity (by Stokes theorem) which we have set to zero by making the variation vanish at infinity. This term contributes nothing to the total variation. Setting the co-efficients of $\delta\tilde{g}^{\mu\nu}$ to zero, we get

$$\tilde{R}_{\mu\nu} - \frac{1}{2}\tilde{g}_{\mu\nu}\tilde{R} = -\frac{2}{\sqrt{-\tilde{g}}}\frac{\delta\mathcal{S}_M}{\delta\tilde{g}^{\mu\nu}} + \phi_{,\mu}\phi_{,\nu} - \tilde{g}_{\mu\nu}\left(\frac{1}{2}(\tilde{\nabla}\phi)^2 + V(\phi)\right)$$

$$\tilde{G}_{\mu\nu} = \tilde{T}^{(M)}_{\mu\nu} + \tilde{T}^{(\phi)}_{\mu\nu}\,. \tag{A.19}$$

Variation of the action (2.13) with respect to the scalar field ϕ leads to

$$\delta\mathcal{S}_E = \int d^4x\sqrt{-\tilde{g}}\left(-\frac{1}{2}\delta(\tilde{\nabla}\phi)^2 - V_{,\phi}\delta\phi\right) + \frac{\delta\mathcal{S}_M}{\delta\phi}\delta\phi$$

$$= \int d^4x\sqrt{-\tilde{g}}\left(-(\tilde{\nabla}_\mu\phi\tilde{\nabla}^\mu\delta\phi) - V_{,\phi}\delta\phi\right) + \frac{\delta\mathcal{S}_M}{\delta g^{\mu\nu}}\frac{\partial g^{\mu\nu}}{\partial\phi}\delta\phi$$

$$= \int d^4x\sqrt{-\tilde{g}}\left((\tilde{\nabla}^\mu\tilde{\nabla}_\mu\phi)\delta\phi - V_{,\phi}\delta\phi + \sqrt{\frac{2}{3}}\frac{1}{\sqrt{-\tilde{g}}}\frac{\delta\mathcal{S}_M}{\delta\tilde{g}^{\mu\nu}}\tilde{g}^{\mu\nu}\delta\phi\right)$$

$$\text{(integrating by parts the first term and using } g^{\mu\nu} = e^{\sqrt{\frac{2}{3}}\phi}\,\tilde{g}_{\mu\nu})$$

$$= \int d^4x\sqrt{-\tilde{g}}\left(\tilde{\Box}\phi - V_{,\phi} - \sqrt{\frac{2}{3}}\frac{\tilde{T}^{(M)}_{\mu\nu}}{2}\tilde{g}^{\mu\nu}\right)\delta\phi\,. \tag{A.20}$$

To get the Klein-Gordon equation, we equate the coefficients of $\delta\phi$ to zero

$$\tilde{\Box}\phi = V_{,\phi} + \frac{1}{\sqrt{6}}\tilde{T}^{(M)}\,. \tag{A.21}$$

Appendix B

Conformal transformation

Using the conformal transformation (2.8) and the relation for inverse of a metric, $g^{\mu\nu} = 1/g_{\mu\nu}$, we get

$$\tilde{g}^{\mu\nu} = \Omega^{-2}\, g^{\mu\nu}\,. \tag{B.1}$$

The determinant of the metric and the d'Alembertian operator transform as

$$\bullet\ \tilde{g} = det\ [\tilde{g}_{\mu\nu}] = \Omega^8\ det\ [g_{\mu\nu}] = \Omega^8\ g$$
$$\text{or,}\ \ \sqrt{-\tilde{g}} = \Omega^4\ \sqrt{-g} \tag{B.2}$$

$$\begin{aligned}\bullet\ \tilde{\Box}\phi &= \frac{1}{\sqrt{-\tilde{g}}}\left(\sqrt{-\tilde{g}}\tilde{g}^{\mu\nu}\phi_{,\nu}\right)_{,\mu} \\ &= \Omega^{-2}\frac{1}{\sqrt{-g}}\left(\sqrt{-g}g^{\mu\nu}\phi_{,\nu}\right)_{,\mu} + 2\Omega^{-3}\Omega_{,\mu}g^{\mu\nu}\phi_{,\nu} \\ &= \Omega^{-2}\left(\Box\phi + 2g^{\mu\nu}\frac{\Omega_{,\mu}}{\Omega}\phi_{,\nu}\right)\,.\end{aligned} \tag{B.3}$$

Christoffel connection coefficients transform as

$$\begin{aligned}\tilde{\Gamma}^{\lambda}{}_{\mu\nu} &= \frac{1}{2}\tilde{g}^{\lambda\alpha}\left(\tilde{g}_{\alpha\nu,\mu} + \tilde{g}_{\mu\alpha,\nu} - \tilde{g}_{\mu\nu,\alpha}\right) \\ &= \frac{1}{2}\Omega^{-2}\ g^{\lambda\alpha}\left((\Omega^2 g_{\alpha\nu})_{,\mu} + (\Omega^2 g_{\mu\alpha})_{,\nu} - (\Omega^2 g_{\mu\nu})_{,\alpha}\right) \\ &= \frac{1}{2}g^{\lambda\alpha}\left(g_{\alpha\nu,\mu} + g_{\mu\alpha,\nu} - g_{\mu\nu,\alpha}\right) + \Omega^{-1}\left(\delta^{\lambda}{}_{\nu}\Omega_{,\mu} + \delta^{\lambda}{}_{\mu}\Omega_{,\nu} - g_{\mu\nu}\Omega^{,\lambda}\right) \\ &= \Gamma^{\lambda}{}_{\mu\nu} + \Omega^{-1}\left(\delta^{\lambda}{}_{\nu}\Omega_{,\mu} + \delta^{\lambda}{}_{\mu}\Omega_{,\nu} - g_{\mu\nu}\Omega^{,\lambda}\right)\,.\end{aligned} \tag{B.4}$$

Hence $\tilde{\Gamma}^{\lambda}{}_{\mu\lambda} = \Gamma^{\lambda}{}_{\mu\lambda} + 4\Omega_{,\mu}/\Omega$. The Ricci tensor in the Einstein frame is defined similar to its Jordan frame counterpart

$$\tilde{R}_{\mu\nu} = \tilde{R}^{\lambda}{}_{\mu\lambda\nu} = \tilde{\Gamma}^{\lambda}{}_{\mu\nu,\lambda} - \tilde{\Gamma}^{\lambda}{}_{\mu\lambda,\nu} + \tilde{\Gamma}^{\lambda}{}_{\mu\nu}\tilde{\Gamma}^{\rho}{}_{\rho\lambda} - \tilde{\Gamma}^{\lambda}{}_{\nu\rho}\tilde{\Gamma}^{\rho}{}_{\mu\lambda}\,. \tag{B.5}$$

Now

$$\begin{aligned} \bullet\ \tilde{\Gamma}^{\lambda}{}_{\mu\nu,\lambda} &= \Gamma^{\lambda}{}_{\mu\nu,\lambda} + \Omega^{-1}\left(\delta^{\lambda}{}_{\nu}\Omega_{,\mu\lambda} + \delta^{\lambda}{}_{\mu}\Omega_{,\nu\lambda} - g_{\mu\nu}\Omega^{,\lambda}{}_{,\lambda} - g_{\mu\nu,\lambda}\Omega^{,\lambda}\right) \\ &\quad - \Omega^{-2}\Omega_{,\lambda}\left(\delta^{\lambda}{}_{\nu}\Omega_{,\mu} + \delta^{\lambda}{}_{\mu}\Omega_{,\nu} - g_{\mu\nu}\Omega^{,\lambda}\right) \\ &= \Gamma^{\lambda}_{\mu\nu,\lambda} + \Omega^{-1}\left(2\Omega_{,\mu\nu} - g_{\mu\nu}\Omega^{,\lambda}{}_{,\lambda} - g_{\mu\nu,\lambda}\Omega^{,\lambda}\right) - \Omega^{-2}\left(2\Omega_{,\mu}\Omega_{,\nu} - g_{\mu\nu}\Omega^{,\lambda}\Omega^{,\lambda}\right) \end{aligned} \tag{B.6}$$

$$\begin{aligned} \bullet\ \tilde{\Gamma}^{\lambda}{}_{\mu\lambda,\nu} &= \Gamma^{\lambda}{}_{\mu\lambda,\nu} + 4\left(\frac{\Omega_{,\mu}}{\Omega}\right)_{,\nu} \\ &= \Gamma^{\lambda}{}_{\mu\lambda,\nu} + 4\Omega^{-1}\left(\Omega_{,\mu\nu} - \Omega^{-1}\Omega_{,\mu}\Omega_{.\nu}\right) \end{aligned} \tag{B.7}$$

$$\begin{aligned} \bullet\ \tilde{\Gamma}^{\lambda}{}_{\mu\nu}\tilde{\Gamma}^{\rho}{}_{\rho\lambda} &= \Gamma^{\lambda}{}_{\mu\nu}\Gamma^{\rho}{}_{\rho\lambda} + 4\Omega^{-1}\Gamma^{\lambda}{}_{\mu\nu}\Omega_{,\lambda} + \Omega^{-1}\Gamma^{\rho}{}_{\rho\lambda}\left(\delta^{\lambda}{}_{\mu}\Omega_{,\nu} + \delta^{\lambda}{}_{\nu}\Omega_{,\mu} - g_{\mu\nu}\Omega^{,\lambda}\right) \\ &\quad + 4\,\Omega^{-2}\Omega_{,\lambda}\left(\delta^{\lambda}{}_{\mu}\Omega_{,\nu} + \delta^{\lambda}{}_{\nu}\Omega_{,\mu} - g_{\mu\nu}\Omega^{,\lambda}\right) \\ &= \Gamma^{\lambda}{}_{\mu\nu}\Gamma^{\rho}{}_{\rho\lambda} + \Omega^{-1}\left(4\Gamma^{\lambda}{}_{\mu\nu}\Omega_{,\lambda} + \Gamma^{\lambda}{}_{\mu\lambda}\Omega_{,\nu} + \Gamma^{\lambda}{}_{\nu\lambda}\Omega_{,\mu} - g_{\mu\nu}\Gamma^{\lambda}{}_{\lambda\rho}\Omega^{,\rho}\right) \\ &\quad + 4\Omega^{-2}\left(2\Omega_{,\mu}\Omega_{,\nu} - g_{\mu\nu}\Omega_{,\lambda}\Omega^{,\lambda}\right) \end{aligned} \tag{B.8}$$

$$\begin{aligned} \bullet\ \tilde{\Gamma}^{\lambda}{}_{\nu\rho}\tilde{\Gamma}^{\rho}{}_{\mu\lambda} &= \Gamma^{\lambda}{}_{\nu\rho}\Gamma^{\rho}{}_{\mu\lambda} + \Omega^{-1}\left(2\Gamma^{\lambda}{}_{\mu\nu}\Omega_{,\lambda} + \Gamma^{\lambda}{}_{\nu\lambda}\Omega_{,\mu} + \Gamma^{\lambda}{}_{\mu\lambda}\Omega_{,\nu} - g_{\mu\lambda}\Gamma^{\lambda}{}_{\nu\rho}\Omega^{,\rho} - g_{\nu\lambda}\Gamma^{\lambda}{}_{\mu\rho}\Omega^{,\rho}\right) \\ &\quad + \Omega^{-2}\left(6\Omega_{,\mu}\Omega_{,\nu} - 2g_{\mu\nu}\Omega_{,\lambda}\Omega^{,\lambda}\right)\,. \end{aligned} \tag{B.9}$$

Combining equations (B.6-B.9), we get

$$\begin{aligned} \tilde{R}_{\mu\nu} &= \left(\Gamma^{\lambda}{}_{\mu\nu,\lambda} - \Gamma^{\lambda}{}_{\mu\lambda,\nu} + \Gamma^{\lambda}{}_{\mu\nu}\Gamma^{\rho}{}_{\rho\lambda} - \Gamma^{\lambda}{}_{\nu\rho}\Gamma^{\rho}{}_{\mu\lambda}\right) \\ &\quad - \Omega^{-1}\left(g_{\mu\nu}\Omega^{,\lambda}{}_{,\lambda} + g_{\mu\nu}\Gamma^{\lambda}{}_{\lambda\rho}\Omega^{,\rho} + 2\Omega_{,\mu\nu} - 2\Gamma^{\lambda}{}_{\mu\nu}\Omega_{,\lambda}\right) + \Omega^{-2}\left(4\Omega_{,\mu}\Omega_{,\nu} - g_{\mu\nu}\Omega_{,\lambda}\Omega^{,\lambda}\right) \\ &= R_{\mu\nu} - \Omega^{-1}\left(g_{\mu\nu}\Box\Omega + 2\nabla_{\mu}\nabla_{\nu}\Omega\right) + \Omega^{-2}\left(4\Omega_{,\mu}\Omega_{,\nu} - g_{\mu\nu}\Omega_{,\lambda}\Omega^{,\lambda}\right)\,, \end{aligned} \tag{B.10}$$

where we have used the relation $g_{\mu\lambda}\Gamma^{\lambda}{}_{\nu\rho}\Omega^{,\rho} + g_{\nu\lambda}\Gamma^{\lambda}{}_{\mu\rho}\Omega^{,\rho} = g_{\mu\nu,\lambda}\Omega^{,\lambda}$. Hence, the Ricci scalar transforms as

$$\begin{aligned}\tilde{R} = \tilde{g}^{\mu\nu}\tilde{R}_{\mu\nu} &= \Omega^{-2}R - \Omega^{-3}\left(4\Box\Omega + 2\Box\Omega\right) + \Omega^{-4}\left(4\Omega_{,\mu}\Omega^{,\mu} - 4\Omega_{,\lambda}\Omega^{,\lambda}\right) \\ &= \Omega^{-2}\left(R - 6\frac{\Box\Omega}{\Omega}\right) . \end{aligned} \tag{B.11}$$

In a similar fashion, we can derive the inverse transformations. The relations are listed below

$$\Gamma^{\lambda}{}_{\mu\nu} = \tilde{\Gamma}^{\lambda}{}_{\mu\nu} - \Omega^{-1}\left(\tilde{\delta}^{\lambda}{}_{\nu}\Omega_{,\mu} + \tilde{\delta}^{\lambda}{}_{\mu}\Omega_{,\nu} - \tilde{g}_{\mu\nu}\Omega^{,\lambda}\right) \tag{B.12}$$

$$\Gamma^{\lambda}{}_{\mu\lambda} = \tilde{\Gamma}^{\lambda}{}_{\mu\lambda} - 4\Omega_{,\mu}/\Omega \tag{B.13}$$

$$R_{\mu\nu} = \tilde{R}_{\mu\nu} + \Omega^{-1}\left(\tilde{g}_{\mu\nu}\tilde{\Box}\Omega + 2\tilde{\nabla}_{\mu}\tilde{\nabla}_{\nu}\Omega\right) - 3\Omega^{-2}\tilde{g}_{\mu\nu}\Omega_{,\lambda}\Omega^{,\lambda} \tag{B.14}$$

$$R = \Omega^{2}\left(\tilde{R} + 6\frac{\tilde{\Box}\Omega}{\Omega} - 12\tilde{g}^{\mu\nu}\frac{\Omega_{,\mu}\Omega_{,\nu}}{\Omega^{2}}\right) . \tag{B.15}$$

For a review on conformal tranformation, see [Dabrowski et al. 2009].

Appendix C

Dynamical systems

A first order nonlinear differential equation can be written as

$$\frac{\mathrm{d}}{\mathrm{dt}}X = F(X,t)\,. \tag{C.1}$$

When the function F does not depend on the independent variable, ie., when the time dependence is not explicitly present, then it is called an autonomous equation. Eq. (C.1) then reduces to

$$\frac{\mathrm{d}}{\mathrm{dt}}X = F(X)\,. \tag{C.2}$$

In this thesis, we are interested only in autonomous systems of the form

$$\begin{aligned} \frac{\mathrm{d}}{\mathrm{dt}}X_1 &= F_1(X_1,\ldots,X_n) \\ &\vdots \\ \frac{\mathrm{d}}{\mathrm{dt}}X_n &= F_n(X_1,\ldots,X_n)\,. \end{aligned} \tag{C.3}$$

The main idea is not to study a particular trajectory in the phase space $\{X_1,\ldots,X_n\}$, but to look for the global picture. We will see that the initial conditions are somewhat less significant than the typical cases of differential equations. The system converges or diverges depending on the topology of the phase space. So this excludes conservative systems which follow the constraint equation

$$\nabla^i F_i = \sum_{i=1}^{n} \partial_{X_i} F_i(X_1,\ldots,X_n) = 0\,. \tag{C.4}$$

Hence, we shall work with non-conservative autonomous systems.

As a first step, we look for the stationary points $\mathrm{dX_i/dt} = 0$ by solving the following system

$$\begin{aligned}
&F_1\left(X_1^{(0)},\ldots,X_n^{(0)}\right) = 0\\
&\vdots\\
&F_n\left(X_1^{(0)},\ldots,X_n^{(0)}\right) = 0\,.
\end{aligned} \tag{C.5}$$

Studying the trajectories in the neighbourhood of these points will allow us to get the evolution of the system. It is sufficient to linearize the equations around the points of equilibrium of the vector field. Thus, we can make a Taylor expansion

$$\begin{aligned}
F_i(X_1,\ldots,X_n) &= F_i\left(X_1^{(0)},\ldots,X_n^{(0)}\right) + \sum_{j=1}^{n}\frac{\partial F_i}{X_j}\left(X_1^{(0)},\ldots,X_n^{(0)}\right)\cdot\left(X_j - X_j^{(0)}\right)\\
&= \sum_{j=1}^{n}\frac{\partial F_i}{X_j}\left(X_1^{(0)},\ldots,X_n^{(0)}\right)\cdot X_j^{(1)}\\
&= \sum_{j=1}^{n} M_{ij}\cdot X_j^{(1)}\,,
\end{aligned} \tag{C.6}$$

and then the system (C.3) can be rewritten as

$$\frac{\mathrm{d}}{\mathrm{dt}}\mathbf{X} = M\cdot\mathbf{X} \tag{C.7}$$

with

$$\mathbf{X} = \begin{pmatrix} X_1^{(1)}\\ X_2^{(1)}\\ \vdots\\ X_n^{(1)}\end{pmatrix} \quad\text{and}\quad M = \begin{pmatrix} \partial_1 F_1\left(X_1^{(0)},\ldots,X_n^{(0)}\right) & \ldots & \partial_n F_1\left(X_1^{(0)},\ldots,X_n^{(0)}\right)\\ \vdots & \ddots & \vdots\\ \partial_1 F_n\left(X_1^{(0)},\ldots,X_n^{(0)}\right) & \ldots & \partial_n F_n\left(X_1^{(0)},\ldots,X_n^{(0)}\right)\end{pmatrix}. \tag{C.8}$$

In order to simplify the calculations, we will discuss the case where $n = 2$. The results can easily be generalized.

For $n = 2$, Eqs. (C.7) can be written as

$$\begin{aligned}
\frac{\mathrm{d}}{\mathrm{dt}}X_1^{(1)} &= M_{11}X_1^{(1)} + M_{12}X_2^{(1)}\\
\frac{\mathrm{d}}{\mathrm{dt}}X_2^{(1)} &= M_{21}X_1^{(1)} + M_{22}X_2^{(1)}\,.
\end{aligned} \tag{C.9}$$

Looking for solutions of the form $\mathbf{X} = \tilde{\mathbf{X}}e^{\omega t}$, we get

$$\begin{aligned}
\omega\tilde{X}_1 &= M_{11}\tilde{X}_1 + M_{12}\tilde{X}_2\\
\omega\tilde{X}_2 &= M_{21}\tilde{X}_1 + M_{22}\tilde{X}_2\,,
\end{aligned} \tag{C.10}$$

which leads to

$$
\begin{aligned}
&(M_{11}-\omega)\tilde{X}_1 + M_{12}\tilde{X}_2 = 0 \\
&M_{21}\tilde{X}_1 + (M_{22}-\omega)\tilde{X}_2 = 0\,.
\end{aligned} \tag{C.11}
$$

We have nontrivial solutions if and only if ω is an eigenvalue of the linear operator M. Thus these eigenvalues will be either real and distinct or real and repeated or complex conjugate.

C.1 Real and distinct roots

We concentrate on the phase space $\{\hat{X}_1, \hat{X}_2\}$, where the eigenvalues are ω_1, ω_2

$$
\begin{aligned}
&\frac{\mathrm{d}}{\mathrm{dt}}\hat{X}_1 = \omega_1\hat{X}_1 \\
&\frac{\mathrm{d}}{\mathrm{dt}}\hat{X}_2 = \omega_2\hat{X}_2\,,
\end{aligned} \tag{C.12}
$$

whose solutions are $\hat{X}_i(t) = \hat{X}_i(0)e^{\omega_i t}$.

Thus we can find the expression of the trajectories eliminating the time in the phase space, and is given by $\left(\hat{X}_1/\hat{X}_1(0)\right)^{1/\omega_1} = \left(\hat{X}_2/\hat{X}_2(0)\right)^{1/\omega_2}$, which gives

$$
\hat{X}_2 \propto \hat{X}_1^{\omega_2/\omega_1}\,. \tag{C.13}
$$

- When ω_1 and ω_2 have the same sign, the fixed point is a *node*. If they are both negative, it is a stable node otherwise its unstable. The trajectory is a parabola opening in the direction of the eigenvalue with the maximum absolute value.
- When ω_1 and ω_2 have opposite signs, the fixed point is a *saddle*. The trajectory is a hyperbola approaching the fixed point in the direction of the eigenvector associated with negative eigenvalue and diverging along the other direction.

C.2 Real and repeated roots

This is the case where we have a single repeated root ω.

If we have the trivial case $M_{11} = M_{22}$ and $M_{12} = M_{21} = 0$, then the linear operator M is proportional to identity. All directions on the plane are eigen directions. The fixed point is then stable or unstable depending on the sign of ω. This fixed point is called a *star*.

In the nontrivial case, we have an eigenvector $\bar{X}_1 = \big(M_{12}, \frac{1}{2}(M_{22} - M_{11})\big)$ associated to the eigenvalue ω. We can then complete the basis by another non-collinear vector $\bar{X}_2$. As we are no longer under the conditions $M_{11} = M_{22}$ and $M_{12} = M_{21} = 0$, we can choose $\bar{X}_2 = (0, 1)$.

It suffices to consider the action of M on the basis as:

$$M\cdot \bar{X}_2 = \bar{X}_1 + \omega \bar{X}_2 \,. \tag{C.14}$$

Thus the system is in the Jordan normal form.

$$\begin{aligned} \frac{\mathrm{d}}{\mathrm{dt}}\bar{X}_1 &= \omega \bar{X}_1 + \bar{X}_2 \,, \\ \frac{\mathrm{d}}{\mathrm{dt}}\bar{X}_2 &= \omega \bar{X}_2 \,, \end{aligned} \tag{C.15}$$

whose solutions are

$$\begin{aligned} \tilde{X}_1(t) &= \tilde{X}_1(0)e^{\omega t} + \tilde{X}_2(0)te^{\omega t} \,, \\ \tilde{X}_2(t) &= \tilde{X}_2(0)e^{\omega t} \,, \end{aligned} \tag{C.16}$$

or in parametric form, it can be written as

$$\tilde{X}_1 \propto \tilde{X}_2 \left(\ln(\tilde{X}_2) + C\right) \,, \tag{C.17}$$

where C is an arbitrary constant. This fixed point is said to be improper node.

C.3 Complex roots

Let the complex conjugate eigenvalues be $\omega_1 = a + ib$ and $\omega_2 = a - ib$. In this case, the operator can be diagonalized in the complex space as

$$\begin{aligned} \frac{\mathrm{d}}{\mathrm{dt}}\tilde{X}_1 &= (a + ib)\tilde{X}_1 \,, \\ \frac{\mathrm{d}}{\mathrm{dt}}\tilde{X}_2 &= (a - ib)\tilde{X}_2 \,, \end{aligned} \tag{C.18}$$

which can be rewritten in the real space in the following way

$$\begin{aligned} \frac{\mathrm{d}}{\mathrm{dt}}\tilde{X}_1 &= a\tilde{X}_1 + b\tilde{X}_2 \,, \\ \frac{\mathrm{d}}{\mathrm{dt}}\tilde{X}_2 &= -b\tilde{X}_1 + a\tilde{X}_2 \,. \end{aligned} \tag{C.19}$$

The solution is of the form

$$\tilde{X}_1(t) = e^{at}\left(\tilde{X}_1(0)\cos(bt) + \tilde{X}_2(0)\sin(bt)\right) ,$$
$$\tilde{X}_2(t) = e^{at}\left(-\tilde{X}_1(0)\sin(bt) + \tilde{X}_2(0)\cos(bt)\right) . \qquad \text{(C.20)}$$

We have a stable or unstable *spiral* critical point depending on whether the sign of a (real part of the eigenvalue) is negative or positive respectively. In the particular case when $a = 0$, ie. the eigenvalue is completely imaginary, the critical point is a *center*.

Bibliography

[**Ade et al. n.d.**]

Ade, P. A. R. et al. "*Planck* 2013 results. I. Overview of products and scientific results." *Astron. Astrophys.,* 571 (A1) (cit. on p. 97).

[**Ade et al. 2014a**]

Ade, P. A. R. et al. (10/2014a). "*Planck* 2013 results. XXII. Constraints on inflation." *Astron. Astrophys.,* 571 (A22) (cit. on p. 24).

[**Ade et al. 2014b**]

Ade, P. A. R. et al. (11/2014b). "*Planck* 2013 results. XXV. Searches for cosmic strings and other topological defects." *Astron. Astrophys.,* 571 (A25) (cit. on p. 19).

[**Ade et al. 2015**]

Ade, P. A. R. et al. (2015). "*Planck* 2015 results. XIV. Dark energy and modified gravity" (cit. on p. 4).

[**Alavirad et al. 2013**]

Alavirad, H. and J. M. Weller (12/2013). "Modified gravity with logarithmic curvature corrections and the structure of relativistic stars." *Phys. Rev. D,* 88 (124034) (cit. on pp. 23, 26).

[**Albrecht et al. 1982**]

Albrecht, A. and P. J. Steinhardt (04/1982). "Cosmology for Grand Unified Theories with Radiatively Induced Symmetry Breaking." *Phys. Rev. Lett.,* 48 (17), pp. 1220–1223 (cit. on p. 3).

[**Alnes et al. 2006**]

Alnes, H. et al. (04/2006). "Inhomogeneous alternative to dark energy?" *Phys. Rev. D,* 73 (083519) (cit. on p. 97).

[**Amendola et al. 2007**]

Amendola, L., R. Gannouji, et al. (04/2007). "Conditions for the cosmological viability of $f(R)$ dark energy models." *Phys. Rev. D,* 75 (083504) (cit. on pp. 24, 74, 98).

[**Amendola et al. 2010**]

Amendola, L. and S. Tsujikawa (2010). *Dark Energy: Theory and Observations.* Cambridge University Press (cit. on pp. 4, 16).

[Amendola et al. 2007]

Amendola, L., D. Polarski, et al. (03/2007). "Are $f(R)$ Dark Energy Models Cosmologically Viable?" *Phys. Rev. Lett.,* 98 (131302) (cit. on p. 98).

[Appleby et al. 2008]

Appleby, S. A. and R. A. Battye (05/2008). "Aspects of cosmological expansion in $f(R)$ gravity models." *J. Cosmol. Astropart. Phys.,* 05 (019) (cit. on p. 24).

[Arapoglu et al. 2011]

Arapoglu, A. S. et al. (07/2011). "Constraints on perturbative $f(R)$ gravity via neutron stars." *J. Cosmol. Astropart. Phys.,* 07 (020) (cit. on pp. 23, 26).

[Astashenok et al. 2013]

Astashenok, A. V. et al. (12/2013). "Further stable neutron star models from $f(R)$ gravity." *J. Cosmol. Astropart. Phys.,* 12 (040) (cit. on pp. 23, 26).

[Babichev et al. 2011]

Babichev, E., S. Chernov, et al. (05/2011). "Perfect fluid and scalar field in the Reissner-Nordström metric." *J. Exp. Theor. Phys.,* 112 (5), pp. 784–793 (cit. on p. 44).

[Babichev et al. 2009]

Babichev, E. and D. Langlois (12/2009). "Relativistic stars in $f(R)$ gravity." *Phys. Rev. D,* 80 (121501), 81 (069901)(E), 03/2010 (cit. on pp. 23, 26).

[Babichev et al. 2010]

Babichev, E. and D. Langlois (06/2010). "Relativistic stars in $f(R)$ and scalar-tensor theories." *Phys. Rev. D,* 81 (124051) (cit. on pp. 23, 26).

[Babichev et al. 2004]

Babichev, E. et al. (07/2004). "Black Hole Mass Decreasing due to Phantom Energy Accretion." *Phys. Rev. Lett.,* 93 (021102) (cit. on p. 44).

[Babichev et al. 2005]

Babichev, E. et al. (03/2005). "The accretion of dark energy onto a black hole." *J. Exp. Theor. Phys.,* 100 (3), pp. 528–538 (cit. on p. 44).

[Babichev et al. 2006]

Babichev, E. et al. (11/2006). "Phantom energy accretion onto black hole." *AIP Conf. Proc.,* 861 (554) (cit. on p. 44).

[Barreiro et al. 2000]

Barreiro, T. et al. (05/2000). "Quintessence arising from exponential potentials." *Phys. Rev. D,* 61 (127301) (cit. on p. 130).

[Bassett et al. 2006]

Bassett, B. A. et al. (05/2006). "Inflation dynamics and reheating." *Rev. Mod. Phys.,* 78 (2), pp. 537–589 (cit. on pp. 3, 17).

[Bean et al. 2007]

Bean, R. et al. (03/2007). “Dynamics of linear perturbations in $f(R)$ gravity.” *Phys. Rev. D,* 75 (064020) (cit. on p. 98).

[Begelman 1978]

Begelman, M. C. (11/1978). “Accretion of $\gamma > 5/3$ Gas by a Schwarzschild Black Hole.” *Astron. Astrophys.,* 70, pp. 583–584 (cit. on p. 44).

[Bekenstein 1995]

Bekenstein, J. D. (06/1995). “Novel ”no-scalar-hair” theorem for black holes.” *Phys. Rev. D,* 51 (R6608) (cit. on p. 27).

[Betschart et al. 2004]

Betschart, G. and C. A. Clarkson (12/2004). “Scalar field and electromagnetic perturbations on locally rotationally symmetric spacetimes.” *Class. Quant. Grav.,* 21 (5587) (cit. on pp. 68–70).

[Bettwieser et al. 1981]

Bettwieser, E. and W. Glatzel (02/1981). “On the growth of primordial black holes.” *Astron. Astrophys.,* 94 (2), pp. 306–312 (cit. on p. 44).

[Binetruy 1999]

Binetruy, P. (08/1999). “Models of dynamical supersymmetry breaking and quintessence.” *Phys. Rev. D,* 60 (063502) (cit. on p. 18).

[Binetruy 2006]

Binetruy, P. (2006). *Supersymmetry: Theory, experiment and cosmology.* Oxford University Press (cit. on p. 15).

[Birrell et al. 1982]

Birrell, N. D. and P. C. W. Davies. (1982). *Quantum Fields in Curved Space.* Cambridge Books Online. Cambridge University Press (cit. on p. 3).

[Blumenthal et al. 1976]

Blumenthal, G. R. and W. G. Mathews (02/1976). “Spherical winds and accretion in general relativity.” *Astrophys. J.,* 203, pp. 714–719 (cit. on p. 44).

[Bondi 1952]

Bondi, H. (04/1952). “On Spherically Symmetrical Accretion.” *Mon. Not. Roy. Astron. Soc.,* 112 (2), pp. 195–204 (cit. on pp. 44, 48, 50, 59).

[Bousso 2002]

Bousso, R. (05/2002). “Adventures in de Sitter space.” *arXiv:hep-th/0205177,* (cit. on p. 89).

[Brans et al. 1961]

Brans, C. and R. H. Dicke (11/1961). “Mach’s Principle and a Relativistic Theory of Gravitation.” *Phys. Rev.,* 124 (3), pp. 925–935 (cit. on p. 13).

[**Brax et al. 1999**]

Brax, P. and J. Martin (11/1999). "Quintessence and supergravity." *Phys. Lett. B,* 468 (1–2), pp. 40–45 (cit. on p. 18).

[**Brinkmann 1980**]

Brinkmann, W. (05/1980). "Adiabatic accretion onto a Schwarzschild black hole." *Astron. Astrophys.,* 85 (1–2), pp. 146–148 (cit. on p. 44).

[**Buchbinder et al. 1992**]

Buchbinder, I. L. et al. (1992). *Effective action in quantum gravity.* CRC Press (cit. on p. 3).

[**Buchert 2000**]

Buchert, T. (01/2000). "On Average Properties of Inhomogeneous Fluids in General Relativity: Dust Cosmologies." *Gen. Rel. Grav.,* 32 (1), pp. 105–125 (cit. on p. 97).

[**Bunch et al. 1977**]

Bunch, T. S. and P. C. W. Davies (09/1977). "Stress Tensor and Conformal Anomalies for Massless Fields in a Robertson-Walker Universe." *Proc. R. Soc. A,* 356 (1687) (cit. on p. 24).

[**Burgay et al. 2003**]

Burgay, M. et al. (12/2003). "An increased estimate of the merger rate of double neutron stars from observations of a highly relativistic system." *Nature,* 426 (02124), pp. 531–533 (cit. on p. 134).

[**Caldwell et al. 1998**]

Caldwell, R. R., R. Dave, et al. (02/1998). "Cosmological Imprint of an Energy Component with General Equation of State." *Phys. Rev. Lett.,* 80 (8), pp. 1582–1585 (cit. on p. 16).

[**Caldwell et al. 2005**]

Caldwell, R. R. and E. V. Linder (09/2005). "Limits of Quintessence." *Phys. Rev. Lett.,* 95 (141301) (cit. on p. 17).

[**Campo et al. 2013**]

Campo, S. del et al. (07/2013). "Thawing models in the presence of a generalized Chaplygin gas." *Phys. Rev. D,* 88 (023532) (cit. on p. 130).

[**Cardenas et al. 2003**]

Cardenas, R. et al. (04/2003). "Model of the universe including dark energy accounted for by both a quintessence field and a (negative) cosmological constant." *Phys. Rev. D,* 67 (083501) (cit. on p. 130).

[**Carloni et al. 2005**]

Carloni, S. et al. (11/2005). "Cosmological dynamics of R^n gravity." *Class. Quant. Grav.,* 22 (4839) (cit. on p. 74).

[Carr et al. 1974]

Carr, B. J. and S. W. Hawking (08/1974). “Black Holes in the Early Universe.” *Mon. Not. Roy. Astron. Soc.,* 168 (2), pp. 399–415 (cit. on p. 44).

[B. W. Carroll et al. 1996]

Carroll, B. W. and D. A. Ostlie (1996). *An Introduction to Modern Astrophysics.* Pearson Addison-Wesley (cit. on p. 5).

[S. M. Carroll 2004]

Carroll, S. M. (2004). “Spacetime and geometry: An introduction to general relativity.” *Addison-Wesley, San Francisco, USA,* 513 pages (cit. on p. 137).

[S. M. Carroll et al. 2006]

Carroll, S. M. et al. (12/2006). “Modified-source gravity and cosmological structure formation.” *New J. Phys.,* 8 (323) (cit. on p. 98).

[Chakrabarti 1996]

Chakrabarti, S. K. (02/1996). “Accretion processes on a black hole.” *Phys. Rept.,* 266 (5–6), pp. 229–390 (cit. on p. 8).

[Chang 1985]

Chang, K. M. (01/1985). “The number of critical points in polytropic accretion onto black holes.” *Astron. Astrophys.,* 142 (1), pp. 212–213 (cit. on p. 44).

[Chiba et al. 2014]

Chiba, T. et al. (07/2014). “Cosmological scaling solutions for multiple scalar fields.” *Phys. Rev. D,* 90 (023516) (cit. on p. 74).

[C. Clarkson 2007]

Clarkson, C. (11/2007). “Covariant approach for perturbations of rotationally symmetric spacetimes.” *Phys. Rev. D,* 76 (104034) (cit. on p. 65).

[C. A. Clarkson et al. 2003]

Clarkson, C. A. and R. K. Barrett (09/2003). “Covariant perturbations of Schwarzschild black holes.” *Class. Quant. Grav.,* 20 (3855) (cit. on pp. 65, 68).

[Clifton 2006]

Clifton, T. (11/2006). “Spherically symmetric solutions to fourth-order theories of gravity.” *Class. Quant. Grav.,* 23 (7445) (cit. on p. 27).

[Clifton et al. 2005]

Clifton, T. and J. D. Barrow (11/2005). “The power of general relativity.” *Phys. Rev. D,* 72 (103005) (cit. on pp. 74, 104, 114).

[Clifton et al. 2013]

Clifton, T., P. Dunsby, et al. (03/2013). “On the absence of the usual weak-field limit, and the impossibility of embedding some known solutions for isolated masses in cosmologies with $f(R)$ dark energy.” *Phys. Rev. D,* 87 (063517) (cit. on p. 26).

[Clifton et al. 2012]

Clifton, T., P. G. Ferreira, et al. (03/2012). "Modified gravity and cosmology." *Phys. Rept.,* 513 (1–3), pp. 1–189 (cit. on p. 4).

[Cooney et al. 2010]

Cooney, A. et al. (09/2010). "Neutron stars in $f(R)$ gravity with perturbative constraints." *Phys. Rev. D,* 82 (064033) (cit. on pp. 23, 26).

[Copeland et al. 2009]

Copeland, E. J., S. Mizuno, et al. (05/2009). "Dynamics of a scalar field in Robertson-Walker spacetimes." *Phys. Rev. D,* 79 (103515) (cit. on p. 130).

[Copeland et al. 2006]

Copeland, E. J., M. Sami, et al. (11/2006). "DYNAMICS OF DARK ENERGY." *Int. J. Mod. Phys. D,* 15 (11), pp. 1753–1936 (cit. on p. 4).

[Cruz et al. n.d.]

Cruz, M. et al. "Black holes structure via dynamical system in $f(R)$ theories." *In preparation,* (cit. on p. 117).

[Dabrowski et al. 2009]

Dabrowski, M. P. et al. (02/2009). "Conformal transformations and conformal invariance in gravitation." *Annalen Phys.,* 18 (1), pp. 13–32 (cit. on p. 145).

[Damour et al. 1993]

Damour, T. and G. Esposito-Farese (04/1993). "Nonperturbative strong-field effects in tensor-scalar theories of gravitation." *Phys. Rev. Lett.,* 70 (15), pp. 2220–2223 (cit. on p. 15).

[Damour et al. 1992]

Damour, T. and J. H. Taylor (03/1992). "Strong-field tests of relativistic gravity and binary pulsars." *Phys. Rev. D,* 45 (6), pp. 1840–1868 (cit. on p. 133).

[Davies 1977]

Davies, P. C. W. (06/1977). "Singularity avoidance and quantum conformal anomalies." *Phys. Lett. B,* 68 (4), pp. 402–404 (cit. on p. 24).

[De Felice et al. 2010]

De Felice, A. and S. Tsujikawa (06/2010). "$f(R)$ Theories." *Living Rev. Rel.,* 13 (3) (cit. on p. 11).

[deRham 2014]

deRham, C. (08/2014). "Massive Gravity." *Living Rev. Rel.,* 17 (7) (cit. on p. 15).

[deRham et al. 2011]

deRham, C. et al. (06/2011). "Resummation of Massive Gravity." *Phys. Rev. Lett.,* 106 (231101) (cit. on p. 15).

[Deruelle et al. 2008]

Deruelle, N. et al. (02/2008). "Junction Conditions in $f(R)$ Theories of Gravity." *Prog. Theor. Phys.,* 119 (2), pp. 237–251 (cit. on p. 26).

[Dicke 1962]

Dicke, R. H. (03/1962). "Mach's Principle and Invariance under Transformation of Units." *Phys. Rev.,* 125 (2163) (cit. on p. 13).

[Dolgov et al. 2003]

Dolgov, A. D. and M. Kawasaki (10/2003). "Can modified gravity explain accelerated cosmic expansion?" *Phys. Lett. B,* 573, pp. 1–4 (cit. on p. 97).

[Eddington 1923]

Eddington, A. S. (1923). *The Mathematical Theory of Reltivity.* Cambridge Books Online. Cambridge University Press (cit. on p. 3).

[Ehlers 1993]

Ehlers, J. (12/1993). "Contributions to the relativistic mechanics of continuous media." *Gen. Rel. Grav.,* 25 (12), 1225–1266 [Abh. Akad. Wiss. Lit. Mainz. Nat. Kl.11, 793(1961)] (cit. on p. 61).

[Einstein 1905]

Einstein, A. (1905). "Does the Inertia of a Body Depend upon its Energy-Content?" *Annalen der Physik,* 18, pp. 639–641 (cit. on p. 1).

[Einstein 1916]

Einstein, A. (1916). "The Foundation of the General Theory of Relativity." *Annalen der Physik,* 49, pp. 769–822 (cit. on p. 1).

[Eisenstein et al. 2005]

Eisenstein, D. J. et al. (11/2005). "Detection of the Baryon Acoustic Peak in the Large-Scale Correlation Function of SDSS Luminous Red Galaxies." *Astrophys. J.,* 633 (2), pp. 560–574 (cit. on p. 4).

[Ellis 1967]

Ellis, G. F. R. (1967). "Dynamics of Pressure-Free Matter in General Relativity." *J. Math. Phys.,* 8 (1171) (cit. on pp. 68, 75).

[Ellis 2009]

Ellis, G. F. R. (03/2009). "Republication of: Relativistic cosmology." *Gen. Rel. Grav.,* 41 (3), 581–660 [Proc. Int. Sch. Phys. Fermi47, 104–182(1971)] (cit. on p. 61).

[Ellis et al. 1999]

Ellis, G. F. R. and H. van Elst (1999). "Cosmological models: Cargése lectures 1998." *NATO Sci. Ser. C,* 541, pp. 1–116 (cit. on p. 61).

[H. v. Elst et al. 1996]

Elst, H. v. and G. F. R. Ellis (05/1996). "The covariant approach to LRS perfect fluid spacetime geometries." *Class. Quant. Grav.,* 13 (1099) (cit. on pp. 68, 75).

[Escobar et al. 2012a]

Escobar, D. et al. (08/2012a). "Phase space analysis of quintessence fields trapped in a Randall–Sundrum braneworld: a refined study." *Class. Quant. Grav.,* 29 (175005) (cit. on p. 129).

[Escobar et al. 2012b]

Escobar, D. et al. (08/2012b). "Phase space analysis of quintessence fields trapped in a Randall–Sundrum braneworld: anisotropic Bianchi I brane with a positive dark radiation term." *Class. Quant. Grav.,* 29 (175006) (cit. on p. 129).

[Escobar et al. 2014]

Escobar, D. et al. (01/2014). "Asymptotic behavior of a scalar field with an arbitrary potential trapped on a Randall-Sundrum's braneworld: the effect of a negative dark radiation term on a Bianchi I brane." *Astrophys. Space Sci.,* 349 (1), pp. 575–602 (cit. on pp. 129, 130).

[Fadragas et al. 2014]

Fadragas, C. R. et al. (03/2014). "Dynamical analysis of anisotropic scalar-field cosmologies for a wide range of potentials." *Class. Quant. Grav.,* 31 (075018) (cit. on p. 129).

[Faraoni 2011]

Faraoni, V. (06/2011). "R^n gravity and the chameleon." *Phys. Rev. D,* 83 (124044) (cit. on p. 24).

[Faraoni 2005]

Faraoni, V. (12/2005). "Stability of modified gravity models." *Phys. Rev. D,* 72 (124005) (cit. on p. 98).

[Faraoni et al. 1999]

Faraoni, V. et al. (1999). "Conformal transformations in classical gravitational theories and in cosmology." *Fund. Cosmic Phys.,* 20 (121) (cit. on p. 13).

[Faulkner et al. 2007]

Faulkner, T. et al. (09/2007). "Constraining $f(R)$ gravity as a scalar-tensor theory." *Phys. Rev. D,* 76 (063505) (cit. on p. 98).

[Frieman et al. 1995]

Frieman, J. A. et al. (09/1995). "Cosmology with Ultralight Pseudo Nambu-Goldstone Bosons." *Phys. Rev. Lett.,* 75 (11), pp. 2077–2080 (cit. on p. 18).

[Frolov 2008]

Frolov, A. V. (08/2008). "Singularity Problem with $f(R)$ Models for Dark Energy." *Phys. Rev. Lett.,* 101 (061103) (cit. on p. 24).

[Fujii et al. 2003]

Fujii, Y. and K.-I. Maeda (2003). *The Scalar-Tensor Theory of Gravitation.* Cambridge Books Online. Cambridge University Press (cit. on p. 13).

[Ganguly et al. 2014]

Ganguly, A., S. G. Ghosh, et al. (09/2014). "Accretion onto a black hole in a string cloud background." *Phys. Rev. D,* 90 (064037) (cit. on p. 43).

[Ganguly et al. 2014]

Ganguly, A. et al. (03/2014). "Neutron stars in the Starobinsky model." *Phys. Rev. D,* 89 (064019) (cit. on p. 23).

[Ganguly et al. 2015]

Ganguly, A. et al. (04/2015). "Global structure of black holes via the dynamical system." *Class. Quant. Grav.,* 32 (105006) (cit. on p. 75).

[Ganguly et al. n.d.]

Ganguly, A. et al. "Black holes structure via dynamical system in $f(R)$ theories." *In preparation,* (cit. on p. 98).

[Gannouji et al. 2012]

Gannouji, R. et al. (09/2012). "Generic $f(R)$ theories and classicality of their scalarons." *Phys. Lett. B,* 716 (2), pp. 255–259 (cit. on pp. 29, 30).

[Ghosh et al. 2014]

Ghosh, S. G. and S. D. Maharaj (04/2014). "Cloud of strings for radiating black holes in Lovelock gravity." *Phys. Rev. D,* 89 (084027) (cit. on p. 19).

[Ginzburg et al. 1971]

Ginzburg, V. L. et al. (08/1971). "The Role of Quantum Fluctuations of the Gravitational Field in General Relativity Theory and Cosmology." *Sov. Phys. JETP,* 33 (2), pp. 242–246 (cit. on p. 24).

[Glass et al. 1998]

Glass, E. N. and J. P. Krisch (05/1998). "Radiation and string atmosphere for relativistic stars." *Phys. Rev. D,* 57 (R5945) (cit. on p. 19).

[Glass et al. 1999a]

Glass, E. N. and J. P. Krisch (1999a). "Scale symmetries of spherical string fluids." *J. Math. Phys.,* 40 (4056) (cit. on p. 19).

[Glass et al. 1999b]

Glass, E. N. and J. P. Krisch (04/1999b). "Two-fluid atmosphere for relativistic stars." *Class. Quant. Grav.,* 16 (1175) (cit. on p. 19).

[Gleyzes et al. 2015]

Gleyzes, J. et al. (05/2015). "New Class of Consistent Scalar-Tensor Theories." *Phys. Rev. Lett.,* 114 (211101) (cit. on p. 15).

[Goheer et al. 2009]

Goheer, N. et al. (05/2009). "Dynamics of $f(R)$-cosmologies containing Einstein static models." *Class. Quant. Grav.,* 26 (105003) (cit. on p. 74).

[**Gonzalez et al. 2007**]

Gonzalez, T., R. Cardenas, et al. (07/2007). "Evolution of density perturbations in double exponential quintessence models." *Astrophys. Space Sci.,* 310 (1), pp. 13–18 (cit. on p. 130).

[**Gonzalez et al. 2006**]

Gonzalez, T., G. Leon, et al. (04/2006). "Dynamics of quintessence models of dark energy with exponential coupling to dark matter." *Class. Quant. Grav.,* 23 (9), pp. 3165–3179 (cit. on p. 130).

[**Goswami et al. 2011**]

Goswami, R. and G. F. R. Ellis (08/2011). "Almost Birkhoff theorem in general relativity." *Gen. Rel. Grav.,* 43 (8), pp. 2157–2170 (cit. on p. 75).

[**Guarnizo et al. 2010**]

Guarnizo, A. et al. (11/2010). "Boundary term in metric $f(R)$ gravity: field equations in the metric formalism." *Gen. Rel. Grav.,* 42 (11), pp. 2713–2728 (cit. on p. 140).

[**Gurovich et al. 1979**]

Gurovich, V. T. and A. A. Starobinsky (1979). "QUANTUM EFFECTS AND REGULAR COSMOLOGICAL MODELS." *Sov. Phys. JETP,* 50 (Zh. Eksp. Teor. Fiz.77,1683(1979)), pp. 844–852 (cit. on p. 98).

[**Guth 1981**]

Guth, A. H. (01/1981). "Inflationary universe: A possible solution to the horizon and flatness problems." *Phys. Rev. D,* 23 (2), pp. 347–356 (cit. on p. 3).

[**Guth et al. 1982**]

Guth, A. H. and S. Y. Pi (10/1982). "Fluctuations in the New Inflationary Universe." *Phys. Rev. Lett.,* 49 (15), pp. 1110–1113 (cit. on p. 4).

[**Hamid et al. 2014**]

Hamid, A. I. M. et al. (07/2014). "Cosmic censorship conjecture revisited: covariantly." *Class. Quant. Grav.,* 31 (135010) (cit. on p. 82).

[**Hawking 1982**]

Hawking, S. W. (09/1982). "The development of irregularities in a single bubble inflationary universe." *Phys. Lett. B,* 115 (4), pp. 295–297 (cit. on p. 4).

[**Hawking et al. 1973**]

Hawking, S. W. and G. F. R. Ellis (1973). *The Large Scale Structure of Space-Time.* Cambridge Books Online. Cambridge University Press (cit. on pp. 73, 81).

[**Hawking et al. 1970**]

Hawking, S. W. and R. Penrose (01/1970). "The Singularities of Gravitational Collapse and Cosmology." *Proc. Roy. Soc. Lond. A,* 314 (1519), pp. 529–548 (cit. on p. 3).

[**Heisenberg et al. 2014**]

Heisenberg, L. et al. (05/2014). "Cosmology of the proxy theory to massive gravity." *Phys. Rev. D,* 89 (103008) (cit. on p. 74).

[Herscovich et al. 2010]

Herscovich, E. and M. G. Richarte (05/2010). “Black holes in Einstein–Gauss–Bonnet gravity with a string cloud background.” *Phys. Lett. B,* 689 (4–5), pp. 192–200 (cit. on p. 19).

[Horndeski 1974]

Horndeski, G. W. (09/1974). “Second-order scalar-tensor field equations in a four-dimensional space.” *Int. J. Theor. Phys.,* 10 (6), pp. 363–384 (cit. on p. 15).

[Hulse et al. 1975]

Hulse, R. A. and J. H. Taylor (01/1975). “Discovery of a pulsar in a binary system.” *Astrophys. J.,* 195 (2), pp. L51–L53 (cit. on p. 133).

[Huterer et al. 1999]

Huterer, D. and M. S. Turner (08/1999). “Prospects for probing the dark energy via supernova distance measurements.” *Phys. Rev. D,* 60 (081301(R)) (cit. on p. 4).

[Israel 1966]

Israel, W. (07/1966). “Singular hypersurfaces and thin shells in general relativity.” *Nuovo Cimento B,* 44 (1), 48(2)(E), 04/1967 (cit. on p. 26).

[Jamil et al. 2008]

Jamil, M. et al. (11/2008). “Charged black holes in phantom cosmology.” *Eur. Phys. J. C,* 58 (2), pp. 325–329 (cit. on p. 44).

[John et al. 2013]

John, A. J. et al. (Nnovember/2013). “Accretion onto a higher dimensional black hole.” *Phys. Rev. D,* 88 (104005) (cit. on p. 44).

[Kainulainen et al. 2007]

Kainulainen, K. et al. (07/2007). “Spherically symmetric spacetimes in $f(R)$ gravity theories.” *Phys. Rev. D,* 76 (024020) (cit. on pp. 23, 26).

[Kallosh et al. 2003]

Kallosh, R. et al. (10/2003). “Observational bounds on cosmic doomsday.” *J. Cosmol. Astropart. Phys.,* (cit. on p. 18).

[Kapner et al. 2007]

Kapner, D. J. et al. (01/2007). “Tests of the Gravitational Inverse-Square Law below the Dark-Energy Length Scale.” *Phys. Rev. Lett.,* 98 (021101) (cit. on p. 29).

[Khoury et al. 2004]

Khoury, J. and A. Weltman (10/2004). “Chameleon Fields: Awaiting Surprises for Tests of Gravity in Space.” *Phys. Rev. Lett.,* 93 (171104) (cit. on p. 29).

[Kibble 1976]

Kibble, T. W. B. (08/1976). “Topology of cosmic domains and strings.” *J. Phys. A,* 9 (1387) (cit. on p. 19).

[Kobayashi et al. 2008]

Kobayashi, T. and K.-I. Maeda (09/2008). "Relativistic stars in $f(R)$ gravity, and absence thereof." *Phys. Rev. D,* 78 (064019), p. 9 (cit. on p. 24).

[Kofinas et al. 2014]

Kofinas, G. et al. (09/2014). "Dynamical behavior in $f(T, T_G)$ cosmology." *Class. Quant. Grav.,* 31 (175011) (cit. on p. 74).

[Komatsu et al. 2009]

Komatsu, E. et al. (02/2009). "FIVE-YEAR WILKINSON MICROWAVE ANISOTROPY PROBE OBSERVATIONS: COSMOLOGICAL INTERPRETATION." *Astrophys. J. Suppl.,* 180 (2), pp. 330–376 (cit. on p. 4).

[Kramer et al. 2009]

Kramer, M. and N. Wex (02/2009). "The double pulsar system: a unique laboratory for gravity." *Class. Quant. Grav.,* 26 (073001) (cit. on p. 3).

[Kramer 2013]

Kramer, M. (03/2013). "Probing gravitation with pulsars (Proceedings of the International Astronomical Union Symposium 291)." *IAU Symp.,* 291, pp. 19–26 (cit. on pp. 133, 134).

[Kundt et al. 1962]

Kundt, W. and M. Trümper (1962). "Beiträge zur Theorie der Gravitations-Strahlungsfelder (German)." *Akad. Wiss. Lit. Mainz, Abhandl. Math.-Nat.Kl.,* 12, pp. 969–1000 (cit. on p. 61).

[Larsen 1997]

Larsen, F. (07/1997). "String model of black hole microstates." *Phys. Rev. D,* 56 (1005) (cit. on p. 19).

[Lattimer et al. 2001]

Lattimer, J. M. and M. Prakash (03/2001). "Neutron Star Structure and the Equation of State." *Astrophys. J.,* 550 (1), pp. 426–442 (cit. on p. 40).

[Leon et al. 2013]

Leon, G. and E. N. Saridakis (03/2013). "Dynamical analysis of generalized Galileon cosmology." *J. Cosmol. Astropart. Phys.,* 03 (025) (cit. on p. 74).

[Letelier 1979]

Letelier, P. S. (09/1979). "Clouds of strings in general relativity." *Phys. Rev. D,* 20 (1294) (cit. on pp. 19–21, 43).

[Leyva et al. 2009]

Leyva, Y. et al. (08/2009). "Dynamics of a self-interacting scalar field trapped in the braneworld for a wide variety of self-interaction potentials." *Phys. Rev. D,* 80 (044026) (cit. on p. 130).

[Liddle et al. 2000]

Liddle, A. R. and D. H. Lyth (2000). *Cosmological Inflation and Large-Scale Structure.* Cambridge University Press (cit. on p. 3).

[Lidsey et al. 2002]

Lidsey, J. E. et al. (07/2002). "Inflaton field as self-interacting dark matter in the braneworld scenario." *Phys. Rev. D,* 66 (023514) (cit. on p. 130).

[Linde 1982]

Linde, A. D. (02/1982). "A new inflationary universe scenario: A possible solution of the horizon, flatness, homogeneity, isotropy and primordial monopole problems." *Phys. Lett. B,* 108 (6), pp. 389–393 (cit. on p. 3).

[Linde 1983]

Linde, A. D. (09/1983). "Chaotic inflation." *Phys. Lett. B,* 129 (3–4), pp. 177–181 (cit. on p. 18).

[Linde 2008]

Linde, A. D. (2008). "Inflationary Cosmology." *Springer Berlin Heidelberg,* 738 (Lect. Notes Phys.), pp. 1–54 (cit. on p. 15).

[Luty et al. 2003]

Luty, M. A. et al. (10/2003). "Strong interactions and stability in the DGP model." *JHEP,* 09 (029) (cit. on p. 15).

[Lyne et al. 2004]

Lyne, A. G. et al. (02/2004). "A Double-Pulsar System: A Rare Laboratory for Relativistic Gravity and Plasma Physics." *Science,* 303 (5661), pp. 1153–1157 (cit. on p. 134).

[Lyth et al. 19991]

Lyth, D. H. and A. Riotto (06/19991). "Particle physics models of inflation and the cosmological density perturbation." *Phys. Rept.,* 314 (1–2), pp. 1–146 (cit. on p. 3).

[Maartens 1997]

Maartens, R. (01/1997). "Linearization instability of gravity waves?" *Phys. Rev. D,* 55 (2), pp. 463–467 (cit. on p. 61).

[K.-I. Maeda 1989]

Maeda, K.-I. (05/1989). "Towards the Einstein-Hilbert action via conformal transformation." *Phys. Rev. D,* 39 (3159) (cit. on p. 13).

[K. Maeda et al. 1980]

Maeda, K. et al. (02/1980). "A New Formalism of the Einstein Equations for Relativistic Rotating Systems." *Prog. Theor. Phys.,* 63 (2), pp. 719–721 (cit. on p. 65).

[Magnano et al. 1994]

Magnano, G. and L. M. Sokolowski (10/1994). "Physical equivalence between nonlinear gravity theories and a general-relativistic self-gravitating scalar field." *Phys. Rev. D,* 50 (5039) (cit. on p. 13).

[Malec 1999]

Malec, E. (10/1999). "Fluid accretion onto a spherical black hole: Relativistic description versus the Bondi model." *Phys. Rev. D,* 60 (104043) (cit. on p. 44).

[Martin 2008]

Martin, J. (06/2008). "QUINTESSENCE: A MINI-REVIEW." *Mod. Phys. Lett. A,* 23 (17n20), pp. 1252–1265 (cit. on p. 15).

[Martin 2012]

Martin, J. (07/2012). "Everything you always wanted to know about the cosmological constant problem (but were afraid to ask)." *Comptes Rendus Physique,* 13 (6–7), pp. 566–665 (cit. on pp. 4, 97).

[Matos et al. 2009]

Matos, T., J.-R. Luevano, et al. (12/2009). "Dynamics of scalar field dark matter with a cosh-like potential." *Phys. Rev. D,* 80 (123521) (cit. on p. 130).

[Matos et al. 2000]

Matos, T. and L. A. Urena-Lopez (2000). "Quintessence and scalar dark matter in the Universe." *Class. Quant. Grav.,* 17 (13), pp. L75–L81 (cit. on p. 130).

[Mazharimousavi et al. 2010]

Mazharimousavi, S. H. et al. (09/2010). "Theorem to generate Einstein-nonlinear Maxwell fields." *Class. Quant. Grav.,* 27 (205022) (cit. on p. 19).

[Mazur et al. 2004]

Mazur, P. O. and E. Mottola (05/2004). "Gravitational vacuum condensate stars." *Proc. Nat. Acad. Sci.,* 101 (26), pp. 9545–9550 (cit. on p. 40).

[Melis et al. 2005]

Melis, M. and S. Mignemi (08/2005). "Global properties of dilatonic Gauss-Bonnet black holes." *Class. Quant. Grav.,* 22 (3169) (cit. on p. 74).

[Michel 1972]

Michel, F. C. (01/1972). "Accretion of matter by condensed objects." *Astrophys. Space Sci.,* 15 (1), pp. 153–160 (cit. on pp. 44–46, 48, 50, 60).

[Mignemi 2000]

Mignemi, S. (06/2000). "Primary scalar hair in dilatonic theories with modulus fields." *Phys. Rev. D,* 62 (024014) (cit. on p. 74).

[Mignemi et al. 1989]

Mignemi, S. and D. L. Wiltshire (07/1989). "Spherically symmetric solutions in dimensionally reduced spacetimes." *Class. Quant. Grav.,* 6 (987) (cit. on p. 74).

[Mignemi et al. 1992]

Mignemi, S. and D. L. Wiltshire (08/1992). "Black holes in higher-derivative gravity theories." *Phys. Rev. D,* 46 (1475) (cit. on pp. 27, 74).

[**Mitchell et al. 1987**]

Mitchell, D. and N. Turok (1987). “Statistical properties of cosmic strings.” *Nucl. Phys. B,* 294, pp. 1138–1163 (cit. on p. 19).

[**Mukhanov et al. 1981**]

Mukhanov, V. F. and G. V. Chibisov (04/1981). “Quantum fluctuations and a nonsingular universe.” *JETP Lett.,* 33 (10), pp. 532–535 (cit. on p. 4).

[**Myung 2011**]

Myung, Y. S. (02/2011). “Graviton and scalar propagations on AdS_4 space in $f(R)$ gravities.” *Eur. Phys. J. C,* 71 (1550) (cit. on p. 98).

[**Myung et al. 2011**]

Myung, Y. S. et al. (06/2011). “Stability of $f(R)$ black holes.” *Phys. Rev. D,* 83 (124009) (cit. on p. 98).

[**Nariai 1973**]

Nariai, H. (01/1973). “Gravitational Instability of Regular Model-Universes in a Modified Theory of General Relativity.” *Prog. Theor. Phys.,* 49 (1), pp. 165–180 (cit. on p. 98).

[**Nayfeh 1973**]

Nayfeh, A. H. (02/1973). “Perturbation Methods.” (Wiley-Interscience) (cit. on p. 30).

[**Nicolis et al. 2009**]

Nicolis, A. et al. (03/2009). “Galileon as a local modification of gravity.” *Phys. Rev. D,* 79 (064036) (cit. on p. 15).

[**Nunez et al. 2004**]

Nunez, A. and S. Solganik (03/2004). “The Content of $f(R)$ gravity.” *arXiv,* hep-th/0403159 (cit. on p. 97).

[**Nzioki et al. 2010**]

Nzioki, A. M., S. Carloni, et al. (04/2010). “New framework for studying spherically symmetric static solutions in $f(R)$ gravity.” *Phys. Rev. D,* 81 (084028) (cit. on p. 28).

[**Nzioki et al. 2014**]

Nzioki, A. M., R. Goswami, et al. (03/2014). “Jebsen-Birkhoff theorem and its stability in $f(R)$ gravity.” *Phys. Rev. D,* 89 (064050) (cit. on pp. 39, 98).

[**Olmo 2005**]

Olmo, G. J. (12/2005). “The Gravity Lagrangian According to Solar System Experiments.” *Phys. Rev. Lett.,* 95 (261102) (cit. on p. 98).

[**Orellana et al. 2013**]

Orellana, M. et al. (02/2013). “Structure of neutron stars in R-squared gravity.” *Gen. Relativ. Gravit.,* 45 (4), pp. 771–783 (cit. on pp. 23, 26).

[**Pacheco 2012**]

Pacheco, J. A. d. F. (2012). “Relativistic Accretion into a Reissner-Nordström Black Hole Revisited.” *J. Thermodynamics,* 2012 (791870) (cit. on pp. 44, 50, 52).

[Pandey 1987]

Pandey, U. S. (08/1987). "Accretion of charged matter by collapsing objects." *Astrophys. Space Sci.,* 136 (1), pp. 195–199 (cit. on p. 44).

[Parthasarathy et al. 1997]

Parthasarathy, R. and K. S. Viswanathan (05/1997). "Modification of black-hole entropy by strings." *Phys. Lett. B,* 400 (1–2), pp. 27–31 (cit. on p. 19).

[Pavluchenko 2003]

Pavluchenko, S. A. (05/2003). "Generality of inflation in closed cosmological models with some quintessence potentials." *Phys. Rev. D,* 67 (103518) (cit. on p. 130).

[Percival et al. 2007]

Percival, W. J. et al. (11/2007). "Measuring the Baryon Acoustic Oscillation scale using the Sloan Digital Sky Survey and 2dF Galaxy Redshift Survey." *Mon. Not. Roy. Astron. Soc.,* 381 (3), pp. 1053–1066 (cit. on p. 4).

[Perlmutter et al. 1999]

Perlmutter, S. et al. (06/1999). "Measurements of Ω and Λ from 42 High-Redshift Supernovae." *Astrophys. J.,* 517 (2), pp. 565–586 (cit. on p. 4).

[Plebanski et al. 2006]

Plebanski, J. and A. Krasinski (2006). *An Introduction to General Relativity and Cosmology.* Cambridge Books Online. Cambridge University Press (cit. on p. 75).

[Poisson 2004]

Poisson, E. (2004). *A Relativist's Toolkit.* Cambridge Books Online. Cambridge University Press (cit. on p. 137).

[Poletti et al. 1994]

Poletti, S. J. and D. L. Wiltshire (12/1994). "Global properties of static spherically symmetric charged dilaton spacetimes with a Liouville potential." *Phys. Rev. D,* 50 (7260), 52 (3753)(E), 09/1995 (cit. on p. 74).

[Press et al. 1972]

Press, W. H. and S. A. Teukolsky (07/1972). "Floating Orbits, Superradiant Scattering and the Black-hole Bomb." *Nature,* 238, pp. 211–212 (cit. on p. 15).

[Psaltis 2008]

Psaltis, D. (11/2008). "Probes and Tests of Strong-Field Gravity with Observations in the Electromagnetic Spectrum." *Living Rev. Relativity,* 11 (9) (cit. on p. 5).

[Ratra et al. 1988]

Ratra, B. and P. J. E. Peebles (06/1988). "Cosmological consequences of a rolling homogeneous scalar field." *Phys. Rev. D,* 37 (3406) (cit. on p. 130).

[Ray 1980]

Ray, D. (02/1980). "Accretion of gas by a Schwarzchild black hole." *Astron. Astrophys.,* 82 (3), pp. 368–369 (cit. on p. 44).

[**Riess et al. 1998**]

Riess, A. G. et al. (09/1998). "Observational Evidence from Supernovae for an Accelerating Universe and a Cosmological Constant." *Astron. J.,* 116 (3), pp. 1009–1038 (cit. on pp. 4, 97).

[**Riess et al. 1999**]

Riess, A. G. et al. (02/1999). "BVRI Light Curves for 22 Type Ia Supernovae." *Astron. J.,* 117 (2), pp. 707–724 (cit. on p. 4).

[**Roy 2014**]

Roy, X. (05/2014). "On the 1+3 Formalism in General Relativity." *arXiv:1405.6319 [gr-qc],* (cit. on p. 61).

[**Sahni et al. 1992**]

Sahni, V., H. Feldman, et al. (01/1992). "Loitering universe." *Astrophys. J.,* 385, pp. 1–8 (cit. on p. 17).

[**Sahni et al. 2000**]

Sahni, V. and A. A. Starobinsky (08/2000). "THE CASE FOR A POSITIVE COSMOLOGICAL Λ-TERM." *Int. J. Mod. Phys. D,* 92 (4), pp. 373–444 (cit. on p. 130).

[**Sahni et al. 2000**]

Sahni, V. and L.-M. Wang (10/2000). "New cosmological model of quintessence and dark matter." *Phys. Rev. D,* 62 (103517) (cit. on p. 130).

[**Sasaki et al. 1980**]

Sasaki, M. et al. (03/1980). "A Method of Determining Apparent Horizons in [(2+1)+1]-Formalism of the Einstein Equations." *Prog. Theor. Phys.,* 63 (3), pp. 1051–1053 (cit. on p. 81).

[**Saslaw et al. 1996**]

Saslaw, W. C. et al. (11/1996). "An Isothermal Universe." *Astrophys. J.,* 471 (2), pp. 571–574 (cit. on p. 103).

[**Sawicki et al. 2007**]

Sawicki, I. and W. Hu (06/2007). "Stability of cosmological solutions in $f(R)$ models of gravity." *Phys. Rev. D,* 75 (127502) (cit. on p. 97).

[**Seifert 2007**]

Seifert, M. D. (09/2007). "Stability of spherically symmetric solutions in modified theories of gravity." *Phys. Rev. D,* 76 (064002) (cit. on p. 97).

[**Sen 1998**]

Sen, A. (07/1998). "Developments in superstring theory." *29th International Conference on High-Energy Physics (ICHEP 98), Vancouver, British Columbia, Canada,* 1 (hep-ph/9810356), pp. 371–381 (cit. on p. 19).

[Senovilla 2013]

Senovilla, J. M. M. (09/2013). "Junction conditions for $f(R)$ gravity and their consequences." *Phys. Rev. D,* 88 (064015) (cit. on p. 26).

[Shapiro 1973a]

Shapiro, S. L. (03/1973a). "Accretion onto Black Holes: the Emergent Radiation Spectrum." *Astrophys. J.,* 180, pp. 531–546 (cit. on p. 44).

[Shapiro 1973b]

Shapiro, S. L. (10/1973b). "Accretion onto Black Holes: the Emergent Radiation Spectrum. II. Magnetic Effects." *Astrophys. J.,* 185, pp. 69–82 (cit. on p. 44).

[Shapiro 1974]

Shapiro, S. L. (04/1974). "Accretion onto Black Holes: the Emergent Radiation Spectrum. III. Rotating (kerr) Black Holes." *Astrophys. J.,* 189, pp. 343–352 (cit. on p. 44).

[Shapiro et al. 1983]

Shapiro, S. L. and S. A. Teukolsky (05/1983). "Black Holes, White Dwarfs and Neutron Stars: The Physics of Compact Objects." *Wiley-VCH,* 663 pages (cit. on pp. 44–46, 48–50, 59, 60).

[Sharif et al. 2011]

Sharif, M. and G. Abbas (07/2011). "PHANTOM ACCRETION BY FIVE-DIMENSIONAL CHARGED BLACK HOLE." *Mod. Phys. Lett. A,* 26 (1731) (cit. on p. 44).

[Sharif et al. 2012]

Sharif, M. and G. Abbas (01/2012). "Phantom Energy Accretion by a Stringy Charged Black Hole." *Chin. Phys. Lett.,* 29 (010401) (cit. on p. 44).

[Song et al. 2007]

Song, Y.-S. et al. (02/2007). "Large scale structure of $f(R)$ gravity." *Phys. Rev. D,* 75 (044004) (cit. on p. 98).

[Sotiriou et al. 2012]

Sotiriou, T. P. and V. Faraoni (02/2012). "Black Holes in Scalar-Tensor Gravity." *Phys. Rev. Lett.,* 108 (081103) (cit. on p. 27).

[Sotiriou et al. 2010]

Sotiriou, T. P. and V. Faraoni (03/2010). "$f(R)$ theories of gravity." *Rev. Mod. Phys.,* 82 (1), pp. 451–497 (cit. on p. 11).

[Starobinsky 1980]

Starobinsky, A. A. (03/1980). "A new type of isotropic cosmological models without singularity." *Phys. Lett. B,* 91 (1), pp. 99–102 (cit. on pp. 11, 24).

[Starobinsky 1982]

Starobinsky, A. A. (11/1982). "Dynamics of phase transition in the new inflationary universe scenario and generation of perturbations." *Phys. Lett. B,* 117 (3–4), pp. 175–178 (cit. on p. 4).

[Starobinsky 1983]

Starobinsky, A. A. (10/1983). "The perturbation spectrum evolving from a nonsingular, initially de Sitter cosmology, and the microwave background anisotropy." *Sov. Astron. Lett.,* 9, pp. 302–304 (cit. on p. 30).

[Starobinsky 2007]

Starobinsky, A. A. (10/2007). "Disappearing cosmological constant in $f(R)$ gravity." *JETP Lett.,* 86 (3), pp. 157–163 (cit. on pp. 28, 30).

[Steinhardt et al. 1999]

Steinhardt, P. J. et al. (05/1999). "Cosmological tracking solutions." *Phys. Rev. D,* 59 (123504) (cit. on p. 18).

[Stelle 1977]

Stelle, K. S. (08/1977). "Renormalization of higher-derivative quantum gravity." *Phys. Rev. D,* 16 (4), pp. 953–969 (cit. on p. 3).

[Stelle 1978]

Stelle, K. S. (04/1978). "Classical gravity with higher derivatives." *Gen. Rel. Grav.,* 9 (4), pp. 353–371 (cit. on p. 29).

[Stephani et al. 2004]

Stephani, H. et al. (2004). *Exact solutions of Einstein's field equations.* Cambridge University Press (cit. on p. 70).

[Stewart et al. 1968]

Stewart, J. M. and G. F. R. Ellis (1968). "Solutions of Einstein's Equations for a Fluid Which Exhibit Local Rotational Symmetry." *J. Math. Phys.,* 9 (1072) (cit. on pp. 68, 69, 75).

[Strominger et al. 1996]

Strominger, A. and C. Vafa (06/1996). "Microscopic origin of the Bekenstein-Hawking entropy." *Phys. Lett. B,* 379 (1–4), pp. 99–104 (cit. on p. 19).

[Sudarsky 1995]

Sudarsky, D. (02/1995). "A simple proof of a no-hair theorem in Einstein-Higgs theory." *Class. Quant. Grav.,* 12 (579) (cit. on p. 27).

[Synge 1960]

Synge, J. L. (01/1960). "Relativity: The General Theory." *North-Holland Publishing Company,* 505 pages (cit. on pp. 19, 43).

[Tegmark et al. 4]

Tegmark, M. et al. (05/004). "Cosmological parameters from SDSS and WMAP." *Phys. Rev. D,* 69 (103501) (cit. on p. 4).

[Tegmark et al. 2006]

Tegmark, M. et al. (12/2006). "Cosmological constraints from the SDSS luminous red galaxies." *Phys. Rev. D,* 74 (123507) (cit. on p. 4).

[Thongkool et al. 2009]

Thongkool, I. et al. (08/2009). "Constraining $f(R)$ gravity models with disappearing cosmological constant." *Phys. Rev. D,* 80 (043523) (cit. on p. 24).

[Thorne et al. 1981]

Thorne, K. S. et al. (06/1981). "Stationary spherical accretion into black holes – I. Equations of structure." *Mon. Not. R. Astron. Soc.,* 194 (2), pp. 475–484 (cit. on p. 44).

[Tolley 2009]

Tolley, A. (2009). "Dark Energy." *Cosmo '09,* (cit. on p. 15).

[Torii et al. 1999]

Torii, T. et al. (02/1999). "Toward the no-scalar-hair conjecture in asymptotically de Sitter spacetime." *Phys. Rev. D,* 59 (064027) (cit. on p. 28).

[Tsujikawa 2013]

Tsujikawa, S. (10/2013). "Quintessence: a review." *Class. Quant. Grav.,* 30 (21) (cit. on p. 15).

[Upadhye et al. 2009]

Upadhye, A. and W. Hu (09/2009). "Existence of relativistic stars in $f(R)$ gravity." *Phys. Rev. D,* 80 (064002) (cit. on p. 24).

[Upadhye et al. 2012]

Upadhye, A., W. Hu, and J. Khoury (07/2012). "Quantum Stability of Chameleon Field Theories." *Phys. Rev. Lett.,* 109 (041301) (cit. on p. 30).

[Urena-Lopez 2012]

Urena-Lopez, L. A. (03/2012). "Unified description of the dynamics of quintessential scalar fields." *J. Cosmol. Astropart. Phys.,* 03 (035) (cit. on p. 129).

[Urena-Lopez et al. 2000]

Urena-Lopez, L. A. and T. Matos (09/2000). "New cosmological tracker solution for quintessence." *Phys. Rev. D,* 62 (081302) (cit. on p. 130).

[Utiyama et al. 1962]

Utiyama, R. and B. S. DeWitt (07/1962). "Renormalization of a Classical Gravitational Field Interacting with Quantized Matter Fields." *J. Math. Phys.,* 3 (4), pp. 608–618 (cit. on p. 3).

[Vilenkin 1981]

Vilenkin, A. (04/1981). "Cosmological Density Fluctuations Produced by Vacuum Strings." *Phys. Rev. Lett.,* 46 (1169), 46 (1496)(E), 06/1981 (cit. on p. 19).

[Vilkovisky 1992]

Vilkovisky, G. A. (1992). "Effective action in quantum gravity." *Class. Quant. Grav.,* 9 (4), pp. 895–903 (cit. on p. 3).

[Wainwright et al. 1997]

Wainwright, J. and G. F. R. Ellis, eds. (1997). *Dynamical Systems in Cosmology.* Cambridge Books Online. Cambridge University Press (cit. on p. 74).

[Wald 1984]

Wald, R. M. (1984). *General Relativity.* Cambridge Books Online. University of Chicago Press (cit. on pp. 2, 13).

[Wands 1994]

Wands, D. (01/1994). "Extended gravity theories and the Einstein–Hilbert action." *Class. Quant. Grav.,* 11 (1), pp. 269–279 (cit. on p. 13).

[Weinberg 1989]

Weinberg, S. (01/1989). "The cosmological constant problem." *Rev. Mod. Phys.,* 61 (1) (cit. on p. 4).

[Wetterich 1988]

Wetterich, C. (06/1988). "Cosmology and the fate of dilatation symmetry." *Nucl. Phys. B,* 302 (4), pp. 668–696 (cit. on p. 130).

[Wex 2014]

Wex, N. (02/2014). "Testing Relativistic Gravity with Radio Pulsars." arXiv:1402.5594[gr-qc] (cit. on p. 133).

[Weyl 1919]

Weyl, H. (1919). "Eine neue Erweiterung der Relativitätstheorie (A New Extension of Relativity Theory)." *Annalen Phys.,* 364 (10), pp. 101–133 (cit. on p. 3).

[Whitt 1984]

Whitt, B. (09/1984). "Fourth-order gravity as general relativity plus matter." *Phys. Lett. B,* 145 (3–4), pp. 176–178 (cit. on p. 27).

[Will 2014]

Will, C. M. (06/2014). "The Confrontation between General Relativity and Experiment." *Living Rev. Rel.,* 17 (4) (cit. on p. 3).

[Wiltshire 1991]

Wiltshire, D. L. (08/1991). "Spherically symmetric solutions in dimensionally reduced spacetimes with a higher-dimensional cosmological constant." *Phys. Rev. D,* 44 (1100) (cit. on p. 74).

[Xiao et al. 2011]

Xiao, K. and J.-Y. Zhu (04/2011). "Stability analysis of an autonomous system in loop quantum cosmology." *Phys. Rev. D,* 83 (083501) (cit. on p. 74).

[Yearsley et al. 1996]

Yearsley, J. and J. D. Barrow (1996). "Cosmological models of dimensional segregation." *Class. Quant. Grav.,* 13 (10), pp. 2693–2706 (cit. on p. 130).

[**Zhang 2007**]

Zhang, P.-J. (07/2007). "Behavior of $f(R)$ gravity in the solar system, galaxies, and clusters." *Phys. Rev. D,* 76 (024007) (cit. on p. 29).

[**Zhou et al. 2009**]

Zhou, S.-Y. et al. (07/2009). "Cosmological constraints on *f(G)* dark energy models." *J. Cosmol. Astropart. Phys.,* 07 (009) (cit. on p. 74).